ANALYSIS OF MITOCHONDRIAL FUNCTION IN MOUSE AND MAN

Dissertation

zur

Erlangung der naturwissenschaftlichen Doktorwürde
(Dr. sc. nat)

vorgelegt der
Mathematisch-naturwissenschaftlichen Fakultät
der
Universität Zürich

von
Robert Acton Jacobs
aus den
Vereinigten Staaten von Amerika

Promotionskomitee

Prof. Dr. Max Gassmann (Vorsitz)
Prof. Dr. Carsten Lundby
Prof. Dr. Hans Hoppeler

Zürich, 2013

Table of Contents

Summary

The mitochondrion, often referred to as the energetic “powerhouse” of the eukaryotic cell, is a vital component for all mammalian life. The oxygen that is breathed in from the environment is ultimately consumed in mitochondria and in turn mitochondria harness energy used to maintain metabolic and biological function. The health of an individual is intimately related to the health of his or her mitochondria and yet much about the mitochondria is unknown.

Research investigating mitochondrial function and its relationship to both health and disease remains at the forefront of a multitude of different scientific fields. Despite the significance of mitochondrial physiology in maintaining both physical and mental health, however, there is paucity of literature that actually examines mitochondrial respiration directly *in vivo* or in intact tissue, *ex vivo*, providing dynamic assessments of electron transfer efficacy and substrate influence on respiration. This dissertationwill review the origin and evolution of the mitochondrion, summarize metabolic pathways fundamental to mitochondrial function, introduce and discuss oxidative phosphorylation together with the structure and function of the electron transport chain, and present 7 studies specific to the investigation of mitochondrial function. The collection of studies included in this dissertationall focus on the study of mitochondrial function through systematic analysis of electron transport system utility.

The results collected in seven independent studies support the following:

1. Human skeletal muscle mitochondria are capable, independent from cytosolic lactate dehydrogenase (LDH), of metabolizing lactate. Respiration is stimulated with the additions of malate + lactate + ADP + NAD^+ in a skeletal muscle preparation that perforates the sarcolemma, facilitating the loss of all soluble cytosolic components including cytosolic LDH. Lactate stimulated respiration despite the loss of cytosolic LDH suggests the existence of a mitochondrial-specific lactate oxidation complex. With the application of specific four different substrate titration protocols, the site of this complex was determined to most likely exist in the mitochondrial intermembrane space.

2. Skeletal muscle predominantly expressing a fast-twitch, glycolytic phenotype is predisposed to age-associated alterations in respiratory chain function. Slow-twitch and more oxidative skeletal muscle does not share this predisposition with aging and appears protected from the progressive lose with senescence. Specific alterations include an amplified respiratory capacity through mitochondrial respiratory complexes I and III with an attendant loss of electron coupling capacity at complex I, both suggestive of a greater oxidant production.

3. Mitochondrial respiratory capacity and control are similar between human and mouse skeletal muscle. The similarities in function, however, are largely dependent on skeletal muscle type with human and mouse quadricep expressing the greatest similarities. One difference that exists across all mouse skeletal muscle with that of human is the phosphorylative restraint of electron transport. Murine muscle electron transport capacity is not limited by the phosphorylative system of mitochondrial complex V, ATP Synthase, whereas human skeletal muscle demonstrates a certain degree of restraint.

4. Eleven days of exposure to high-altitude does not markedly modify integrated measures of mitochondrial functional capacity in human skeletal muscle despite significant decrements in the concentrations of certain enzymes involved in the tricarboxylic acid cycle and oxidative phosphorylation. Though respiratory capacities and efficiency are largely unaffected throughout an eleven-day sojourn to high altitude, mass-specific maximal state 3 respiration, oxidative phosphorylation capacity, does demonstrate a tendency to diminish over time.

5. One month of exposure to high-altitude, however, reduces respiratory capacity in human skeletal muscle while the efficiency of electron transport improves. Specifically, electron transport capacity specific to complex I-, complex II-, and maximal state-3 oxidative phosphorylation capacity all diminished independent from any measureable loss in mitochondrial content. Leak control

coupling, respiratory control ratio, and oligomycin-induced leak respiration, all measures of mitochondrial efficiency, improved with hypoxic exposure.

6. Integrative functional differences in mitochondrial function are apparent across groups of individuals that differ in aerobic capacities. Respiration capacities representative of fat oxidation, maximal oxidative phosphorylation, and electron transport system capacity all correspondingly improve with aerobic capacity. These observations are apparent even when controlling for differences in mitochondrial content in the skeletal muscle. Though differences in respiratory capacity are apparent, electron-coupling control for fat oxidation does not differ.

7. Maximal state-3 respiratory capacity, oxidative phosphorylation capacity, is the strongest predictor of endurance performance across a group of highly trained athletes. Mitochondrial content, however, which was similar across all subjects, had no predictive value of performance. Overall exercise performance, including incremental exercise performance in addition to endurance capacity, are best predicted by the measures of maximal oxygen consumption, total hemoglobin mass, maximal state-3 respiration, and electron transport system capacity of the skeletal muscle.

In brief, respiratory capacity and substrate control are dependent on both quantitative as well as qualitative characteristics. The mammalian reliance on this dynamic organelle, capable of utilizing many different substrates through multiple pathways, is fairly consistent across species. The capacity for oxygen utilization is extremely plastic, and modified through various modes of metabolic stress (i.e. hypoxia and exercise) to optimize the benefit of the host organism.

Zusammenfassung

Mitochondrien, oft als auch Kraftwerke der eukaryotischen Zelle bezeichnet, sind lebenswichtige Komponenten für alle Säugetiere. Der aus der Umwelt aufgenommene Sauerstoff wird von den Mitochondrien zur Energiegewinung für metabolische und biologische Funktionen eingesetzt. Die Gesundheit des Menschen hängt unmittelbar mit dem Gesundheitszustand der Mitochondrien zusammen, jedoch ist noch vieles über das Mitochondrium unbekannt.

Die Erforschung der Mitochondrien-Funktion und deren Einfluss auf Gesundheit und Krankheit bleibt weiterhin ein wichtiger Bestandteil in vielen unterschiedlichen wissenschaftlichen Forschungsbereichen. Trotz der hohen Bedeutung der mitochondriale Physiologie in der Aufrechterhaltung von physischer und psychischer Gesundheit, gibt es nur unzureichend Literatur zur Forschung der mitochondrialen Respiration in vivo oder in intaktem Gewebe, ex vivo. Damit lassen sich nur schwer dynamische Einschätzungen zur Elektronentransfereffizienz und zum Einfluss von Substraten auf die Respiration abgeben. In dieser Doktorarbeit soll der Ursprung und die Evolution der Mitochondrien zusammengetragen werden. Zudem werden die fundamentalen Stoffwechselwege der Mitochondrien zusammengefasst und die oxidative Phosphorylierung zusammen mit der Struktur und der Funktion der Elektronentransportkette diskutiert. Es werden 7 spezifische Studien in die Doktorarbeit miteinbezogen, welche sich auf die Funktion der Mitochondrien durch systematischen Analyse des Elektronentransportsystems, konzentrieren.

Die gesammelten Daten der sieben unabhängigen Studien unterstützen folgende Aussagen:

1. Humane Skelettmuskelmitochondrien sind fähig, unabhängig von zytosolischer Laktatdehydrogenase (LDH), Laktat zu metabolisieren. Die Atmung wird mittels Malat + Laktat + ADP + NAD+ Zusatz in einem Skelettmuskelpräparat mit perforiertem Sarkolemm stimuliert, um so den Verlust von allen löslichen zytosolischen Komponenten, inklusive der

zytosolischen LDH, zu erleichtern. Laktat stimuliert auch ohne zytosolisches LDH die Atmung welches auf die Existenz eines mitochondrien-spezifischen Laktatoxidationskomplexes zurückschliessen lässt. Dieser Komplex kommt mit grosser Wahrscheinlichkeit im Membranzwischenraum der Mitochondrien vor, welches anhand von mehreren unterschiedlichen Substrat-Titrationsprotokollen bestimmt wurde.

2. Der vorwiegend schnell-kontrahierende, glycolytische Skelettmuskel ist besonders anfällig für altersabhängige Veränderungen in der Atmungskettenfunktion. Langsame und hauptsächlich oxidative Skelettmuskel unterliegen nicht dieser altersabhängigen Veränderungen und scheinen vor dem progressiven Verlust durch Seneszenz geschützt zu sein. Spezifische Veränderungen sind dabei die erhöhte respiratorische Kapazität durch die respiratorischen Komplexe I und III bei gleichzeitigem Verlust der Elektronenkopplungskapazität im Komplex I. Beides lässt auf eine grössere oxidative Produktion zurückschliessen.

3. Die menschliche Skelettmuskulatur ähnelt – in Bezug auf respiratorische Kapazität und mitochondrialer Kontrolle – der Skelettmuskulatur der Maus. Funktionelle Gemeinsamkeiten sind allerdings stark vom Skelettmuskeltyp abhängig. Der Quadrizeps bei Mensch und Maus zeigt dabei die grössten Ähnlichkeiten auf. Ein wesentlicher Unterschied zur Maus ist jedoch die Hemmung des Elektronentransports durch die ATP-Synthase beim Menschen. Während die Muskelelektronentransportkapazität in allen Skelettmusklen von Mäusen nicht durch das phosphorylierende System des Mitochondrienkomplex V, ATP Synthase begrenzt wird, zeigt die menschliche Skelettmuskulatur eine entsprechende Limitierung.

4. Eine 11-tägige Höhenexposition verändert die die funktionelle Kapazität der Mitochondrien in der humanen Skelettmuskulatur – trotz signifikanter Abnahme von Enzymen des Tricarbonsäurezyklus und der oxidativen Phosphorylierung – nicht. Obwohl die respiratorische Kapazität und die Effizienz weitgehend unverändert bleiben, zeigt die massespezifische

maximale „state-3“ Respiration bzw. die oxidative Phosphorylierungskapazität eine tendenzielle Abnahme in dieser Zeit.

5. Eine Höhenexpostition von einem Monat reduziert jedoch die respiratorische Kapazität im humanen Skelettmuskel, während die Effizienz des Elektronentransportes verbessert wird. Vor allem die Elektronentransportkapazität im Komplex I- und Komplex II-, sowie die maximale „state-3“ oxidative Phosphorylierungskapazität werden unabhängig von jeglichem messbaren Verlust des Mitochondriengehalts reduziert. Die Leak-Kontrollkopplung, das respiratorische Kontrollverhältnis und die Oligomycin-induzierte Leak-Respiration – alles Effizienzmessgrössen der Mitochondrien – verbesserten sich während des Aufenthaltes in der Höhe.

6. Integrative funktionelle Differenzen in den Mitochondrien kommen in Individuen vor, welche sich in ihrer aerobischen Kapazität unterscheiden. Respiratorische Kapazitäten wie die Fettoxidation, die maximale oxidative Phosphorylierung und die Kapazität des Elektronentransportsystems verbessern sich alle entsprechend der aerobischen Kapazität. Sogar wenn die Unterschiede im Mitochondriengehalt der Skelettmuskulatur berücksichtigt werden zeigen sich diese Beobachtungen auf. Trotz der Unterschiede in der respiratorischen Kapazität ist kein Unterschied in der Elektronenkopplungskontrolle der Fettoxidation zusehen.

7. Die maximale „state-3“ respiratorische Kapazität – also die Kapazität der oxidativen Phosphorylierung - ist der beste Indikator für die Ausdauerleistung in einer Gruppe von gut trainierten Athleten. Der Mitochondriengehalt, welcher in allen Probanden vergleichbar war, stand jedoch nicht im Zusammenhang mit der Leistung. Die gesamte Leistungsfähigkeit, inklusive Stufentestleistung und Ausdauerkapazität, wird am besten durch den maximalen Sauerstoffverbrauch, die totale Hämoglobinmasse, die maximale state-3 Respiration und die Kapazität des Elektronetransportsystems im Skelettmuskel bestimmt.

Zusammenfassend kann man sagen, dass die respiratorische Kapazität und Substratsteuerung abhängig von den quantitativen sowie auch von qualitativen

Eigenschaften der Mitochondrien sind. Dieses dynamische Organell mit der Fähigkeit viele unterschiedliche Substrate über mehrere Substratwege zu nutzen, ist in einer Vielzahl von Säugetieren anzutreffen. Die Kapazität der Sauerstoffumsetzung ist extrem plastisch und passt sich verschiedenen Arten von metabolischem Stress (z.B Hypoxie und körperlicher Belastung) an, um den Nutzen des Wirtsorganismus zu optimieren.

Acknowledgments

"If I have seen further than others it is by standing upon the shoulders of giants."
– Sir Isaac Newton

My many, many thanks to all whose support have allowed me to reach the conclusion of my doctoral studies. First of all I would like to thank those who provided me the opportunity to learn and prosper in the world of science. I would not have been able to complete this work if it wasn't for the collective support and guidance of Prof. Dr. Carsten Lundby and Prof. Dr. med. vet. Max Gassmann. I would like to give an additional thanks to Prof. Dr. med. Hans Hoppeler for taking the necessary time to help steer the direction of my studies and participate in my education as a part of my Ph.D. committee. My committee as a whole provided the challenges and support necessary to shape a young scientist and I will be forever grateful.

I thank my many colleagues that over the course of four years I now have the privilege to call friends, specifically Dr. Christoph Siebenmann, Dr. Dominik Pesta, Dr. Sergey Yakushev, Dr. Víctor Díaz, and Dr. Peter Rasmussen. I am truly lucky to have been given the chance to work with such a phenomenal group of young scientists. Their support, teamwork, and friendship have been of immense help and inspiration to me.

Enough cannot be said about the loving support of my parents, Richard James and Jane Ellen Jacobs. They have been with me, truly, since the beginning. There is no monetary equivalent for the unconditional love and support they have provided me the over the last 31 years. It has been through their sacrifice that I was allowed to follow my interests and dreams. I am and will be forever indebted to them.

Lastly, I without a doubt thank my beautiful wife, Angela Jeau Jacobs, for carrying me through the last two years of my studies. It is with her I found life anew. She instills in me a hunger for living that cannot be satisfied. I am so extremely happy to be able to share this accomplishment with the person who functions, among many other relations, as my best friend and biggest supporter. I love you!

1. Introduction

Origin

Atmospheric concentrations of molecular oxygen (O_2) rapidly increased approximately 2.5 billion years ago (16, 90), either as a consequence of oxygenic photosynthesis (156) and/or via an abiotic shift of the oxidant/reducant equilibrium in the Earth's surface (90, 154, 158).

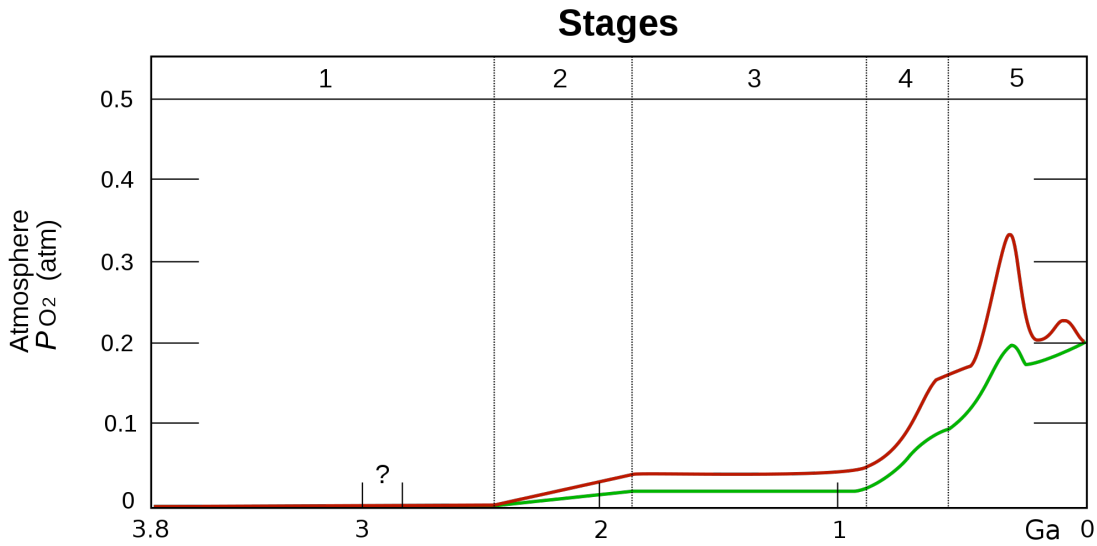

Figure 1. The history of oxygen on the earth. Adapted from (113). Atmospheric concentrations of oxygen on the earth presented in 5 stages with years (Gyr) on the x-axis with the red and green lines representing the estimated range: 1.) The atmosphere was essentially anoxic; 2.) Oxygen concentration in shallow portions of the oceans rose slightly; 3.) Maintenance period for low atmospheric concentrations of oxygen, with no significant changes; 4.) Acritarch and early protistan morphotypes sank to the sediment rich ocean floor resulting in a biological upsurge forming, among other organisms, algae; 5.) Oxygen formation from the ocean diffused into the environment and into land surfaces.

Primordial life was threatened in the precipitously oxygen-rich environment and was forced to adapt accordingly. This ambient accumulation of O_2 and the biological means to control it was a considerable boon in the evolution of *Homo sapiens*. The invaluable characteristic of this particular diradical gas is its instability - deficient by two additional electrons would spin pair both unpaired electrons in the outer orbital (2p) (9). While this instability has served as the lynchpin in the development and maintenance of mammalian life, there is a corollary threat attendant to this dependence on O_2. The volatility of O_2 can also precipitate cellular damage, as it is quite proficient in "stealing" electrons from various molecules through non-specific and non-facilitated means. In fact, O_2 is so adept at taking electrons from other molecules that the general process has been termed "oxidation" (189). Specific

adaptations to a high environmental O_2 concentration, in part, limited the uncontrolled oxidation of biological material by establishing an exact and coordinated cellular system of electron transfer with the final acceptor being O_2. Evolution found a way to provide O_2 with exactly what it desired, electrons, and in turn developed a system that harnessed the transfer of energy attendant to the transport of electrons from unusable organic material into biologically accessible sources, termed oxidative phosphorylation. This exploited O_2 and the potentially undesirable characteristics in favor of a massive biological thermodynamic advantage. While mammalian bioenergetics expands beyond aerobic means, the maintenance of mammalian life is now ultimately determined by O_2 availability and the capacity for aerobic metabolism. The ability to enzymatically restrain and lower the kinetic barrier of O_2 has guided adaptation over hundreds of millions of years and drastically increased the ceiling of metabolic potential. Cellular processes central to the utilization of O_2, now collectively referred to as aerobic metabolism, became possible through the synergistic fusion and evolution of ancestral eukaryotes with α-bacterial-like endosymbionts such as rhizobacteria and rickettsia (239, 319) eventually forming what is now known as the mitochondrion. Hitherto, our understanding of this subcellular structure, fundamental in O_2 metabolism and the transduction of energy into biologically usable means, has yet to catch up its evolution. Whereas primordial organisms labored with the initial exposure and utilization of O_2, mammals now find themselves in an impossible struggle to maintain cellular O_2 availability. The primary focus of this dissertation revolves around this subcellular structure that serves as the primary energetic source in mammals that controls the systematic conduction of electrons to O_2, the mitochondrion.

The mitochondrion

Mitochondria are organelles common to eukaryotic cells and are ubiquitous throughout the organism, albeit specific content varies across cell types (176, 258). Mitochondrial morphologies also vary considerably across different cell types, for example fibroblast mitochondria present as long and thin filaments, hepatocyte mitochondria more spherical and individual (325), and skeletal muscle mitochondria exist as an intricate interconnected reticular network (148).

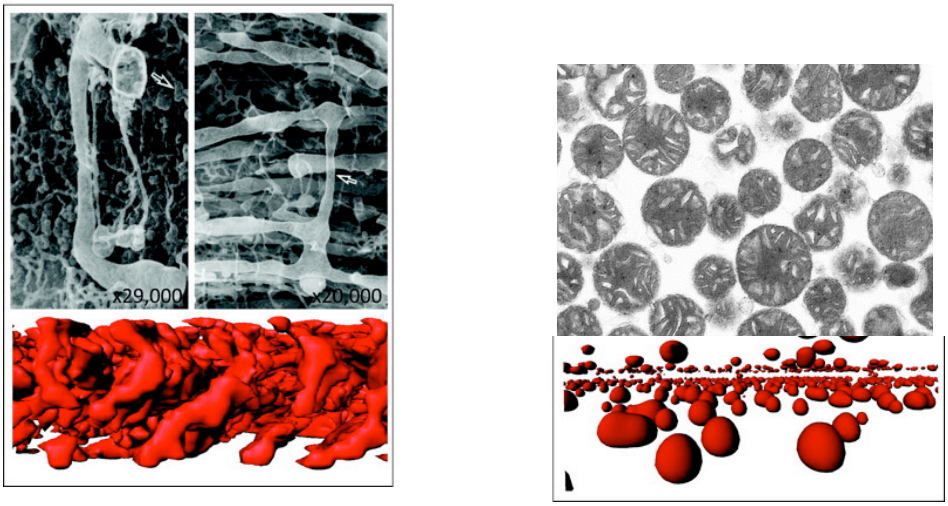

Figure 2. Mitochondrial morphology. Mitochondrial structure presenting as a reticular network within skeletal muscle (left) and as a spherical organelle in the liver (right). Figure adapted from references (148, 177, 215, 231)

Mitochondria are extremely dynamic subcellular structures and constantly adapt to accommodate their cellular environment (325). For example, mitochondrial volume density in human skeletal muscle, percent volume of the muscle fiber taken up by mitochondria, is approximately 5% but can range from 3 to 7% (76, 119, 295).

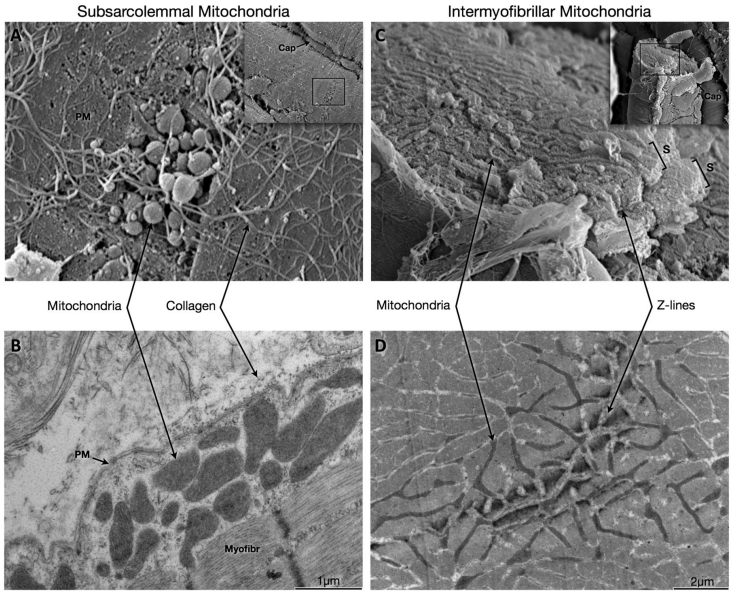

Figure 3. Skeletal muscle mitochondria. Figure from reference (233). Subsarcolemmal and intermyofibrillar mitochondrial morphology using scanning electron microscopy (EM) (A, B) and transmission EM (B,D) of a freeze-fractured intact mouse soleus sample. PM – plasma membrane; Myofibr – myofibrils; S – sarcomeres; Cap – capillary. Scanning electron microscopy (SEM) images were captured at magnifications of ×10,300 (A) and ×1,140 (A, inset), and ×5,800 (B) and ×1,310 (C, inset).

Structural and morphological mitochondrial adaptations include alterations in size (fission/fusion) or a change in number (mitochondrial biogenesis). Mitochondrial fusion increases or improves reticular interconnectivity network by the amalgamation mitochondrial plasma membranes from two previously separate organelles (185). This usually occurs in response to cellular stress and metabolic demand (325). Mitochondrial fission involves the replication of mtDNA and division of the organelle, creating new mitochondria. This process is essential for adequate

mitochondrial population within a given cell (325). Mitochondrial biogenesis is the concerted process of creating mitochondria *de novo* through the coordinated upregulation of mitochondrial and nuclear transcription, translation, and assembly of mitochondrial proteins (317). This also occurs in response to a cellular metabolic stress (325). Mitochondria are even capable of moving throughout some cells, such as has been observed in hepatocytes, as they respond to their cellular environment (146). Alternatively mitochondria can also be anchored to a location by the cellular cytoskeleton to help maintain energy provision to an area with consistently high local metabolic demand. This occurs in cardiomyocytes, where mitochondria are anchored in close proximity to the contractile elements of the muscle (320) and also in sperm where they are woven around the motile flagellum (40). The regulation of mitochondrial morphology is extremely complex and still highly studied. This is important, as mitochondrial function is highly dependent upon its structure.

Mitochondrial structure

Mitochondria are composed of two separate and very different plasma membranes. The mitochondrial outer membrane (MOM) is a semi-permeable phospholipid bilayer that separates the cellular cytosol from the mitochondrial intermembrane space (MIS). This outer membrane encompasses the entirety of the organelle. The MOM is rich in transmembrane proteins called porins, which facilitate the passive diffusion of molecules across plasma membranes. This allows the MOM to be rather permeable to molecules up to approximately 4 kDa that lack a net charge and strong dipoles (20, 50), however it remains impermeable to larger molecules, such as cytochrome c (19). Accordingly, MIS functions near chemical equilibrium with the cytosol in respect to small molecules. The mitochondrial inner membrane (MIM) is an impermeable phospholipid bilayer that separates the MIS and the mitochondrial matrix (MM). This membrane ribbons back and forth, folding over itself creating invaginations, or mitochondrial cristae, which creates a large surface area. The impermeability of the MIM is fundamental to mammalian bioenergetics and thus all ions and molecules require a transport protein in order to transverse the MIM. Found within the MIM are a series of membrane bound proteins that are collectively referred to as the electron transport system. This system is ultimately responsible for transferring electrons to O_2 while transforming unusable chemical energy into biologically viable sources. A

portion of the sequential disassembly of chemical sources ultimately used for energetic transduction occurs in the MM. The MM is the space within the organelle that is enclosed by the MIM. The mitochondrial matrix possesses hundreds of enzymes, including all those involved in the tricarboxylic acid (TCA) cycle, fatty acid metabolism, or β-oxidation, protein metabolism, and many more. The MM also contains the mitochondrial genome.

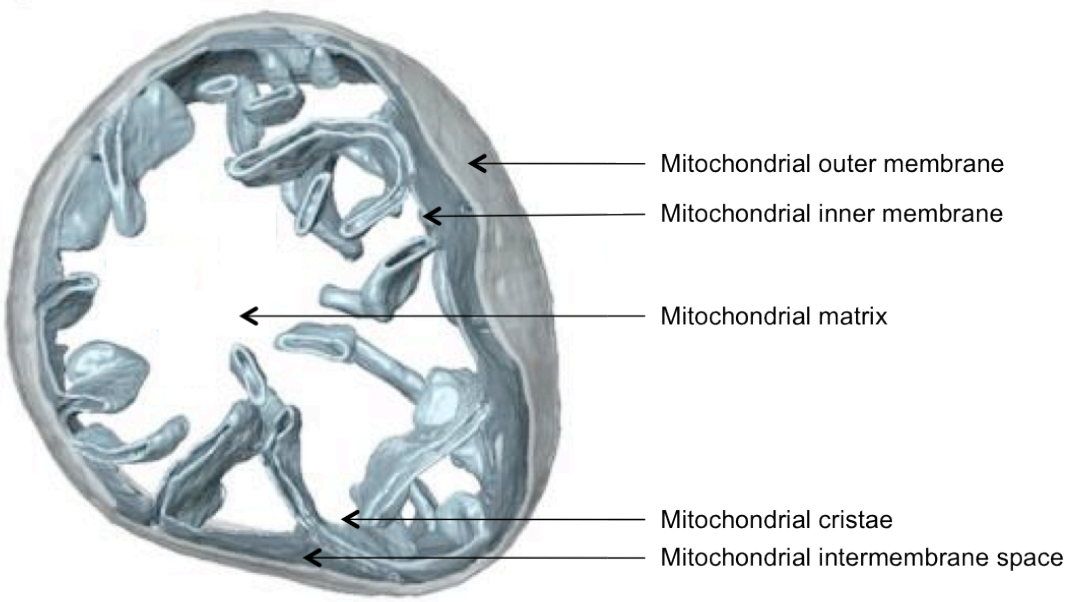

Figure 4. Depiction of a mitochondrion from the transverse plane. Adapted from reference (54).

Gene expression

Mitochondria possess their own genetic material separate from the nucleus, making them unique from other cellular organelles (258). This genetic material is referred to as mitochondrial DNA (mtDNA). Opposed to the more common α-helical structure of nuclear DNA (nDNA), mtDNA is a closed 16.6 kb circular double-stranded molecule (6, 306). Mammalian mtDNA is maternally inherited, which is also disparate from nDNA (141, 268). While the bacterial ancestors to the mitochondrion expressed a complete genome that encoded for all genes necessary to sustain autonomous and independent life, mitochondria are genetically semiautonomous. Mitochondria rely greatly on nuclear expression within their host as mtDNA have only retained the genes that encode for 2 rRNA, 22 tRNA, and 13 mRNA that are essential for mitochondrial protein synthesis, specifically 13 polypeptides that are involved in oxidative phosphorylation. These 13 polypeptides are translated on mitochondrial

ribosomes and serve as structural subunits for mitochondrial complexes involved in the electron transport system, including mitochondrial respiratory complexes I, III, IV, and V (258). The additional ~1500 genes specific to the mitochondrial genome are expressed throughout nDNA. These mitochondrial proteins that are encoded in nDNA are incorporated into the mitochondria via selective importation following extramitochondrial translation via cytosolic ribosomes (91). Mitochondrial respiratory complex II, for example, is entirely encoded for by nDNA and transported into the mitochondria after translation via cytosolic ribosomes. Mitochondria proteins specific for the organelle typically undergo posttranslational modification once in the mitochondria prior to incorporation as a functional unit (302). Therefore the mitochondrion is entirely symbiotic, relying on both mt and nDNA for complete expression and function.

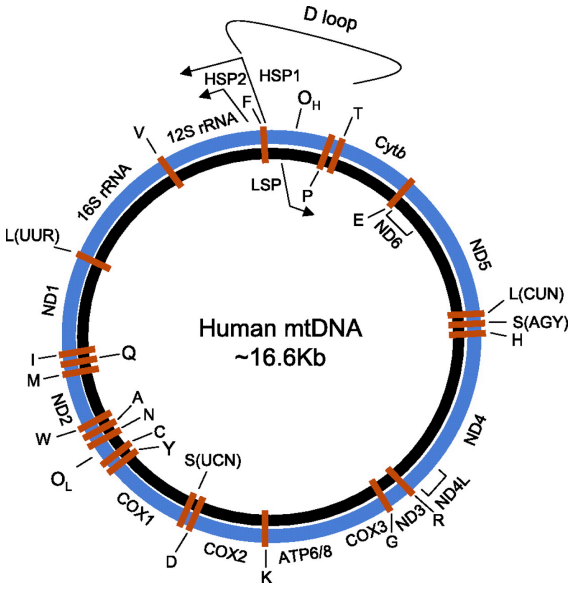

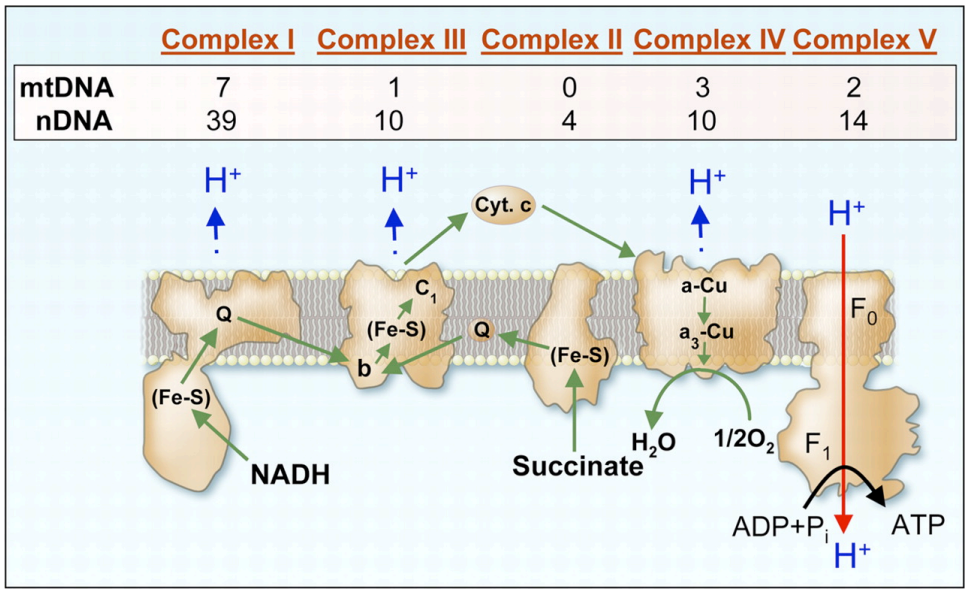

Figure 5. Mitochondrial genetic expression. Illustration of mitochondrial (mt) DNA (top) and an illustration of the electron transport system with the location of their expression (bottom). nDNA – nuclear DNA. Both figures are from reference (258).

Mitochondrial function

The term “mitochondrial function” serves as a general umbrella term in reference to several processes, as the mitochondria are intimately involved in many different cellular functions. Mitochondrial functions in cellular calcium regulation/signaling (6), inflammatory responses (151), redox signaling (31, 63), nitrogen metabolism (237), heme biosynthesis (178), and apoptosis (208) among others. The primary function of the mitochondrion, however, is to harness biologically inaccessible energy into viable sources providing the foundation of aerobic metabolism establishing life as we know it. Therefore, throughout this dissertation the term mitochondrial function specifically refers to the bioenergetic capabilities of the mitochondria.

Chemical sources of biological energy

All life requires a source of energy to survive. The energy source for life on earth ultimately comes from the sun. Mammals obtain this energy via indirect means through chemical sources in the form of nutrients including carbohydrates, fats/lipids, and proteins. The energy in these nutrients is stored within their chemical bonds. Accordingly there are necessary processes that systematically break down and transform this chemical form of energy from nutrients into biologically usable sources. This energy is used to maintain metabolic function and overall homeostasis in organisms. Most of these pathways involve the mitochondria either directly or indirectly and are discussed below.

Glycolysis

Glucose is the predominant carbohydrate metabolized by mammals for energetic means. The metabolism of glucose begins outside of the mitochondria in the cytosol by means of glycolysis. Overall, glycolysis involves the metabolism of 1 molecule of D-glucose to form 2 molecules of pyruvate, which also nets 2 molecules of adenosine-5'-triphosphate (ATP) and 2 reduced nicotinamide adenine dinucleotides (NADH) in the process. When one molecule of glucose ($C_6H_{12}O_6$) is completely metabolized (aerobically, + $6O_2$) to $6CO_2$ + $6H_2O$, there is approximately 2937 kJ/mol of energy released. The complete hydrolysis of ATP to AMP releases about 50 kJ/mol under physiologic conditions. Thus the energetic efficiency of glycolysis alone is roughly 3.4%. Though glycolysis is capable of capturing some chemical energy

into biologically useable ATP through substrate-level phosphorylation (phosphorylation of ADP to ATP at the expense – oxidation – of the substrate), this process is incredibly inefficient and could not support a long-term, high metabolic demand. Some of the energy stored in the chemical bonds of glucose is lost as heat during glycolysis, however a significant amount of chemical energy remains in the bonds of the pyruvate molecules and the reduced coenzymes, NADH. To harness the remaining energy from pyruvate and NADH, these molecules are transferred into the mitochondrial matrix where they are fully metabolized and ultimately account for approximately 30 additional molecules of ATP, improving efficiency of energy transfer from glucose metabolism by 51% over glycolysis alone!

It quickly becomes obvious that glycolysis did not persist throughout evolution as a result of its energetic efficiency. The benefit of this process is the rate at which glycogen and/or glucose can be broken down and partially metabolized, which functions about 100 times faster than the complete aerobic metabolism of glucose. For example, approximately 32 ATP are gained through the complete aerobic metabolism of a single molecule of glucose. Theoretically, if 100 molecules of glucose could be aerobically metabolized in one minute then the net gain in ATP would be about 3,200. In that same amount of time glycolosis, netting just 2 ATP per molecule of glucose, could produce approximately 20,000 ATP but at the expense of glucose expenditure (10,000 molecules!). This sacrifice of metabolic brevity over efficiency with glycolysis comes at the expense of accumulating metabolic by-products. Also, cytosolic redox balance becomes severely challenged during times of high metabolic demand with an increasing NADH to NAD ratio as glycolysis functions at a rate far beyond the capacity of mitochondria. If left alone this unequal distribution of reduced coenzymes will inhibit glycolysis and potentially threaten life with metabolic arrest. During the periods of high glycolytic flux, such as intense exercise like sprinting, an additional pathway is necessary in order to maintain cytosolic redox balance. This is partially achieved by converting pyruvate into lactate via lactate dehydrogenase (LDH), which oxidizes NADH back to NAD^+ in the process. There are several fates then for lactate. One of the greatest debates in regards to lactate metabolism is whether it can then be taken up and oxidized by the mitochondria itself, similar to pyruvate. This specific question is tested and presented later an accompanied manuscript entitled *Lactate oxidation in human skeletal muscle mitochondria*. For this

to occur pyruvate is shuttled into the mitochondria and decarboxylated into acetyl-CoA via pyruvate dehydrogenase, also forming NADH. It is then in the mitochondria that acetyl-CoA then enters the TCA cycle.

The tricarboxylic acid (TCA) cycle

Mitochondria generate biologically accessible energy by oxidizing carbohydrate and lipid metabolites alike (Lehninger AL. The Mitochondrion. New York: Benjamin, 1965). In this process metabolites of both carbohydrates and lipids must first transverse the TCA cycle in the mitochondrial matrix. The first step in the TCA cycle is the formation of citrate and coenzyme A (CoA)-SH through the condensation of acetyl-CoA and oxaloacetate. Acetyl-CoA is primarily produced via glycolysis in the case of carbohydrates, which was previously discussed, or from β-oxidation during lipid metabolism, which will be discussed in the next section. This exergonic reaction is catalyzed by citrate synthase (CS) and is irreversible. Feedback inhibition is necessary to limit this reaction, as NADH and succinyl-CoA, both by products of the TCA cycle, allosterically inhibit CS. Next in the TCA cycle is the isomerization of citrate into isocitrate. This step is catalyzed by aconitase. This reaction occurs near equilibrium. The facilitated shift of the hydroxyl group changes a tertiary alcohol of which is very difficult to oxidize, citrate, into a secondary alcohol that is much easier to further oxidize, isocitrate. Accordingly, isocitrate dehydrogenase then catalyzes the oxidation of isocitrate to oxalosuccinate and NADH, which then spontaneously decarboxylates to form α-ketoglutarate and CO_2. This is another exergonic and irreversible reaction, allosterically activated by ADP and inhibited by both NADH and ATP. Then there is another oxidative decarboxylation reaction that occurs with α-ketoglutarate being converted to succinyl-CoA, CO_2 and NADH. Similar to the previous reaction, this is highly exergonic and irreversible. Succinyl-CoA synthetase then converts succinyl-CoA to succinate. This highly exergonic reaction is coupled to the endergonic substrate level phosphorylation of guanosine-5'-diphosphate (GDP) and inorganic phosphate into a high-energy phosphate, GTP. This GTP is later converted to the more common energetic cellular currency, ATP. Succinate dehydrogenase then oxidizes succinate to form fumarate and reduce flavin adenine dinucleotide ($FADH_2$). This is also an exergonic reaction, however the energy released is not sufficient to reduce NAD and thus FAD serves as the electron acceptor

in the reaction. Succinate dehydrogenase is the only membrane bound protein in the TCA cycle, as all other enzymes involved in the TCA cycle are soluble. Succinate dehydrogenase also serves as a respiratory complex II in the electron transport system. The role of succinate dehydrogenase in the electron transport system will be discussed later in greater detail. Fumerate is then hydrated to form malate via fumarase. Finally, the last step in the TCA cycle is the oxidation of malate back to oxaloacetate, also reducing NAD^+ to NADH. In all, the TCA cycle alone only accounts for the production of two ATP via substrate level phosphorylation, however there is still the energy that was transferred into the reduced coenzymes produced, NADH and $FADH_2$. These coenzymes are then shuttled into the electron transport system.

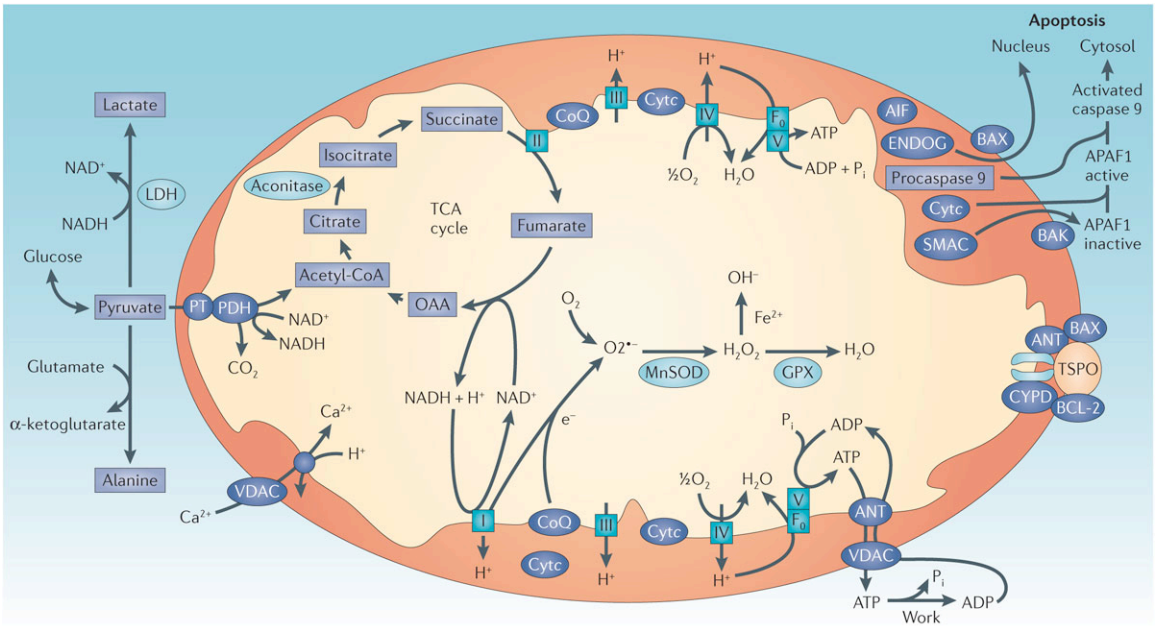

Figure 6. The tricarboxylic acid (TCA) cycle and mitochondrial function. A summary of the TCA cycle in the mitochondrial matrix, which demonstrates its integration with other mitochondrial functions. This graph is from reference (303).

Amino acids can also be metabolized for energetic means through the TCA cycle, however under normal conditions their contribution to total energy transduction is low respective to carbohydrates and lipids. A more significant contribution of amino acids to aerobic metabolism include their role in the anaplerotic reactions that help maintain the necessary concentration of TCA cycle intermediates. A significant amount of amino acids, specifically the branched-chain amino acids, can be metabolized during

times of extreme metabolic stress such as starvation, however this is transient and progressively shifts primarily to fat oxidation (38, 39, 236).

β-oxidation

Fat is the most energetically rich and abundant nutrient for mammals, with a large capacity for fat storage. In addition to their favorable energetic abundance, lipids are hydrophobic molecules, ergo they are stored without water (non hydrated), as is the case with glucose when stored as glycogen. Fatty acids are stored as triacylglycerols primarily in adipocytes however various tissues also are capable of limited fat storage. The metabolism of fatty acids for energy primarily occurs in the mitochondria. Short chain fatty acids are directly transported into the mitochondria for oxidation whereas long chained fatty acids require activation prior to their entry. This is done by acyl-CoA sythetase located on the MOM (250). The activated acyl-CoA requires specific transport into the mitochondrial matrix. This is done in a series of steps. First, the acyl group is transferred from CoA to the hydroxyl group of carnitine via carnitine acyltransferase I, which is bound to the MOM forming acyl-carnitine. Acyl-carnitine is transported across the MIM, where in the matrix it is converted back to acyl-CoA via carnitine acyltransferase II returning carnitine to the MIS.

In the mitochondrial matrix the fatty acyl-CoA molecules are broken down through an enzymatic process referred to as β-oxidation. The first reaction is catalyzed by the enzyme acyl-CoA dehydrogenase, which has a FAD prosthetic group that is reduced during the metabolism of the fatty acid molecule. The now reduced $FADH_2$ then transfers its electrons to a flavoprotein known as electron transfer flavoprotein (ETF). ETF reoxidizes by transferring electrons to an oxidoreductase that directly transports the electrons to coenzyme Q_{10} (CoQ, also known as ubiquinone) of the electron transport system, discussed later in more detail. The next step in β-oxidation is the hydration of the fatty acid moiety by enoyl-CoA hydratase, converting transenoyl-CoA into L-β-hydroxyacyl-CoA. L-hydroxyacyl-CoA dehydrogenase then oxidizes L-β-hydroxyacyl-CoA to β-ketoacyl-CoA, reducing NAD^+ to NADH. This reducing agent is then transported to mitochondrial respiratory complex I of the electron transport system. In the final step of β-oxidation, thiolase ultimately catalyzes the formation of acetyl-CoA and an acyl-CoA molecule that is 2 carbons shorter. This

cycle is repeated until the fatty acid has been completely broken down into acetyl CoA molecules. The acetyl-CoA produced from β-oxidation is then transported into the TCA cycle as discussed previously.

Up to this point in the discussion only 3 molecules of ATP have been formed through one cycle of glycolysis and the TCA cycle. Activation of fatty acids in order to enter the mitochondrion requires energy, so with one round of β-oxidation included there has only been one net ATP produced. There are several reduced coenzymes that have also been produced as well. These reducing agents are then transported to the electron transport system. The mitochondrial electron transport system serves as the bioenergetic hub of aerobic metabolism. The analysis and study of respiratory control and efficiency involves the examination of the electron transport system directly.

Oxidative phosphorylation

Uncovering the science behind cellular respiration, and explaining oxidative phosphorylation through Peter Mitchell's chemiosmotic theory (199) not only led to a Nobel Prize in Chemistry in 1978 but easily serves as one of the most important biological findings of the past century. Our understanding of mitochondrial respiration is now much more complete however much remains unknown in regards to mitochondrial respiration. The fundamental force facilitating oxidative phosphorylation is the proton motive force (pmf) that is developed from the active traslocation of protons across the MIM into the MIS via a system of enzymes that couples this translocation with a systemic transfer of electrons. The pmf describes the electrochemical gradient across the MIM composed of both a chemical gradient and an electrical gradient. This gradient is established by a selective set of enzymes associated with the MIM referred to as the electron transport system.

The electron transport system

The electron transport system is a collection of mitochondrial enzymes located either within or attached to the MIM. These enzymes serve as electrogenic proton pumps and oxidizing agents that reduce products (NADH and $FADH_2$) of the TCA cycle and β-oxidation. This occurs through a systematic transfer of electrons down a gradient while simultaneously pumping protons into the MIS, creating an electrochemical

gradient across the MIM. This electrochemical potential is often referred to as mitochondrial membrane potential. The mitochondrial membrane potential that develops across the MIM facilitates the conduction of energy into the phosphate bonds of ATP (199). Each enzyme of the electron transport system plays a specific role in the final step of aerobic metabolism. Electron input occurs from four sources: 1.) NADH transmitted through mitochondrial respiratory complex I; 2.) TCA cycle specific $FADH_2$ through mitochondrial respiratory complex II; 3.) electron transfer from the metabolism of fatty acids through β-oxidation through the electron-transferring-flavoprotein (ETF) dehydrogenase (flavoprotein–ubiquinone oxidoreductase); and 4.) electrons transferred from glycerophosphate dehydrogenase to CoQ that originated from cytosolic NADH via the glycerophosphate shuttle. (321).

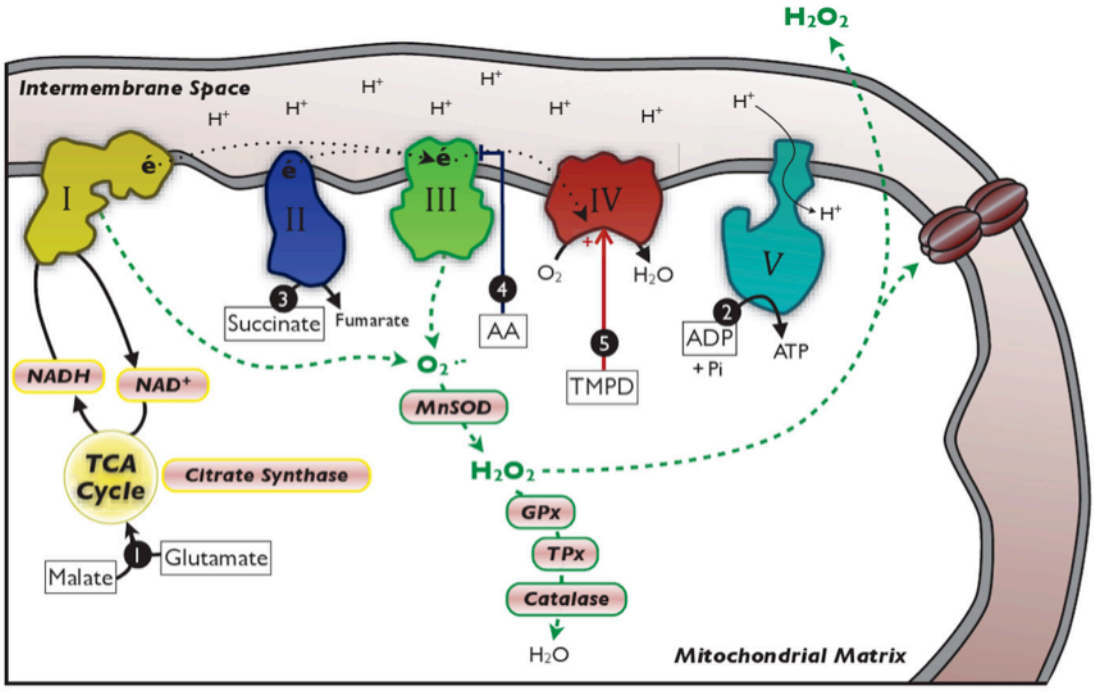

Figure 7. Electron transport system. Electron transport chain complexes I to V; NAD^+ – nicotinamide adenine nucleotide; NADH – reduced NAD^+; TCA – tricarboxilic acid cycle; MnSOD – manganese superoxide dismutase; GPx – glutathione peroxidase; TPx – thioredoxin peroxidase; AA – antimycin A; and TMPD – N,N,N′,N′-tetramethyl-p-phenylenediamine. Modified from reference (232).

1.1 Mitochondrial respiratory complex I (CI) – NADH dehydrogenase

Mitochondrial respiratory complex I (CI) is the largest and most complicated enzyme of the respiratory system. It is composed of 14 central units (310) and 32 accessory subunits (41, 74, 111), making it one of the largest membrane-bound proteins in general, with the size of about 1,000 kDa. Seven of the 46 polypeptides that compose CI are genetically encoded in the mtDNA (302). There are two primary sections of CI

that give it an L-shaped appearance, a hydrophobic membrane-bound arm of the protein and a hydrophilic peripheral arm, which extends into the mitochondrial matrix (28, 256, 257). The specific mechanisms by which CI functions and the roles of all accessory subunits remain largely unknown (28, 68). In general there are three primary functions of CI: i.) electron attainment and subsequent oxidation of NADH; ii.) electron release to CoQ; and iii.) the translocation of protons across the MIM. First, NADH binds (44) and transfers its electrons to the flavin mononucleotide (FMN) prosthetic group, similar to FAD, creating $FMNH_2$ (245). $FMNH_2$ delivers a single electron (in a two-to-one conversion) onto an iron-sulfur cluster binding motif (104, 216), which is then shuttled from one set of iron-sulfur clusters to another before finally being transferred to CoQ (57, 104, 216). The FMN and up to 8 or 9 iron-sulfur clusters exist in the peripheral arm of CI (104) while the membrane-bound arm contains the proton-pumping structures (256, 257). For every $2e^-$ transferred through CI, there is a reciprocal 4 H^+ pumped across the MIM into the MIS (79, 80). The mechanism linking these two phenomena are not clear but evidence suggests that there is an indirect redox-dependent conformational change that occurs in the membrane-bound arm of CI facilitating the translocation of protons (17, 29, 66).

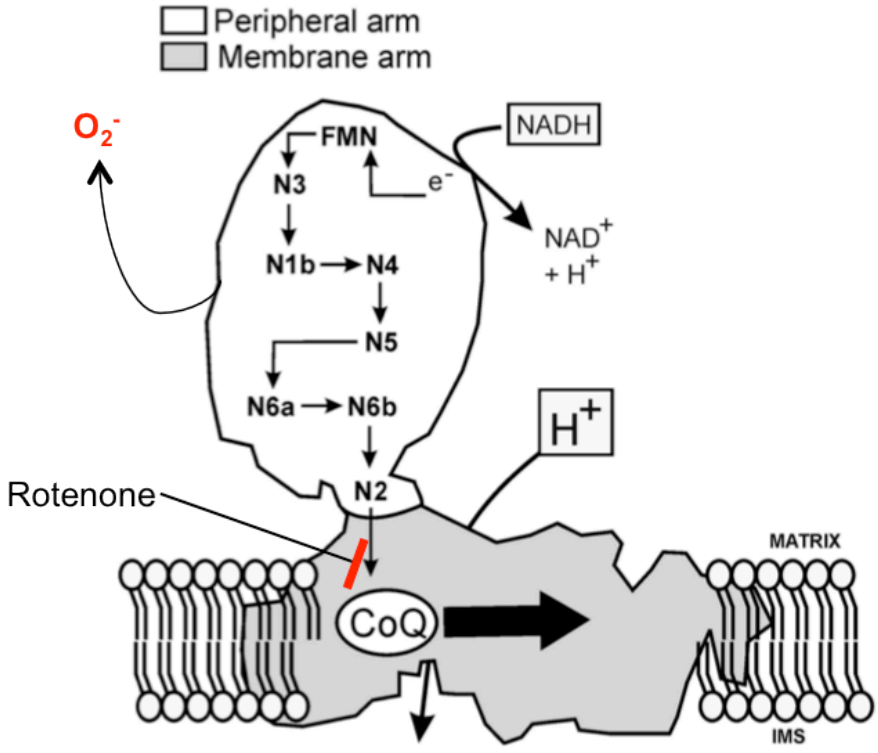

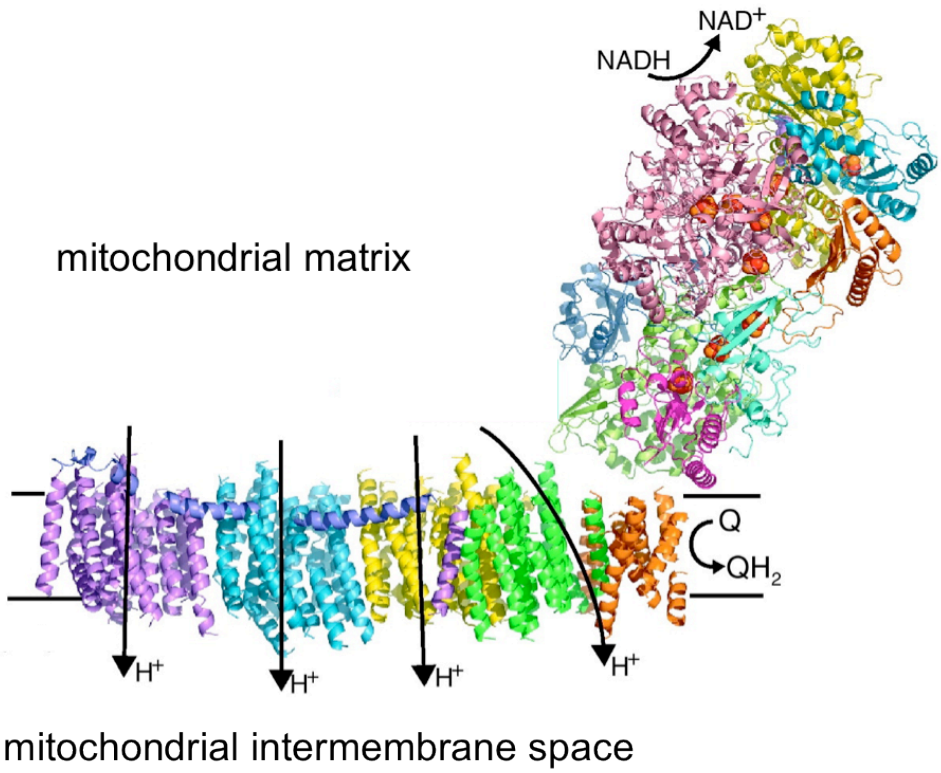

Figure 8. Mitochondrial respiratory complex I (CI) – NADH dehydrogenase. Illustrations depicting CI. IMS - intermembrane space; O_2^- - superoxide dismutase; N – iron-sulfur clusters; CoQ and Q – coenzyme Q. Modified from references (68, 155).

The impermeability of the MIM is not perfect and sometimes electrons slip from their molecular transfer cascade or protons leak across the MIM back into the matrix. The uncontrolled leak of electrons from coenzymes or prosthetic groups of the electron transport system then reacts with O_2 to form reactive oxygen species (ROS). Mitochondria are a primary site of ROS production. The progression of ROS production beyond hormetic concentrations precipitates deleterious and indiscriminate oxidation of nucleic acids, proteins, and lipids (128, 272, 285). Mitochondrial-derived ROS are largely accounted for by superoxide (O_2^-) production into the mitochondrial matrix at mitochondrial complex I (CI) (161, 162, 287) and into both the matrix and mitochondrial intermembrane space at mitochondrial complex III (CIII) (43, 96, 99, 205, 286, 323). There are three different conditions in which CI is postulated to produce ROS: 1.) During conditions where the respiratory system is blocked downstream from CI and electrons become congested in the iron-sulfur clusters (65, 78); 2.) reduced FMN reacts with O_2 dependent on the ratio of NADH/NAD^+ (110); and 3.) during reverse electron transfer (RET) as electrons flow back to CI from CoQ

via mitochondrial complex II (95, 298). A high mitochondrial membrane potential is necessary for the latter to occur (64, 298).

In summary, mitochondrial CI oxidizes NADH, transfers the associated electrons down the electron transport system to CoQ, and reciprocally pumps the coupled H^+ ions across the MIM (330). Mitochondrial CI is also one of the principal contributors to mitochondrially-derives ROS. As NADH serves as a substrate for CI, rotenone is a common inhibitor. It works as an antagonist for the reduction of CoQ by inhibiting the transfer of electrons from the iron-sulfur clusters to CoQ (28). All the actions of CI work in parallel oppose to linearly with those of mitochondrial complex II during oxidative phosphorylation.

1.2 Mitochondrial respiratory complex II (CII) – Succinate dehydrogenase

Mitochondrial respiratory complex II (CII) is the smallest respiratory complex in the electron transport system at approximately 120 kDa and is completely nDNA-encoded (302). In most mammals, CII is composed of four polypeptide subunits, all encoded for by nDNA (248, 276, 302). Additionally it contains 5 prosthetic groups: one covalently linked FAD, a b-type heme, and three iron-sulfur clusters (281). The series of redox centers are arranged so that there is limited ROS formation at CII, accounting for approximately 0.1–0.2% total ROS formation (238, 321). CII is the only enzyme that participates directly in both the TCA cycle and the electron transport system.

In the TCA cycle CII catalyzes succinate to fumarate, reducing FAD^+, and in the respiratory system it transfers the electrons gained from reducing equivalents ($FADH_2$) first to a iron-sulfur cluster and then onto CoQ (165). Two of its larger subunits out of the four and one of the three iron-sulfur clusters catalyze the transfer of electrons from succinate to an electron acceptor (165, 184). Unlike mitochondrial complexes I, III, and IV, the enzymatic activity of CII is not coupled with the pumping of protons across the MIM (61). While this is the only respiratory complex with no portion of the enzyme within the MIM, CII is anchored to the inner membrane by two subunits (217).

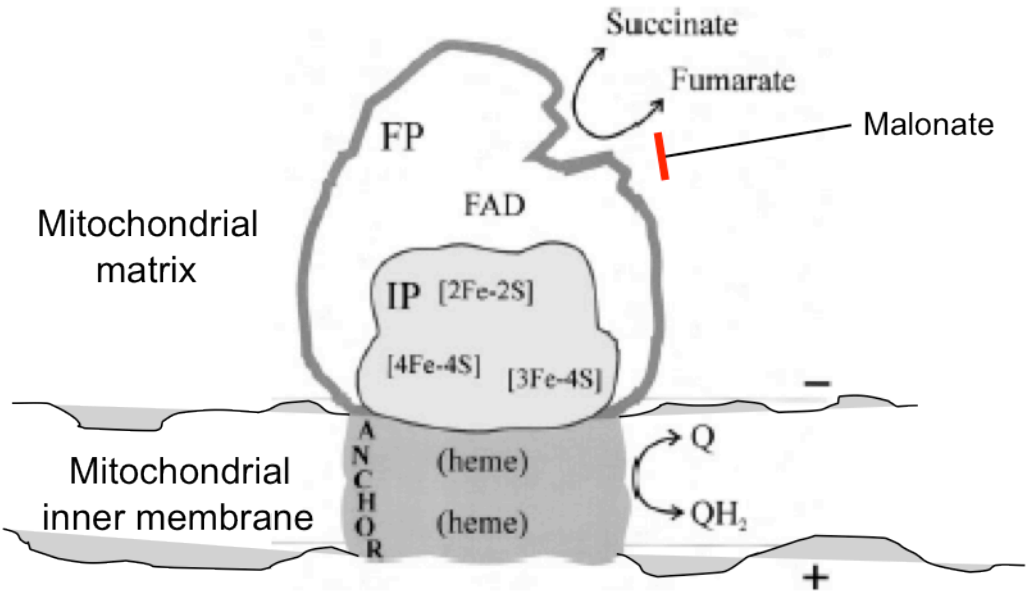

Figure 9. Mitochondrial respiratory complex II (CII) – Succinate dehydrogenase. Q – coenzyme Q; FP – flavoprotein; IP – iron protein. Modified from reference (97).

In summary, mitochondrial complex II transfers electrons from $FADH_2$ to mitochondrial complex III via CoQ. Substrates for CII include flavin based redox cofactors, specifically those reduced in the reaction catalyzed by succinate dehydrogenase during the TCA cycle. The flavin based reducing agents specific to β-oxidation are often mistakenly referred as CII substrates (157, 167, 168, 170), however their electrons are transferred through the electron transfer flavoprotein (ETF) discussed above, during β-oxidation. Malonate and oxaloacetate are competitive inhibitor of CII (97). Malonate serves as a CII competitive inhibitor as it binds to the same catalytic site as succinate (235).

1.3 Mitochondrial respiratory complex III (CIII) – Cytochrome bc_1 complex

A dissolved pool of CoQ molecules in the MIM function to transport electrons from CI and CII to mitochondrial respiratory complex III (CIII) (18, 172, 173). CIII is a 248 kDa enzyme consisting of 11 polypeptide subunits and four prosthetic groups (259). All four points of entry into the electron transport system (CI, CII, ETF, and glycerophosphate shuttle) converge at CIII. In addition to CoQ, the essential redox components of CIII are three heme components, two b-type hemes and one c-type (bL, bH, and c1, respectively), one high potential iron-sulfur cluster, and cytochrome c (318). Cytochrome b is the one of 11 polypeptides that is mtDNA-encoded in CIII

(302). The role of CIII in electron transport is to transfer the electrons received from CoQ to a soluble cytochrome c. This transfer of electrons is coupled to the concomitant translocation of two H^+ across the MIM for every CoQ oxidized (109, 200, 201, 282).

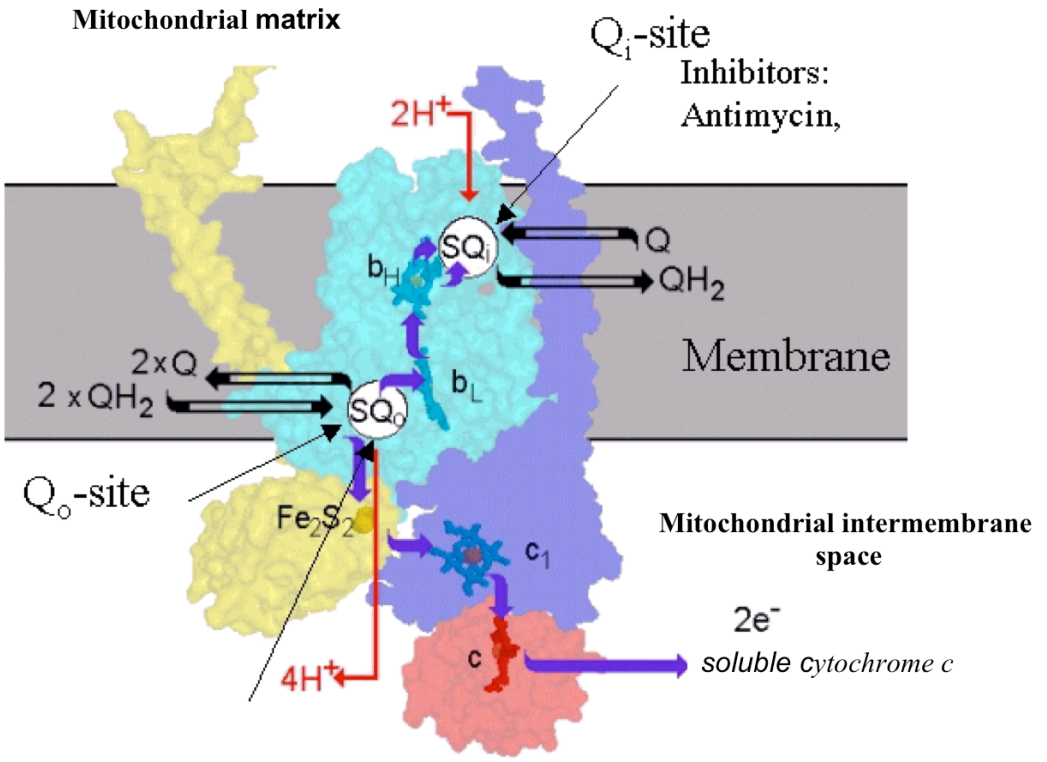

Figure 10. Mitochondrial respiratory complex III (CIII) – cytochrome bc_1 complex. Red arrows show the translocation of protons across the mitochondrial inner membrane and the purple arrows show the pathway of electron transport. Q_i-site – catalytic site on the negative side of the mitochondrial inner membrane; Q_o-site – catalytic site on the positive side of the mitochondrial inner membrane; Q and QH_2 – oxidized and reduced coenzyme Q, respectively. Modified from references (318, 328)

The mechanism that connects the translocation of protons with the transfer of electrons within CIII is the proton-motive Q cycle (201). While the mechanistic specifics involved in the proton-motive Q cycle are still being discussed, the most general and widely accepted model involves the bifurcated flow of electrons through CIII (200, 282). There are two CoQ binding sites on CIII: one specific for CoQ oxidation (Qp or Q_o on the positive side or MIS of the enzyme) and the other for CoQ reduction (Qn or Q_i located on the negative side or matrix side of the enzyme) (82, 329). During the proton-motive Q cycle, a fully reduced CoQ (ubiquinol) binds to Q_o and is sequentially oxidized. One of these electrons is transferred to cytochrome c via the iron-sulfur cluster and cytochrome c1 prosthetic groups. The other electron is transferred directly to the bL and then bH heme groups before partially reducing CoQ

(ubiquinone) bound to the Q_i site. The CoQ at the Q_i site is only partially reduced (semiquinone). Thus another Q cycle is necessary for the CoQ in the Q_i site to become fully reduced, and a total of 4 H+ (2 per cycle) are translocated across the MIM into the MIS (53, 58, 200, 201, 218, 244, 282).

Although the process is exceptionally efficient overall, the two catalytic sites facilitating the same reaction in opposing directions (oxido-reduction of CoQ) leads to the potential for electron build-up and potential backflow allowing oxygen serve as an oxygen donor, producing superoxide ($O_2^{\bullet-}$) (53, 277) $O_2^{\bullet-}$ can be generated at two different sites, Q_O and Q_i, within complex III. The two catalytic site result in two points of ROS production. The Q_O site on the positive side of the enzyme releases $O_2^{\bullet-}$ into the MIS, whereas Q_i associated ROS production is released into the mitochondrial matrix (43, 96, 99, 205, 286, 323). Most of the $O_2^{\bullet-}$ generated by complex III, however, is generated at the Q_O catalytic center (26).

In summary, mitochondrial complex III is responsible for catalyzing the transfer of electrons from a fully reduced CoQ to cytochrome c. This transfer of electrons is coupled to the translocation of protons across the MIM from the matrix the MIS at a ratio of $4H^+$ per $2e^-$. Accordingly mitochondrial complex III assists in developing the electrochemical proton gradient that ultimately drives energy transduction. The transfer of electrons, while efficient, is not perfect and serves as a primary source of ROS production in the mitochondria. While technically CoQ serves as the substrate for CIII, durohydroquinone (duroquinol oxidase, DHQ) can serve as an artificial electron donor for CIII for analysis of electron transport from CIII to mitochondrial complex IV (100, 174, 246, 308). Antimycin A is an inhibitor of CIII as it binds to the Q_i catalytic site of the enzyme rendering it incapacitated (82).

1.4 Mitochondrial complex IV (CIV) – Cytochrome c oxidase

Mitochondrial complex IV (CIV; cytochrome c oxidase) is a large transmembrane protein (200 kDa) that serves as the terminal electron-accepting enzyme in the respiratory system and is responsible for approximately 95% of all oxygen metabolism in mammals (189, 283). Thirteen subunits collectively represent CIV with 3 of those 13 encoded by mtDNA, subunits I-III (9, 284, 302).

In general, CIV transfers electrons from cytochrome c to naturally unstable O_2, forming metabolic H_2O (292). The reduction of O_2 by CIV is also linked with the translocation of protons across the MIM, further developing the proton motive force across the inner membrane (23, 315). This occurs at a ratio of $4e^-$ to $2H_2O$ and $2H^+$ (193). All redox centers in CIV are located on just 2 of the 13 subunits; subunits I and II (9). Accordingly these two subunits are responsible for the entirety of the protein's energy transduction as the rest are involved in enzyme regulation (107). Electrons are transferred from soluble cytochrome c to the copper A (Cu_A) center of subunit two. The electrons are then transferred to heme a and onto the binuclear center consisting of heme a_3 and copper B (Cu_B), all located on subunit one. The binuclear center is where O_2 is reduced to H_2O (127, 283, 284). The catalytic cycle of CIV can be divided into 2 parts, the oxidative and the reductive phases (292). In the oxidative phase the enzyme is reduced, which consists of the heme and copper centers all possessing electrons with four in total. The heme a_3-Cu_B center on subunit II then interacts with the bound O_2, reducing it to H_2O (9). All redox centers are then re-reduced by cytochrome c during the reductive phase prior to the binding of the next O_2 (292).

The evolutionary dominance of O_2 metabolism by CIV most likely occurred as a result of the chemical difficulty of executing the complete reaction with the effective and efficient success that CIV achieves (189). Despite the high traffic of electron transport and close proximity to O_2, CIV is not considered a primary site of ROS production (26). Endogenously, reduced cytochrome c serves as the primary CIV substrate however non-biological substances such as N,N,N′,N′-tetramethyl-p-phenylenediamine dihydrochloride (TMPD) can also serve as electron donors to CIV for analysis. For example, respiratory rates following inhibition of respiratory complexes upstream of CIV allows for assessment of CIV activity with TMPD serving as the electron donor to cytochrome c and ascorbate maintaining TMPD in the reduced state (89). The binuclear catalytic center of CIV is inhibited by cyanide (209, 214, 316), which blocks O_2 binding and respiration (229). The transport of electrons across the MIM at CIV is the final step along the respiratory chain that builds the proton motive force of which is used for energy transduction at ATP synthase.

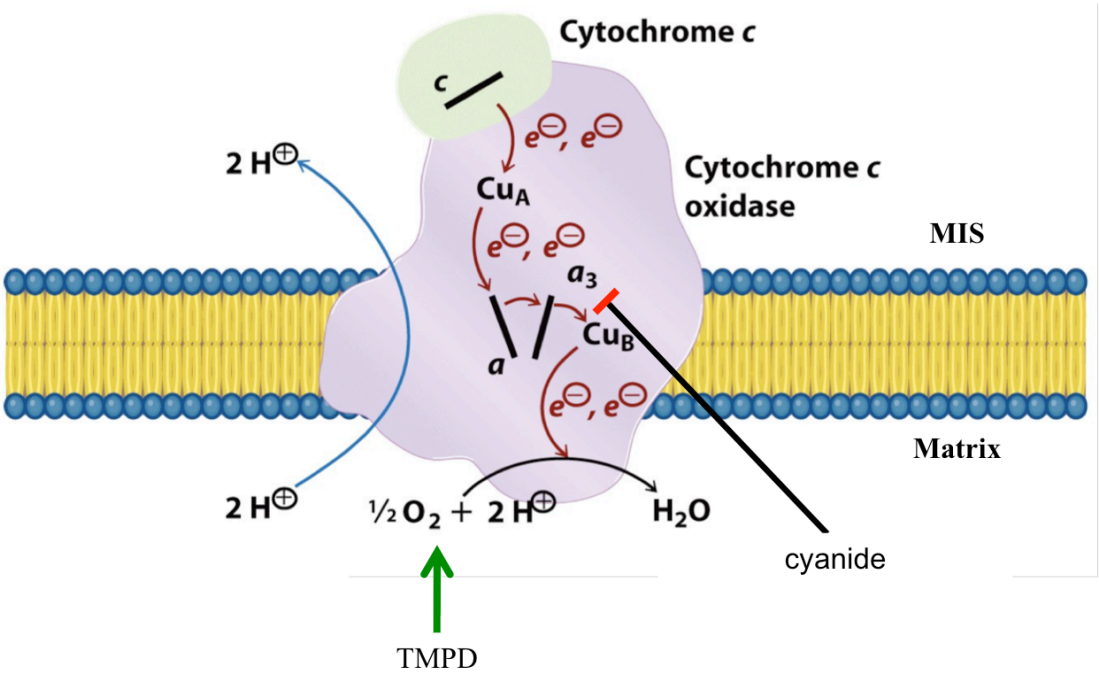

Figure 11. Mitochondrial respiratory complex IV (CIV) – Cytochrome c oxidase. The Blue arrow shows the translocation of protons across the mitochondrial inner membrane and the red arrows show the pathway of electron transport. MIS – mitochondrial intermembrane space; TMPD – N,N,N′,N′-tetramethyl-p-phenylenediamine dihydrochloride. Modified from reference (123).

1.5 Mitochondrial complex V (CV) – ATP synthase

The ability to harness and utilize energy is a requisite of life. The most fundamental molecule in mammalian bioenergetics is ATP. The average person synthesizes his/her body weight in ATP per day (25). Mitochondrial respiratory complex V (CV, ATP synthase) is the enzyme responsible for the majority of this ATP synthesis, excluding that obtained from substrate level phosphorylation. The characteristic folds of the mitochondrial cristae have been observed via electron tomography to possess high concentrations of CV dimers (55, 275).

The fifth mitochondrial respiratory complex, with a mass of ~600 kDa (10), is a bipartite molecule consisting of an embedded membrane domain (F_0) involved in proton translocation and a peripheral catalytic domain (F_1) that extends into the mitochondrial matrix (265). This enzyme, which can also function as an ATPase, is collectively comprised of, including the regulatory subunit (IF_1), 16 polypeptides (48, 247, 301), two of which are encoded on mtDNA (302). The membranous subcomplex F_0 consists of subunits a, b, c_8, d, e, f, g, A6L, and F_6 (10, 48) and the extramembranous F_1 subcomplex consists of subunits α_3, β_3, γ, δ, and ε (2, 3, 24). A central stalk, consisting of the γ, δ, and ε subunits from the F_1 domain, and a

peripheral stalk composed of the oligomycin sensitivity conferral protein (OSCP) and subunits b, d, and F_6 from the F_0 domain connect the two subcomplexes (48, 49, 84). Collectively this enzyme functions similar to a hydroelectric dam with the electrochemical gradient established by CI, CIII, and CIV being the dammed water and CV as both the turbine and generator used to convert gradient (potential) energy into chemical energy. This chemical energy is harnessed by converting ADP and phosphate (Pi) into ATP.

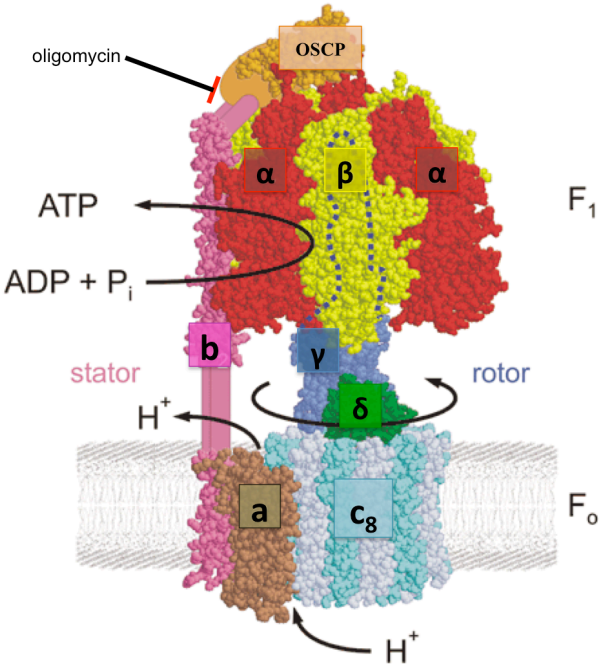

Figure 12. Mitochondrial respiratory complex V (CV) – ATP synthase. The F_1 domain resides in the mitochondrial matrix as the F_0 domain is primarily in the mitochondrial inner membrane. OSCP – oligomycin sensitivity conferral protein. Modified from reference (265).

The specifics of ATP synthesis and hydrolysis are complex and intricate. Simply put, the flow of protons through F_0 creates a torque that facilitates the synthesis of ATP at F_1. This process is fully reversible such that ATP hydrolysis at F_1 can actively pump protons back out of the matrix through F_0 (70, 147, 305). Much of the mechanism explaining the synthesis of ATP via CV in fact has derived from studies investigating the effect of ATP hydrolysis on enzyme mechanics (142, 211) although the forward mechanism has also been observed (126).

The process of ATP synthesis at CV begins with proton translocation from the MIS down the gradient into the mitochondrial matrix through the F_0 domain causing its c_8 (subunit) ring to rotate (211). The protons ionize carboxylate residues on glutamate in the c_8 subunit. This ionization drives the movement of these residues via Brownian motion in attempt to reach a more hydrophobic environment, causing the c-ring to turn. Eventually the carboxylate reaches an environment where it is reionized and the proton is released (140). This rotational force causes the entire asymmetric central stalk to turn which then applies a rotary torque on the γ chain that runs through core

of the $\alpha_3\beta_3$ assemblage of the F_1 domain (222, 255, 274). Rotation of this γ chain propagates conformational changes in the β subunits and facilitates ATP synthesis (152, 211). Rotation of the γ subunit occurs in discrete 120° clockwise increments – from an F_0 vantage point – of which are composed of 80° and 40° substeps, at approximately 100 rotations per second (210, 307, 322). This rotational torque is however resisted by the peripheral stalk, which stabilizes the catalytic component of F_1 (300). The globular F_1 domain has three catalytic β chains, and each chain is separated by a corresponding non-catalytic α subunit (2). There are three potential nucleotide-binding sites on the β subunits located at the αβ interface (25, 152, 265). These catalytic sites undergo conformational changes facilitated by the rotational torque of the central stalk and the γ subunit. The catalytic conformations correspond to the binding of the nucleotide, which are "open", "loose", and "tight" (25). Within a 360° turn each site progresses through all three conformations, and so each 120° rotation of the central stalk approximately 1 molecule of ATP is made (307).

The synthesis of ATP is highly efficient with the P/O ratio varying according to c-ring size. The P/O ratio is defined as the number of ATP molecules synthesized per pair of electrons that traverse the electron transport system (75). The number of translocated protons necessary to generate one 360° turn is the same as the number of c-subunits on the c-ring (307). A mammalian c-ring with eight c-subunits has an electrochemical cost of 3.7 protons per ATP produced (307). This equates with a P/O ratio of 2.7 and 1.6 for CI and CII specific electron entry into the respiratory system, respectively (108, 307). Every $2e^-$ that enters the respiratory system at CI results in 10 H^+ ions translocated across the MIM (4 at CI, 2 at CIII, and 4 at CIV) and thus the P/O ratio is 2.7 (10÷3.7). Alternatively, electron entry at CII only result in 6 H+ translocated since CII does not actively transport protons across the MIM (2 at CIII and 4 at CIV) resulting in a P/O ratio of 1.6 (6÷3.7) (75, 108, 307).

While ADP and ATP obviously function as substrates for CV, oligomycin acts as an inhibitor. Oligomycin reacts with OSCP facilitating a conformational change in the OSCP-bdF_6 subcomplex of F_0, which prevents binding of ADP or the release of ATP at the catalytic sites of F_1 (225, 247).

Synopsis of the mitochondrion and cellular respiration

In summary, the mammalian mitochondrion is believed to have evolved from the synergistic fusion of ancestral glycolytic proto-eukaryotes with oxidative α-bacterial-like endosymbionts. Overtime a mitonuclear coadaptation occurred such that the previously autonomous bacterial ancestors became reliant on its host's nuclear DNA despite retaining some genetic self-sufficiency, specifically the genes that encode for 12S and 16S rRNA, 22 tRNAs essential for mitochondrial protein synthesis, and 13 polypeptides that are involved in oxidative phosphorylation. In addition to the genetic reliance of the mitochondrion on the eukaryotic cell came the energetic reliance of the eukaryotic cell on the mitochondrion. The mitochondrion emerged as the lynchpin in mammalian evolution allowing for the exploitation of oxygen's instability and providing the facilities to transduce energy from chemical sources into biologically accessible forms of which are used to maintain metabolic homeostasis. This process, termed oxidative phosphorylation, oxidizes the metabolites of macronutrients (glucose, fatty acids, and amino acids) via a superlative and intricate set of synchronized and coupled reactions. Though the origin of the process varies depending on the macronutrient oxidized, ultimately all carbon sources coalesce in the mitochondrial matrix and precede through the TCA cycle. The systematic metabolization and oxidation of these chemical sources generate reducing equivalents such as NADH and $FADH_2$. These reducing equivalents serve as the electron sources necessary to build an electrochemical gradient across the MIM that facilitates the energetic transduction. Electron input occurs from four sources: 1.) NADH transmitted through mitochondrial respiratory complex I; 2.) TCA cycle specific $FADH_2$ through mitochondrial respiratory complex II; 3.) electron transfer from the metabolism of fatty acids through β-oxidation through the electron-transferring-flavoprotein (ETF) dehydrogenase (flavoprotein–ubiquinone oxidoreductase); and 4.) electrons transferred from glycerophosphate dehydrogenase to CoQ that originated from cytosolic NADH via the glycerophosphate shuttle. All electrons are passed onto dissolved pool of CoQ molecules in the MIM where they converge and are passed onto mitochondrial respiratory complex III. The electrons are then shuttled to mitochondrial respiratory complex IV via soluble cytochrome c. It is here that oxygen is reduced to metabolic water and carbon dioxide. The transport of electrons through complexes I, III, and IV result in the attendant transfer of protons from the

mitochondrial matrix, across the MIM and into the MIS. This develops a proton motive force that is then channeled through mitochondrial respiratory complex V (ATP synthase), which is coupled to the phosphorylation of ADP to ATP. As this process is vital to metabolic homeostasis and the maintenance of life, small alterations in mitochondrial function can have drastic influences on health.

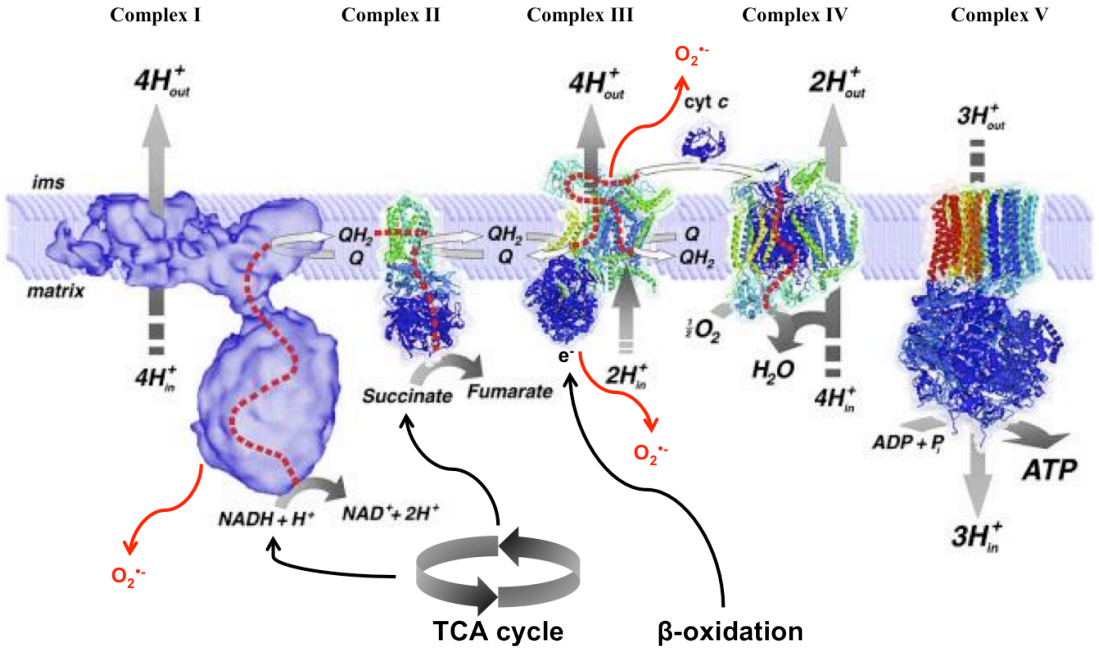

Figure 13. Oxidative phosphorylation. This figure illustrates the process of oxidative phosphorylation with: Substrate provision to mitochondrial complex I and complex II from the TCA cycle and to mitochondrial complex III via electron transferring flavoprotein from β-oxidation; The collective flow of electrons (red-dashed lines and white arrows); Translocation of hydrogen (grey arrows); The production of superoxide ($O_2^{\bullet-}$); The reduction of molecular O_2 to H_2O at mitochondrial complex IV; and The phosphorylation of ADP + inorganic phosphate (P_i) to ATP at mitochondrial complex V. ims – intermitochondrial space; Q and QH2 – oxidized and reduced coenzyme Q, respectively; cyt c – cytochrome C. Figure modified from reference (326).

Appropriately, research investigating mitochondrial function and its relationship to both health and disease remains at the forefront of a multitude of different scientific fields. Despite the significance of mitochondrial physiology in maintaining both physical and mental health, however, there is paucity of literature that actually examines mitochondrial respiration directly *in vivo* or in intact tissue, *ex vivo*, providing dynamic assessments of electron transfer sufficiency and substrate influence on respiration. In the following section the specific reason for conducting the studies included in this dissertationwill be addressed.

Aim of Study 1: Analysis of lactate metabolism in human skeletal muscle mitochondria

Lactate is an intermediate metabolite of glucose, a by-product of glycolysis, and is essential for human bioenergetics and maintaining overall homeostasis (85, 87, 289). The cell-cell lactate shuttle (CCLS) has been confirmed throughout the years (12, 21, 106, 187, 196, 290), verifying that lactate released from one cell can serve as a carbon source for bioenergetic means throughout the body (32, 34). Though many different tissues, including the heart, brain, kidney, adipose tissue, liver and skeletal muscle, consume lactate (62, 195, 289, 290), the mechanism of lactate metabolism is debated.

The lactate shuttle hypothesis (34), which has served as the epicenter of the debate, initially proposed that lactate was transported into the mitochondrial matrix where it was oxidized (35, 36). While much evidence refutes this hypothesis, the specifics of lactate metabolism within skeletal muscle mitochondria remain obscure (33, 36, 37, 86, 241, 249, 324). One similarity across the majority of studies is the mitochondrial preparation utilized to assess mitochondria-specific lactate oxidation (36, 234, 241, 249, 324). This crude method of mitochondrial extraction results in a varying % yield of mitochondria by mechanical homogenization and differential centrifugation. Although the methods were grossly similar across labs, the dispute regarding the mechanisms of mitochondrial lactate oxidation consists of challenging the exact method used for mitochondrial isolation or the success achieved in purity and completeness of the mitochondrial isolations (33, 37, 241).

As reviewed in the introduction, mitochondria subsist in skeletal muscle as a reticular tubular network and not as the discrete organelles achieved with mitochondrial isolation (148). The isolation procedures disrupt this native reticulum resulting in artificially spherical and discrete organelles that represent only a portion of the entire mitochondrial network (231, 263). Such disruption carries the risk of: i) contaminating the mitochondrial fraction with proteins foreign to the mitochondria (46, 231), ii) depleting mitochondrial specific contents (33, 37, 231), and iii) altering mitochondrial function (164, 251, 254). Indeed, mitochondrial isolation has repeatedly been shown to affect mitochondrial respiratory function (19, 159, 198, 221,

230, 294). Unlike those studies that have utilized isolation techniques, we wanted to examined the ability of mitochondria to oxidize lactate by means of high-resolution respirometry on preparations of human skeletal muscle *in situ*. This technique allows for the analysis of mitochondrial function by chemically permeabilizing the sarcolemma, allowing access to unaltered mitochondria for direct manipulation. In the process of sarcolemmal perturbation, soluble cytosolic proteins, including LDH, are concomitantly lost (160, 164, 254). This is an additional benefit of this technique, as it not only allows access to an entire innate mitochondrial network within the skeletal muscle but also eliminates the confounding effects of cytosolic LDH on lactate metabolism.

Accordingly, the primary aim of this study was to challenge the hypothesis that mitochondria can directly oxidize lactate. Assuming that a lactate oxidation complex exists within skeletal muscle mitochondria (102), our hypothesis was that mitochondrial preparations of human skeletal muscle *in situ* would display the ability for lactate to facilitate mitochondrial respiration independent from any addition of exogenous LDH.

Aim of Study 2: Identify and describe age-induced alterations in mitochondria

As introduced in the prologue, oxygen is unstable, and because of that instability there are varying degrees of oxidant production with aerobic metabolism (101). As the mitochondrion monopolizes aerobic metabolism, these subcellular structures also consequently serve as the primary source of *in vivo* oxidant production (11, 15, 285, 304), mostly accounted for the production at CI (161, 162, 287) and CIII (43, 96, 99, 205, 286, 323). A certain degree of oxidant production is beneficial and facilitates healthy adaptation via systematic and controlled cellular signaling cascades. Oxidant production beyond these hormetic concentrations, however, precipitates deleterious and indiscriminate oxidation of nucleic acids, proteins, and lipids (128, 272, 285). The mitochondrial theory of aging asserts that the actual biological aging process is facilitated by a gradual impairment in electron transport efficiency that increases oxidant production, which damages mtDNA damage causing additional functional

impairment, and so on; a vicious cycle of functional impairment, oxidant production, and cellular damage (77). This theory has yet to be entirely confirmed.

Senescence does correlate with evidence of nuclear and mtDNA damage (98, 194, 266, 267) and mtDNA induced mutations are associated with premature aging (224). Additionally, models of increased oxidant production also associate with premature aging (71, 153, 191), while prevention of oxidative stress via upregulation of endogenous antioxidant alternatively increases lifespan (262). Despite these findings, any age-induced alterations in actual electron transport function have not been demonstrated (11).

Accordingly the aim of this study was to examine mitochondrial protein expression and both respiratory capacity and control via high-resolution respirometry. The use of isolated mitochondrial preparations to study the effects of aging on mitochondrial amplifies the age induced changes in mitochondrial function, embellishing the actual alterations (230). Mitochondrial isolation techniques alter innate mitochondrial characteristics (33, 37, 46, 122, 159, 198, 221, 230, 294) such as the loss of mitochondrial membrane integrity (19, 314) and the ability to oxidize fatty acids (221). For respirometric analysis we used saponin permeabilized skeletal muscle preparations allowing direct access to skeletal muscle mitochondria while maintaining both the cytocellular ultrastructure (88, 164, 179, 226, 231, 252, 254) and subcellular interactions with mitochondria (164, 179, 198, 231, 254, 291). Cellular bioenergetics and metabolic channeling are predicated upon these factors (88, 144, 164, 254). Accordingly, this specific mitochondrial preparation serves as the best model to examine respiratory capacity and control with aging. Respirometric analyses were carried out on soleus (SOL), quadricep (QUAD), and lateral gastrocnemius (GAST) skeletal muscles, which represent type 1 slow twitch oxidative (SOL) and type 2 fast twitch glycolytic muscle (QUAD and GAST), respectively, in young (10-12 wk) and mature (74-76 wk) mice. We hypothesized that actual electron transport function is modified with age however the effects of age may vary across skeletal muscle types,.

Aim of Study 3: Compare and contrast mitochondrial function in mouse and man

Mouse modeling for the study of both human health and disease is an extremely powerful tool that is widely used. The degree of conservation between mouse and human genomes allows for the study of murine biology to largely characterize that of humans (52). There remains, however, a biological divergence between species that are not always so apparent and can lead to scientific misdirection if not properly recognized. The exact biological processes differ between humans and mice regards to certain aspects of cancer (240), aging (59), and metabolic disease (83, 278). Mechanisms of sarcopenia in rodents and humans are different (242) as are those regulating hemodynamic control (22, 60), and even the metabolic profile of skeletal muscle (260). These differences must be accounted for when applying the results from rodent studies towards the progression of human health and well-being.

Our understanding and interpretation of mitochondrial physiology is often derived from mouse models (197, 220, 230, 264). Furthermore, one of the most common tissues used to analyze mitochondria is skeletal muscle because of its accessibility, relative mass to body weight ratio, and high metabolic rate. Differences between mouse and human skeletal muscle have brought into question the validity of studying mouse mitochondria and alternative animal models have already been proposed to ostensibly replace the mouse for the study of human mitochondrial physiology (171). Additionally, differences in metabolic expression across skeletal muscle types has brought into question the proper mouse muscle to analyze when attempting to mimic human biology (145).

Accordingly our objective was to compare and contrast mitochondrial function across different skeletal muscle types in the mouse and determine if they can properly represent human skeletal muscle mitochondrial function. If so, we wanted to identify the mouse skeletal muscle that best represents human muscle. We hypothesize that i) the mouse can serve as a viable model for the study of mitochondrial function in humans, and ii) that the mouse soleus would best represent mitochondrial function in human skeletal muscle as a result of the molecular similarities between muscles (145).

Aim of Studies 4 & 5: Examine the adaptation of skeletal muscle mitochondria to hypoxia

The study of acclimatization and adaptation to hypoxia in humans is a timely topic of research. Approximately 16.5 million km^2 of the earth's surface exists at or above an elevation of 2,000 m (69), and between 140 and 150 million people reside at high altitudes while 35 million lowland dwellers visit or commute to elevation above 3,000 m annually (203, 313). Exposure of humans to high altitudes is a challenge to biological homeostasis as oxygen delivery becomes progressively more limited as a result of the gradual decrease in the partial pressure of oxygen (PO_2) attendant to the diminishing barometric pressure (311). The collection of past literature that has examined mitochondrial alterations with high altitude exposure are difficult to collectively interpret. While early studies (112, 243, 280, 288) reported greater expression of indirect markers suggestive of oxidative potential in both animals and humans native to high altitude (112), later studies reported a loss of skeletal muscle mitochondria with altitude exposure (120, 124, 175) or negligible changes in mitochondrial characteristics (92-94, 175, 181, 202).

The majority of these studies investigating mitochondrial modifications during acclimatization have focused primarily on morphological examinations and biochemical analysis of expression. Relying exclusively, however, on static measurements to characterize the very dynamic activities of the mitochondrion is incomplete. A proper evaluation of mitochondrial-specific adaptations requires a complement of direct and functional measures in intact mitochondria to, for example, assess potential changes in oxidative phosphorylation, electron transport, coupling control and efficiency. In two separate studies we set out to assess hypoxia-facilitated changes to mitochondrial respiratory chain function and biochemical expression of mitochondrial specific enzymes using high-resolution respirometry. We hypothesized that the previous literature suggesting a diminished oxidative phosphorylation capacity with altitude exposure would be represented in functional measurements with an attendant loss in respiratory capacity.

Aim of Studies 6 & 7: Investigate mitochondrial differences across various athletes

The majority of mitochondrial research is directed toward understanding the integrative functions of the organelle in relation to various diseases and disorders. The good intensions of this research may be limited to an extent, as it is difficult to characterize mitochondrial "dysfunction" prior to fully understanding healthy mitochondrial function. The physiological boundaries of human skeletal muscle mitochondrial performance are unknown, as are the benefits having healthy and fully functional mitochondria. Measures of whole-body cardiorespiratory fitness ostensibly represent the state of health in humans (1, 81, 136, 143, 150, 180, 219). Accordingly we sought to i) identify and describe mitochondrial function across of healthy, young individuals that possess different aerobic capacities; and ii) analyze mitochondrial function in a more homogenous group, composed of highly-trained athletes.

Mitochondrial expression and function seem to parallel that of overall health and fitness. Mitochondrial density increases in response to training (114, 115, 119) and differ between untrained and trained individuals (121, 166, 192, 331). Skeletal muscle oxidative capacity also increases with training (228) and varies across groups differing in activity level (166, 192, 331). There is debate whether the increase in skeletal muscle respiration capacity that parallels aerobic fitness can be explained by quantitative differences in mitochondrial content alone (263, 309) or whether qualitative adaptations such as functional modifications in respiratory control and capacity also improve along with whole body aerobic capacity (88). The aim of this study was therefore to analyze mitochondrial differences, both quantitative and qualitative, across four different groups of healthy and physically active subjects that differ in aerobic capacity. We hypothesized that differences in mitochondria from AT to ET individuals would possess distinct qualitative differences.

Differences in mitochondrial function across groups that largely differ in aerobic capacity should be more obvious than the more subtle differences within a more homogenous group of individuals. Highly trained endurance athletes place a inordinate amount of metabolic strain on their bodies and greatly rely on aerobic metabolism to perform. Yet, the description of respiratory capacity and/or efficiency

in the top athletes is lacking. Overall endurance performance can roughly be determined by the product of an athlete's maximal oxygen consumption (VO_{2max}) x lactate threshold x exercise efficiency can predict endurance performance (14, 137-139), but this general calculation is vague in regards to specific physiological variables important to exercise performance. The purpose of this study is therefore to isolate the most dominant physiological variables of performance and identify the strongest determinant(s) of exercise performance in highly trained endurance athletes. As oxidative capacity of the skeletal muscle appears to have the most common interrelation between VO_{2max}, lactate threshold, and exercise efficiency we hypothesize that maximal oxidative phosphorylation capacity of the skeletal muscle is the strongest determinant time trial performance in highly trained athletes.

2. Manuscripts

2.1 Lactate metabolism in human skeletal muscle mitochondria

2.2 Fast-twitch glycolytic skeletal muscle is predisposed to age-induced impairments in mitochondrial function

2.3 The C57Bl/6 mouse serves as a suitable model of human skeletal muscle mitochondrial function

2.4 Mitochondrial function in human skeletal muscle following high-altitude exposure

2.5 Twenty-eight days at 3454-m altitude diminishes respiratory capacity but enhances efficiency in human skeletal muscle mitochondria

2.6 Determinants of time trial performance and maximal incremental exercise in highly trained endurance athletes

2.7 Mitochondria express enhanced quality as well as quantity in association with aerobic fitness across recreationally active individuals up to elite athletes

Am J Physiol Endocrinol Metab 304: E686–E694, 2013.
First published February 5, 2013; doi:10.1152/ajpendo.00476.2012.

Lactate oxidation in human skeletal muscle mitochondria

Robert A. Jacobs,[1,2,3] Anne-Kristine Meinild,[3] Nikolai B. Nordsborg,[4] and Carsten Lundby[1,3]

[1]*Zurich Center for Integrative Human Physiology, Zurich, Switzerland;* [2]*Institute of Veterinary Physiology, Vetsuisse Faculty, University of Zurich, Zurich, Switzerland;* [3]*Institute of Physiology, University of Zurich, Zurich, Switzerland;* [4]*Department of Exercise and Sport Sciences, University of Copenhagen, Copenhagen, Denmark*

Submitted 20 September 2012; accepted in final form 30 January 2013

Jacobs RA, Meinild AK, Nordsborg NB, Lundby C. Lactate oxidation in human skeletal muscle mitochondria. *Am J Physiol Endocrinol Metab* 304: E686–E694, 2013. First published February 5, 2013; doi:10.1152/ajpendo.00476.2012.—Lactate is an important intermediate metabolite in human bioenergetics and is oxidized in many different tissues including the heart, brain, kidney, adipose tissue, liver, and skeletal muscle. The mechanism(s) explaining the metabolism of lactate in these tissues, however, remains unclear. Here, we analyze the ability of skeletal muscle to respire lactate by using an in situ mitochondrial preparation that leaves the native tubular reticulum and subcellular interactions of the organelle unaltered. Skeletal muscle biopsies were obtained from vastus lateralis muscle in 16 human subjects. Samples were chemically permeabilized with saponin, which selectively perforates the sarcolemma and facilitates the loss of cytosolic content without altering mitochondrial membranes, structure, and subcellular interactions. High-resolution respirometry was performed on permeabilized muscle biopsy preparations. By use of four separate and specific substrate titration protocols, the respirometric analysis revealed that mitochondria were capable of oxidizing lactate in the absence of exogenous LDH. The titration of lactate and NAD^+ into the respiration medium stimulated respiration ($P \leq 0.003$). The addition of exogenous LDH failed to increase lactate-stimulated respiration ($P = 1.0$). The results further demonstrate that human skeletal muscle mitochondria cannot directly oxidize lactate within the mitochondrial matrix. Alternately, these data support previous claims that lactate is converted to pyruvate within the mitochondrial intermembrane space with the pyruvate subsequently taken into the mitochondrial matrix where it enters the TCA cycle and is ultimately oxidized.

lactate metabolism; mitochondrial function; lactate oxidation complex

OUR UNDERSTANDING OF LACTATE METABOLISM has evolved greatly over the past century (30, 32, 86). The omnipresent intermediate by-product of glycolysis is now recognized as an essential and common metabolite involved in human bioenergetics. It is ubiquitously utilized by different tissues throughout the body, including the heart, brain, kidney, adipose tissue, liver, and skeletal muscle (25, 59, 86, 87) and is produced even at rest despite a sufficient supply of oxygen to the tissue (7, 17, 34, 59). The lactate shuttle hypothesis (15) helped propel our current understanding of lactate metabolism. The premise for the cell-cell lactate shuttle (CCLS) is that lactate released from one cell could serve as a precursor carbon source for either oxidative phosphorylation or gluconeogenesis in other cells throughout the body (13, 15). The majority of this theory has been confirmed throughout the years (4, 8, 38, 56, 60, 87).

Address for reprint requests and other correspondence: R. A. Jacobs, Institute of Veterinary Physiology, Zurich Center for Integrative Human Physiology (ZIHP), Winterthurerstrasse 260, CH-8057 Zurich, Switzerland (e-mail: jacobs@vetphys.uzh.ch).

The observations of high cytosolic ratios of lactate to pyruvate in skeletal muscle, especially apparent during exercise, along with the understanding that lactate can serve as a precursor for cellular respiration, led to the intracellular lactate shuttle (ILS) hypothesis. This hypothesis has transformed over the years from the initial speculation that lactate was transported into the mitochondrial matrix where it was subsequently oxidized (16, 18) into its current position (36, 37). It is now proposed that glycolytically produced lactate passively diffuses across the mitochondrial outer membrane (MOM) into the mitochondrial intermembrane space (MIS). An increase in lactate concentrations in the MIS facilitates conversion back into pyruvate catalyzed by an isoform of lactate dehydrogenase (LDH) located in the mitochondria (mLDH). Pyruvate is then shuttled across the mitochondrial inner membrane (MIM) into the matrix via a mitochondrial monocarboxylate transporter (mMCT), where it is oxidized (37), The MCTs most likely involved are MCT1 (36, 37) and/or the high-affinity pyruvate transporter MCT2, which has been reported to subsist in both subsarcolemmal and intermyofibrillar mitochondrial populations (95).

The specifics of lactate metabolism within skeletal muscle mitochondria are ardently debated (14, 18, 19, 31, 74, 75, 95). Previous investigations into the functional assessment of mitochondria-specific lactate oxidation have primarily utilized isolated mitochondrial preparations (18, 73–75, 95), for which mitochondria are extracted and purified by mechanical homogenization and differential centrifugation. Consequently, the dispute regarding mitochondrial lactate oxidation consists of challenging either the method used for mitochondrial isolation or the success achieved in purity and completeness of the mitochondrial isolations (14, 19, 74).

Mitochondria subsist in skeletal muscle as a reticular tubular network as opposed to discrete organelles (45). Mitochondrial isolation disrupts the native heterogeneous reticulum, producing somewhat artificially homogeneous spherical and discrete organelles (71, 82). Such disruption carries the risk of *1*) contaminating the mitochondrial fraction with proteins foreign to the mitochondria (21, 71), *2*) depleting contents specific to mitochondria (14, 19, 71), and *3*) altering mitochondrial function (51, 76, 80). Indeed, mitochondrial isolation has repeatedly been shown to affect mitochondrial respiratory function (5, 48, 61, 67, 70, 90).

Unlike previous studies, here we test the ability of mitochondria to oxidize lactate by means of high-resolution respirometry on preparations of human skeletal muscle biopsies. With this technique, the sarcolemma is chemically permeabilized, and soluble cytosolic proteins, including LDH, are lost without affecting native mitochondrial structure, allowing access to unaltered mitochondria for direct manipulation and investigation of respiratory control (49, 51, 80). The primary

aim of the current study is to challenge the hypothesis that mitochondria can directly oxidize lactate. Assuming that a lactate oxidation complex exists within skeletal muscle mitochondria (36), our hypothesis was that mitochondrial preparations of human skeletal muscle in situ would display the ability for lactate to facilitate mitochondrial respiration independent of any addition of exogenous LDH. Indeed, we demonstrate the ability of unaltered, intact mitochondria to utilize lactate as a substrate for respiration in human skeletal muscle. The additional titration of exogenous LDH fails to further stimulate respiration. Our results provide evidence that demonstrate the ability of human skeletal muscle mitochondria to utilize lactate as a substrate.

Glossary

C1	Complex I (NADH dehydrogenase)
C2	Complex II (succinate dehydrogenase)
CCLS	Cell-cell lactate shuttle
DTT	Dithiothreitol
ILS	Intracellular lactate shuttle
K-MES	2-(*N*-morpholino)ethanesulfonic acid hydrate
LDH	Lactate dehydrogenase
L_N	Leak respiration in absence of adenylates
MIM	MMitochondrial inner membrane
MiR05	Mitochondrial respiration medium
MiR06	MiR05 + catalase
MIS	Mitochondrial intermembrane space
mLDH	Mitochondria-specific LDH
mMCT	Mitochondrial-specific monocarboxylate transporters
MOM	Mitochondrial outer membrane
NAD	Nicotinamide adenine dinucleotide
P_{ETF}	Fatty acid oxidative capacity
P_{C1}	Submaximal respiratory state specific to complex I
P_{C2}	Submaximal respiratory state specific to complex II
P	Maximal state 3 respiration and oxidative phosphorylation capacity
ROX	Residual oxygen consumption
SIRT	Sirtuin

MATERIALS AND METHODS

Ethical Approval

Experimental protocols involving human subjects were approved by the ethics committees for the Eidgenössische Technische Hochschule in Zürich (EK 2011-N-51) and the Regional Ethics Committee of Region Hovedstaden in Denmark (H-1-2011-052), in accordance with the Declaration of Helsinki. Prior to the start of the experiments, informed oral and written consent was obtained from all participants.

Experimental Design

Sixteen young and healthy subjects (14 male and 2 female) voluntarily participated in this study. For logistic reasons, the subjects were divided into two groups of eight. The first eight subjects (*group 1*, 6 males and 2 females) and the second group of eight subjects (*group 2*, 8 males) had their skeletal muscle samples analyzed with separate substrate titration protocols. These protocols are explained in detail below.

Skeletal Muscle Sampling

Skeletal muscle biopsies were obtained from the vastus lateralis muscle under local anesthesia (1% Lidocaine) of the skin and superficial muscle fascia, using the Bergström technique (9) with a needle modified for suction. The biopsy was immediately dissected free of fat and connective tissue and divided into sections for measurements of mitochondrial respiration.

Skeletal Muscle Preparation

The biopsy was sectioned into parts to measure mitochondrial respiration. Each part was immediately placed in ice-cold biopsy preservation solution (BIOPS) containing 2.77 mM CaK_2EGTA buffer, 7.23 mM K_2EGTA buffer, 0.1 μM free calcium, 20 mM imidazole, 20 mM taurine, 50 mM 2-(*N*-morpholino)ethanesulfonic acid hydrate (K-MES), 0.5 mM dithiothreitol (DTT), 6.56 mM $MgCl_2{\cdot}6H_2O$, 5.77 mM ATP, and 15 mM phosphocreatine (pH 7.1). Muscle samples were then gently dissected with the tips of two 18-gauge needles, achieving a high degree of fiber separation verified microscopically, followed by chemical permeabilization via incubation in 2 ml of BIOPS with saponin (50 μg/ml) for 30 min at 4°C (50). Last, samples were washed with a mitochondrial respiration medium (MiR05) containing 0.5 mM EGTA, 3 mM $MgCl_2{\cdot}6H_2O$, 60 mM K-lactobionate, 20 mM taurine, 10 mM KH_2P0_4, 20 mM HEPES, 110 mM sucrose, and 1 g/l bovine serum albumin (pH 7.1) for 10 min at 4°C. Cytosolic components of the skeletal muscle sample are lost during skeletal muscle preparation, including LDH (49, 53, 69, 78, 89).

Mitochondrial Respiration Measurements

Muscle bundles were blotted dry and measured for wet weight in a balance-controlled scale (XS205 DualRange Analytical Balance; Mettler-Toledo, Switzerland) maintaining constant relative humidity, providing hydration consistency as well as stability of weight measurements. Respiration measurements were performed in mitochondrial respiration medium 06 (MiR06; MiR05 + catalase 280 IU/ml). Measurements of oxygen consumption were performed at 37°C using the high-resolution Oxygraph-2k (Oroboros, Innsbruck, Austria) with all additions in each protocol added in series. The Oxygraph-2k is a two-chamber titration-injection respirometer with an oxygen detection limit of 0.5 $pmol{\cdot}s^{-1}{\cdot}ml^{-1}$. Standardized instrumental calibrations were performed to correct for back-diffusion of oxygen into the chamber from the various components, leak from the exterior, oxygen consumption by the chemical medium, and sensor oxygen consumption. Oxygen flux was resolved by software allowing nonlinear changes in the negative time derivative of the oxygen concentration signal (DatLab; Oroboros, Innsbruck, Austria). All experiments were carried out in a hyperoxygenated environment to prevent any potential oxygen diffusion limitation. This technique of permeabilization allows for the study of mitochondrial function in intact skeletal muscle samples in situ without altering the natural mitochondrial reticulum in small biopsy samples using high-resolution respirometry (41, 42, 51).

Respiratory Titration Protocols

Four different titration protocols were applied in the study, and they are illustrated in Table 1. Each protocol was specific to the examination of individual aspects of lactate-stimulated respiratory control through a sequence of coupling and substrate states induced via separate titrations. All titrations were added in series as presented.

LDH^-/NAD^- Titration Protocol

Leak respiration in absence of adenylates (L_N) was induced with the addition of malate (2 mM) and octanoyl carnitine (0.2 mM). This state represents the resting oxygen consumption of an unaltered and intact electron transport system in the absence of adenylates. In the L_N state, the chemiosmotic gradient is at maximum, specific to the substrates provided, and oxygen flux is at a minimum indicating proton leak, slip, cation cycling, and overall dyscoupling (33, 69). Fatty acid oxidative capacity and maximal electron transport through electron transferring flavoprotein (ETF) was determined following the

AJP-Endocrinol Metab • doi:10.1152/ajpendo.00476.2012 • www.ajpendo.org

Table 1. *Experimental design of respirometric analysis*

	M	OC	ADP	Lac			Pyr	S	CytC	Rot	AmA
LDH^-/NAD^- *group 1* ($n = 8$)	2 mM	0.2 mM	5 mM	30 mM	X	X	5 mM	10 mM	10 μM	0.5 μM	2.5 μM
NAD^+/LDH^-/ *group 2* ($n = 8$)	2 mM	0.2 mM	5 mM	30 mM	X	NAD(2mM)	5 mM	10 mM	10 μM	0.5 μM	2.5 μM
NAD^+/LDH^+ *group 2* ($n = 8$)	2 mM	0.2 mM	5 mM	30 mM	NAD(2mM)	LDH(6IU/l)	5 mM	10 mM	10 μM	0.5 μM	2.5 μM
LDH^+/NAD^+ *group 1* ($n = 8$)	2 mM	0.2 mM	5 mM	30 mM	LDH(6IU/l)	NAD(2mM)	5 mM	10 mM	10 μM	0.5 μM	2.5 μM

Four different titration protocols were used in this study. They are indicated in the furthest *left* column, from *top* to *bottom*: *1*) LDH^-/NAD^-; 2) NAD^+/LDH^-; *3*) NAD^+/LDH^+; *4*) LDH^+/NAD^+. Below the protocol is the subject group for which skeletal muscle specimens were analyzed with that specific protocol. T*op*: substrate or inhibitor added to the respiration medium. The sequence of the titrations into the chamber follows the order of substrates and inhibitors presented from *left* to *right*. Concentration of substrate or inhibitor (columns) added during respirometric analysis is indicated in the box located in the respective protocol of interest (row). M, malate; OC, octanoyl carnitine; ADP, adenosine diphosphate; Lac, lactate; NAD, nicotinamide adenine dinucleotide; LDH, lactate dehydrogenase; Pyr, pyruvate; S, succinate; Cyt C, cytochrome *c*; Rot, rotenone; AmA, antimycin A.

addition of ADP (P_{ETF}, 5 mM). Here, the transfer of electrons requires the metabolism of CoA, hence the previous addition of malate, to allow β-oxidation to proceed. Following P_{ETF}, lactate (30 mM) was added to the chamber to measure the oxidation of lactate. Next, pyruvate (5 mM) was added. Pyruvate is a common substrate used to stimulate electron flow through complex I (C1; NADH dehydrogenase) providing a submaximal state 3 respiratory state specific to C1 (P_{C1}). Maximal state 3 respiration, oxidative phosphorylation capacity (P), was induced with the addition of succinate (10 mM). Maximal state 3 P represents respiration that is resultant to saturating concentrations of ADP as well as substrates specific for C1 and succinate dehydrogenase, complex II (C2) and demonstrates an intact electron transport system's capacity to catalyze a sequential set of redox reactions that are partially coupled to the production of ATP via ATP synthase. Convergent electron input to C1 and C2 provides higher respiratory values compared with the isolated respiration of either C1 (pyruvate/glutamate + malate) or C2 (succinate + rotenone) (33); accordingly, it is more representative and physiologically relevant to the study of mitochondrial function and necessary to establish confirmation of a complete and intact electron transport system (10). As an additional internal control for damaged mitochondria, the integrity of the outer mitochondrial membrane was assessed with the addition of cytochrome *c* (10 μM). Rotenone (0.5 μM) and antimycin A (2.5 μM) were finally added, in sequence, to terminate respiration by inhibiting C1, achieving state 3 respiration through C2 (P_{C2}), and complex III (cytochrome bc_1 complex), respectively. Inhibition of respiration allows for the determination and correction of residual oxygen consumption (ROX), indicative of nonmitochondrial oxygen consumption in the chamber. The concentrations of substrates and inhibitors used were based on prior experiments conducted for optimization of the titration protocols.

NAD^+/LDH^- Titration Protocol. The only difference in the NAD^+/LDH^- titration protocol was that NAD (2 mM) was titrated into the respiration medium following the addition of lactate and before the addition of pyruvate.

NAD^+/LDH^+ Titration Protocol. The NAD^+/LDH^+ titration protocol also titrated NAD (2 mM) following the addition of lactate. However, LDH (3 IU/ml) was then added following stabilization of NAD-stimulated respiration and prior to the titration of pyruvate. This concentration of LDH, which has been previously used (75, 95), is supraphysiological and not limited to lactate-stimulated respiration.

LDH^+/NAD^+ Titration Protocol. Finally, the LDH^+/NAD^+ titration protocol had LDH (3 IU/ml) titrated into the respiratory medium following the addition of lactate followed by the addition of NAD (2 mM) before the addition of pyruvate.

Control for Sirtuin Influence on Mitochondrial Respiration

To address any question of whether respiration in the presence of lactate is truly due to lactate or rather to an enhancement of fatty acid metabolism or electron transport chain activity in response to the NAD^+, we measured P_{EFT} and mitochondrial lactate respiration in 18 separate human subjects from another study. As opposed to the titration protocols detailed above in this study, we added NAD^+ (6 mM) prior to lactate (60 mM) in the titration protocol. We analyzed respirometric values using a one-way ANOVA on repeated measurements with a Bonferroni adjustment to specify location of differences (SPSS Statistics 17.0; SPSS, Chicago, IL).

Enzyme Activities

LDH activities were assayed in homogenates of the skeletal muscle samples used in respiration measurements: The contents of the Oxygraph-2k chambers (2 ml each) were removed after each respiration experiment and washed once with 2 ml of MiR05. One percent Triton X-100 and 2 μl of a protease inhibitor cocktail (Sigma Aldrich cat. 539134) were added to the combined solutions (content and wash) and then homogenized for 30 s with a T10 basic ULTRA-TURRAX homogenizer near maximum speed. The homogenate was then centrifuged for 15 min at 4°C, and the supernatant was removed, frozen in liquid nitrogen, and stored at −80°C. LDH activity was measured fluorometrically at 450 nm and 37°C according to the manufacturer (LDH-Cytotoxicity Assay Kit, BioVision).

Data Analysis

For all statistical evaluations, a P value of <0.05 was considered significant. Statistical analysis of changes to respiration within each respective titration protocol was analyzed by one-way ANOVA on repeated measurements (SPSS Statistics 17.0). Differences in percent changes among respiratory states across all titration protocols and LDH activities across samples were analyzed using a one-way ANOVA. When appropriate, a Bonferroni adjustment was used to specify location of differences.

RESULTS

Lactate Dehydrogenase

There was a significant difference in LDH between samples that did not have exogenous LDH added from those samples that did (Fig. 1, $P < 0.001$). The LDH^- group showed trace amounts of LDH (38.9 ± 13.4 mU/mg wet wt), whereas the LDH^+, as expected, presented with a concentration of LDH indicative of the amount added to the mitochondrial medium during respirometric analysis (2,850 ± 687 mU/ml).

Respirometric Analysis

Differential respiratory capacities across the mitochondrial respiratory system were made evident throughout each separate titration protocol (Fig. 2, *A–D*).

LDH^-/NAD^- respirometric analysis. Respirometric analysis of the skeletal muscle samples using the LDH^-/NAD^- titration protocol is illustrated in Fig. 2*A*. Malate and octanoyl carnitine induced leak respiration, L_N. Respiration significantly

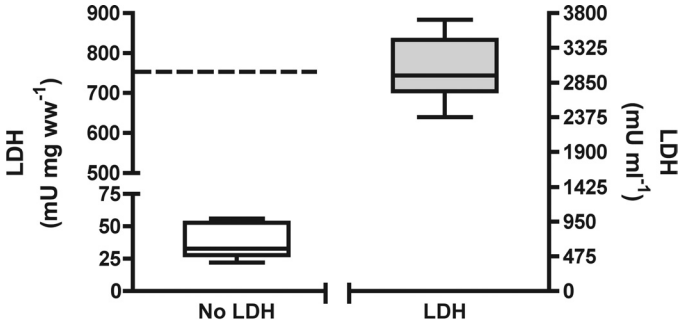

Fig. 1. Box-whisker plot representing lactate dehydrogenase (LDH) concentrations. Measurements of LDH activity (mU/mg wet wt) in permeabilized samples (*left y*-axis) that never had exogenous LDH added to the respiratory chamber and those that did have LDH activity (mU/ml) added to the respirometric chamber (*right y*-axis). LDH activity between the 2 sets of samples was significantly different ($P < 0.0001$). Black dashed line represents average skeletal muscle LDH activity (763 mU/mg wet wt) resported from active and inactive males and females (20, 43).

increased following the addition of ADP, demonstrating the capacity for fatty acid oxidation, P_{ETF} ($P < 0.001$). There was no increase from fat respiration following the addition of lactate (L). Respiration did, as expected, increase following pyruvate addition (P_{C1}, $P < 0.001$) and again following the titration of succinate ($P < 0.001$), the latter of which represents oxidative phosphorylation capacity, P. Finally, respiration diminished after inhibition of C1 with rotenone (P_{C2}, $P = 0.001$).

NAD^+/LDH^- respirometric analysis. Respirometric analysis of the skeletal muscle samples using the NAD^+/LDH^- protocol is illustrated in Fig. 2*B*. Malate and octanoyl carnitine induced L_N. Respiration significantly increased following the addition of ADP signifying P_{ETF} ($P < 0.001$). No increase was evident following the addition of lactate (L; 30 mM). Respiration did increase with the titration NAD ($P < 0.01$). There was another increase following the addition of pyruvate (P_{C1}, $P < 0.05$). Respiration again increased with the addition of succinate (P, $P \leq 0.001$). Finally, respiration diminished after inhibition of C1 with rotenone (P_{C2}, $P < 0.001$).

NAD^+/LDH^+ respirometric analysis. Respirometric analysis of the skeletal muscle samples using the NAD^+/LDH^+ protocol is illustrated in Fig. 2*C*. Malate and octanoyl carnitine induced L_N. Respiration significantly increased following the addition of ADP signifying P_{ETF} ($P \leq 0.001$). No increase was evident following the addition of lactate (L; 30 mM). Respiration did then increase with the titration NAD ($P \leq 0.001$). There was no further increase, however, with the addition of LDH. Respiration showed a trend to increase with pyruvate (P_{C1}, $P = 0.062$). Respiration did increase with the addition of succinate ($P < 0.001$). Finally, respiration diminished after inhibition of C1 with rotenone (P_{C2}, $P < 0.05$).

LDH^+/NAD^+ respirometric analysis. Respirometric analysis of the skeletal muscle samples using the LDH^+/NAD^+ protocol is illustrated in Fig. 2*D*. Malate and octanoyl carnitine induced L_N. Respiration significantly increased following the addition of ADP signifying P_{ETF} ($P < 0.001$). No increase was evident following the addition of lactate (L; 30 mM). Again, there was no increase in respiration following the titration of LDH. Respiration did then increase with the addition of NAD ($P \leq 0.01$). There was an increase following the addition of pyruvate (P_{C1}, $P < 0.01$). Respiration again increased with the addition of succinate (P, $P < 0.01$). Finally, respiration diminished after inhibition of C1 with rotenone (P_{C2}, $P < 0.01$).

Test of Mitochondrial Membrane Integrity

Across all titration protocols, cytochrome *c* had no additive effect on respiration. Respiration changed by −0.4% ($P = 0.962$), 3.1% ($P = 0.758$), −0.3% ($P = 0.971$), and −0.9% ($P = 0.846$) in groups LDH^-/NAD^-, NAD^+/LDH^-, NAD^+/LDH^+, or LDH^+/NAD^+, respectively (Figs. 2, *A–D*). The negligible changes in respiration from oxidative phosphorylation capacity, P, to the exogenous cytochrome *c*-stimulated respiration confirmed MOM intactness throughout all skeletal muscle samples.

Differences in Percent Changes Between Respiratory States Across Groups

Table 2 displays specific percent changes in respiration rates between different substrate-induced respiratory states across all groups. Only two significant differences were calculated, and both were between the NAD^+/LDH^+ and LDH^+/NAD^+ protocols. *1*) There was a difference in percent change from lactate-stimulated respiration and respirometric values obtained following the titration of LDH ($P < 0.001$); and *2*) There was a difference in percent change from the recorded LDH-stimulated respiration and respirometric values obtained following the titration of pyruvate ($P < 0.001$). The only difference between these two protocols is the order in which LDH and NAD were titrated into the respiratory chambers during analysis. As such, the former protocol, NAD^+/LDH^+, contained 2 mM NAD in the LDH-induced respiratory state, whereas the latter protocol, LDH^+/NAD^+, did not.

DISCUSSION

The current study was conducted to test whether human skeletal muscle mitochondria can oxidize lactate. The results *1*) confirm that lactate cannot be taken up directly by human skeletal muscle mitochondria into the mitochondrial matrix and oxidized; *2*) suggest that lactate is converted to pyruvate within the mitochondrial intermembrane space and that the pyruvate is then taken into the mitochondrial matrix where it consequently enters the TCA cycle and is ultimately oxidized; and *3*) is consistent with the existence of a functional lactate oxidation complex in human skeletal muscle mitochondria. The novelty of this study is the mitochondrial preparation and multiple substrate titrations utilized to examine the mechanism by which lactate is oxidized. In contrast to mitochondrial fractions from isolated preparations, the mitochondrial preparation applied in the current study preserved both structural integrity and functional interactions with cellular components (Figs. 2).

Lactate is undoubtedly a metabolic precursor for oxidative phosphorylation in human skeletal muscle (3, 56, 59, 60, 62, 87) as well as other tissues such as the brain (88). Hitherto, the primary disagreement in regard to the metabolism of lactate is whether mitochondria, independently of cytosolic enzymes and pathways, are capable of lactate metabolism and how, specifically, lactate is used as a substrate for cellular respiration.

It was reported that, in mitochondrial preparations isolated from rat hindlimb skeletal muscle, "malate+lactate"-stimulated respiration was similar to "malate+pyruvate"-stimulated respiration (18). Moreover, malate+lactate-stimulated respiration was greatly diminished when oxamate, a competitive

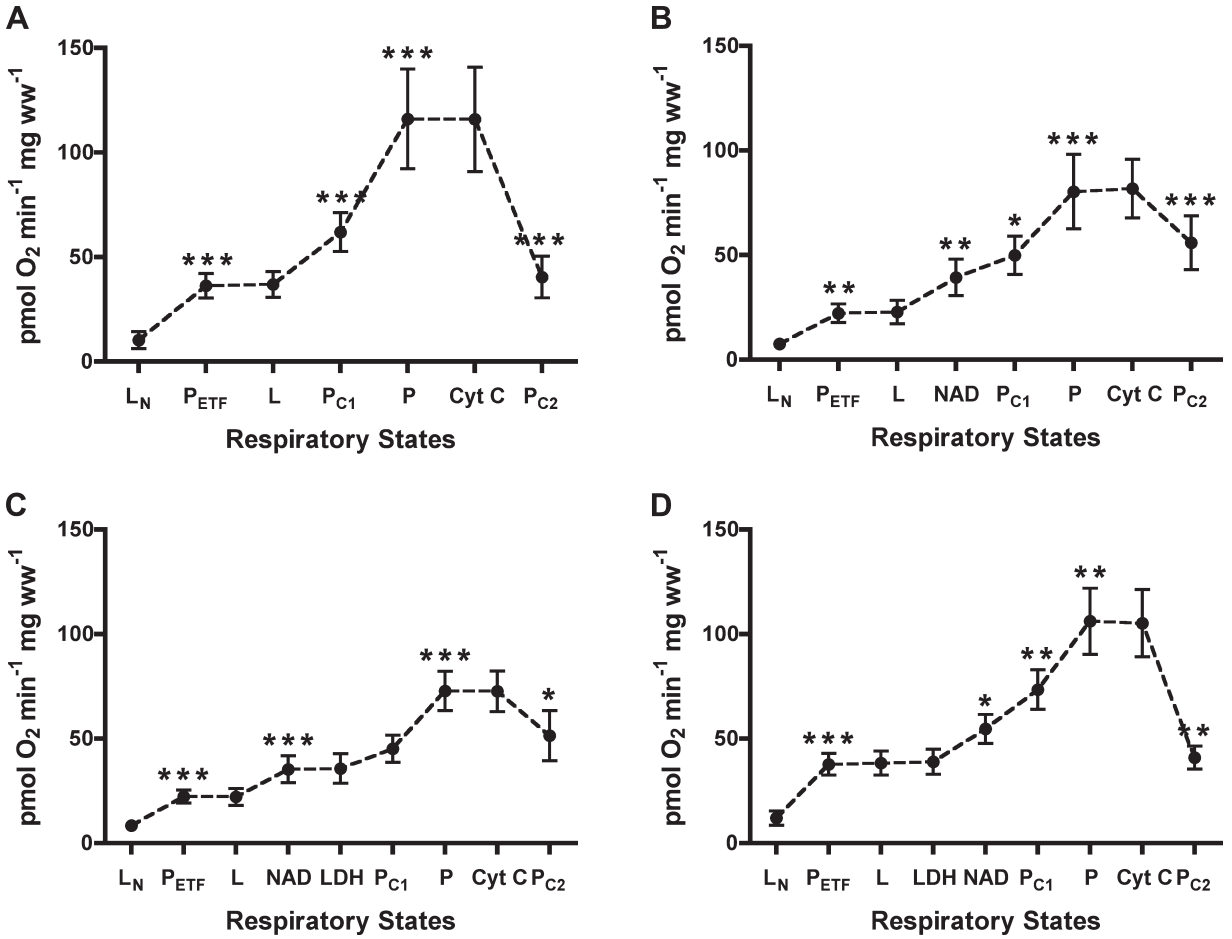

Fig. 2. Mass-specific respirometric analysis. Titration protocols for skeletal muscle samples with all titrations, presented from *left* to *right*, added in series. *A*: protocol without addition of LDH or NAD (LDH^-/NAD^-). *B*: protocol with NAD added but without LDH (NAD^+/LDH^-). *C*: protocol with NAD and LDH both added to respiration medium in successive order (NAD^+/LDH^+). *D*: protocol with LDH and NAD both added to respiration medium in successive order (LDH^+/NAD^+). L_N, respiration in absence of adenylates; P_{ETF}, capacity for fatty acid oxidation; L, lactate; P_{CI}, submaximal state 3 respiration through complex I stimulated with pyruvate; P, maximal state 3 respiration minus oxidative phosphorylation capacity; Cyt C, cytochrome *c*; P_{C2}, submaximal state 3 respiration through complex II following addition of rotenone. Differential respiratory capacities across the mitochondrial respiratory system were made evident throughout the titration protocol utilized, validating our mitochondrial preparation. Values are presented as means ± SD. *, **, and ***, difference in the specific respiration state between groups; $P \leq 0.05$, $P \leq 0.01$, $P \leq 0.001$, respectively.

inhibitor of LDH (58), was included in the respirometric analysis. The presence of LDH was reported in the intermembrane space, inner membrane, and matrix fractions of the skeletal muscle (18). Mitochondria isolated from skeletal muscle, however, are often so fraught with cytosolic LDH contamination that the inclusion of an LDH inhibitor, such as oxamate, is recommended to improve enzymatic analyses in mitochondrial preparations (21).

Several studies (73–75, 94, 95) across different laboratories have reported evidence in opposition to these findings (18), challenging the capacity for lactate oxidation in skeletal muscle mitochondria. These studies (73–75, 94, 95) reported the inability of various skeletal muscles across different species, including humans, to directly oxidize lactate. These studies were also unable to verify the presence of LDH in the mitochondrial fraction of skeletal muscle homogenates, further challenging the existence of a lactate oxidation complex in skeletal muscle mitochondria (74, 75, 95). All respirometric measurements collected in these studies, however, were obtained using isolated mitochondrial preparations. Accordingly,

Table 2. *Percent changes in respiration across all groups*

	L_N to FAT	FAT to Lac	Lac to NAD	Lac to LDH	NAD to Pyr	NAD to LDH	LDH to NAD	LDH to Pyr	Lac to Pyr
LDH^-/NAD^- *group 1* (n = 8)	307 ± 71	2 ± 4							69 ± 14*
NAD^+/LDH^- *group 2* (n = 8)	233 ± 69	2 ± 6	75.2 ± 28.1		29 ± 18				126 ± 52*
NAD^+/LDH^+ *group 2* (n = 8)	182 ± 87	1 ± 9	60.7 ± 20.9	62 ± 19*	30 ± 20	1 ± 5		29 ± 19*	108 ± 34
LDH^+/NAD^+ *group 1* (n = 8)	226 ± 66	2 ± 4	50.9 ± 10.3	2 ± 2*	35 ± 14		41.7 ± 17.2	90 ± 20*	93 ± 18

Values are presented as means ± SD. Percent change from one substrate-induced respiratory state to another (columns) is presented across all titration protocols (rows) used throughout the study. Respiration in absence of adenylates (L_N), capacity for fatty acid oxidation (P_{ETF}), lactate (Lac), LDH, and pyruvate (Pyr). *Significant difference in specific respiration state between groups, $P < 0.05$.

they have been theoretically rebutted due to the possibility of mLDH depletion during the isolation procedure (14, 19).

Mitochondrial isolation techniques disrupt the native mitochondrial reticular networks in skeletal muscle, producing unnaturally discrete and spherical organelles through unknown and unregulated means (6, 71, 82). This is often associated with an alteration to natural mitochondrial characteristics (14, 19, 21, 48, 61, 67, 70, 90) such as the loss of mitochondrial membrane integrity (5, 93) and the ability to oxidize fatty acids (67). Crude skeletal muscle homogenizations often result in mitochondrial damage but are required for high fractional yield. Maintaining integrity of mitochondrial membranes during isolation using a more temperate homogenization comes at the expense of a lower mitochondrial yield (52). Consequently, the isolation procedure often limits mitochondrial yield, preventing examination of the total mitochondrial population. As such, conclusive deductions regarding mitochondrial utilization of lactate through respirometric investigations using isolated mitochondria are difficult to establish.

Eukaryotic cells represent an integrated multicompartmental system, making it difficult to isolate and study mitochondrial function in living cells. Mitochondrial structure and function are intricately associated (76). Techniques using selective permeabilization in skeletal muscle samples, as applied in the current study, allow direct access to skeletal muscle mitochondria unaffected by the preparation and remain intact within their natural cytoarchitectural environment (33, 51, 53, 69, 71, 77, 80). They also preserve subcellular interactions with the nucleus, endoplasmic reticulum (51), and sarcoplasmic reticulum (71, 89) in addition to the cytoskeleton (53, 61, 80). Metabolic channeling and the intracellular transfer of energy are dependent on these interactions (33, 44, 51, 80).

The current study used saponin treatment to permeabilize the skeletal muscle samples. Saponin preferentially interacts with membranes rich in cholesterol such as the sarcolemmal membrane, which has a greater cholesterol concentration than both the MOM and MIM (24, 47). This preferential perforation of the sarcolemma initiates the loss of soluble cytosolic metabolites, cofactors, enzymes, and coenzymes (49, 53, 78, 89), allowing rapid equilibration with the respiration medium and the ability to manipulate mitochondrial respiration (Fig. 2). The samples in the current study showed LDH concentrations that were ~5% of previously reported LDH activities from the vastus lateralis muscle in both males and females (20, 43), which is similar to the volume density of mitochondria in skeletal muscle (29, 40, 91). The presence of LDH within mitochondria has repeatedly been demonstrated in different tissues and cell types across several species (1, 2, 11, 12, 18, 22, 26–28, 37, 46, 54, 55, 57, 63, 65, 68, 83–85, 92), and there is also evidence that LDH has a genetic tag for mitochondrial allocation (39); yet opposing reports maintain skepticism as to its mitochondrial subsistence (74, 75, 95). The most likely explanation to this discrepancy is the location of LDH in the mitochondria, which appears to reside in the MIS on the outside layer of the MIM (2, 37), making this soluble enzyme easily lost with the disruption of mitochondrial membrane integrity (68). Another possibility that cannot be fully discounted is the tethering of LDH to the outside of the MOM, opposed to within the MIS. The coprecipitation of LDH and mitochondrial respiratory complex IV cytochrome *c* oxidase, however, supports the existence of LDH to be within the MIS (37). The results of the current study closely reflect those presented from rat liver mitochondria that also identified the location of mitochondrial LDH in the intermembrane space (84). While we cannot definitively exclude the possibility that lactate- and NAD^+-stimulated respiration was facilitated by remnants of cytosolic LDH, our data, specifically the required addition of NAD+ in combination with the negligible response to exogenous LDH titration and successful control of mitochondrial membrane integrity, suggest a successful preparation in which cytosolic LDH is routinely lost (49, 51, 80) and the existence of LDH is within the MIS but not the matrix.

Despite the loss of cytosolic LDH concomitant to the perforation of the sarcolemma, the integrity of the mitochondrial outer and inner membranes was confirmed, as exogenous cytochrome *c* had no effect on respiration across all groups (respiration LDH^-/NAD^-, NAD^+/LDH^-, NAD^+/LDH^+, and LDH^+/NAD^+ groups changed by −0.4%, 3.1%, −0.3%, and −0.9%, respectively; Fig. 2). Endogenous cytochrome *c* is lost during skeletal muscle preparations that corrupt mitochondrial membrane integrity. Titration of exogenous cytochrome *c* confirms damage by stimulating respiration (51, 79). Acceptable elevation in respiration following exogenous cytochrome *c* that substantiates membrane integrity is typically between 5 and 15% (51). In addition to our control of mitochondrial membrane integrity, we also show a functional capacity for fatty acid oxidation, which can be altered with mitochondrial isolation (67), as well as discernible responses in respiration to all substrates and inhibitors alike (Fig. 2), all of which demonstrate a complete, intact, and functional respiratory system.

The results presented in this study directly conflict with those reported in a prior study using similar mitochondrial preparation techniques. They reported the inability of rat skeletal muscle to directly oxidize lactate (72). These results were later challenged with the suggestion that mLDH was lost during skeletal muscle preparation (37). While the MOM is rather permeable to molecules up to ~4 kDa that lack a net charge and strong dipoles (6, 23), it is impermeable to large molecules, such as cytochrome *c* (5). Cytochrome *c* has a molecular mass of ~12 kDa, whereas LDH has a molecular mass of ~140 kDa. The loss of mLDH is highly unlikely if much smaller molecules, such as cytochrome *c*, are not lost during mitochondrial preparation (Fig. 2). Unfortunately, Ponsot et al. (72) failed to confirm the integrity of the MOM.

A more likely explanation for the inability of rat skeletal muscle to oxidize lactate in the study by Ponsot et al. (72) is the loss of cytosolic reducing agents during the skeletal muscle preparation. Assuming that a lactate oxidation complex exists in skeletal muscle mitochondria as proposed (37), then the presence of both lactate and NAD^+ are necessary to facilitate the conversion to pyruvate and NADH in the MIS via mLDH. Small molecules in the MIS such as NAD^+ equilibrate with cytosolic concentrations and would be lost during skeletal muscle preparation. We demonstrate that "lactate-stimulated" respiration does increase above P_{EFT} with the addition of NAD^+ (Fig. 2, *B* and *C*); however, lactate-stimulated respiration was not sufficient to support P_{C1}.

The failure of lactate to stimulate respiration independently from exogenous titrations of NAD^+ brought into question our interpretation of the results. Certain mitochondrial proteins, such as sirtuins (SIRT), are bioenergetic cellular sensors that are dependent on NAD^+ concentrations (64). Specifically,

AJP-Endocrinol Metab • doi:10.1152/ajpendo.00476.2012 • www.ajpendo.org

SIRT3, in skeletal muscle mitochondria (66), modifies functional expression of mitochondrial proteins involved in β-oxidation and electron transport by deacetylation (35, 81). Post-translational modification of these enzymes via SIRT3 are reported to alter mitochondrial fatty acid oxidation and oxidative phosphorylation (64). However, we found no difference ($P = 0.958$) between P_{ETF} (with mean ± SD of 20.4 ± 3.5 pmol $O_2 \cdot min^{-1} \cdot mg\ wet\ wt^{-1}$) and respiration following NAD^+ (6 mM) titration into the respiration medium (20.1 ± 3.0 pmol $O_2 \cdot min^{-1} \cdot mg\ wet\ wt^{-1}$). In agreement with the current study's findings, we did observe an increase ($P < 0.001$) when lactate was then added into the respiration medium (46.5 ± 9.5 pmol $O_2 \cdot min^{-1} \cdot mg\ wet\ wt^{-1}$; data not shown).

In conclusion, we have demonstrated the ability of skeletal muscle mitochondria to utilize lactate as a substrate for respiration, which is consistent with the existence of a lactate oxidation complex in human skeletal muscle mitochondria. The data suggest that the mitochondrial utilization of lactate as a substrate requires conversion of lactate to pyruvate prior to entry into the mitochondrial matrix and that this conversion occurs independently of cytosolic LDH. These findings were obtained using a mitochondrial preparation that prevents mitochondrial disruption and provides direct access to intact mitochondria in their natural reticular network with functional subcellular interactions. This allows for data interpretation to be autonomous of possible contamination of nonmitochondrial proteins or loss of mitochondrial-specific proteins.

ACKNOWLEDGMENTS

We sincerely thank Dr. Bengt Saltin for taking skeletal muscle biopsies, Drs. Steen Larsen and Víctor Díaz for the provision of necessary solutions, substrates, and inhibitors on short notice, Dr. Henriette Pilegaard for allowing us access to her laboratory equipment, and Jens Jung Nielsen for technical assistance in the laboratory.

DISCLOSURES

No conflicts of interest, financial or otherwise, are declared by the author(s).

AUTHOR CONTRIBUTIONS

Author contributions: R.A.J. conception and design of research; R.A.J. and A.-K.M. performed experiments; R.A.J. and A.-K.M. analyzed data; R.A.J., A.-K.M., N.B.N., and C.L. interpreted results of experiments; R.A.J. prepared figures; R.A.J. drafted manuscript; R.A.J., A.-K.M., N.B.N., and C.L. edited and revised manuscript; R.A.J., A.-K.M., N.B.N., and C.L. approved final version of manuscript.

REFERENCES

1. **Agostoni A, Vergani C, Villa L.** Intracellular distribution of the different forms of lactic dehydrogenase. *Nature* 209: 1024–1025, 1966.
2. **Baba N, Sharma HM.** Histochemistry of lactic dehydrogenase in heart and pectoralis muscles of rat. *J Cell Biol* 51: 621–635, 1971.
3. **Baldwin KM, Hooker AM, Herrick RE.** Lactate oxidative capacity in different types of muscle. *Biochem Biophys Res Commun* 83: 151–157, 1978.
4. **Bangsbo J, Gollnick PD, Graham TE, Saltin B.** Substrates for muscle glycogen synthesis in recovery from intense exercise in man. *J Physiol* 434: 423–440, 1991.
5. **Benz R.** Permeation of hydrophilic solutes through mitochondrial outer membranes: review on mitochondrial porins. *Biochim Biophys Acta* 1197: 167–196, 1994.
6. **Benz R.** Porin from bacterial and mitochondrial outer membranes. *CRC Crit Rev Biochem* 19: 145–190, 1985.
7. **Bergman BC, Horning MA, Casazza GA, Wolfel EE, Butterfield GE, Brooks GA.** Endurance training increases gluconeogenesis during rest and exercise in men. *Am J Physiol Endocrinol Metab* 278: E244–E251, 2000.
8. **Bergman BC, Wolfel EE, Butterfield GE, Lopaschuk GD, Casazza GA, Horning MA, Brooks GA.** Active muscle and whole body lactate kinetics after endurance training in men. *J Appl Physiol* 87: 1684–1696, 1999.
9. **Bergström J.** Muscle electrolytes in man. *Scand J Clin Lab Invest* 68: 1–110, 1962.
10. **Brand MD, Nicholls DG.** Assessing mitochondrial dysfunction in cells. *Biochem J* 435: 297–312, 2011.
11. **Brandt RB, Laux JE, Spainhour SE, Kline ES.** Lactate dehydrogenase in rat mitochondria. *Arch Biochem Biophys* 259: 412–422, 1987.
12. **Brody IA, Engel WK.** Isozyme histochemistry: the display of selective lactate dehydrogenase isozymes in sections of skeletal muscle. *J Histochem Cytochem* 12: 689–695, 1964.
13. **Brooks GA.** Cell-cell and intracellular lactate shuttles. *J Physiol* 587: 5591–5600, 2009.
14. **Brooks GA.** Lactate shuttle—between but not within cells? *J Physiol* 541: 333–334, 2002.
15. **Brooks GA.** Lactate: Glycolytic end product and oxidative substrate during sustained exercise in mammals—the "lactate shuttle". In: *Circulation, Respiration, and Metabolism: Current Comparative Approaches*, edited by Gilles R. Berlin: Springer-Verlag, 1985, p. 208–218.
16. **Brooks GA.** Mammalian fuel utilization during sustained exercise. *Comp Biochem Physiol B Biochem Mol Biol* 120: 89–107, 1998.
17. **Brooks GA, Butterfield GE, Wolfe RR, Groves BM, Mazzeo RS, Sutton JR, Wolfel EE, Reeves JT.** Decreased reliance on lactate during exercise after acclimatization to 4,300 m. *J Appl Physiol* 71: 333–341, 1991.
18. **Brooks GA, Dubouchaud H, Brown M, Sicurello JP, Butz CE.** Role of mitochondrial lactate dehydrogenase and lactate oxidation in the intracellular lactate shuttle. *Proc Natl Acad Sci USA* 96: 1129–1134, 1999.
19. **Brooks GA, Hashimoto T.** Investigation of the lactate shuttle in skeletal muscle mitochondria. *J Physiol* 584: 705–706; author reply 707–708, 2007.
20. **Burke ER, Cerny F, Costill D, Fink W.** Characteristics of skeletal muscle in competitive cyclists. *Med Sci Sports* 9: 109–112, 1977.
21. **Chretien D, Pourrier M, Bourgeron T, Sene M, Rotig A, Munnich A, Rustin P.** An improved spectrophotometric assay of pyruvate dehydrogenase in lactate dehydrogenase contaminated mitochondrial preparations from human skeletal muscle. *Clin Chim Acta* 240: 129–136, 1995.
22. **Coleman RA, Ramp WK, Toverud SU, Hanker JS.** Electron microscopic localization of lactate dehydrogenase in osteoclasts of chick embryo tibia. *Histochem J* 8: 543–558, 1976.
23. **Colombini M.** VDAC structure, selectivity, dynamics. *Biochim Biophys Acta* 1818: 1457–1465, 2012.
24. **Comte J, Maisterrena B, Gautheron DC.** Lipid composition and protein profiles of outer and inner membranes from pig heart mitochondria. Comparison with microsomes. *Biochim Biophys Acta* 419: 271–284, 1976.
25. **Donovan CM, Pagliassotti MJ.** Quantitative assessment of pathways for lactate disposal in skeletal muscle fiber types. *Med Sci Sports Exerc* 32: 772–777, 2000.
26. **Dubouchaud H, Butterfield GE, Wolfel EE, Bergman BC, Brooks GA.** Endurance training, expression, and physiology of LDH, MCT1, and MCT4 in human skeletal muscle. *Am J Physiol Endocrinol Metab* 278: E571–E579, 2000.
27. **Fahimi HD, Amarasingham CR.** Cytochemical localization of lactic dehydrogenase in white skeletal muscle. *J Cell Biol* 22: 29–48, 1964.
28. **Fahimi HD, Karnovsky MJ.** Cytochemical localization of two glycolytic dehydrogenases in white skeletal muscle. *J Cell Biol* 29: 113–128, 1966.
29. **Ferretti G, Antonutto G, Denis C, Hoppeler H, Minetti AE, Narici MV, Desplanches D.** The interplay of central and peripheral factors in limiting maximal O2 consumption in man after prolonged bed rest. *J Physiol* 501: 677–686, 1997.
30. **Gladden LB.** 200th anniversary of lactate research in muscle. *Exerc Sport Sci Rev* 36: 109–115, 2008.
31. **Gladden LB.** Is there an intracellular lactate shuttle in skeletal muscle? *J Physiol* 582: 899, 2007.
32. **Gladden LB.** Lactate metabolism: a new paradigm for the third millennium. *J Physiol* 558: 5–30, 2004.
33. **Gnaiger E.** Capacity of oxidative phosphorylation in human skeletal muscle: new perspectives of mitochondrial physiology. *Int J Biochem Cell Biol* 41: 1837–1845, 2009.
34. **Graham TE, Saltin B.** Estimation of the mitochondrial redox state in human skeletal muscle during exercise. *J Appl Physiol* 66: 561–566, 1989.

35. **Hallows WC, Lee S, Denu JM.** Sirtuins deacetylate and activate mammalian acetyl-CoA synthetases. *Proc Natl Acad Sci USA* 103: 10230–10235, 2006.
36. **Hashimoto T, Brooks GA.** Mitochondrial lactate oxidation complex and an adaptive role for lactate production. *Med Sci Sports Exerc* 40: 486–494, 2008.
37. **Hashimoto T, Hussien R, Brooks GA.** Colocalization of MCT1, CD147, and LDH in mitochondrial inner membrane of L6 muscle cells: evidence of a mitochondrial lactate oxidation complex. *Am J Physiol Endocrinol Metab* 290: E1237–E1244, 2006.
38. **Henderson GC, Horning MA, Lehman SL, Wolfel EE, Bergman BC, Brooks GA.** Pyruvate shuttling during rest and exercise before and after endurance training in men. *J Appl Physiol* 97: 317–325, 2004.
39. **Holmes RS, Goldberg E.** Computational analyses of mammalian lactate dehydrogenases: human, mouse, opossum and platypus LDHs. *Comput Biol Chem* 33: 379–385, 2009.
40. **Hoppeler H, Howald H, Conley K, Lindstedt SL, Claassen H, Vock P, Weibel ER.** Endurance training in humans: aerobic capacity and structure of skeletal muscle. *J Appl Physiol* 59: 320–327, 1985.
41. **Jacobs RA, Boushel R, Wright-Paradis C, Calbet JA, Robach P, Gnaiger E, Lundby C.** Mitochondrial function in human skeletal muscle following high altitude exposure. *Exp Physiol* doi:10.1113/expphysiol.2012.066092: 2012.
42. **Jacobs RA, Rasmussen P, Siebenmann C, Diaz V, Gassmann M, Pesta D, Gnaiger E, Nordsborg NB, Robach P, Lundby C.** Determinants of time trial performance and maximal incremental exercise in highly trained endurance athletes. *J Appl Physiol* 111: 1422–1430, 2011.
43. **Karlsson J, Diamant B, Saltin B.** Lactate dehydrogenase activity in muscle after prolonged severe exercise in man. *J Appl Physiol* 25: 88–91, 1968.
44. **Kay L, Nicolay K, Wieringa B, Saks V, Wallimann T.** Direct evidence for the control of mitochondrial respiration by mitochondrial creatine kinase in oxidative muscle cells in situ. *J Biol Chem* 275: 6937–6944, 2000.
45. **Kirkwood SP, Munn EA, Brooks GA.** Mitochondrial reticulum in limb skeletal muscle. *Am J Physiol Cell Physiol* 251: C395–C402, 1986.
46. **Kline ES, Brandt RB, Laux JE, Spainhour SE, Higgins ES, Rogers KS, Tinsley SB, Waters MG.** Localization of L-lactate dehydrogenase in mitochondria. *Arch Biochem Biophys* 246: 673–680, 1986.
47. **Korn ED.** Cell membranes: structure and synthesis. *Annu Rev Biochem* 38: 263–288, 1969.
48. **Kunz WS, Kudin A, Vielhaber S, Elger CE, Attardi G, Villani G.** Flux control of cytochrome c oxidase in human skeletal muscle. *J Biol Chem* 275: 27741–27745, 2000.
49. **Kunz WS, Kuznetsov AV, Schulze W, Eichhorn K, Schild L, Striggow F, Bohnensack R, Neuhof S, Grasshoff H, Neumann HW, Gellerich FN.** Functional characterization of mitochondrial oxidative phosphorylation in saponin-skinned human muscle fibers. *Biochim Biophys Acta* 1144: 46–53, 1993.
50. **Kuznetsov AV, Schneeberger S, Seiler R, Brandacher G, Mark W, Steurer W, Saks V, Usson Y, Margreiter R, Gnaiger E.** Mitochondrial defects and heterogeneous cytochrome *c* release after cardiac cold ischemia and reperfusion. *Am J Physiol Heart Circ Physiol* 286: H1633–H1641, 2004.
51. **Kuznetsov AV, Veksler V, Gellerich FN, Saks V, Margreiter R, Kunz WS.** Analysis of mitochondrial function in situ in permeabilized muscle fibers, tissues and cells. *Nat Protoc* 3: 965–976, 2008.
52. **Lanza IR, Nair KS.** Functional assessment of isolated mitochondria in vitro. *Methods Enzymol* 457: 349–372, 2009.
53. **Lin A, Krockmalnic G, Penman S.** Imaging cytoskeleton–mitochondrial membrane attachments by embedment-free electron microscopy of saponin-extracted cells. *Proc Natl Acad Sci USA* 87: 8565–8569, 1990.
54. **Machado de Domenech E, Domenech CE, Aoki A, Blanco A.** Association of the testicular lactate dehydrogenase isozyme with a special type of mitochondria. *Biol Reprod* 6: 136–147, 1972.
55. **Mattisson AG, Johansson RG, Bostrom SL.** The cellular localization of lactate dehydrogenase in skeletal muscle of eel (*Anguilla anguilla*). *Comp Biochem Physiol B* 41: 475–482, 1972.
56. **Mazzeo RS, Brooks GA, Schoeller DA, Budinger TF.** Disposal of blood [1-^{13}C]lactate in humans during rest and exercise. *J Appl Physiol* 60: 232–241, 1986.
57. **McClelland GB, Brooks GA.** Changes in MCT 1, MCT 4, and LDH expression are tissue specific in rats after long-term hypobaric hypoxia. *J Appl Physiol* 92: 1573–1584, 2002.
58. **McPherson A Jr.** Binding of oxamate to the apoenzyme of dogfish M4 lactate dehydrogenase. *J Mol Biol* 76: 528–531, 1973.
59. **Miller BF, Fattor JA, Jacobs KA, Horning MA, Navazio F, Lindinger MI, Brooks GA.** Lactate and glucose interactions during rest and exercise in men: effect of exogenous lactate infusion. *J Physiol* 544: 963–975, 2002.
60. **Miller BF, Fattor JA, Jacobs KA, Horning MA, Suh SH, Navazio F, Brooks GA.** Metabolic and cardiorespiratory responses to "the lactate clamp". *Am J Physiol Endocrinol Metab* 283: E889–E898, 2002.
61. **Milner DJ, Mavroidis M, Weisleder N, Capetanaki Y.** Desmin cytoskeleton linked to muscle mitochondrial distribution and respiratory function. *J Cell Biol* 150: 1283–1298, 2000.
62. **Mole PA, Van Handel PJ, Sandel WR.** Extra O2 consumption attributable to NADH2 during maximum lactate oxidation in the heart. *Biochem Biophys Res Commun* 85: 1143–1149, 1978.
63. **Nakae Y, Stoward PJ, Shono M, Matsuzaki T.** Localisation and quantification of dehydrogenase activities in single muscle fibers of mdx gastrocnemius. *Histochem Cell Biol* 112: 427–436, 1999.
64. **Nogueiras R, Habegger KM, Chaudhary N, Finan B, Banks AS, Dietrich MO, Horvath TL, Sinclair DA, Pfluger PT, Tschop MH.** Sirtuin 1 and sirtuin 3: physiological modulators of metabolism. *Physiol Rev* 92: 1479–1514, 2012.
65. **Novikoff AB, Masek B.** Survival of lactic dehydrogenase and DPNH-diaphorase activities after formol-calcium fixation. *J Histochem Cytochem* 6: 217, 1958.
66. **Onyango P, Celic I, McCaffery JM, Boeke JD, Feinberg AP.** SIRT3, a human SIR2 homologue, is an NAD-dependent deacetylase localized to mitochondria. *Proc Natl Acad Sci USA* 99: 13653–13658, 2002.
67. **Pande SV, Blanchaer MC.** Preferential loss of ATP-dependent long-chain fatty acid activating enzyme in mitochondria prepared using Nagarse. *Biochim Biophys Acta* 202: 43–48, 1970.
68. **Passarella S, de Bari L, Valenti D, Pizzuto R, Paventi G, Atlante A.** Mitochondria and L-lactate metabolism. *FEBS Lett* 582: 3569–3576, 2008.
69. **Pesta D, Gnaiger E.** High-resolution respirometry. OXPHOS protocols for human cell cultures and permeabilized fibres from small biopsies of human muscle. *Mitochondrial Bioenergetics: Methods and Protocols* 810: 25–58, 2011.
70. **Picard M, Ritchie D, Wright KJ, Romestaing C, Thomas MM, Rowan SL, Taivassalo T, Hepple RT.** Mitochondrial functional impairment with aging is exaggerated in isolated mitochondria compared with permeabilized myofibers. *Aging Cell* 9: 1032–1046, 2010.
71. **Picard M, Taivassalo T, Gouspillou G, Hepple RT.** Mitochondria: isolation, structure and function. *J Physiol* 589: 4413–4421, 2011.
72. **Ponsot E, Zoll J, N'Guessan B, Ribera F, Lampert E, Richard R, Veksler V, Ventura-Clapier R, Mettauer B.** Mitochondrial tissue specificity of substrates utilization in rat cardiac and skeletal muscles. *J Cell Physiol* 203: 479–486, 2005.
73. **Popinigis J, Antosiewicz J, Crimi M, Lenaz G, Wakabayashi T.** Human skeletal muscle: participation of different metabolic activities in oxidation of L-lactate. *Acta Biochim Pol* 38: 169–175, 1991.
74. **Rasmussen HN, van Hall G, Rasmussen UF.** Lactate dehydrogenase is not a mitochondrial enzyme in human and mouse vastus lateralis muscle. *J Physiol* 541: 575–580, 2002.
75. **Sahlin K, Fernstrom M, Svensson M, Tonkonogi M.** No evidence of an intracellular lactate shuttle in rat skeletal muscle. *J Physiol* 541: 569–574, 2002.
76. **Saks V, Guzun R, Timohhina N, Tepp K, Varikmaa M, Monge C, Beraud N, Kaambre T, Kuznetsov A, Kadaja L, Eimre M, Seppet E.** Structure-function relationships in feedback regulation of energy fluxes in vivo in health and disease: mitochondrial interactosome. *Biochim Biophys Acta* 1797: 678–697, 2010.
77. **Saks VA, Belikova YO, Kuznetsov AV.** In vivo regulation of mitochondrial respiration in cardiomyocytes: specific restrictions for intracellular diffusion of ADP. *Biochim Biophys Acta* 1074: 302–311, 1991.
78. **Saks VA, Kaambre T, Sikk P, Eimre M, Orlova E, Paju K, Piirsoo A, Appaix F, Kay L, Regitz-Zagrosek V, Fleck E, Seppet E.** Intracellular energetic units in red muscle cells. *Biochem J* 356: 643–657, 2001.
79. **Saks VA, Vasil'eva E, Belikova Yu O, Kuznetsov AV, Lyapina S, Petrova L, Perov NA.** Retarded diffusion of ADP in cardiomyocytes: possible role of mitochondrial outer membrane and creatine kinase in cellular regulation of oxidative phosphorylation. *Biochim Biophys Acta* 1144: 134–148, 1993.
80. **Saks VA, Veksler VI, Kuznetsov AV, Kay L, Sikk P, Tiivel T, Tranqui L, Olivares J, Winkler K, Wiedemann F, Kunz WS.** Permeabilized cell

and skinned fiber techniques in studies of mitochondrial function in vivo. *Mol Cell Biochem* 184: 81–100, 1998.
81. **Schwer B, Bunkenborg J, Verdin RO, Andersen JS, Verdin E.** Reversible lysine acetylation controls the activity of the mitochondrial enzyme acetyl-CoA synthetase 2. *Proc Natl Acad Sci USA* 103: 10224–10229, 2006.
82. **Schwerzmann K, Hoppeler H, Kayar SR, Weibel ER.** Oxidative capacity of muscle and mitochondria: correlation of physiological, biochemical, and morphometric characteristics. *Proc Natl Acad Sci USA* 86: 1583–1587, 1989.
83. **Sjodin B.** Lactate dehydrogenase in human skeletal muscle. *Acta Physiol Scand* Suppl 436: 1–32, 1976.
84. **Skilleter DN, Kun E.** The oxidation of L-lactate by liver mitochondria. *Arch Biochem Biophys* 152: 92–104, 1972.
85. **Szczesna-Kaczmarek A.** Regulating effect of mitochondrial lactate dehydrogenase on oxidation of cytoplasmic NADH via an "external" pathway in skeletal muscle mitochondria. *Int J Biochem* 24: 657–661, 1992.
86. **van Hall G.** Lactate kinetics in human tissues at rest and during exercise. *Acta Physiol (Oxf)* 199: 499–508, 2010.
87. **Van Hall G, Jensen-Urstad M, Rosdahl H, Holmberg HC, Saltin B, Calbet JA.** Leg and arm lactate and substrate kinetics during exercise. *Am J Physiol Endocrinol Metab* 284: E193–E205, 2003.
88. **van Hall G, Stromstad M, Rasmussen P, Jans O, Zaar M, Gam C, Quistorff B, Secher NH, Nielsen HB.** Blood lactate is an important energy source for the human brain. *J Cereb Blood Flow Metab* 29: 1121–1129, 2009.
89. **Veksler VI, Kuznetsov AV, Sharov VG, Kapelko VI, Saks VA.** Mitochondrial respiratory parameters in cardiac tissue: a novel method of assessment by using saponin-skinned fibers. *Biochim Biophys Acta* 892: 191–196, 1987.
90. **Villani G, Greco M, Papa S, Attardi G.** Low reserve of cytochrome c oxidase capacity in vivo in the respiratory chain of a variety of human cell types. *J Biol Chem* 273: 31829–31836, 1998.
91. **Vogt M, Puntschart A, Geiser J, Zuleger C, Billeter R, Hoppeler H.** Molecular adaptations in human skeletal muscle to endurance training under simulated hypoxic conditions. *J Appl Physiol* 91: 173–182, 2001.
92. **Walker DG, Seligman AM.** The use of formalin fixation in the cytochemical demonstration of succinic and DPN- and TPN-dependent dehydrogenases in mitochondria. *J Cell Biol* 16: 455–469, 1963.
93. **Wicker U, Bucheler K, Gellerich FN, Wagner M, Kapischke M, Brdiczka D.** Effect of macromolecules on the structure of the mitochondrial inter-membrane space and the regulation of hexokinase. *Biochim Biophys Acta* 1142: 228–239, 1993.
94. **Willis WT, Thompson A, Messer JI, Thresher JS.** Vmax of mitochondrial electron shuttles in rat skeletal muscle and liver. *Med Sci Sports Exerc* 35: S396, 2003.
95. **Yoshida Y, Holloway GP, Ljubicic V, Hatta H, Spriet LL, Hood DA, Bonen A.** Negligible direct lactate oxidation in subsarcolemmal and intermyofibrillar mitochondria obtained from red and white rat skeletal muscle. *J Physiol* 582: 1317–1335, 2007.

Journals of Gerontology: BIOLOGICAL SCIENCES
Cite journal as: J Gerontol A Biol Sci Med Sci
doi:10.1093/gerona/gls335

Fast-Twitch Glycolytic Skeletal Muscle Is Predisposed to Age-Induced Impairments in Mitochondrial Function

Robert A. Jacobs,[1,2,4] Víctor Díaz,[1–3] Lavinia Soldini,[4] Thomas Haider,[2] Martin Thomassen,[5] Nikolai B. Nordsborg,[5] Max Gassmann,[1,2,6] and Carsten Lundby[1,4]

[1]Zurich Center for Integrative Human Physiology (ZIHP) and
[2]Institute of Veterinary Physiology, Vetsuisse Faculty, University of Zurich, Switzerland.
[3]Department of Health and Human Performance, Universidad Politécnica de Madrid, Spain.
[4]Institute of Physiology, University of Zurich, Switzerland.
[5]Department of Exercise and Sport Sciences, University of Copenhagen, Copenhagen, Denmark.
[6]Universidad Peruana Cayetano Heredia (UPCH), Lima, Peru.

Address correspondence to Robert A. Jacobs, MSc, Institute of Veterinary Physiology and Zurich Center for Integrative Human Physiology (ZIHP), Winterthurerstrasse 260, CH-8057 Zurich, Switzerland. E-mail: jacobs@vetphys.uzh.ch

The etiology of mammalian senescence is suggested to involve the progressive impairment of mitochondrial function; however, direct observations of age-induced alterations in actual respiratory chain function are lacking. Accordingly, we assessed mitochondrial function via high-resolution respirometry and mitochondrial protein expression in soleus, quadricep, and lateral gastrocnemius skeletal muscles, which represent type 1 slow-twitch oxidative muscle (soleus) and type 2 fast-twitch glycolytic muscle (quadricep and gastrocnemius), respectively, in young (10–12 weeks) and mature (74–76 weeks) mice. Electron transport through mitochondrial complexes I and III increases with age in quadricep and gastrocnemius, which is not observed in soleus. Mitochondrial coupling efficiency during respiration through complex I also deteriorates with age in gastrocnemius and shows a tendency ($p = .085$) to worsen in quadricep. These data demonstrate actual alterations in electron transport function that occurs with age and are dependent on skeletal muscle type.

Key Words: Mitochondria—Respiratory chain—Function theory of aging.

Received October 2, 2012; Accepted December 19, 2012

Decision Editor: Rafael de Cabo, PhD

An inherent flaw of the bioenergetic reliance on aerobic metabolism to sustain life is the corollary oxidant production (1), and consequently mitochondria serve as the primary source of in vivo oxidant production (2–5). Mitochondria-derived reactive oxygen species are largely accounted for by superoxide (O_2^-) production into the mitochondrial matrix at mitochondrial complex I (CI) (6–8) and into both the matrix and mitochondrial intermembrane space at mitochondrial complex III (CIII) (9–14). The progression of reactive oxygen species production beyond hormetic concentrations precipitates deleterious and indiscriminate oxidation of nucleic acids, proteins, and lipids (5,15,16). These pernicious effects then correspondingly impair mitochondrial function, which result in greater oxidant production, and so on leading to a "vicious cycle" and eminent cellular demise (4,15,17). The mitochondrial theory of aging asserts that the biological aging process is facilitated by this progressive accrual of mitochondrial DNA (mtDNA) damage and reciprocal decline of mitochondrial function (18). Although evidence of increasing mtDNA alteration with age is supported by the literature, data suggestive of an impairment of mitochondrial function with aging are inconsistent.

Senescence corresponds with mounting indications of nuclear and mtDNA damage in both humans and animals (19–22). Moreover, mtDNA facilitated mutations lead to premature aging in mice (23) and humans (24). Transgenic studies show that reducing whole-body or tissue-specific mitochondrial superoxide dismutase, the enzyme that catalyses the dismutation of mitochondria-generated O_2^- to H_2O_2 (25), increases evidence of oxidative damage and premature aging (26–28). Alternatively, overexpression of endogenous mitochondrial catalase lessens oxidant damage, reduces an overall burden of disease (29), and increases life span (30). Indications of impaired mitochondrial function extending beyond measures of oxidant production or damage are lacking. Whether there are age-induced alterations in actual electron transport function remain unanswered (4).

Reports of functional impairments to mitochondria with aging are seemingly paradoxical. Mitochondrial enzymatic expression, protein synthesis, volume density, and oxidative capacity have been reported to decrease with age in humans and animals quadricep (QUAD) skeletal muscle (19,31–37) as well as in a collection of lower limb skeletal muscle representative of mixed glycolytic and oxidative fibers (38–40). The age-induced loss of mitochondrial protein expression and oxidative capacity, however, fails to decrease

in skeletal muscle primarily composed of type 2 fast-twitch glycolytic fibers (41–43). Modifications of mitochondrial content also differ with aging between *m. vastus lateralis* and *m. gastrocnemius* in humans (44). These differences have led to speculation that mitochondrial impairment with aging may differ across different skeletal muscle types (19,45). In vivo metabolic imaging techniques have provided preliminary evidence to support this assumption with skeletal muscle primarily composed of fast-twitch fibers exhibiting the greatest age-induced impairments (46,47).

Accordingly, the aim of this study is to examine mitochondrial protein expression along with analysis of respiratory capacity and control via high-resolution respirometry. Respirometric analyses using isolated mitochondrial preparations have been reported to exaggerate age-induced changes in mitochondrial function (48). Mitochondrial isolation techniques disturb native mitochondrial reticular networks in skeletal muscle (49) producing atypical and individual organelles through unregulated means (50–52). This alters innate mitochondrial characteristics (48,53–60) such as the loss of mitochondrial membrane integrity (61,62) and the ability to oxidize fatty acids (56). For respirometric analysis, we use saponin-permeabilized skeletal muscle preparations. This preparation allows for direct access to skeletal muscle mitochondria while maintaining both the cytocellular ultrastructure (51,63–68) and subcellular interactions with mitochondria (51,53,64,67–69). Cellular bioenergetics and metabolic channeling are predicated upon these factors (63,64,67,70). We have previously demonstrated that respirometric analysis using this in situ preparation in conjunction with biochemical assessment of mitochondria is more appropriate when attempting to differentiate between isolated changes in enzymatic expression versus an alteration in the functional capacity of a subcellular system (71–74). Accordingly, this specific mitochondrial preparation serves as the best model to examine respiratory capacity and control with aging. Respirometric analyses were carried out on soleus (SOL), QUAD, and lateral gastrocnemius (GAST) skeletal muscles, which represent type 1 slow-twitch oxidative muscle (SOL) and type 2 fast-twitch glycolytic muscle (QUAD and GAST), respectively, in young (10–12 weeks) and mature (74–76 weeks) mice. Taking into account the inconsistent reports of mitochondrial impairment with age across different skeletal muscles, we hypothesize that alterations in mitochondrial function with age vary across skeletal muscle types, explaining the seemingly inconsistent past findings on this topic.

Experimental Procedures

Ethical Approval

The experimental protocols using laboratory animals were approved by the Kantonales Veterinäramt Zürich (217/2010) and were performed in accordance with the Swiss animal protection laws and institutional guidelines.

Experimental Animals

A total of 24 male C57Bl/6 mice were used in the completion of this study, 12 young (10–12 week old) and 12 mature (74–76 week old) mice. All mice were housed in standard rodent cages (T3) with fixed temperature (21 ± 1°C), free access to food and water, and a 12-hour light–dark cycle. Animals were euthanized by means of carbon dioxide followed by rapid excision of SOL, QUAD, and GAST. These muscles represent a type 1 slow-twitch oxidative muscle (SOL) and a type 2 fast-twitch glycolytic muscle (QUAD and GAST), respectively. The skeletal muscles from one leg were quickly excised and placed in ice-cold biopsy solution for immediate respirometric analyses. The corresponding skeletal muscles from the opposite hind limb were then removed, frozen in liquid nitrogen, and stored at −80°C until processed for protein expression analysis (see Muscle Lysate Preparation, and Sodium Dodecyl Sulfate–Polyacrylamide Gel Electrophoresis and Western Blotting sections).

Muscle Lysate Preparation

The muscle samples were homogenized (Qiagen TissueLyser II, Retsch, Haan, Germany) in a fresh batch of buffer containing the following (in millimolar): 10% glycerol, 20 sodium-pyrophosphate, 150 NaCl, 50 4-(2-hydroxyethyl) piperazine-1-ethanesulfonic acid (HEPES) (pH 7.5), 1% NP-40, 20 β-glycerophosphate, 2 Na_3VO_4, 10 NaF, 2 phenylmethanesulfonyl fluoride, 1 ethylenediaminetetraacetic acid (pH 8.0), 1 ethylene glycol-bis(2-aminoethylether)-N,N,N′,N′-tetraacetic acid (EGTA) (pH 8.0), 10 µg/mL aprotinin, 10 µg/mL leupeptin, and 3 benzamidine. Afterward samples were rotated end over end for 1 hour at 4°C and centrifuged at 16,500*g* for 30 minutes at 4°C, and the supernatant (lysate) was used for further analysis. Total protein concentration in each sample was determined by a bovine serum albumin standard kit (Pierce, Rockford, IL), and all samples were diluted to the same protein concentration in ddH_2O and a modified 6× Laemmli buffer (7 mL 0.5 M Tris base [pH 6.8], 3 mL glycerol, 0.93 g dithiothreitol, 1 g sodium dodecyl sulfate, and 1.2 mg bromophenol blue).

Sodium Dodecyl Sulfate–Polyacrylamide Gel Electrophoresis and Western Blotting

Methods have been previously described in detail (75–77). Equal amounts (10 µg) of total muscle lysate proteins, determined during optimization of the different antibodies, were loaded in each well. Samples were loaded together with protein markers (Precision Plus All Blue and Dual Color, Bio-Rad Laboratories, Hercules, CA) on precasted gels (Bio-Rad Laboratories). Proteins were separated by sodium dodecyl sulfate–polyacrylamide gel electrophoresis and

semidry transferred to a polyvinylidene fluoride membrane (Millipore). The membranes were blocked in either 2% skimmed milk or 3% bovine serum albumin in Tris-buffered saline, including 0.1% Tween 20 before an overnight incubation in primary antibody at 4°C. Thereafter, membranes were washed in Tris-buffered saline, including 0.1% Tween 20 and incubated for 1 hour at room temperature in horseradish peroxidase-conjugated secondary antibody. Membranes were then washed 3 × 15 minutes in Tris-buffered saline, including 0.1% Tween 20 before the bands were visualized with ECL (Millipore) and recorded with a digital camera (ChemiDoc MP Imaging System, Bio-Rad). Quantification of the Western blot band intensity was done using the Image Lab software programme (Bio-Rad) and determined as the total band intensity minus the background intensity. Primary antibodies were optimized by use of mouse muscle lysates to secure that the protein amount loaded would result in band signal intensities localized on the steep and linearly part of a standard curve. To determine changes in total protein expression, the following antibodies were used with the localization of the quantified signal noted: 3-hydroxyacyl coenzyme a dehydrogenase (HAD): 83 kDa, polyclonal ab54477 (Abcam, UK); Mitochondrial Complex IV subunit 4, COXIV, (CIV): 16 kDa, monoclonal sc-58348 (Santa Cruz Biotechnology, Santa Cruz, CA); and Mitochondrial Complex I subunit NDUFB8 (CI): 20 kDa (monoclonal ab110242), Mitochondrial Complex II, Succinate Dehydrogenase complex subunit B (CII): 30 kDa (monoclonal ab14714), Mitochondrial Complex III subunit Core 2 (CIII): 45 kDa (monoclonal ab14745), Mitochondrial Complex V ATP Synthase subunit alpha (CV): 55 kDa (monoclonal ab14748) all four included in the MitoProfile Total OXPHOS Human WB Antibody Cocktail (ab110411, Abcam). The secondary antibodies used were horseradish peroxidase-conjugated goat anti-mouse and goat anti-rabbit (P-0447 and P-0448, DAKO, Denmark). All samples from the same muscle type were loaded on the same gel with young and mature muscles mixed. Signal intensity from each muscle sample was normalized to the mean signal intensity of the human standard.

Skeletal Muscle Preparation

Each part was immediately placed in ice-cold biopsy preservation solution containing 2.77 mM CaK_2EGTA buffer, 7.23 mM K_2EGTA buffer, 0.1 µM free calcium, 20 mM imidazole, 20 mM taurine, 50 mM 2-(*N*-morpholino) ethanesulfonic acid hydrate (K-MES), 0.5 mM dithiothreitol, 6.56 mM $MgCl_2$•$6H_2O$, 5.77 mM ATP, and 15 mM phosphocreatine (pH 7.1). Muscle samples were then gently dissected with a pair of fine-tipped forceps achieving a high degree of fiber separation verified microscopically. Chemical permeabilization followed via incubation in 2 mL of biopsy preservation solution with saponin (50 µg/mL) for 30 minutes in 4°C. Last, samples were washed with a mitochondrial respiration medium (MiR05) containing 0.5 mM EGTA, 3 mM $MgCl_2$•$6H_2O$, 60 mM K-lactobionate, 20 mM taurine, 10 mM KH_2PO_4, 20 mM HEPES, 110 mM sucrose, and 1 g/L bovine serum albumin (pH 7.1) for 10 minutes at 4°C.

Mitochondrial Respiration Measurements

Muscle bundles were blotted dry and measured for wet weight in a balance-controlled scale (XS205 DualRange Analytical Balance, Mettler-Toledo AG, Switzerland) maintaining constant relative humidity, providing hydration consistency as well as stability of weight measurements. Respiration measurements were performed in mitochondrial respiration medium 06 (MiR06; MiR05 + catalase 280 IU/mL). Measurements of oxygen consumption were performed at 37°C using the high-resolution Oxygraph-2k (Oroboros, Innsbruck, Austria) with all additions in each substrate, uncoupler, and inhibitor titration protocol added in series. Standardized instrumental calibrations were performed to correct for back diffusion of oxygen into the chamber from the various components, leak from the exterior, oxygen consumption by the chemical medium, and sensor oxygen consumption. Oxygen flux was resolved by software allowing nonlinear changes in the negative time derivative of the oxygen concentration signal (Oxygraph-2k, Oroboros). All experiments were carried out in a hyperoxygenated environment to prevent any potential oxygen diffusion limitation.

Respiratory Titration Protocols

Each titration protocol was specific to the examination of individual aspects of respiratory control through a sequence of coupling and substrate states induced via separate titrations, which were added in series as presented. The concentrations of substrates, uncouplers, and inhibitors used were based on prior experiments conducted for optimization of the titration protocols (71–73). A description of all three protocols is given in Table 1.

Table 1. Respirometric Titration Protocols

1	M: 2 mM	OC: 0.2 mM	ADP: 5 mM	G: 10 mM	S: 10 mM	Cyt C: 10 µM	FCCP: 1.5–3 µM	Rot: 0.5 µM	AmA: 2.5 µM
2	M: 2 mM	P: 5 mM	ADP: 5 mM	Cyt C: 10 µM	FCCP: 1.5–3 µM	Rot: 0.5 µM	AmA: 2.5 µM	—	—
3	Rot: 0.5 µM	S: 10 mM	ADP: 5 mM	Cyt C: 10 µM	FCCP: 1.5–3 µM	AmA: 2.5 µM	—	—	—

Notes: The three different titration protocols utilized in this study. Each row presents the substrate, uncoupler, or inhibitor and concentration titrated into the respiration medium, with all additions occurring sequentially as presented from left to right. ADP = adenosine diphosphate; AmA = antimycin A; Cyt C = cytochrome c; FCCP = carbonyl cyanide *p*-(trifluoromethoxy) phenylhydrazone; G = glutamate; M = malate; OC = octanoyl carnitine; Rot = rotenone; S = succinate.

Titration protocol 1

- Leak respiration in absence of adenylates (L_N) was induced with the addition of malate (2 mM) and octanoyl carnitine (0.2 mM). The L_N state represents the resting oxygen consumption of an unaltered and intact electron transport system (ETS) free of adenylates.
- Maximal electron flow through electron-transferring flavoprotein (ETF) and fatty acid oxidative capacity, P_{ETF}, were both determined following the addition of ADP (5 mM). In the P_{ETF} state, the ETF-linked transfer of electrons requires the metabolism of acetyl-CoA, hence the addition of malate, in order to facilitate convergent electron flow into the Q-junction from both CI and ETF allowing β-oxidation to proceed. The contribution of electron flow through CI is far below capacity and so here the rate-limiting metabolic branch is electron transport through ETF such that malate + octanoyl carnitine + ADP-stimulated respiration is representative of, rather than specific to, electron capacity through ETF (71,78,79).
- Submaximal state 3 respiratory capacity specific to CI, P_{CI}, was induced following the additions of glutamate (10 mM).
- Maximal state 3 respiration, oxidative phosphorylation capacity, P, was then induced with the addition of succinate (10 mM). P demonstrates a naturally intact ETS's capacity to catalyze a sequential set of redox reactions that are partially coupled to the production of ATP via ATP Synthase. P maintains an electrochemical gradient across the inner mitochondrial membrane dictated by the degree of coupling to the phosphorylation system (63,65). This maximal state 3 state represents respiration that is resultant to saturating concentrations of ADP and substrate supply for both CI and succinate dehydrogenase, CII. Convergent electron input to CI and CII provides higher respiratory values compared with the isolated respiration of either CI (pyruvate and/or glutamate + malate or glutamate + malate) or CII (succinate + rotenone) (63, 80). Consequently, P presents more physiological relevance to the study of mitochondrial function (81) and is necessary to establish confirmation of a complete and intact ETS.
- As an internal control for compromised integrity of the mitochondrial preparation, the mitochondrial outer membrane was assessed with the addition of cytochrome c (10 μM). If respiration significantly increased following titration of cytochrome c, then the measurement was removed and not included in statistical analysis. There was no indication of mitochondrial damage in the measurements included in the study as demonstrated by the average 3.5%, 2.9%, 7.5%, 5.3%, 6.3%, and 2.3% change in young and mature QUAD, SOL, and GAST respiration, respectively. All were either below or within the accepted 5%–15% elevation in respiration following exogenous cytochrome c titration, successfully verifying the integrity of the outer mitochondrial membrane (64).
- Phosphorylative restraint of electron transport was assessed by uncoupling ATP Synthase, CV from the ETS with the titration of the proton ionophore, and carbonyl cyanide *p*-(trifluoromethoxy) phenylhydrazone (0.5 μM per addition up to optimum concentrations ranging from 1.5 to 3 μM) reaching ETS capacity. The inner mitochondrial membrane potential is completely collapsed with an open transmembrane proton circuit in the ETS respiratory state. The uninhibited flow of electrons through the respiratory system can, therefore, indirectly serve as an indication of maximal mitochondrial membrane potential.
- Finally, rotenone (0.5 μM) and antimycin A (2.5 μM) were added, in sequence, to terminate respiration by inhibiting CI and CIII, respectively. With CI inhibited, electron flow is specific to CII, providing submaximal state 3 respiration through CII (P_{CII}).
- Inhibition of respiration with antimycin A then allows for the determination and correction of residual oxygen consumption, indicative of nonmitochondrial oxygen consumption in the chamber.

Titration protocol 2.—This titration protocol was necessary for determination of coupling control of electrons through CI.

- L_N–malate (2 mM) and pyruvate (5 mM).
- P_{CI}–ADP (5 mM).
- Internal control for mitochondrial outer membrane integrity–cytochrome c (10 μM). There was no indication of mitochondrial damage in the measurements included in the study as demonstrated by the 0.3%, 1.3%, 0.1%, −0.3%, 4.3%, and −0.1% change in mouse young and mature QUAD, SOL, and GAST respiration, respectively.
- ETS–carbonyl cyanide *p*-(trifluoromethoxy) phenylhydrazone (0.5 μM per addition up to optimum concentrations ranging from 1.5 to 3 μM).
- CI inhibition–rotenone (0.5 μM).
- Residual oxygen consumption–antimycin A (2.5 μM).

Titration protocol 3.—This titration protocol was necessary for determination of coupling control of electrons through CII.

- CI inhibition–rotenone (0.5 μM).
- L_N–succinate (10 mM).
- P_{CII}–ADP (5 mM).
- Internal control for mitochondrial outer membrane integrity–cytochrome c (10 μM). There was no indication of mitochondrial damage in the measurements included in the study as demonstrated by the 7.3%, 2.6%, 9.8%, 13.4%, 5.1%, and 7.3% change in mouse young and mature QUAD, SOL, and GAST respiration, respectively.

- ETS–carbonyl cyanide *p*-(trifluoromethoxy) phenylhydrazone (0.5 μM per addition up to optimum concentrations ranging from 1.5 to 3 μM).
- Residual oxygen consumption–antimycin A (2.5 μM).

Respirometric values representing P_{CI} and P_{CII} did not differ across titration protocols. Consequently all P_{CI} and P_{CII} values achieved with the titration protocols for 2 and 3, respectively, were grouped with complementing respiratory state from titration protocol 1.

Data Analysis

All mass-specific respirometric values were controlled to account for the differences in mitochondrial content, as indicated by CII protein expression, across age and fiber types. In doing so, all CII protein expression data were adjusted to a value of 1. The degree by which the protein expression had to be adjusted to equal 1 was then applied to all mass-specific respirometric values corresponding with the appropriate age and skeletal muscle type, respectively. Values of P_{CI} controlling for CI protein expression, P_{ETF} controlling for HAD protein expression, and P controlling for CIII protein expression all were also adjusted using the same method.

For all statistical evaluations, a p value of less than .05 was considered significant. Differences in respiratory capacities and protein expression with age and across skeletal muscle groups were initially compared using a two-way analysis of variance. When an analysis of variance was significant, differences in respiratory capacities and protein expression with age and across skeletal muscle groups were evaluated using pairwise comparisons with a Bonferroni adjustment (SPSS Statistics 17.0, SPSS, Inc., Chicago, IL). Indices of mitochondrial efficiency did not express a Gaussian distribution and therefore a Kruskal–Wallis analysis of variance and the U-Mann Whitney tests were used to reveal differences between younger and older muscle as well as comparisons across muscle groups within the respective age groups.

Results

Skeletal Muscle Protein Expression

As shown in Figure 1, protein expression for all mitochondrial enzymes was greatest in the slow-twitch SOL muscle. In young animals only the expression of CII and CIV differed between QUAD and GAST, both of which were lost with age. Only SOL expressed a change in mitochondrial protein content with age as CI, CII, and CV all increased (Figure 1A, B, and E, respectively). Though no significant changes in protein expression of CIII (Figure 1C) or CIV (Figure 1D) were apparent, both complexes showed a tendency to diminish with age in GAST (p = .060 and .063, respectively). Collectively, this analysis illustrates that the protein content for enzymes involved in mitochondrial oxidative phosphorylation is largely unaffected in primarily fast-twitch glycolytic muscle (QUAD and GAST) but slightly increased in primarily slow-twitch oxidative muscle (SOL) with age.

Mitochondrial Respiration

Main effects of age on mass-specific respiration (pmol O_2/min/mg ww) were observed for P_{ETF} (p = .011) and P_{CII} (p = .008). This was reflected by the higher P_{ETF} and P_{CII} in mature QUAD (p = .031 and .037, respectively; Figure 2E) and GAST (p = .011 and .016, respectively; Figure 2I) versus their younger counterparts. There was also a main effect of muscle type on mass-specific respiration as SOL has greater respiration across all states compared with both QUAD and GAST (p < .001; Figure 2A).

Mass-specific respiration does not take into account differences in mitochondrial content between samples (Figure 1). Accordingly, all respirometric analyses were adjusted for CII protein content, a biomarker shown to express the best concordance with mitochondrial content and total cristae area as measured by transmission electron microscopy as well as myocellular respiratory capacity over protein concentrations for all other mitochondrial complexes (82). When controlling respiration to mitochondrial content, the main effect of age on respiration capacity (pmol O_2/min/CII) appeared to be silenced by the divergent fluctuations in mitochondrial function across skeletal muscle types in response to age. Respiratory states representing P_{CI}, P, and ETS in QUAD and P_{CI}, P, ETS, and P_{CII} in SOL all lost respiratory capacity in response to age (Figure 2F and H). Conversely, GAST increased respiratory capacity at every respiratory state measured (Figure 2J) in response to age. The differences in respiratory capacity when controlling for mitochondrial content across skeletal muscle in younger and older mice are shown in Figure 2B and D, respectively.

Respiratory Capacity and Coupling Control Specific to Mitochondrial Complexes I and III

Electron transport and control specifically through CI and CIII are of particular interest as reactive oxygen species production at each respective complex accounts for the majority of mitochondria-specific oxidant production (9–14). In order to isolate analysis to these specific complexes, all P_{CI} values, including respirometric values from both titration protocols 1 and 2, and maximal state 3 respirometric values, P, were adjusted to account for the differences in CI and CIII protein expression, respectively, with age and across muscle groups (Figure 1A and C).

There were main effects of age (p = .001) on P_{C1} respiration when controlling for CI expression (pmol O_2/min/CI), which increased with age in both QUAD and GAST (p < .001) and decreased in SOL (p = .003; Figure 3A–C). The

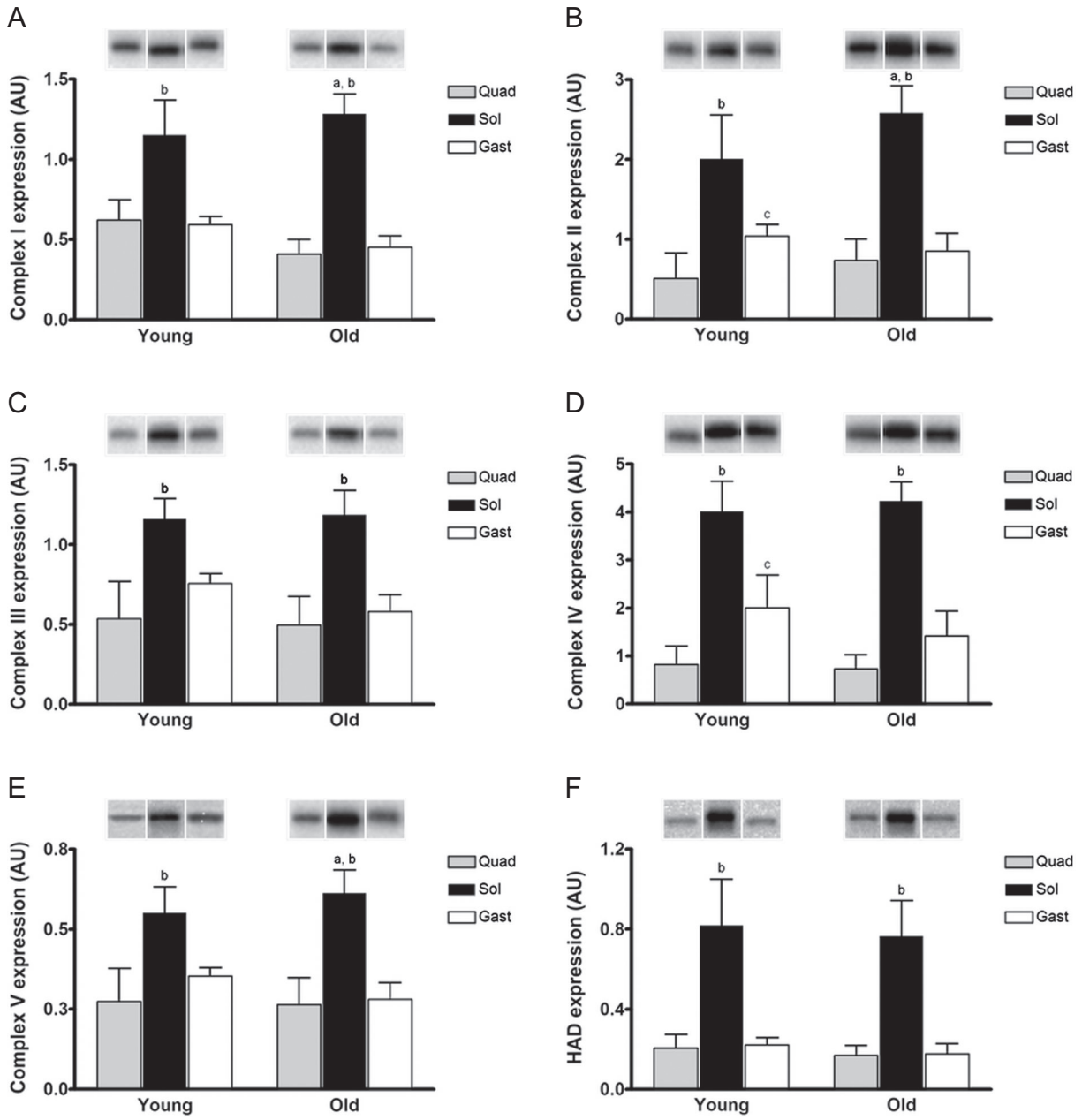

Figure 1. Protein expression of mitochondrial complexes and proteins with age. Skeletal muscle protein expression determined in young (10–12 weeks) and mature (74–76 weeks) C57Bl/6 mice. Protein expression for (A) CI, mitochondrial complex I or NADH dehydrogenase; (B) CII, mitochondrial complex II or succinate dehydrogenase; (C) CIII, mitochondrial complex III or cytochrome bc_1 complex; (D) CIV, mitochondrial complex IV or cytochrome c oxidase; (E) CV, mitochondrial complex V or ATP Synthase; and (F) HAD, 3-hydroxyacyl coenzyme a dehydrogenase, is illustrated in response to age and across skeletal muscles. Example blots for one analysis from one animal are shown above the graph. Values are means ± *SD*. In figure, a indicates significant difference in age within a skeletal muscle, $p < .05$; b shows significant difference between soleus (black) from both quadricep (grey) and lateral gastrocnemius (white) within the same age, $p < .05$; and c indicates differences between quadricep and gastrocnemius within the same age, $p < .05$.

coupling efficiency during P_{CI} respiration deteriorated with age in GAST ($p = .043$) and showed a tendency to diminish in QUAD as well ($p = .085$; Table 2). Though no differences in respiratory capacity were observed across all young muscle groups during P_{CI} when controlling for CI, the coupling control was superior in young QUAD and GAST over SOL ($p = .021$ and .009, respectively). In the older muscle both QUAD and GAST presented with higher P_{CI} than SOL ($p < .001$) and both, again, expressed a tighter coupling efficiency than SOL ($p = .004$ and $p < .001$).

There were also main effects of age ($p = .009$) on maximal state 3 respiration and oxidative phosphorylation capacity, P, when controlling for CIII protein expression (pmol O_2/min/CIII) (Figure 4A–C). Respiration capacity in both QUAD and GAST increased with age ($p = .009$ and .001, respectively), whereas SOL did not change ($p = .144$).

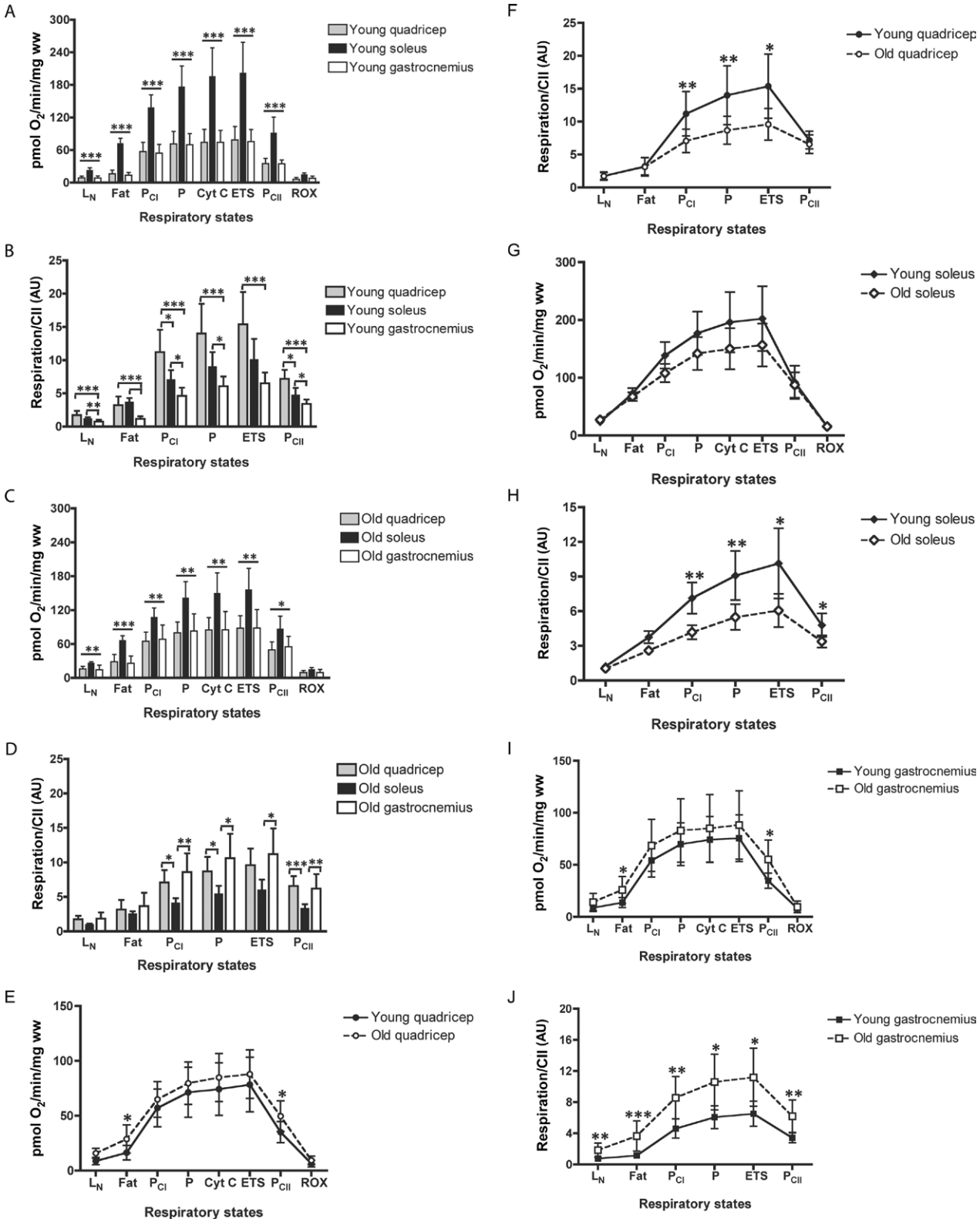

Figure 2. Skeletal muscle respirometric analysis. Mass-specific respiration across muscle groups in (A) young and (C) mature animals. Mass-specific respiration with age in mouse (E) quadricep, (G) soleus, and (I) gastrocnemius skeletal muscles. Mitochondrial-specific respiration controlling for mitochondrial content, as assessed by mitochondrial complex II protein expression (82), across skeletal muscles in (B) young and (D) mature animals. Mitochondrial-specific respiration with age in mouse (F) quadricep, (H) soleus, and (J) gastrocnemius skeletal muscles. L_N, leak respiration without adenylates; P_{EFT}, maximal fatty acid oxidation; P_{CI}, submaximal state 3 respiration through mitochondrial complex I (CI); P, maximal state 3 respiration–oxidative phosphorylation capacity; Cyt C, cytochrome c, internal test of mitochondrial membrane integrity; ETS, electron transport system capacity; and P_{CII}, submaximal state 3 respiration through mitochondrial complex II (CII). Data presented as mean ± *SD*. *, **, and *** indicate significant difference of $p \leq .05$, $p \leq .01$, and $p \leq .001$, respectively.

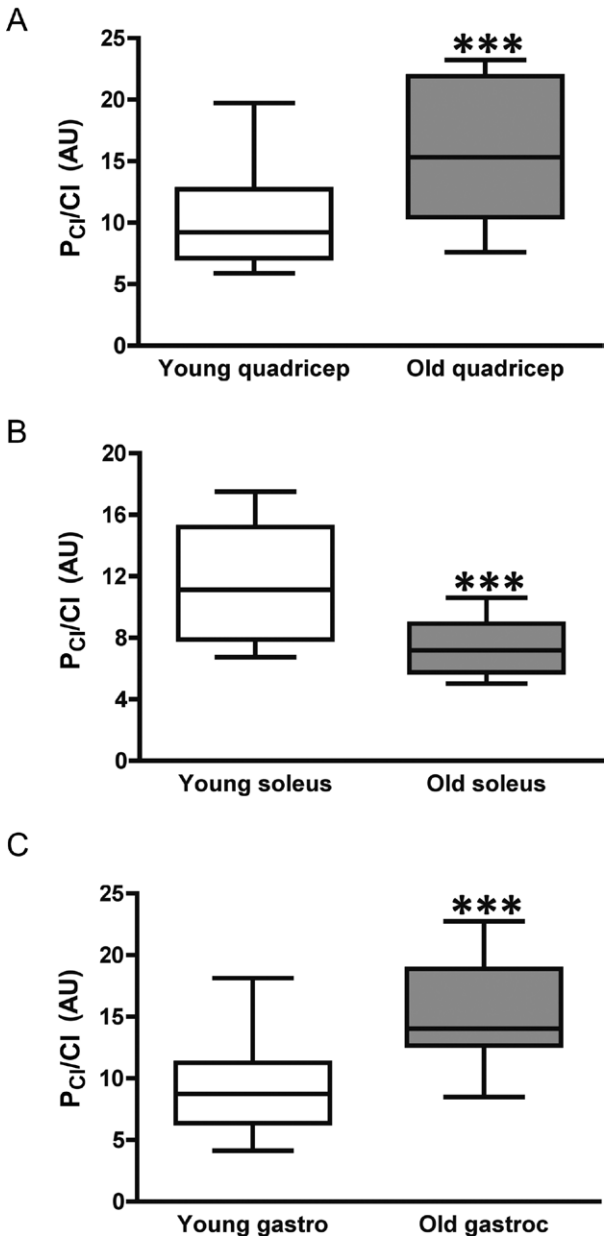

Figure 3. Respiratory capacity and control through mitochondrial complex I (CI). Submaximal state 3 respiratory capacity specific to CI (P_{CI}) when controlling for CI protein expression with age in (A) quadricep, (B) soleus, and (C) gastrocnemius skeletal muscles. *, **, and *** indicate significant difference of age, $p \leq .05$, $p \leq .01$, and $p \leq .001$, respectively.

Differences across young muscle groups were evident between both QUAD and SOL versus GAST ($p = .023$ and .001, respectively) and across mature muscle groups with QUAD greater than SOL ($p = .020$).

Respiratory Capacity and Control Specific to β-Oxidation

Only values of fatty acid oxidative capacity, P_{ETF}, were adjusted to account for the differences in HAD protein expression (Figure 1D). P_{ETF} (pmol O_2/min/HAD) increased with age in QUAD ($p = .004$) and showed a tendency to increase in GAST ($p = .065$) (Figure 5). Differences across young and mature muscle groups were evident with both QUAD and GAST far below SOL ($p < .001$). Though P_{ETF}, when controlling for HAD, did not change in SOL (Figure 5), the coupling efficiency during β-oxidation diminished with age (Table 2). Despite this decrease with age, the coupling control of electron transport during β-oxidation in SOL was significantly better than younger and older QUAD ($p = .01$ and .05, respectively). Coupling control during fat oxidation did not change with age in QUAD or GAST, though it did differ between young SOL and GAST ($p = .05$). This difference was lost with age (Table 2).

Discussion

The aim of this study was to analyze the effect of biological aging on respiratory capacities and mitochondrial coupling control across different skeletal muscle types as a function of age. Our main findings are (i) mitochondrial function is dependent on skeletal muscle type, irrespective of age; (ii) submaximal state 3 respiration specific to CI, P_{CI}, increased in both QUAD and GAST but decreased in SOL when controlling for complex I protein expression; (iii) coupling control during P_{CI} was also lost with age in GAST and indicated a tendency for deterioration in QUAD but remained unchanged in SOL; (iv) maximal state 3 respiration and oxidative phosphorylation capacity, P, increased with age in QUAD and GAST but not SOL when controlling for CIII protein expression; and finally (v) although the capacity for fat respiration increased with age in QUAD when controlling for differences in HAD protein expression across skeletal muscle types, the

Table 2. Mitochondrial Coupling Efficiency With Age

	Young QUAD	Mature QUAD	Young SOL	Mature SOL	Young GAST	Mature GAST
LCR_{ETF}	0.54±0.16†	0.53±0.18†	0.33±0.09*,†,‡	0.41±0.05*,†	0.57±0.29‡	0.52±0.10
LCR_{CI}	0.15±0.03†,§	0.20±0.07†,§	0.24±0.11†,‡	0.29±0.06†,‡	0.12±0.06*,‡	0.17±0.03*,‡
LCR_{CII}	0.69±0.13	0.76±0.07	0.54±0.25	0.72±0.11	0.68±0.19	0.66±0.11

Notes: Leak control ratios (LCR) as indices of mitochondrial coupling and respiratory control across different skeletal muscles with age. GAST = gastrocnemius; LCR_{ETF} = coupling efficiency of electron transfer through electron-transferring flavoprotein (ETF) during β-oxidation; P_{CI} = coupling efficiency of electron transfer during respiration through mitochondrial complex I (CI); P_{CII} = coupling efficiency of electron transfer during respiration through mitochondrial complex II (CII); QUAD = quadriceps; SOL = soleus.

*,†,‡Effect of age, difference between QUAD vs SOL, and difference in SOL vs GAST, respectively, with $p < .05$.

§Difference with age, $p = .085$. Data are presented as mean ± *SD*.

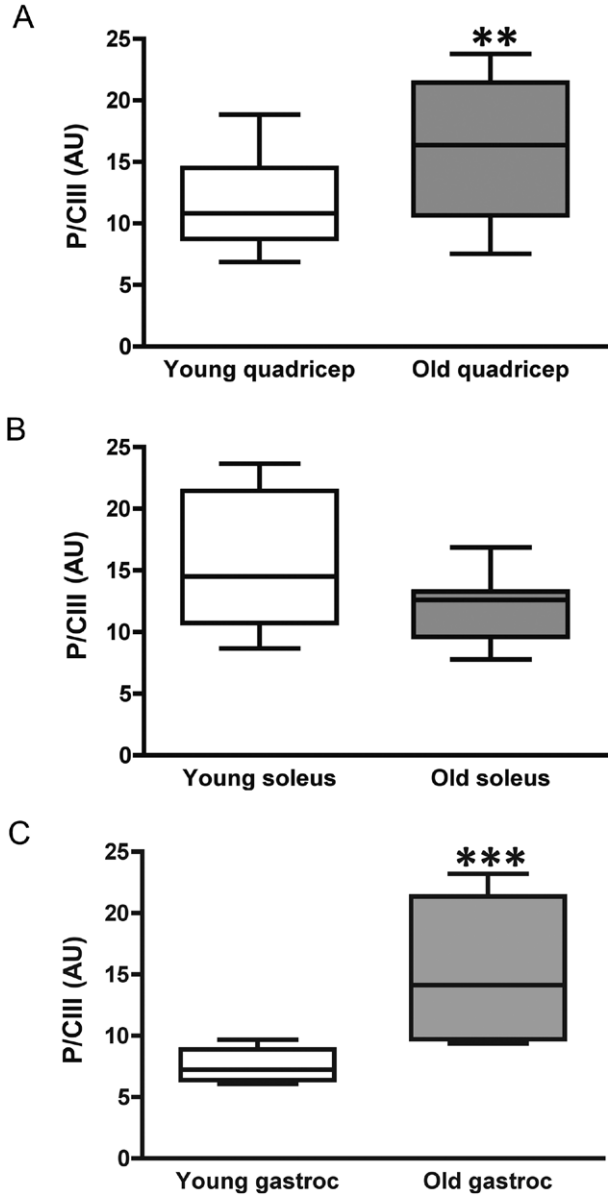

Figure 4. Respiratory capacity and control through mitochondrial complex III (CIII). Maximal state 3 respiration and oxidative phosphorylation capacity (P) when controlling for CIII protein expression with age in (A) quadricep, (B) soleus, and (C) gastrocnemius skeletal muscles. *, **, and *** indicate significant difference of age, $p \leq .05$, $p \leq .01$, and $p \leq .001$, respectively.

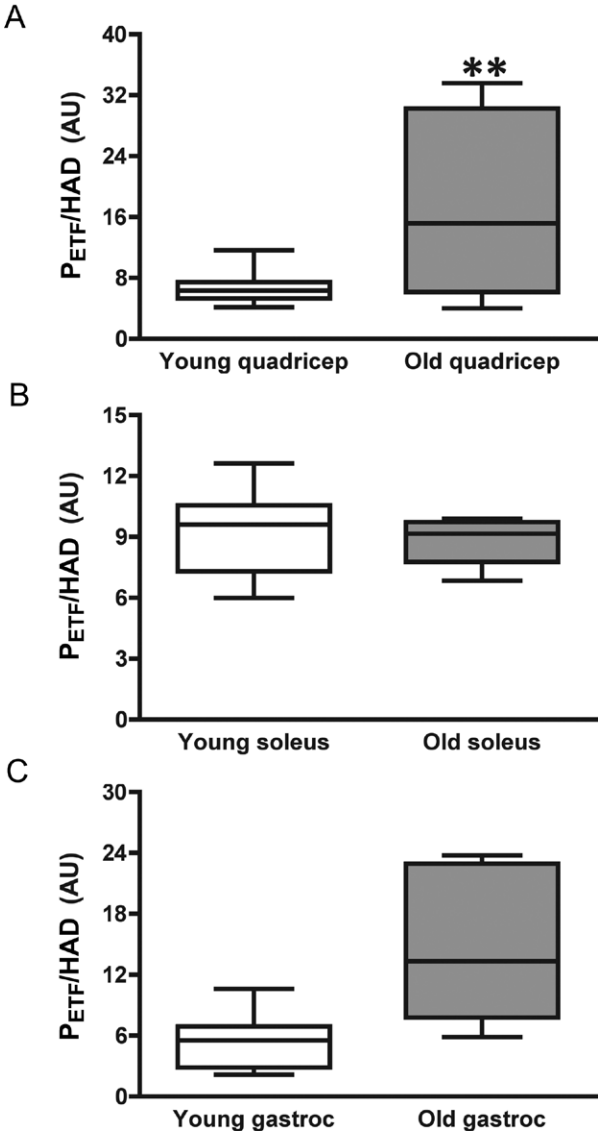

Figure 5. Respiratory capacity and control through electron transferring flavoprotein (ETF) during maximal fat respiration. Submaximal state 3 respiratory capacity specific to the capacity for fat oxidation and electron transfer through ETF (P_{ETF}) when controlling for 3-hydroxyacyl coenzyme a dehydrogenase (HAD) protein expression with age in (A) quadricep, (B) soleus, and (C) gastrocnemius skeletal muscles. *, **, and *** indicate significant difference of age, $p \leq .05$, $p \leq .01$, and $p \leq .001$, respectively. # indicates a tendency of a difference with age, $p = .065$.

coupling control during fat oxidation worsened with age only in SOL.

Variations in Mitochondrial Function Across Fiber Types

There is some dispute on whether differences in respiratory capacity fluctuate across different skeletal muscle types that vary in their biochemical makeup, tailoring oxidative function to specific metabolic demand (83). Initial reports suggested that respiratory differences could be accounted for simply by the differences in mitochondrial content (50,84). This has since been refuted as various skeletal muscles have been shown to express respiratory differences across muscle types (46,47,85,86). We recently substantiated these differences in mitochondrial function across muscle types as respiration capacities in both GAST and QUAD were greater than those in SOL at P_{CI}, P_{CII}, P, and ETS respiratory states when normalizing mass-specific respiration to citrate synthase activity (87). Although it seems evident that differences in function exist across different skeletal muscle fiber types, even when controlling for the disproportionate expression of mitochondria, the data

presented here demonstrate how important normalization of the mass-specific respirometric values can be to overall data interpretation.

Our findings specific to mitochondrial protein expression are contrary to studies suggestive of a progressive loss of mitochondria with age (34,48). We cannot exclude the possibility that some mitochondrial protein/fragments may have been lost as a result of our homogenization and centrifugation procedures. Thus, we cannot confirm that our mitochondrial protein determination is representative of the total per volume of muscle mass, possibly explaining the differences between studies. Alternatively, however, our results are in accordance with several studies reporting negligible to minor changes in mitochondrial protein expression with age, including an increase of expression that is dependent on skeletal muscle type (32,33,45,88). There is also evidence in mice of *increased* skeletal muscle mitochondrial protein synthesis with advancing age (88). Although it is unlikely that the preferential loss of mitochondrial protein during homogenization and centrifugation procedures biased our results, we cannot definitively exclude this possibility.

Skeletal Muscle Mitochondrial Respiratory Capacity and Control Across Skeletal Muscle Types With Age

Mitochondrial respiratory capacities across several different states diminished with age in QUAD and SOL (Figure 2F and H). These results coincide with previous reports where oxidative capacity is reported to decline with age in either QUAD or mixed muscle homogenates (19,31,33,35,36,38,39). Alternatively, mitochondrial respiratory capacities across all states increased with age in GAST (Figure 2J). The increase in respiratory capacity with age in GAST also corresponds with previous work that demonstrated a greater reliance with age of oxidative phosphorylation for ATP synthesis in primarily type 2 fast-twitch glycolytic skeletal muscle (41,42,89).

Mitochondria serve as a primary source of in vivo oxidant production (2–5) with the primary oxidant production occurring at CI (6–8) and CIII (9–14). Despite the macro decreases in mitochondrial-specific respiratory capacity in QUAD (Figure 2F), respiration and electron flow specifically through CI and CIII increased (Figures 3A and 4A). Coupling control during P_{CI} also had a tendency to deteriorate in QUAD ($p = .085$) in response to age (Table 2). Respiration and electron flow specifically through CI and CIII also increased in GAST, whereas coupling control during P_{CI} worsened with age (Table 2). Electron coupling control is indicative of oxidant production as mitochondrial production of superoxide is closely related to mitochondrial coupling efficiency during respiration (9). Moreover, increased mitochondrial respiration capacity also results in increased oxidative damage and shorter life span (27). Respiratory capacity through CI diminished, whereas capacity through CIII and electron coupling control through CI remained unaffected by age in the slow-twitch oxidative SOL (Figures 3B and 4B, and Table 2, respectively). Highly glycolytic skeletal muscle has been shown to have higher oxidant production with a reciprocal lower capacity for oxidant scavenging compared with highly oxidative muscle (90). Predominantly fast-twitch skeletal muscle also has been reported to accrue age-associated oxidative damage, as assessed with protein carbonyl profiles across different skeletal muscle types, more rapidly than slow-twitch oxidative muscle (91). Collectively, the results from this study, in corroboration with these previous findings, provide the direct evidence of a predisposition to ETS dysfunction with age in type 2 fast-twitch glycolytic skeletal muscle that is not observed in type 1 slow-twitch oxidative muscle and has been previously suggested in humans using indirect metabolic imaging techniques (46,47). Preliminary evidence suggests that caloric restriction (92) and exercise (93) reduce mitochondrial oxidant production and may serve to counterbalance these age-related impairments in electron transport.

Ratios of coupling control are based on the supposition that a tightly coupled system can be distinguished from a dyscoupled system by the magnitude of difference between two steady respiratory states with identical substrate supply (94). We used leak control ratios as our indices of mitochondrial coupling control efficiency (Table 2). Leak control ratios are produced between two reciprocal respiratory states; a low flux state (ie, L_N with malate and pyruvate, state 4 respiration) compared with an equivalent high respiratory flux state (ie, P_{CI}, submaximal state 3 respiration). An identical substrate supply is necessary to pair corresponding states. Flux control ratios demonstrate coupling efficiency using a theoretical minimum of 0.0, which indicates a fully coupled system, to a value of 1.0 representing a fully noncoupled or dyscoupled system (63). Although we show evidence of a loss of coupling control with aging during P_{CI} in GAST and a tendency in QUAD, unfortunately coupling efficiency during maximal state 3 respiration could not be determined with the titration protocols utilized as there was no reciprocal leak state measured for P.

Respiratory Capacity and Control of Fat Oxidation With Aging

We found that the capacity for fat respiration increased with age without a reciprocal loss of coupling efficiency during β-oxidation in QUAD when controlling for differences in HAD protein expression (Figure 5 and Table 2, respectively). Conversely, capacity for fat respiration was unaltered with age in SOL, though the coupling control during fat oxidation diminished. Neither respiratory capacity nor control of fat oxidation was altered in GAST. Skeletal muscle intramyocellular lipid stores increase in

parallel with age-related decreases in mitochondria (37). Moreover, intramyocellular lipid content is also reported to drift away from the mitochondrial reticulum with age (37). The dysregulation of fat metabolism within skeletal muscle is associated with the development of insulin resistance and metabolic disease (95–97). The loss of mitochondrial coupling efficiency in type 1 slow-twitch fibers, such as observed here, may in part explain the reported insulin resistance in healthy, lean, elderly participants (38). This is of interest in regards to metabolic disease as well as aging and merits further investigation.

Conclusions

Here, we directly demonstrate impairments of mitochondrial function in response to aging in skeletal muscle. The specific age-induced alteration in function is dependent on skeletal muscle type. Skeletal muscle composed primarily of type 2 fast-twitch glycolytic fibers are predisposed to progressive impairments in mitochondrial function with age as type 1 slow-twitch oxidative fibers appear to protect against this effect.

Author Contributions

All respirometric measurements were performed at the Institute of Physiology at University of Zurich (R.A.J., V.D., L.S.), whereas the Western blot analyses were done at the Department of Exercise and Sport Sciences at University of Copenhagen (M.T.). The following is a list stating the contribution of each author to specific aspects of the study: (i) Conception and design of the experiments (R.A.J. and C.L.); (ii) Contribution of reagents, facilities, and analytical tools (T.H., N.B.N., M.G., and C.L.); (iii) Collection of data (R.A.J., V.D., L.S., and M.T.); (iv) Analysis and interpretation of data (R.A.J., V.D., M.T.); and (v) Drafting the article or revising it critically for important intellectual content (R.A.J., V.D., T.H., M.T., N.B.N., M.G., and C.L.).

References

1. Harman D. Aging: a theory based on free radical and radiation chemistry. *J Gerontol*. 1956;11:298–300.
2. Beckman KB, Ames BN. The free radical theory of aging matures. *Physiol Rev*. 1998;78:547–581.
3. Wallace DC. Mitochondrial diseases in man and mouse. *Science*. 1999;283:1482–1488.
4. Balaban RS, Nemoto S, Finkel T. Mitochondria, oxidants, and aging. *Cell*. 2005;120:483–495.
5. Turrens JF. Mitochondrial formation of reactive oxygen species. *J Physiol (Lond)*. 2003;552:335–344.
6. Kussmaul L, Hirst J. The mechanism of superoxide production by NADH:ubiquinone oxidoreductase (complex I) from bovine heart mitochondria. *Proc Natl Acad Sci USA*. 2006;103:7607–7612.
7. Kushnareva Y, Murphy AN, Andreyev A. Complex I-mediated reactive oxygen species generation: modulation by cytochrome c and NAD(P)+ oxidation-reduction state. *Biochem J*. 2002;368:545–553.
8. Turrens JF, Boveris A. Generation of superoxide anion by the NADH dehydrogenase of bovine heart mitochondria. *Biochem J*. 1980;191:421–427.
9. Yin Y, Yang S, Yu L, Yu CA. Reaction mechanism of superoxide generation during ubiquinol oxidation by the cytochrome bc1 complex. *J Biol Chem*. 2010;285:17038–17045.
10. Chen Q, Vazquez EJ, Moghaddas S, Hoppel CL, Lesnefsky EJ. Production of reactive oxygen species by mitochondria: central role of complex III. *J Biol Chem*. 2003;278:36027–36031.
11. Turrens JF, Alexandre A, Lehninger AL. Ubisemiquinone is the electron donor for superoxide formation by complex III of heart mitochondria. *Arch Biochem Biophys*. 1985;237:408–414.
12. Guzy RD, Hoyos B, Robin E, et al. Mitochondrial complex III is required for hypoxia-induced ROS production and cellular oxygen sensing. *Cell Metab*. 2005;1:401–408.
13. Han D, Williams E, Cadenas E. Mitochondrial respiratory chain-dependent generation of superoxide anion and its release into the intermembrane space. *Biochem J*. 2001;353:411–416.
14. Muller FL, Liu Y, Van Remmen H. Complex III releases superoxide to both sides of the inner mitochondrial membrane. *J Biol Chem*. 2004;279:49064–49073.
15. Jacobs HT. The mitochondrial theory of aging: dead or alive? *Aging Cell*. 2003;2:11–17.
16. Stadtman ER, Levine RL. Protein oxidation. *Ann N Y Acad Sci*. 2000;899:191–208.
17. Bishop NA, Lu T, Yankner BA. Neural mechanisms of ageing and cognitive decline. *Nature*. 2010;464:529–535.
18. Fleming JE, Miquel J, Cottrell SF, Yengoyan LS, Economos AC. Is cell aging caused by respiration-dependent injury to the mitochondrial genome? *Gerontology*. 1982;28:44–53.
19. Short KR, Bigelow ML, Kahl J, et al. Decline in skeletal muscle mitochondrial function with aging in humans. *Proc Natl Acad Sci USA*. 2005;102:5618–5623.
20. Hamilton ML, Van Remmen H, Drake JA, et al. Does oxidative damage to DNA increase with age? *Proc Natl Acad Sci USA*. 2001;98:10469–10474.
21. Michikawa Y, Mazzucchelli F, Bresolin N, Scarlato G, Attardi G. Aging-dependent large accumulation of point mutations in the human mtDNA control region for replication. *Science*. 1999;286:774–779.
22. Shigenaga MK, Hagen TM, Ames BN. Oxidative damage and mitochondrial decay in aging. *Proc Natl Acad Sci USA*. 1994;91:10771–10778.
23. Trifunovic A, Wredenberg A, Falkenberg M, et al. Premature ageing in mice expressing defective mitochondrial DNA polymerase. *Nature*. 2004;429:417–423.
24. Payne BA, Wilson IJ, Hateley CA, et al. Mitochondrial aging is accelerated by anti-retroviral therapy through the clonal expansion of mtDNA mutations. *Nat Genet*. 2011;43:806–810.
25. McCord JM, Fridovich I. Superoxide dismutase. An enzymic function for erythrocuprein (hemocuprein). *J Biol Chem*. 1969;244:6049–6055.
26. Melov S, Schneider JA, Day BJ, et al. A novel neurological phenotype in mice lacking mitochondrial manganese superoxide dismutase. *Nat Genet*. 1998;18:159–163.
27. Kokoszka JE, Coskun P, Esposito LA, Wallace DC. Increased mitochondrial oxidative stress in the Sod2 (+/-) mouse results in the age-related decline of mitochondrial function culminating in increased apoptosis. *Proc Natl Acad Sci USA*. 2001;98:2278–2283.
28. Esposito LA, Melov S, Panov A, Cottrell BA, Wallace DC. Mitochondrial disease in mouse results in increased oxidative stress. *Proc Natl Acad Sci USA*. 1999;96:4820–4825.
29. Treuting PM, Linford NJ, Knoblaugh SE, et al. Reduction of age-associated pathology in old mice by overexpression of catalase in mitochondria. *J Gerontol A Biol Sci Med Sci*. 2008;63:813–822.
30. Schriner SE, Linford NJ, Martin GM, et al. Extension of murine life span by overexpression of catalase targeted to mitochondria. *Science*. 2005;308:1909–1911.
31. Conley KE, Jubrias SA, Esselman PC. Oxidative capacity and ageing in human muscle. *J Physiol (Lond)*. 2000;526(Pt 1):203–210.
32. Larsen S, Hey-Mogensen M, Rabøl R, Stride N, Helge JW, Dela F. The influence of age and aerobic fitness: effects on mitochondrial respiration in skeletal muscle. *Acta Physiol (Oxf)*. 2012;205:423–432.
33. Rasmussen UF, Krustrup P, Kjaer M, Rasmussen HN. Experimental evidence against the mitochondrial theory of aging. A study of

isolated human skeletal muscle mitochondria. *Exp Gerontol*. 2003;38:877–886.
34. Rooyackers OE, Adey DB, Ades PA, Nair KS. Effect of age on in vivo rates of mitochondrial protein synthesis in human skeletal muscle. *Proc Natl Acad Sci USA*. 1996;93:15364–15369.
35. Tonkonogi M, Fernström M, Walsh B, et al. Reduced oxidative power but unchanged antioxidative capacity in skeletal muscle from aged humans. *Pflugers Arch*. 2003;446:261–269.
36. Trounce I, Byrne E, Marzuki S. Decline in skeletal muscle mitochondrial respiratory chain function: possible factor in ageing. *Lancet*. 1989;1:637–639.
37. Crane JD, Devries MC, Safdar A, Hamadeh MJ, Tarnopolsky MA. The effect of aging on human skeletal muscle mitochondrial and intramyocellular lipid ultrastructure. *J Gerontol A Biol Sci Med Sci*. 2010;65:119–128.
38. Petersen KF, Befroy D, Dufour S, et al. Mitochondrial dysfunction in the elderly: possible role in insulin resistance. *Science*. 2003;300:1140–1142.
39. Hepple RT, Hagen JL, Krause DJ, Jackson CC. Aerobic power declines with aging in rat skeletal muscles perfused at matched convective O2 delivery. *J Appl Physiol*. 2003;94:744–751.
40. Figueiredo PA, Ferreira RM, Appell HJ, Duarte JA. Age-induced morphological, biochemical, and functional alterations in isolated mitochondria from murine skeletal muscle. *J Gerontol A Biol Sci Med Sci*. 2008;63:350–359.
41. Lanza IR, Befroy DE, Kent-Braun JA. Age-related changes in ATP-producing pathways in human skeletal muscle in vivo. *J Appl Physiol*. 2005;99:1736–1744.
42. Lanza IR, Larsen RG, Kent-Braun JA. Effects of old age on human skeletal muscle energetics during fatiguing contractions with and without blood flow. *J Physiol (Lond)*. 2007;583:1093–1105.
43. Chretien D, Gallego J, Barrientos A, et al. Biochemical parameters for the diagnosis of mitochondrial respiratory chain deficiency in humans, and their lack of age-related changes. *Biochem J*. 1998;329(Pt 2):249–254.
44. Houmard JA, Weidner ML, Gavigan KE, Tyndall GL, Hickey MS, Alshami A. Fiber type and citrate synthase activity in the human gastrocnemius and vastus lateralis with aging. *J Appl Physiol*. 1998;85:1337–1341.
45. Picard M, Ritchie D, Thomas MM, Wright KJ, Hepple RT. Alterations in intrinsic mitochondrial function with aging are fiber type-specific and do not explain differential atrophy between muscles. *Aging Cell*. 2011;10:1047–1055.
46. Conley KE, Amara CE, Jubrias SA, Marcinek DJ. Mitochondrial function, fibre types and ageing: new insights from human muscle in vivo. *Exp Physiol*. 2007;92:333–339.
47. Amara CE, Shankland EG, Jubrias SA, Marcinek DJ, Kushmerick MJ, Conley KE. Mild mitochondrial uncoupling impacts cellular aging in human muscles in vivo. *Proc Natl Acad Sci USA*. 2007;104:1057–1062.
48. Picard M, Ritchie D, Wright KJ, et al. Mitochondrial functional impairment with aging is exaggerated in isolated mitochondria compared to permeabilized myofibers. *Aging Cell*. 2010;9:1032–1046.
49. Kirkwood SP, Munn EA, Brooks GA. Mitochondrial reticulum in limb skeletal muscle. *Am J Physiol*. 1986;251:C395–C402.
50. Schwerzmann K, Hoppeler H, Kayar SR, Weibel ER. Oxidative capacity of muscle and mitochondria: correlation of physiological, biochemical, and morphometric characteristics. *Proc Natl Acad Sci USA*. 1989;86:1583–1587.
51. Picard M, Taivassalo T, Gouspillou G, Hepple RT. Mitochondria: isolation, structure and function. *J Physiol (Lond)*. 2011;589:4413–4421.
52. Benz R. Porin from bacterial and mitochondrial outer membranes. *CRC Crit Rev Biochem*. 1985;19:145–190.
53. Milner DJ, Mavroidis M, Weisleder N, Capetanaki Y. Desmin cytoskeleton linked to muscle mitochondrial distribution and respiratory function. *J Cell Biol*. 2000;150:1283–1298.
54. Kunz WS, Kudin A, Vielhaber S, Elger CE, Attardi G, Villani G. Flux control of cytochrome c oxidase in human skeletal muscle. *J Biol Chem*. 2000;275:27741–27745.
55. Villani G, Greco M, Papa S, Attardi G. Low reserve of cytochrome c oxidase capacity in vivo in the respiratory chain of a variety of human cell types. *J Biol Chem*. 1998;273:31829–31836.
56. Pande SV, Blanchaer MC. Preferential loss of ATP-dependent long-chain fatty acid activating enzyme in mitochondria prepared using Nagarse. *Biochim Biophys Acta*. 1970;202:43–48.
57. Brooks GA. Lactate shuttle – between but not within cells? *J Physiol (Lond)*. 2002;541:333–334.
58. Brooks GA, Hashimoto T. Investigation of the lactate shuttle in skeletal muscle mitochondria. *J Physiol (Lond)*. 2007;584:705–706; author reply 707–708.
59. Chretien D, Pourrier M, Bourgeron T, et al. An improved spectrophotometric assay of pyruvate dehydrogenase in lactate dehydrogenase contaminated mitochondrial preparations from human skeletal muscle. *Clin Chim Acta*. 1995;240:129–136.
60. Horan MP, Pichaud N, Ballard JW. Review: quantifying mitochondrial dysfunction in complex diseases of aging. *J Gerontol A Biol Sci Med Sci*. 2012;67:1022–1035.
61. Benz R. Permeation of hydrophilic solutes through mitochondrial outer membranes: review on mitochondrial porins. *Biochim Biophys Acta*. 1994;1197:167–196.
62. Wicker U, Bücheler K, Gellerich FN, Wagner M, Kapischke M, Brdiczka D. Effect of macromolecules on the structure of the mitochondrial inter-membrane space and the regulation of hexokinase. *Biochim Biophys Acta*. 1993;1142:228–239.
63. Gnaiger E. Capacity of oxidative phosphorylation in human skeletal muscle: new perspectives of mitochondrial physiology. *Int J Biochem Cell Biol*. 2009;41:1837–1845.
64. Kuznetsov AV, Veksler V, Gellerich FN, Saks V, Margreiter R, Kunz WS. Analysis of mitochondrial function in situ in permeabilized muscle fibers, tissues and cells. *Nat Protoc*. 2008;3:965–976.
65. Pesta D, Gnaiger E. High-resolution respirometry. OXPHOS protocols for human cells and permeabilized fibers from small biopsies of human muscle. *Mitochondria Bioenergy Meth Protocols*. 2011;810:25–58.
66. Saks VA, Belikova YO, Kuznetsov AV. In vivo regulation of mitochondrial respiration in cardiomyocytes: specific restrictions for intracellular diffusion of ADP. *Biochim Biophys Acta*. 1991;1074:302–311.
67. Saks VA, Veksler VI, Kuznetsov AV, et al. Permeabilized cell and skinned fiber techniques in studies of mitochondrial function in vivo. *Mol Cell Biochem*. 1998;184:81–100.
68. Lin A, Krockmalnic G, Penman S. Imaging cytoskeleton–mitochondrial membrane attachments by embedment-free electron microscopy of saponin-extracted cells. *Proc Natl Acad Sci USA*. 1990;87:8565–8569.
69. Veksler VI, Kuznetsov AV, Sharov VG, Kapelko VI, Saks VA. Mitochondrial respiratory parameters in cardiac tissue: a novel method of assessment by using saponin-skinned fibers. *Biochim Biophys Acta*. 1987;892:191–196.
70. Kay L, Nicolay K, Wieringa B, Saks V, Wallimann T. Direct evidence for the control of mitochondrial respiration by mitochondrial creatine kinase in oxidative muscle cells in situ. *J Biol Chem*. 2000;275:6937–6944.
71. Jacobs RA, Boushel R, Wright-Paradis C, et al. Mitochondrial function in human skeletal muscle following high altitude exposure. *Exp Physiol*. 2012. doi:10.1113/expphysiol.2012.066092
72. Jacobs RA, Lundby C. Mitochondria express enhanced quality as well as quantity in association with aerobic fitness across recreationally active individuals up to elite athletes. *J Appl Physiol*. 2012. doi:10.1152/japplphysiol.01081.2012
73. Jacobs RA, Rasmussen P, Siebenmann C, et al. Determinants of time trial performance and maximal incremental exercise in highly trained endurance athletes. *J Appl Physiol*. 2011;111:1422–1430.

74. Jacobs RA, Siebenmann C, Hug M, Toigo M, Meinild AK, Lundby C. 28 days at 3,454 m altitude diminishes respiratory capacity but enhances efficiency in human skeletal muscle mitochondria. *FASEB J*. 2012. doi:10.1096/fj.12-218206.
75. Nordsborg NB, Siebenmann C, Jacobs RA, et al. Four weeks of normobaric "live high-train low" do not alter muscular or systemic capacity for maintaining pH and K^+ homeostasis during intense exercise. *J Appl Physiol*. 2012;112:2027–2036.
76. Nordsborg N, Ovesen J, Thomassen M, et al. Effect of dexamethasone on skeletal muscle Na+,K+ pump subunit specific expression and K+ homeostasis during exercise in humans. *J Physiol (Lond)*. 2008;586:1447–1459.
77. Thomassen M, Rose AJ, Jensen TE, et al. Protein kinase Cα activity is important for contraction-induced FXYD1 phosphorylation in skeletal muscle. *Am J Physiol Regul Integr Comp Physiol*. 2011;301:R1808–R1814.
78. Eaton S, Bartlett K, Pourfarzam M. Mammalian mitochondrial beta-oxidation. *Biochem J*. 1996;320(Pt 2):345–357.
79. Lanza IR, Nair KS. Mitochondrial function as a determinant of life span. *Pflugers Arch*. 2010;459:277–289.
80. Rasmussen UF, Rasmussen HN. Human quadriceps muscle mitochondria: a functional characterization. *Mol Cell Biochem*. 2000;208:37–44.
81. Brand MD, Nicholls DG. Assessing mitochondrial dysfunction in cells. *Biochem J*. 2011;435:297–312.
82. Larsen S, Nielsen J, Hansen CN, et al. Biomarkers of mitochondrial content in skeletal muscle of healthy young human subjects. *J Physiol (Lond)*. 2012;590:3349–3360.
83. Picard M, Hepple RT, Burelle Y. Mitochondrial functional specialization in glycolytic and oxidative muscle fibers: tailoring the organelle for optimal function. *Am J Physiol Cell Physiol*. 2012;302:C629–C641.
84. Hoppeler H, Hudlicka O, Uhlmann E. Relationship between mitochondria and oxygen consumption in isolated cat muscles. *J Physiol (Lond)*. 1987;385:661–675.
85. Jackman MR, Willis WT. Characteristics of mitochondria isolated from type I and type IIb skeletal muscle. *Am J Physiol*. 1996;270:C673–C678.
86. Picard M, Csukly K, Robillard ME, et al. Resistance to Ca2+-induced opening of the permeability transition pore differs in mitochondria from glycolytic and oxidative muscles. *Am J Physiol Regul Integr Comp Physiol*. 2008;295:R659–R668.
87. Jacobs RA, Diaz V, Meinild AK, Gassmann M, Lundby C. The C57Bl/6 mouse serves as a suitable model of human skeletal muscle mitochondrial function. *Exp Physiol*. 2012. doi:10.1113/expphysiol.2012.07003.
88. Miller BF, Robinson MM, Bruss MD, Hellerstein M, Hamilton KL. A comprehensive assessment of mitochondrial protein synthesis and cellular proliferation with age and caloric restriction. *Aging Cell*. 2012;11:150–161.
89. Lanza IR, Russ DW, Kent-Braun JA. Age-related enhancement of fatigue resistance is evident in men during both isometric and dynamic tasks. *J Appl Physiol*. 2004;97:967–975.
90. Anderson EJ, Neufer PD. Type II skeletal myofibers possess unique properties that potentiate mitochondrial H(2)O(2) generation. *Am J Physiol Cell Physiol*. 2006;290:C844–C851.
91. Feng J, Navratil M, Thompson LV, Arriaga EA. Principal component analysis reveals age-related and muscle-type-related differences in protein carbonyl profiles of muscle mitochondria. *J Gerontol A Biol Sci Med Sci*. 2008;63:1277–1288.
92. Chen Y, Hagopian K, McDonald RB, et al. The influence of dietary lipid composition on skeletal muscle mitochondria from mice following 1 month of calorie restriction. *J Gerontol A Biol Sci Med Sci*. 2012;67:1121–1131.
93. Alves RM, Vitorino R, Figueiredo P, Duarte JA, Ferreira R, Amado F. Lifelong physical activity modulation of the skeletal muscle mitochondrial proteome in mice. *J Gerontol A Biol Sci Med Sci*. 2010;65:832–842.
94. Chance B, Williams GR. Respiratory enzymes in oxidative phosphorylation. III. The steady state. *J Biol Chem*. 1955;217:409–427.
95. Amati F, Dubé JJ, Alvarez-Carnero E, et al. Skeletal muscle triglycerides, diacylglycerols, and ceramides in insulin resistance: another paradox in endurance-trained athletes? *Diabetes*. 2011;60:2588–2597.
96. Chomentowski P, Coen PM, Radiková Z, Goodpaster BH, Toledo FG. Skeletal muscle mitochondria in insulin resistance: differences in intermyofibrillar versus subsarcolemmal subpopulations and relationship to metabolic flexibility. *J Clin Endocrinol Metab*. 2011;96:494–503.
97. Coen PM, Goodpaster BH. Role of intramyocelluar lipids in human health. *Trends Endocrinol Metab*. 2012;23:391–398.

Research Paper

The C57Bl/6 mouse serves as a suitable model of human skeletal muscle mitochondrial function

Robert A. Jacobs[1,2,4], Víctor Díaz[1,2,3], Anne-Kristine Meinild[1,4], Max Gassmann[1,2,5] and Carsten Lundby[1,4]

[1] *Zurich Center for Integrative Human Physiology (ZIHP) and*
[4] *Institute of Physiology, University of Zurich, Switzerland*
[2] *Institute of Veterinary Physiology, Vetsuisse Faculty, University of Zurich, Switzerland*
[3] *Department of Health and Human Performance, Universidad Politécnica de Madrid, Spain*
[5] *Universidad Peruana Cayetano Heredia (UPCH), Lima, Peru*

New Findings

- **What is the central question of this study?**
  Do mouse skeletal muscle mitochondria resemble human skeletal muscle mitochondria sufficiently to serve as a proper model and how do differences of skeletal muscle type affect the comparison?
- **What is the main finding and its importance?**
  We find that mouse skeletal muscle respiratory capacity and control function rather similar to human m. vastus lateralis, with the mouse quadricep being overall the most similar. This resemblance is not universal, however, because the coupling control of electron transport during fat oxidation in type I murine muscle is more comparable to human vastus lateralis.

It is debatable whether differences in mitochondrial function exist across skeletal muscle types and whether mouse skeletal muscle mitochondrial function can serve as a valid model for human skeletal muscle mitochondrial function. The aims of this study were to compare and contrast three different mouse skeletal muscles and to identify the mouse muscle that most closely resembles human skeletal muscle respiratory capacity and control. Mouse quadriceps ($QUAD_M$), soleus (SOL_M) and gastrocnemius ($GAST_M$) skeletal muscles were obtained from 8- to 10-week-old healthy mice ($n = 8$), representing mixed, oxidative and glycolytic muscle, respectively. Skeletal muscle samples were also collected from young, active, healthy human subjects ($n = 8$) from the vastis lateralis ($QUAD_H$). High-resolution respirometry was used to examine mitochondrial function in all skeletal muscle samples, and mitochondrial content was quantified with citrate synthase activity. Mass-specific respiration was higher across all respiratory states in SOL_M *versus* both $GAST_M$ and $QUAD_H$ ($P < 0.01$). When controlling for mitochondrial content, however, SOL_M respiration was lower than $GAST_M$ and $QUAD_H$ ($P < 0.05$ and $P < 0.01$, respectively). When comparing respiratory capacity between mouse and human muscle, $QUAD_M$ exhibited only one different respiratory state when compared with $QUAD_H$. These results demonstrate that qualitative differences in mitochondrial function exist between different mouse skeletal muscles types when respiratory capacity is normalized to mitochondrial content, and that skeletal muscle respiratory capacity in young, healthy $QUAD_M$ does correspond well with that of young, healthy $QUAD_H$.

(Received 21 September 2012; accepted after revision 19 November 2012; first published online 23 November 2012)
Corresponding author R. A. Jacobs: Institute of Physiology and Zurich Center for Integrative Human Physiology (ZIHP), Winterthurerstrasse 190, CH-8057 Zurich, Switzerland. Email: jacobs@vetphys.uzh.ch

DOI: 10.1113/expphysiol.2012.070037

Experimental Physiology

Mouse modelling for the study of human health and disease is an extremely powerful tool that is widely used. The degree of conservation between mouse and human genomes permits the study of murine biology largely to characterize that of humans (Mouse Genome Sequencing Consortium *et al.* 2002). There remains, however, a biological divergence between species that is not always readily apparent and can lead to scientific misdirection if not properly recognized. There are certain fundamental differences in mouse models that mimic human disease with regard to cancer (Rangarajan & Weinberg, 2003), ageing (Demetrius, 2006) and metabolic disease (Svenson *et al.* 2007; Garland *et al.* 2011) that must be taken into account. The use of rodents for research on human muscle disuse and sarcopenia is fraught with dissimilarities between species (Rennie *et al.* 2010). The differences between mice and humans extend beyond diseased states. Haemodynamic control differs between healthy humans and mice (Desai *et al.* 1997; Bernstein, 2003), as do normal metabolic profiles of some skeletal muscles (Schiaffino *et al.* 2007). Accordingly, data extrapolation from mouse studies modelling human physiological function, in both healthy and diseased states, can have limitations if the differences between species are not identified and controlled for.

Mitochondria are associated with the aetiology of many disease states and disorders, including ageing (Jacobs, 2003) and metabolic disease (Lowell & Shulman, 2005; Chomentowski *et al.* 2011). The roles of mitochondrial function in these diseases are often studied using mouse models (Picard *et al.* 2010; Miller *et al.* 2012; Paglialunga *et al.* 2012; Sebastián *et al.* 2012). The most common tissue used to analyse mitochondria is skeletal muscle, because of its accessibility, relative mass-to-body weight ratio and high metabolic rate. Differences between mouse and human skeletal muscle have brought into question the validity of studying mouse mitochondria, and alternative animal models have already been proposed ostensibly to replace the mouse for the study of human mitochondrial physiology (Lemieux & Warren, 2012).

Skeletal muscle anatomy and function vary between mice and humans. These recognized differences have led to comparisons of molecular expression across different mouse and human muscles in an attempt to identify the best phenotypic association between species (Kho *et al.* 2006). The mouse soleus (SOL_M) has been reported to express the closest molecular resemblance to several human skeletal muscles (Kho *et al.* 2006). However, mitochondrial function across different murine skeletal muscles has never been empirically compared with a human skeletal muscle, namely the vastus lateralis, because that is the most common human skeletal muscle sampled. The aim of this study, therefore, is to analyse respiratory capacity and control across several mouse muscles and to evaluate those results with skeletal muscle mitochondrial function measured from young and healthy human subjects.

Our first objective is to compare and contrast mitochondrial function across the lateral portion of mouse quadriceps ($QUAD_M$), SOL_M and lateral gastrocnemius ($GAST_M$). Hitherto, differences in mitochondrial function across skeletal muscles have been attributed primarily to the differences in mitochondrial content (Hoppeler *et al.* 1987; Schwerzmann *et al.* 1989). Such studies, however, used preparations of isolated mitochondria for respirometric analysis with limited substrate supply, never reaching maximal state 3 respiration or oxidative phosphorylation capacity (P) of the entire respiratory system. We have previously demonstrated that differences in mitochondrial respiratory capacity and control are apparent only when substrate provision for both complex I (CI; NADH dehydrogenase) and complex II (CII; succinate dehydrogenase) is provided (Jacobs & Lundby, 2012). Our first objective is to confirm differences in respiratory capacity and control between different skeletal muscles as suggested by previous studies in humans (Amara *et al.* 2007; Conley *et al.* 2007). Our second objective is to determine whether mouse skeletal muscle can properly represent human skeletal muscle mitochondrial function and, if so, to identify the mouse skeletal muscle that best represents human muscle. Our hypotheses are as follows: (i) that the mouse can serve as a viable model for the study of mitochondrial function in humans; and (ii) that SOL_M will best represent mitochondrial function in human skeletal muscle, as a result of the molecular similarities between muscles (Kho *et al.* 2006).

Methods

Ethical approval

The experimental protocols using laboratory animals were approved by the Kantonales Veterinäramt Zürich (73/2011) and were performed in accordance with the Swiss animal protection laws and institutional guidelines. The Regional Ethics Committee of Region Hovedstaden in Denmark approved experimental protocols involving human subjects (H-1-2011-052), which were in accordance with the Declaration of Helsinki. Prior to the start of the experiments, informed oral and written consent was obtained from all participants.

Experimental animals

A total of eight C57Bl/6J wild-type mice were used in this study. All mice were housed in standard rodent cages with fixed temperature ($21 \pm 1^{\circ}C$), free access to food and water, and a 12 h–12 h light–dark cycle. Mice ranged from 8 to 10 weeks of age when they were killed and

skeletal muscles collected. Animals were killed by means of carbon dioxide inhalation, followed by rapid excision of $QUAD_M$, SOL_M and $GAST_M$. These muscles represent a mixed oxidative and glycolytic muscle, an oxidative muscle and a glycolytic muscle, respectively.

Human subjects

Eight young and physically active subjects voluntarily participated in this study. Subject characteristics (means ± SD) were as follows: age, 26 ± 5 years; height, 175 ± 9 cm; and body weight, 70 ± 7 kg. All subjects were recreationally active. No subjects were taking any sort of prescription medication or had any known family history of type 2 diabetes, severe obesity or cardiovascular diseases.

Human skeletal muscle sampling

Skeletal muscle biopsies were obtained from the vastus lateralis. Samples were collected under local anaesthesia (1% lidocaine) of the skin and superficial muscle fascia, using the Bergström technique (Bergström, 1962) with a needle modified for suction. The biopsy was immediately dissected free of fat and connective tissue and divided into sections for measurements of mitochondrial respiration.

Skeletal muscle preparation

Both human and mouse skeletal muscle samples were immediately placed in ice-cold biopsy preservation solution containing 2.77 mM CaK_2EGTA buffer, 7.23 mM K_2EGTA buffer, 0.1 μM free calcium, 20 mM imidazole, 20 mM taurine, 50 mM 2-(*N*-morpholino)ethanesulfonic acid hydrate (K-Mes), 0.5 mM dithiothreitol, 6.56 mM $MgCl_2.6H_2O$, 5.77 mM ATP and 15 mM phosphocreatine (pH 7.1). Muscle samples were then gently dissected with either a pair of fine-tipped forceps or the tip of two 18-gauge needles for murine and human skeletal muscle samples, respectively, achieving a high degree of fibre separation that was verified microscopically. Chemical permeabilization was carried out by incubation in 2 ml of biopsy preservation solution with saponin (50 μg ml^{-1}) for 30 min at 4°C (Kuznetsov *et al.* 2004). Finally, samples were washed with a mitochondrial respiration medium 05 (MiR05) containing 0.5 mM EGTA, 3 mM $MgCl_2.6H_2O$, 60 mM potassium lactobionate, 20 mM taurine, 10 mM KH_2P0_4, 20 mM Hepes, 110 mM sucrose and 1 g l^{-1} bovine serum albumin (pH 7.1) for 10 min at 4°C.

Mitochondrial respiration measurements

Muscle bundles were blotted dry and measured for wet weight in a balance-controlled scale (XS205 DualRange Analytical Balance; Mettler-Toledo AG, Greifensee, Switzerland), at constant relative humidity in order to provide hydration consistency as well as stability of weight measurements. Respiration measurements were performed in mitochondrial respiration medium 06 (MiR06; MiR05 + catalase 280 IU ml^{-1}). Measurements of oxygen consumption were performed at 37°C using the high-resolution Oxygraph-2k (Oroboros, Innsbruck, Austria), with all additions in each substrate, uncoupler and inhibitor titration protocol being added in series. Standardized instrumental calibrations were performed to correct for back diffusion of oxygen into the chamber from the various components, leak from the exterior, oxygen consumption by the chemical medium and oxygen consumption by the sensor. Oxygen flux was resolved by software allowing non-linear changes in the negative time derivative of the oxygen concentration signal (Oxygraph-2k; Oroboros). All experiments were carried out in a hyperoxygenated environment to prevent any potential oxygen diffusion limitation.

Respiratory titration protocol

The titration protocol was specific to the examination of individual aspects of respiratory control through a sequence of coupling and substrate states induced via separate titrations. All respirometric analyses were made in duplicate, and all titrations were added in series as presented. The concentrations of substrates, uncouplers and inhibitors used were based on prior experiments conducted for optimization of the titration protocols (Jacobs *et al.* 2011, 2012; Jacobs & Lundby, 2012).

Leak respiration in the absence of adenylates (L_N) was induced with the addition of malate (2 mM) and octanoyl carnitine (0.2 mM). The L_N state represents the resting oxygen consumption of an unaltered and intact electron transport system free of adenylates.

Maximal electron flow through electron-transferring flavoprotein (ETF) and fatty acid oxidative capacity (P_{ETF}) were both determined following the addition of ADP (5 mM). In the P_{ETF} state, the ETF-linked transfer of electrons requires the metabolism of acetyl-CoA, hence the addition of malate, in order to facilitate convergent electron flow into the Q-junction from both CI and ETF, allowing β-oxidation to proceed. The contribution of electron flow through CI is far below capacity and so here the rate-limiting metabolic branch is electron transport through ETF such that malate + octanoyl carnitine + ADP-stimulated respiration is representative of, rather than specific to, electron capacity through ETF (Eaton *et al.* 1996; Saks *et al.* 1998; Gnaiger, 2009; Pesta & Gnaiger, 2011; Pesta *et al.* 2011).

Submaximal state 3 respiratory capacity specific to CI (P_{CI}) was induced following the additions of

pyruvate (5 mM) and glutamate (10 mM). Maximal state 3 respiration, oxidative phosphorylation capacity (P), was then induced with the addition of succinate (10 mM). Oxidative phosphorylation capacity demonstrates the capacity of a naturally intact electron transport system to catalyse a sequential set of redox reactions that are partially coupled to the production of ATP via ATP synthase. Oxidative phosphorylation capacity maintains an electrochemical gradient across the inner mitochondrial membrane that is dictated by the degree of coupling to the phosphorylation system (Gnaiger, 2009; Pesta & Gnaiger, 2011). This maximal state represents respiration that is resultant to saturating concentrations of ADP and substrate supply for both CI and CII. Convergent electron input to CI and CII provides higher respiratory values compared with the isolated respiration of either CI (pyruvate/glutamate + malate or glutamate + malate) or CII (succinate + rotenone; Rasmussen & Rasmussen, 2000; Gnaiger, 2009). Consequently, P presents more physiological relevance to the study of mitochondrial function (Brand & Nicholls, 2011) and is necessary to establish confirmation of a complete and intact electron transport system.

As an internal control for compromised integrity of the mitochondrial preparation, the mitochondrial outer membrane was assessed with the addition of cytochrome *c* (10 μM). There was no indication of mitochondrial damage, because the 3.5, 2.1, 5.5 and –0.4% change in mouse $QUAD_M$, SOL_M, $GAST_M$ and $QUAD_H$ respiration, respectively, was either below or within the accepted 5–15% elevation in respiration following exogenous cytochrome *c*, verifying integrity of the outer mitochondrial membrane (Kuznetsov *et al.* 2008).

Phosphorylative restraint of electron transport was assessed by uncoupling ATP synthase (complex V) from the electron transport system with the titration of the proton ionophore, carbonyl cyanide *p*-(trifluoromethoxy) phenylhydrazone (FCCP; 0.5 μM per addition up to optimal concentrations ranging from 1.5 to 3 μM), reaching electron transport system (ETS) capacity. In the ETS respiratory state, the inner mitochondrial membrane potential is completely collapsed, with an open transmembrane proton circuit. The uninhibited flow of electrons through the respiratory system can therefore serve indirectly as an indication of maximal mitochondrial membrane potential.

Finally, rotenone (0.5 μM) and antimycin A (2.5 μM) were added, in sequence, to terminate respiration by inhibiting CI and complex III (CIII; cytochrome bc_1 complex), respectively. With CI inhibited, electron flow is specific to CII, providing submaximal state 3 respiration through CII (P_{CII}). There are negligible differences in P_{CII} when measured with or without a prior addition of FCCP (Jacobs *et al.* 2012), because the capacity for electron flow through CII is much less than that of CIII and complex IV (CIV; cytochrome *c* oxidase), and thus is rate limiting (Gnaiger, 2009). Inhibition of respiration with antimycin A then allows for the determination and correction of residual oxygen consumption, indicative of non-mitochondrial oxygen consumption in the chamber.

Citrate synthase activities

Citrate synthase (CS) activities were assayed in homogenates of the skeletal muscle samples used in respiration measurements. The contents of the Oxygraph-2k chambers (2 ml each) were removed after each respiration experiment and washed once with 2 ml of MiR05. One per cent Triton X-100 and 2 μl of a protease inhibitor cocktail (Sigma Aldrich catalogue no. 539134) were added to the combined solutions (content and wash) and then homogenized for 30 s with a T10 basic ULTRA-TURRAX® homogenizer near maximal speed (setting 4). The homogenate was then centrifuged for 15 min at 4°C, and the supernatant was removed, frozen in liquid nitrogen and stored at –80°C. As has been previously described (Srere, 1969), CS activity was measured fluorometrically at 412 nm and 25°C (Citrate Synthase Assay Kit; Sigma-Aldrich), according to the manufacturer.

Muscle lysate preparation

Muscle tissue ($QUAD_M$, SOL_M and $GAST_M$) was collected from a subgroup of mice ($n = 4$) to measure the protein expression of several mitochondria-specific proteins and compare quantification of those with our measure of CS activity to establish its validity as a biomarker of mitochondrial content in mouse skeletal muscle. The muscle samples were homogenized (Qiagen Tissuelyser II, Retsch, Haan, Germany) in a fresh batch of buffer containing the following: 10% glycerol, 20 mM sodium pyrophosphate, 150 mM NaCl, 50 mM Hepes (pH 7.5), 1% NP-40, 20 mM β-glycerophosphate, 2 mM Na_3VO_4, 10 mM NaF, 2 mM phenylmethylsulfonyl fluoride, 1 mM EDTA (pH 8.0), 1 mM EGTA (pH 8.0), 10 μg ml^{-1} aprotinin, 10 μg ml^{-1} leupeptin and 3 mM benzamidine. Afterwards, samples were rotated end over end for 1 h at 4°C and centrifuged at 16,500*g* for 30 min at 4°C, and the supernatant (lysate) was used for further analysis. The total protein concentration in each sample was determined by a bovine serum albumin standard kit (Pierce, Rockford, IL, USA), and samples were mixed with a modified 6× Laemmli buffer [7 ml 0.5 M Tris base (pH 6.8), 3 ml glycerol, 0.93 g dithiothreitol, 1 g SDS and 1.2 mg Bromophenol blue].

SDS-PAGE and Western blotting

Methods have been described in detail previously (Nordsborg *et al.* 2008, 2012; Thomassen *et al.* 2011). Equal amounts (10 μg) of total muscle lysate proteins, determined during optimization of the different antibodies, were loaded in each well. Samples were loaded together with protein markers (Precision Plus All Blue and Dual Colour; Bio-Rad Laboratories, Hercules, CA, USA) on precasted gels (Bio-Rad Laboratories). Proteins were separated by SDS-PAGE and semi-dry transferred to a polyvinylidene fluoride membrane (Millipore, Billerica, MA, USA). The membranes were blocked in either 2% skimmed milk or 3% bovine serum albumin in Tris-buffered saline, including 0.1% Tween 20 (TBST) before an overnight incubation in primary antibody at 4°C. Thereafter, membranes were washed in TBST and incubated for 1 h at room temperature in horseradish peroxidase-conjugated secondary antibody. Membranes were then washed three times for 15 min in TBST before the bands were visualized with ECL (Millipore) and recorded with a digital camera (ChemiDoc MP Imaging System; Bio-Rad). Quantification of the Western blot band intensity was done using the Image Lab software program (Bio-Rad) and determined as the total band intensity minus the background intensity. Primary antibodies were optimized by use of mouse muscle lysates to ensure that the amount of protein loaded would result in band signal intensities localized on the steep and linear part of a standard curve.

In order to determine changes in total protein expression, the following antibodies were used, with the localization of the quantified signal noted: 3-hydroxyacyl coenzyme *a* dehydrogenase (HAD), 83 kDa, polyclonal ab54477 (Abcam, Cambridge, UK); citrate synthase (CS), 48 kDa, polyclonal ab96600 (Abcam); mitochondrial complex IV subunit 4, (CIV), 16 kDa, monoclonal sc-58348 (Santa Cruz Biotechnology, Santa Cruz, CA, USA); and mitochondrial complex I subunit NDUFB8 (CI), 20 kDa (monoclonal ab110242), mitochondrial complex II, succinate dehydrogenase complex subunit B (CII), 30 kDa (monoclonal ab14714), mitochondrial complex III subunit core 2 (CIII), 45 kDa (monoclonal ab14745) and mitochondrial complex V ATP synthase subunit α (CV), 55 kDa (monoclonal ab14748), all four of which are included in the MitoProfile® Total OXPHOS Human WB Antibody Cocktail (ab110411; Abcam). The secondary antibodies used were horseradish peroxidase-conjugated goat anti-mouse and goat anti-rabbit (P-0447 and P-0448; Dako, Glostrup, Denmark).

All samples from the same muscle type were loaded on the same gel. The signal intensity from each muscle sample was normalized to the mean signal intensity of a human standard loaded together with the samples.

Data analysis

For all statistical evaluations, a P value of <0.05 was considered significant. Linear regression was used to calculate the strength of association between CS activity and the quantification of mitochondria-specific proteins from the tricarboxylic acid cycle, β-oxidation pathway and electron transport system across all types of murine skeletal muscles. Respiratory capacities, CS activity and indices of mitochondrial efficiency did not show a Gausian distribution; therefore a Kruskal–Wallis ANOVA and the Mann–Whitney U test were used to reveal differences between muscles. Pearson correlation coefficients were calculated for the strength of association between P and CS activity.

Results

Mass-specific respiration across mouse skeletal muscle

Differences in mass-specific respiratory capacity across different skeletal muscles in the mouse are presented in Fig. 1*A*. For all respiratory states, SOL_M was significantly ($P < 0.01$) greater than both $QUAD_M$ and $GAST_M$. The only difference observed between $QUAD_M$ and $GAST_M$ was in maximal fatty acid oxidation capacity, P_{ETF}, where $QUAD_M$ expressed a greater capacity ($P = 0.028$).

Mitochondrial respiratory capacity and content

Mass-specific respiration does not take into account differences in mitochondrial content. When controlling mass-specific respiration for mitochondrial content, the differences in respiratory capacities across all mouse skeletal muscles change (Fig. 1*B*). Specifically, both $QUAD_M$ and $GAST_M$ were greater than SOL_M during submaximal state 3 respiration through CI (P_{CI}; $P = 0.005$ and 0.001, respectively), maximal state 3 respiration (P; $P = 0.007$ and $P < 0.001$, respectively), electron transport system capacity (ETS; $P = 0.01$ and $P < 0.001$, respectively) and submaximal state 3 respiration through CII (P_{CII}; $P = 0.021$ and $P = 0.001$, respectively). Mitochondrial content correlates directly with overall respiratory capacity (Larsen *et al.* 2012). This is shown here, because maximal state 3 respiration, or oxidative phosphorylation capacity, P, strongly correlates ($r = 0.932$, $P < 0.001$) with CS activity across all mouse muscles (Fig. 1*C*). When analysing differences in CS activity across groups, SOL_M presents with more CS activity than any other skeletal muscle ($P < 0.001$). The only other difference was that CS activity in $GAST_M$ was less than in $QUAD_H$ ($P < 0.002$).

Mitochondria-specific respiration across mouse muscles

Although CS activity has been shown to correlate strongly with mitochondrial content in humans (Larsen *et al.* 2012) and also in horses (Hoppeler, 1990), it was necessary to establish this in mouse skeletal muscle. In order to validate measures of CS activity in mouse skeletal muscle, we correlated those values to quantification of mitochondrial enzymes from a subgroup of animals included in this study ($n = 4$). The quantification of all mitochondrial proteins analysed in $QUAD_M$, SOL_M and $GAST_M$ is

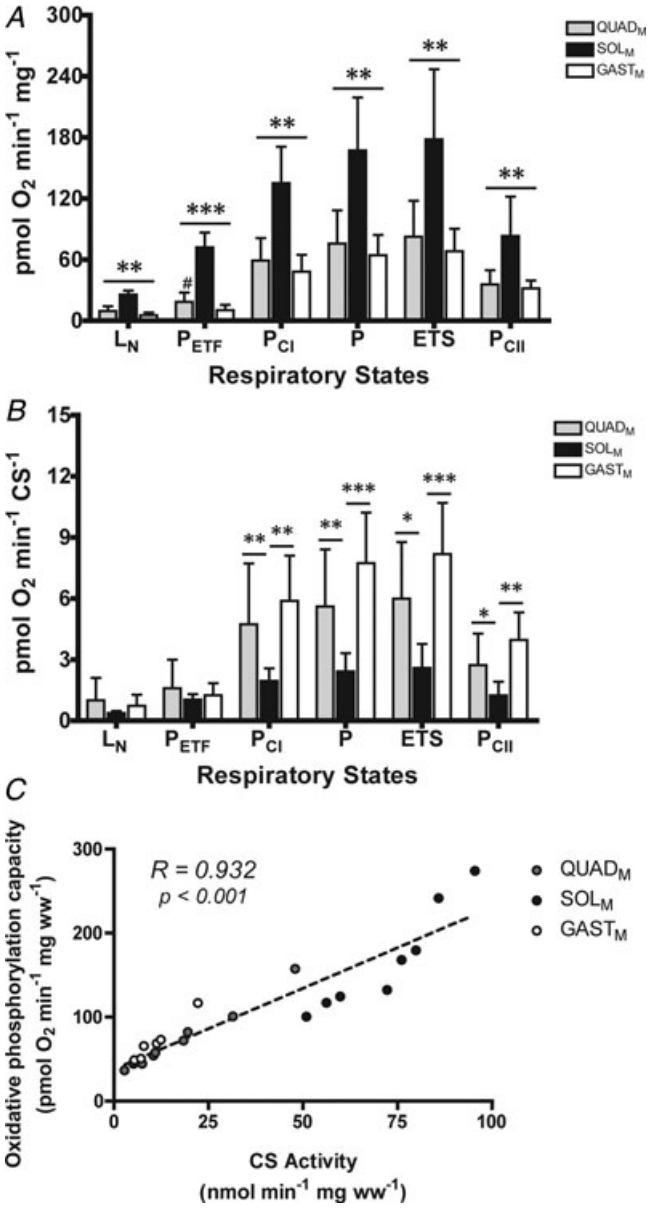

Figure 1. Comparison of respiratory capacity and control in mouse skeletal muscles
Mass-specific (*A*) and mitochondria-specific respiration (*B*) across mouse quadriceps ($QUAD_M$; grey bars), soleus (SOL_M; filled bars) and gastrocnemius ($GAST_M$; open bars). Abbreviations: L_N, leak respiration without adenylates; P, maximal state 3 respiration, i.e. oxidative phosphorylation capacity; P_{CI}, submaximal state 3 respiration through complex I (CI); P_{CII}, submaximal state 3 respiration through complex II (CII); and P_{ETF}, maximal fatty acid oxidation. Data are presented as means + SD. $^{*}P \leq 0.05$, $^{**}P \leq 0.01$ and $^{***}P \leq 0.001$. #Significant difference from $GAST_M$, $P < 0.05$. *C*, Pearson correlation of maximal oxidative phosphorylation system capacity, maximal state 3 respiration (P), *versus* citrate synthase (CS) activity. Citrate synthase activity (*x*-axis) is plotted against P (*y*-axis) for all mouse skeletal muscles. The grey circles represent $QUAD_M$, the filled circles SOL_M and the open circles $GAST_M$. $r = 0.932$, $P < 0.001$.

illustrated in the Supplemental material (Fig. S1). All quantifications of mitochondrial proteins correlated strongly with measures of CS activity (Supplemental material, Fig. S1), establishing its use as a valid biomarker of mitochondrial content in mouse skeletal muscle.

Mitochondrial function in mouse quadriceps *versus* human quadriceps

Mass-specific respirometric comparisons of $QUAD_M$ differed from its human counterpart during P_{ETF} ($P = 0.007$), P_{CI} ($P = 0.05$), P ($P = 0.015$) and ETS ($P = 0.002$) respiratory states (Fig. 2*A*). When controlling for mitochondrial content, the only difference between $QUAD_M$ and $QUAD_H$ was observed at ETS ($P = 0.038$; Fig. 2*B*).

Mitochondrial function in mouse soleus *versus* human quadriceps

Mass-specific respiratory values from SOL_M and $QUAD_H$ mitochondria are presented in Fig. 3*A*. They differed during leak respiration in absence of adenylates (L_N; $P < 0.001$), P_{ETF} ($P < 0.001$), P_{CI} ($P = 0.005$) and P_{CII} ($P = 0.002$). When controlling for mitochondrial content, the differences between SOL_M and $QUAD_H$ were observed at P_{ETF} ($P = 0.002$), P_{CI} ($P < 0.001$), P ($P < 0.001$) and ETS ($P < 0.001$) respiratory states (Fig. 3*B*).

Mitochondrial function in mouse gastrocnemius *versus* human quadriceps

Mass-specific differences for all respiratory states except P_{CII} were lower in $GAST_M$ when compared with $QUAD_H$ (Fig. 4*A*; L_N, $P = 0.05$; P_{ETF}, $P < 0.001$; P_{CI}, $P = 0.003$; P, $P = 0.003$; and ETS, $P < 0.001$). When controlling for mitochondrial content, the only differences between $GAST_M$ and $QUAD_H$ were at P_{CI} ($P = 0.05$) and P_{CII} ($P = 0.007$) respiratory states (Fig. 4*B*).

Mitochondrial coupling control

The leak control ratio during β-oxidation (LCR_{ETF}), representing the electron coupling control during fat oxidation, differed between $QUAD_M$ and SOL_M ($P = 0.015$) and between $QUAD_M$ and $QUAD_H$ ($P = 0.005$). The phosphorylation system control ratio (PSCR) did not differ between any mouse muscles (Fig. 5); however, all the mouse muscles presented with a higher PSCR than the human muscle ($P < 0.001$).

Discussion

The aim of this study was to analyse respiratory capacity and control in several mouse muscles and to compare and contrast those values with skeletal muscle mitochondrial function measured in muscle from young and healthy human subjects. We have several main findings, as follows: (i) qualitative differences in mitochondrial function exist between mouse skeletal muscles; (ii) respiratory capacity in young, healthy mouse skeletal muscle does correspond well to that of young, healthy human skeletal muscle; and (iii) in contrast to our hypothesis, mitochondrial function of the $QUAD_M$, not SOL_M, more closely resembles that of human skeletal muscle.

There is discussion on whether the respiratory capacity of skeletal muscle depends solely on mitochondrial content or whether differences exist across skeletal muscles with varying biochemical make-up (Picard *et al.* 2012). There is some evidence in support of the supposition that differences in oxidative potential between skeletal muscles can be accounted for by the mitochondrial volume density between the muscles (Hoppeler *et al.* 1987; Schwerzmann *et al.* 1989), although these studies were limited either by measuring P_{CI} and P_{CII} only individually, but not collectively, in preparations of isolated mitochondria or by perfusion limitations to the skeletal muscle. Other evidence suggests, as do the results presented here, that a respiratory difference between oxidative and glycolytic muscle mitochondria does exist when taking into account mitochondrial content (Jackman & Willis, 1996; Picard *et al.* 2008). All data reporting differences between oxidative and glycolytic muscles report a higher respiratory capacity per mitochondrion in glycolytic muscle (Jackman & Willis, 1996; Picard *et al.* 2008). Respiratory differences across skeletal muscle fibre types have also been shown in human subjects using *in vivo* imaging techniques (Amara *et al.* 2007; Conley *et al.* 2007). Here we maintain that there are differences in respiratory capacity per mitochondrion across different skeletal muscles and that the more glycolytic muscle possesses greater respiratory capacity for a given mitochondrial content (Fig. 1*B*).

The mechanism(s) explaining these functional differences across skeletal muscle fibre types are largely unknown. Mitochondria do, however, vary morphometrically between fibre types, with mitochondria of fast-twitch muscles possessing a thinner and longer reticular network and mitochondria of slow-twitch muscles expressing a thicker and more truncated reticulum (Ogata & Yamasaki, 1997). The mitochondria expressed in different fibre types are also sometimes subjected to very a different metabolic strain. Glycogen stores are markedly greater in fast-twitch glycolytic muscles when compared with slow-twitch oxidative muscles (Greenhaff *et al.* 1991; Tsintzas *et al.* 1995),

as are the maximal rates of glycogenolysis within each respective muscle type (Greenhaff *et al.* 1991). The greater respiratory capacity per mitochondrion in glycolytic muscle is necessary and may be explained by the greater glycolytic strain per unit mitochondria during intense to maximal exertion. Biochemical protein expression supports this idea, because several mitochondrial enzymes directly involved in the function of the tricarboxylic acid cycle and electron transport chain, e.g. NADH dehydrogenase, have been reported to possess greater expression in glycolytic compared with oxidative skeletal muscle (Glancy & Balaban, 2011).

Normalization of respiration plays a large role in whether or not differences are observed between oxidative and glycolytic fibres; oxidative fibres express greater respiratory capacity when normalized to tissue weight (Fig. 1*A*), because they possess considerably higher mitochondrial content (Fig. 1*C*). This is in

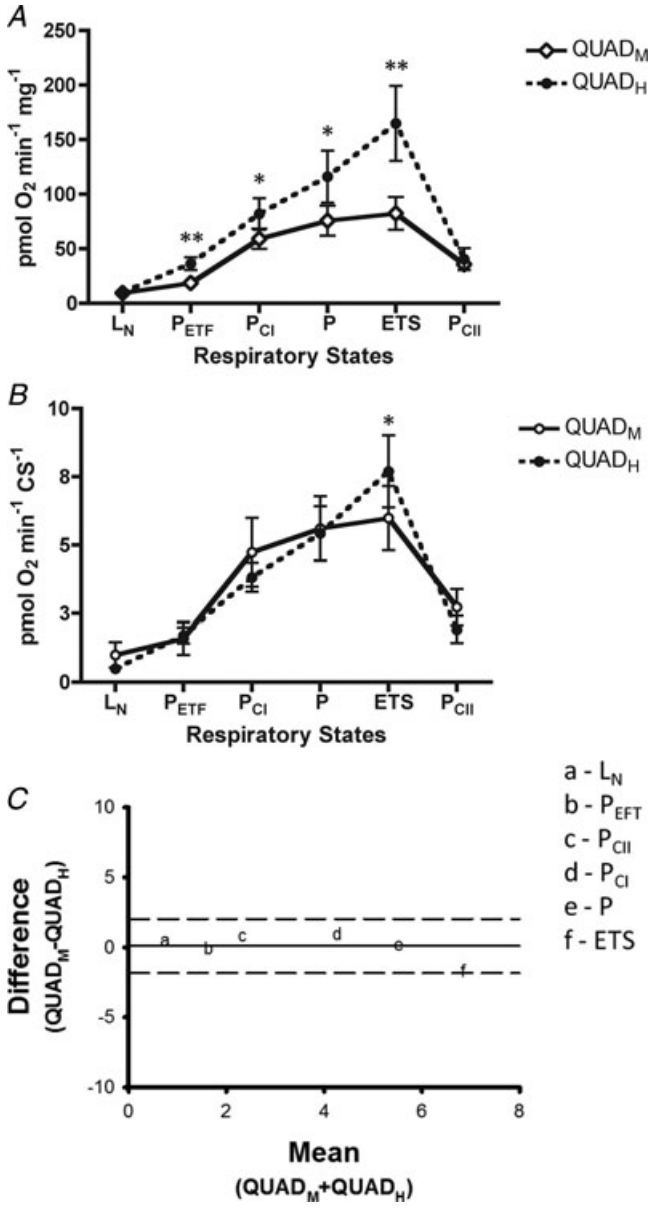

Figure 2. Respiratory capacity and control between mouse quadriceps ($QUAD_M$) and human quadriceps ($QUAD_H$)
Mass-specific (*A*) and mitochondria-specific respiration (*B*). Data are presented as means + SD. $^{*}P \leq 0.05$ and $^{**}P \leq 0.01$. *C*, Bland–Altman plots representing the mean difference and the limit of agreement between $QUAD_M$ and $QUAD_H$ across respiratory states. The continuous line represents the mean of the differences between $QUAD_M$ and $QUAD_H$ and the dashed lines represent the level of agreement (mean ± 2SD). The smaller the range between these two limits, the better the agreement.

agreement with previous reports (Ponsot *et al.* 2005; Picard *et al.* 2008). Normalization to mitochondrial content is required for comparison of true differences in respiratory capacity between skeletal muscles. Respirometric analysis of mitochondria isolated from rat soleus, extensor digitorum longus, gastrocnemius and tibialis anterior found no difference in respiratory capacity in subsarcolemmal or intermyofibrillar populations when normalized to mitochondrial protein content (Yajid *et al.* 1998). Mitochondrial isolation, however, disrupts the united heterogeneous mitochondrial reticulum, resulting in unnaturally circular and disconnected organelles (Schwerzmann *et al.* 1989; Picard *et al.* 2011). This carries the risk of contaminating the isolated fractions

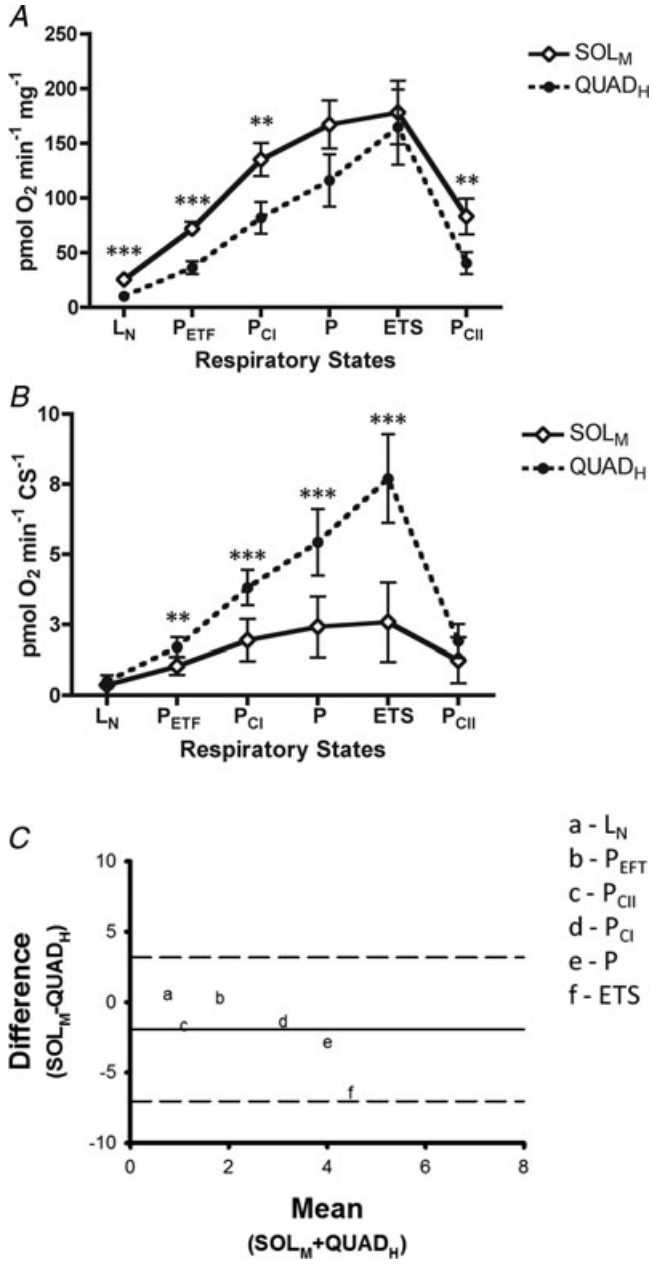

Figure 3. Respiratory capacity and control between mouse soleus (SOL_M) and human quadriceps ($QUAD_H$)
Mass-specific (*A*) and mitochondria-specific respiration (*B*). Data are presented as means + SD. $^{**}P \leq 0.01$ and $^{***}P \leq 0.001$. *C*, Bland–Altman plots representing the mean difference and the limit of agreement between SOL_M and $QUAD_H$ across respiratory states. The continuous line represents the mean of the differences between SOL_M and $QUAD_H$ and the dashed lines represent the level of agreement (mean ± 2SD). The smaller the range between these two limits, the better the agreement.

with proteins not native to the mitochondria (Chretien *et al.* 1995; Picard *et al.* 2011), losing mitochondria-specific contents (Brooks, 2002; Brooks & Hashimoto, 2007; Picard *et al.* 2011) and modifying overall function (Pande & Blanchaer, 1970; Benz, 1994; Saks *et al.* 1998, 2010; Villani *et al.* 1998; Kunz *et al.* 2000; Milner *et al.* 2000; Kuznetsov *et al.* 2008; Picard *et al.* 2010). Moreover, respirometric normalization to mitochondrial protein following mitochondrial isolation has since been rebutted, because it does not correlate with the total area of the cristae (Leary *et al.* 2003). Respirometric normalization to a biomarker of mitochondrial content, such as CS, which is different between muscles, was not analysed (Yajid *et al.* 1998). In human skeletal muscle, CS activity can serve as a valid representative biomarker of mitochondrial volume density, total cristae area and respiratory capacity (Larsen

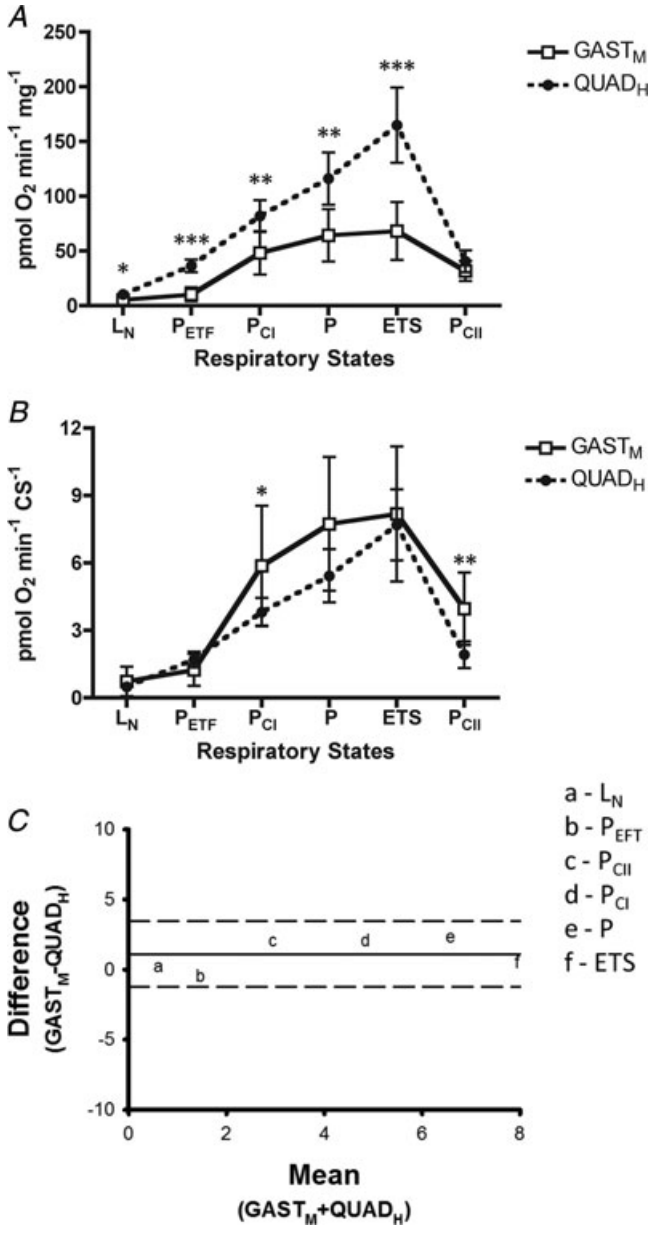

Figure 4. Respiratory capacity and control between mouse gastrocnemius ($GAST_M$) and human quadriceps ($QUAD_H$)
Mass-specific (*A*) and mitochondria-specific respiration (*B*). Data are presented as means + SD. $^{*}P \leq 0.05$, $^{**}P \leq 0.01$ and $^{***}P \leq 0.001$. *C*, Bland–Altman plots representing the mean difference and the limit of agreement between $GAST_M$ and $QUAD_H$ across respiratory states. The continuous line represents the mean of the differences between $GAST_M$ and $QUAD_H$ and the dashed lines represent the level of agreement (mean ± 2SD). The smaller the range between these two limits, the better the agreement.

et al. 2012). We also validate CS activity as a representative biomarker of mitochondrial content in mouse skeletal muscle, because there were strong correlations with CS activity and quantification of all mitochondrial proteins analysed (Supplemental material, Fig. S1). An additional benefit to the use of measurements of CS activity is that they can be made from the same skeletal muscle preparation used to collect respirometric values (Picard *et al.* 2008; Larsen *et al.* 2012), as was done in the present study.

The ability to use animal models for human mitochondrial function is important, because mitochondria are intimately associated with both health and disease. Use of the mouse as a representative model of human mitochondrial function, however, has come into question (Lemieux & Warren, 2012). Differences in molecular profiles between mouse and human skeletal muscle indirectly support these claims. However, the assertion that mouse mitochondrial function deviates greatly from that in the human has never empirically been tested until now. Using saponin-permeabilized skeletal muscle preparations from $QUAD_M$ and $QUAD_H$, we show that the differences in respiratory control across species are minor or negligible (Fig. 2*B*). In contrast to isolated mitochondrial preparations, this specific mitochondrial preparation allows for direct access to skeletal muscle mitochondria while preserving the cytocellular ultrastructure (Lin *et al.* 1990; Saks *et al.* 1991, 1998; Kuznetsov *et al.* 2008; Gnaiger, 2009; Pesta & Gnaiger, 2011; Picard *et al.* 2011) as well as subcellular interactions (Veksler *et al.* 1987; Lin *et al.* 1990; Saks *et al.* 1998; Milner *et al.* 2000; Kuznetsov *et al.* 2008; Picard *et al.* 2011). Cellular bioenergetics and metabolic channelling are reliant upon these characteristics (Saks *et al.* 1998; Kay *et al.* 2000; Kuznetsov *et al.* 2008; Gnaiger, 2009). Accordingly, this specific mitochondrial preparation serves as the best model in which to examine differences between skeletal muscle types and also to compare and contrast function across species.

In contrast to our hypothesis, it was respiratory capacity and control of the $QUAD_M$, not SOL_M, that better represents human skeletal muscle mitochondrial function (Figs 2*B versus* 3*B*). These data also refute previous reports that the SOL_M may serve as a better representative of human skeletal muscle based on molecular modelling (Kho *et al.* 2006). Bland–Altman plots further verified this finding (Figs 2*C*, 3*C* and 4*C*). These Bland–Altman plots are graphical representations of the differences between the respirometric analysis of mouse muscle and human muscle against the mean for each respective respiratory state. This method determines the mean difference (measurement bias) between the two measurements in question, as well as the 95% limit of agreement of the mean difference (2SD). The smaller the range between these two limits, the better the agreement.

It should be noted that mitochondrial electron coupling control during fat oxidation is more similar between SOL_M and $QUAD_H$ (Fig. 5). The LCR_{ETF} is determined from two respiratory states, a leak state (L_N) and a higher respiratory state (P_{EFT}). These corresponding states are paired by an identical substrate supply (malate + octanoyl carnitine). The ratio of these two states reflects electron coupling efficiency during fat oxidation, from a theoretical minimum of 0.0, indicating a fully coupled system, to a value of 1.0, representing a fully non-coupled (dyscoupled) system (Gnaiger, 2009). Thus, while $QUAD_M$ was most similar to $QUAD_H$ respiratory capacities, it may be more accurate to state that mouse skeletal muscles can provide a useful model to test hypotheses relating to human skeletal muscle with the caveat that species differences are real, very specific, different across muscle types, and must be considered before extrapolating directly to human skeletal muscle. We also confirmed that young, healthy mice may serve as representative models of mitochondrial performance in young, healthy and non-sedentary humans. The comorbidities of a sedentary, caged and *ad libitum*-fed lifestyle (Martin *et al.* 2010) do not appear to affect mitochondrial function within the first 8–10 weeks of life.

One difference that did exist between all mouse skeletal muscles and the human muscle was the PSCR. This is the ratio of maximal state 3 respiration to ETS capacity and represents the degree of constraint of the maximal oxidative phosphorylation capacity by the phosphorylation system or ATP synthase (Gnaiger, 2009). With no restriction, the PSCR approaches a ratio of 1.0, which we observed in all mouse muscles (Fig. 5), as seen in other studies (ter Veld *et al.* 2005; Aragonés *et al.* 2008). We observed that human skeletal muscle

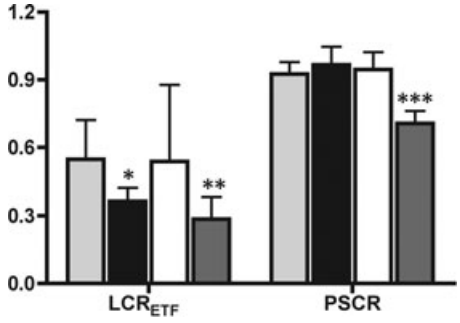

Figure 5. Mitochondrial coupling control across all groups
Leak-control ratios (LCRs) for the coupling control of electron transport through the electron-transferring flavoprotein (ETF) during β-oxidation (LCR_{ETF}) and phosphorylation system control ratio (PSCR) across mouse quadriceps ($QUAD_M$; light grey bars), mouse soleus (SOL_M; dark grey bars), mouse gastrocnemius ($GAST_M$; open bars) and human quadriceps ($QUAD_H$; filled bars). Data are presented as means + SD. $^*P \leq 0.05$, $^{**}P \leq 0.01$ from $QUAD_M$. $^{***}P < 0.001$ from all mouse skeletal muscle.

presented with an average PSCR of 0.71, which is also comparable to other reported values (Boushel *et al.* 2007). A ratio less than 1.0, as observed in humans, suggests that electron transport through complexes I–IV is limited by ADP phosphorylation. When facilitating non-coupled respiration with the proton ionophore FCCP by collapsing the electron gradient prior to phosphorylation, a higher electron transport and attendant respiration is reached ($QUAD_H$ respiration; Fig. 2*B*). Oxidative phosphorylation capacity (P) is more than capable of utilizing the oxygen delivered during maximal whole-body exercise (Boushel *et al.* 2011), where oxygen delivery is limiting. Thus, the excess capacity for electron transport following uncoupling in human skeletal muscle mitochondria possibly serves a functional role during exercise in isolated muscle groups where maximal work is not limited by oxygen supply (Andersen & Saltin, 1985). The functional role of an excess electron transport capacity in human skeletal muscle mitochondria merits further investigation.

Conclusion

If differences in murine and human mitochondrial function did exist then it would be both difficult and cavalier to apply results collected from mice to a larger and different human population, particularly if neither the group sampled nor the population was clearly defined. Here we discriminate between skeletal muscle mitochondrial function in mice and humans. We provide evidence disproving any excessive discordance or discrepancy that has been claimed to exist between mouse and human mitochondria unless specifically examining the phosphorylative restraint of ATP synthase on oxidative phosphorylation (Lemieux & Warren, 2012). Specifically, young, healthy mouse quadriceps serves as a suitable representative for mitochondrial function in young, healthy human vastus lateralis. This allows for more assurance when progressing from descriptive to inferential statistics between healthy young mouse and human mitochondria.

References

Amara CE, Shankland EG, Jubrias SA, Marcinek DJ, Kushmerick MJ & Conley KE (2007). Mild mitochondrial uncoupling impacts cellular aging in human muscles *in vivo*. *Proc Natl Acad Sci U S A* **104**, 1057–1062.

Andersen P & Saltin B (1985). Maximal perfusion of skeletal muscle in man. *J Physiol* **366**, 233–249.

Aragonés J, Schneider M, Van Geyte K, Fraisl P, Dresselaers T, Mazzone M *et al.* (2008). Deficiency or inhibition of oxygen sensor Phd1 induces hypoxia tolerance by reprogramming basal metabolism. *Nat Genet* **40**, 170–180.

Benz R (1994). Permeation of hydrophilic solutes through mitochondrial outer membranes: review on mitochondrial porins. *Biochim Biophys Acta* **1197**, 167–196.

Bergström J (1962). Muscle electrolytes in man. *Scand J Clin Lab Invest* **68**, 1–110.

Bernstein D (2003). Exercise assessment of transgenic models of human cardiovascular disease. *Physiol Genomics* **13**, 217–226.

Boushel R, Gnaiger E, Calbet JA, Gonzalez-Alonso J, Wright-Paradis C, Sondergaard H, Ara I, Helge JW & Saltin B (2011). Muscle mitochondrial capacity exceeds maximal oxygen delivery in humans. *Mitochondrion* **11**, 303–307.

Boushel R, Gnaiger E, Schjerling P, Skovbro M, Kraunsøe R & Dela F (2007). Patients with type 2 diabetes have normal mitochondrial function in skeletal muscle. *Diabetologia* **50**, 790–796.

Brand MD & Nicholls DG (2011). Assessing mitochondrial dysfunction in cells. *Biochem J* **435**, 297–312.

Brooks GA (2002). Lactate shuttle – between but not within cells? *J Physiol* **541**, 333–334.

Brooks GA & Hashimoto T (2007). Investigation of the lactate shuttle in skeletal muscle mitochondria. *J Physiol* **584**, 705–706; author reply 707–708.

Chomentowski P, Coen PM, Radiková Z, Goodpaster BH & Toledo FG (2011). Skeletal muscle mitochondria in insulin resistance: differences in intermyofibrillar *versus* subsarcolemmal subpopulations and relationship to metabolic flexibility. *J Clin Endocrinol Metab* **96**, 494–503.

Chretien D, Pourrier M, Bourgeron T, Séné M, Rötig A, Munnich A & Rustin P (1995). An improved spectrophotometric assay of pyruvate dehydrogenase in lactate dehydrogenase contaminated mitochondrial preparations from human skeletal muscle. *Clin Chim Acta* **240**, 129–136.

Conley KE, Amara CE, Jubrias SA & Marcinek DJ (2007). Mitochondrial function, fibre types and ageing: new insights from human muscle *in vivo*. *Exp Physiol* **92**, 333–339.

Demetrius L (2006). Aging in mouse and human systems: a comparative study. *Ann N Y Acad Sci* **1067**, 66–82.

Desai KH, Sato R, Schauble E, Barsh GS, Kobilka BK & Bernstein D (1997). Cardiovascular indexes in the mouse at rest and with exercise: new tools to study models of cardiac disease. *Am J Physiol Heart Circ Physiol* **272**, H1053–H1061.

Eaton S, Bartlett K & Pourfarzam M (1996). Mammalian mitochondrial β-oxidation. *Biochem J* **320**, 345–357.

Garland T Jr, Schutz H, Chappell MA, Keeney BK, Meek TH, Copes LE, Acosta W, Drenowatz C, Maciel RC, van Dijk G, Kotz CM & Eisenmann JC (2011). The biological control of voluntary exercise, spontaneous physical activity and daily energy expenditure in relation to obesity: human and rodent perspectives. *J Exp Biol* **214**, 206–229.

Glancy B & Balaban RS (2011). Protein composition and function of red and white skeletal muscle mitochondria. *Am J Physiol Cell Physiol* **300**, C1280–C1290.

Gnaiger E (2009). Capacity of oxidative phosphorylation in human skeletal muscle: new perspectives of mitochondrial physiology. *Int J Biochem Cell Biol* **41**, 1837–1845.

Greenhaff PL, Ren JM, Söderlund K & Hultman E (1991). Energy metabolism in single human muscle fibers during contraction without and with epinephrine infusion. *Am J Physiol Endocrinol Metab* **260**, E713–E718.

Hoppeler H (1990). *The Dynamic State of Muscle Fibers*. Walter de Gruyter, Berlin.

Hoppeler H, Hudlicka O & Uhlmann E (1987). Relationship between mitochondria and oxygen consumption in isolated cat muscles. *J Physiol* **385**, 661–675.

Jackman MR & Willis WT (1996). Characteristics of mitochondria isolated from type I and type IIb skeletal muscle. *Am J Physiol Cell Physiol* **270**, C673–C678.

Jacobs HT (2003). The mitochondrial theory of aging: dead or alive? *Aging Cell* **2**, 11–17.

Jacobs RA & Lundby C. (2012). Mitochondria express enhanced quality as well as quantity in association with aerobic fitness across recreationally active individuals up to elite athletes. *J Appl Physiol*, doi:10.1152/japplphysiol.01081.2012.

Jacobs RA, Rasmussen P, Siebenmann C, Díaz V, Gassmann M, Pesta D, Gnaiger E, Nordsborg NB, Robach P & Lundby C (2011). Determinants of time trial performance and maximal incremental exercise in highly trained endurance athletes. *J Appl Physiol* **111**, 1422–1430.

Jacobs RA, Siebenmann C, Hug M, Toigo M, Meinild AK & Lundby C (2012). Twenty-eight days at 3454-m altitude diminishes respiratory capacity but enhances efficiency in human skeletal muscle mitochondria. *FASEB J* **26**, 5192–5200.

Kay L, Nicolay K, Wieringa B, Saks V & Wallimann T (2000). Direct evidence for the control of mitochondrial respiration by mitochondrial creatine kinase in oxidative muscle cells *in situ*. *J Biol Chem* **275**, 6937–6944.

Kho AT, Kang PB, Kohane IS & Kunkel LM (2006). Transcriptome-scale similarities between mouse and human skeletal muscles with normal and myopathic phenotypes. *BMC Musculoskelet Disord* **7**, 23.

Kunz WS, Kudin A, Vielhaber S, Elger CE, Attardi G & Villani G (2000). Flux control of cytochrome *c* oxidase in human skeletal muscle. *J Biol Chem* **275**, 27741–27745.

Kuznetsov AV, Schneeberger S, Seiler R, Brandacher G, Mark W, Steurer W, Saks V, Usson Y, Margreiter R & Gnaiger E (2004). Mitochondrial defects and heterogeneous cytochrome *c* release after cardiac cold ischemia and reperfusion. *Am J Physiol Heart Circ Physiol* **286**, H1633–H1641.

Kuznetsov AV, Veksler V, Gellerich FN, Saks V, Margreiter R & Kunz WS (2008). Analysis of mitochondrial function *in situ* in permeabilized muscle fibers, tissues and cells. *Nat Protoc* **3**, 965–976.

Larsen S, Nielsen J, Hansen CN, Nielsen LB, Wibrand F, Stride N, Schroder HD, Boushel R, Helge JW, Dela F & Hey-Mogensen M (2012). Biomarkers of mitochondrial content in skeletal muscle of healthy young human subjects. *J Physiol* **590**, 3349–3360.

Leary SC, Lyons CN, Rosenberger AG, Ballantyne JS, Stillman J & Moyes CD (2003). Fiber-type differences in muscle mitochondrial profiles. *Am J Physiol Regul Integr Comp Physiol* **285**, R817–R826.

Lemieux H & Warren BE (2012). An animal model to study human muscular diseases involving mitochondrial oxidative phosphorylation. *J Bioenerg Biomembr* **44**, 503–512.

Lin A, Krockmalnic G & Penman S (1990). Imaging cytoskeleton–mitochondrial membrane attachments by embedment-free electron microscopy of saponin-extracted cells. *Proc Natl Acad Sci U S A* **87**, 8565–8569.

Lowell BB & Shulman GI (2005). Mitochondrial dysfunction and type 2 diabetes. *Science* **307**, 384–387.

Martin B, Ji S, Maudsley S & Mattson MP (2010). "Control" laboratory rodents are metabolically morbid: why it matters. *Proc Natl Acad Sci U S A* **107**, 6127–6133.

Miller BF, Robinson MM, Bruss MD, Hellerstein M & Hamilton KL (2012). A comprehensive assessment of mitochondrial protein synthesis and cellular proliferation with age and caloric restriction. *Aging Cell* **11**, 150–161.

Milner DJ, Mavroidis M, Weisleder N & Capetanaki Y (2000). Desmin cytoskeleton linked to muscle mitochondrial distribution and respiratory function. *J Cell Biol* **150**, 1283–1298.

Nordsborg N, Ovesen J, Thomassen M, Zangenberg M, Jøns C, Iaia FM, Nielsen JJ & Bangsbo J (2008). Effect of dexamethasone on skeletal muscle Na^+,K^+ pump subunit specific expression and K^+ homeostasis during exercise in humans. *J Physiol* **586**, 1447–1459.

Nordsborg NB, Siebenmann C, Jacobs RA, Rasmussen P, Diaz V, Robach P & Lundby C (2012). Four weeks of normobaric "live high-train low" do not alter muscular or systemic capacity for maintaining pH and K^+ homeostasis during intense exercise. *J Appl Physiol* **112**, 2027–2036.

Ogata T & Yamasaki Y (1997). Ultra-high-resolution scanning electron microscopy of mitochondria and sarcoplasmic reticulum arrangement in human red, white, and intermediate muscle fibers. *Anat Rec* **248**, 214–223.

Paglialunga S, van Bree B, Bosma M, Valdecantos MP, Amengual-Cladera E, Jörgensen JA, van Beurden D, den Hartog GJ, Ouwens DM, Briedé JJ, Schrauwen P & Hoeks J (2012). Targeting of mitochondrial reactive oxygen species production does not avert lipid-induced insulin resistance in muscle tissue from mice. *Diabetologia* **55**, 2759–2768.

Pande SV & Blanchaer MC (1970). Preferential loss of ATP-dependent long-chain fatty acid activating enzyme in mitochondria prepared using Nagarse. *Biochim Biophys Acta* **202**, 43–48.

Pesta D & Gnaiger E (2011). High-resolution respirometry: OXPHOS protocols for human cell cultures and permeabilized fibers from small biopsies of human muscle. *Methods Mol Biol* **810**, 25–58.

Pesta D, Hoppel F, Macek C, Messner H, Faulhaber M, Kobel C, Parson W, Burtscher M, Schocke M & Gnaiger E (2011). Similar qualitative and quantitative changes of mitochondrial respiration following strength and endurance training in normoxia and hypoxia in sedentary humans. *Am J Physiol Regul Integr Comp Physiol* **301**, R1078–R1087.

Picard M, Csukly K, Robillard ME, Godin R, Ascah A, Bourcier-Lucas C & Burelle Y (2008). Resistance to Ca^{2+}-induced opening of the permeability transition pore differs in mitochondria from glycolytic and oxidative muscles. *Am J Physiol Regul Integr Comp Physiol* **295**, R659–R668.

Picard M, Hepple RT & Burelle Y (2012). Mitochondrial functional specialization in glycolytic and oxidative muscle fibers: tailoring the organelle for optimal function. *Am J Physiol Cell Physiol* **302**, C629–C641.

Picard M, Ritchie D, Wright KJ, Romestaing C, Thomas MM, Rowan SL, Taivassalo T & Hepple RT (2010). Mitochondrial functional impairment with aging is exaggerated in isolated mitochondria compared to permeabilized myofibers. *Aging Cell* **9**, 1032–1046.

Picard M, Taivassalo T, Gouspillou G & Hepple RT (2011). Mitochondria: isolation, structure and function. *J Physiol* **589**, 4413–4421.

Ponsot E, Zoll J, N'Guessan B, Ribera F, Lampert E, Richard R, Veksler V, Ventura-Clapier R & Mettauer B (2005). Mitochondrial tissue specificity of substrates utilization in rat cardiac and skeletal muscles. *J Cell Physiol* **203**, 479–486.

Rangarajan A & Weinberg RA (2003). Opinion: Comparative biology of mouse versus human cells: modelling human cancer in mice. *Nat Rev Cancer* **3**, 952–959.

Rasmussen UF & Rasmussen HN (2000). Human skeletal muscle mitochondrial capacity. *Acta Physiol Scand* **168**, 473–480.

Rennie MJ, Selby A, Atherton P, Smith K, Kumar V, Glover EL & Philips SM (2010). Facts, noise and wishful thinking: muscle protein turnover in aging and human disuse atrophy. *Scand J Med Sci Sports* **20**, 5–9.

Saks V, Guzun R, Timohhina N, Tepp K, Varikmaa M, Monge C, Beraud N, Kaambre T, Kuznetsov A, Kadaja L, Eimre M & Seppet E (2010). Structure–function relationships in feedback regulation of energy fluxes in vivo in health and disease: mitochondrial interactosome. *Biochim Biophys Acta* **1797**, 678–697.

Saks VA, Belikova YO & Kuznetsov AV (1991). In vivo regulation of mitochondrial respiration in cardiomyocytes: specific restrictions for intracellular diffusion of ADP. *Biochim Biophys Acta* **1074**, 302–311.

Saks VA, Veksler VI, Kuznetsov AV, Kay L, Sikk P, Tiivel T, Tranqui L, Olivares J, Winkler K, Wiedemann F & Kunz WS (1998). Permeabilized cell and skinned fiber techniques in studies of mitochondrial function in vivo. *Mol Cell Biochem* **184**, 81–100.

Schiaffino S, Sandri M & Murgia M (2007). Activity-dependent signaling pathways controlling muscle diversity and plasticity. *Physiology (Bethesda)* **22**, 269–278.

Schwerzmann K, Hoppeler H, Kayar SR & Weibel ER (1989). Oxidative capacity of muscle and mitochondria: correlation of physiological, biochemical, and morphometric characteristics. *Proc Natl Acad Sci U S A* **86**, 1583–1587.

Sebastián D, Hernández-Alvarez MI, Segalés J, Sorianello E, Muñoz JP, Sala D, Waget A, Liesa M, Paz JC, Gopalacharyulu P, Orešič M, Pich S, Burcelin R, Palacín M & Zorzano A (2012). Mitofusin 2 (Mfn2) links mitochondrial and endoplasmic reticulum function with insulin signaling and is essential for normal glucose homeostasis. *Proc Natl Acad Sci U S A* **109**, 5523–5528.

Srere PA (1969). Citrate synthase. *Methods Enzymol* **13**, 3–11.

Svenson KL, Von Smith R, Magnani PA, Suetin HR, Paigen B, Naggert JK, Li R, Churchill GA & Peters LL (2007). Multiple trait measurements in 43 inbred mouse strains capture the phenotypic diversity characteristic of human populations. *J Appl Physiol* **102**, 2369–2378.

ter Veld F, Jeneson JA & Nicolay K (2005). Mitochondrial affinity for ADP is twofold lower in creatine kinase knock-out muscles. Possible role in rescuing cellular energy homeostasis. *FEBS J* **272**, 956–965.

Thomassen M, Rose AJ, Jensen TE, Maarbjerg SJ, Bune L, Leitges M, Richter EA, Bangsbo J & Nordsborg NB (2011). Protein kinase Cα activity is important for contraction-induced FXYD1 phosphorylation in skeletal muscle. *Am J Physiol Regul Integr Comp Physiol* **301**, R1808–R1814.

Tsintzas OK, Williams C, Boobis L & Greenhaff P (1995). Carbohydrate ingestion and glycogen utilization in different muscle fibre types in man. *J Physiol* **489**, 243–250.

Veksler VI, Kuznetsov AV, Sharov VG, Kapelko VI & Saks VA (1987). Mitochondrial respiratory parameters in cardiac tissue: a novel method of assessment by using saponin-skinned fibers. *Biochim Biophys Acta* **892**, 191–196.

Villani G, Greco M, Papa S & Attardi G (1998). Low reserve of cytochrome *c* oxidase capacity *in vivo* in the respiratory chain of a variety of human cell types. *J Biol Chem* **273**, 31829–31836.

Mouse Genome Sequencing Consortium, Waterston RH, Lindblad-Toh K, Birney E, Rogers J, Abril JF et al. (2002). Initial sequencing and comparative analysis of the mouse genome. Nature 420, 520-562. Consortium MGS, Waterston RH, Lindblad-Toh K, Birney E, Rogers J, Abril JF & al. e. (2002). Initial sequencing and comparative analysis of the mouse genome. *Nature* **420,** 520–562.

Yajid F, Mercier JG, Mercier BM, Dubouchaud H & Préfaut C (1998). Effects of 4 wk of hindlimb suspension on skeletal muscle mitochondrial respiration in rats. *J Appl Physiol* **84**, 479–485.

Supporting Information

Additional Supporting Information may be found in the online version of this article:

SUPPLEMENTAL FIGURE S1. Quantification of mitochondria-specific enzymes across mouse skeletal muscles. Using a subsection of animals (n = 4) the expression of various mitochondrial proteins were quantified (mean ± SD) in quadricep (QUAD, grey bars), soleus (SOL, black bars), and lateral gastrocnemius (GAST, white bars). The respective correlation of these values to citrate synthase (CS) activity was also examined in QUAD (grey filled points), SOL (black filled points), and GAST (white filled points). Protein quantification and correlation to CS activity for mitochondrial complex I (A & B), mitochondrial complex II (C&D), mitochondrial complex III (E & F), mitochondrial complex IV (G & H), mitochondrial complex V (I & J), 3-hydroxyacyl coenzyme a dehydrogenase (HAD, K & L), and CS (M & N).

Research Paper

Mitochondrial function in human skeletal muscle following high-altitude exposure

Robert A. Jacobs[1,2], Robert Boushel[3,4], Cynthia Wright-Paradis[3], Jose A. L. Calbet[3,5], Paul Robach[6], Erich Gnaiger[7] and Carsten Lundby[1,8]

[1] *Center for Integrative Human Physiology (ZIHP) and* [8] *Institute of Physiology, University of Zurich, Zurich, Switzerland*
[2] *Institute of Veterinary Physiology, Vetsuisse Faculty, University of Zurich, Zurich, Switzerland*
[3] *The Copenhagen Muscle Research Centre, Copenhagen, Denmark*
[4] *Heart & Circulatory Unit, Department of Biomedical Sciences, University of Copenhagen, Copenhagen, Denmark*
[5] *Department of Physical Education, University of Las Palmas, Canary Islands, Spain*
[6] *Département Médical, Ecole Nationale de Ski et d'Alpinisme, site de l'Ecole Nationale des Sports de Montagne, Q4 Chamonix, France*
[7] *Department of General and Transplant Surgery, D. Swarovski Research Laboratory, Medical University of Innsbruck, Innsbruck, Austria*

Studies regarding mitochondrial modifications in human skeletal muscle following acclimatization to high altitude are conflicting, and these inconsistencies may be due to the prevalence of representing mitochondrial function through static and isolated measurements of specific mitochondrial characteristics. The aim of this study, therefore, was to investigate mitochondrial function in response to high-altitude acclimatization through measurements of respiratory control in the vastus lateralis muscle. Skeletal muscle biopsies were obtained from 10 lowland natives prior to and again after a total of 9–11 days of exposure to 4559 m. High-resolution respirometry was performed on the muscle samples to compare respiratory chain function and respiratory capacities. Respirometric analysis revealed that mitochondrial function was largely unaffected, because high-altitude exposure did not affect the capacity for fat oxidation or individualized respiration capacity through either complex I or complex II. Respiratory chain function remained unaltered, because neither coupling nor respiratory control changed in response to hypoxic exposure. High-altitude acclimatization did, however, show a tendency ($P = 0.059$) to limit mass-specific maximal oxidative phosphorylation capacity. These data suggest that 9–11 days of exposure to high altitude do not markedly modify integrated measures of mitochondrial functional capacity in skeletal muscle despite significant decrements in the concentrations of enzymes involved in the tricarboxylic acid cycle and oxidative phosphorylation.

(Received 17 March 2012; accepted after revision 24 May 2012; first published online 25 May 2012)
Corresponding author C. Lundby: Zürich Center for Integrative Human Physiology (ZIHP), University of Zurich, Institute of Physiology, Office 23 H 6, Winterthurerstraße 190, 8057 Zürich, Switzerland. Email: carsten.lundby@access.uzh.ch

Surprisingly little is known regarding hypoxia-dependent control of mitochondrial function. Previous observations of mitochondrial modifications following acclimatization to altitude have been inconsistent. Initial studies (Tappan *et al.* 1957; Valdivia, 1958; Reynafarje, 1962; Hochachka *et al.* 1983) reported greater expression of indirect markers suggestive of oxidative potential in both animals and humans native to high altitude, leading investigators to speculate that acclimatization may improve respiratory capacity and mitochondrial function in response to an increasingly hypoxic environment (Hochachka *et al.* 1983). This preliminary theory was challenged when further studies of lowlanders sojourning to high/extreme altitudes reported either a dramatic loss of skeletal muscle mitochondria (Hoppeler *et al.* 1990; Howald *et al.* 1990; Levett *et al.* 2012) or negligible changes in

DOI: 10.1113/expphysiol.2012.066092

mitochondrial characteristics, such as enzyme activities, following acclimatization (Green *et al.* 1989, 1992, 2000*a*; MacDougall *et al.* 1991; Mizuno *et al.* 2008; Levett *et al.* 2012), even despite significant reductions in skeletal muscle mass (MacDougall *et al.* 1991; Mizuno *et al.* 2008). Additionally, several studies have reported evidence to suggest an improvement in mechanical efficiency during exercise at sea level following prolonged or intermittent hypoxic exposure (Green *et al.* 2000*b*; Gore *et al.* 2001; Katayama *et al.* 2004; Saunders *et al.* 2009). Other studies have failed to verify this change in exercise economy through consistent and intermittent hypoxic exposure (Lundby *et al.* 2007; Siebenmann *et al.* 2012). Intermittent hypoxic exposure has also failed to facilitate changes in mitochondrial efficiency (Robach *et al.* 2012). Hitherto, in humans, hypoxia-mediated changes in mitochondrial physiology are far from understood.

Changes in muscle oxidative capacity have often been implied by static measurements of mitochondrial protein concentrations/activity or morphometric analysis, representing mitochondrial content or volume, respectively. Relying exclusively on such measurements for the characterization of mitochondrial function and oxidative potential is incomplete, because the evaluation of mitochondrial function requires direct functional measures of intact mitochondria to assess potential changes in oxidative phosphorylation, electron transport, coupling control and efficiency. For example, mass-specific maximal oxidative phosphorylation capacity (P), as measured by high-resolution respirometry, was revealed to be the strongest determinant of endurance performance in highly trained athletes, while the correlation between performance as a measure of mitochondrial content was negligible (Jacobs *et al.* 2011).

Altitude-induced alterations in whole-body protein turnover (Holm *et al.* 2010), including several mitochondrial proteins (Viganò *et al.* 2008) from this study, have previously been reported. Enzyme levels involved in the tricarboxylic acid (TCA) cycle and oxidative phosphorylation were lower following acclimatization, as was previously reported with a similar length of hypoxic exposure (Mizuno *et al.* 1990). To elucidate whether these enzymatic alterations are reflected in mitochondrial respiratory chain function, we assessed mitochondrial respiration in permeabilized skeletal muscle fibres at sea level and after 9–11 days of exposure to high altitude. We hypothesized that mass-specific oxidative phosphorylation capacities would parallel these findings and also diminish following acclimatization to high altitude.

Methods

Subjects

Ten healthy, young and physically active lowland male subjects voluntarily participated in this study. Subject characteristics (means ± SEM) were as follows: age, 26 ± 1 years; height, 181 ± 1 cm; and weight, 79 ± 2 kg. All subjects were scanned for body composition in a dual-energy X-ray absorptiometer (DEXA; Lunar, GE Medical Systems, Madison, WI, USA) prior to high-altitude ascent and again 1 day after return to sea level. Body composition as measured by DEXA showed no differences between sea level baseline (BL) scans compared with those collected after 9–11 days of high-altitude acclimatization (HA), because fat mass was 13.4 ± 4.2 and 13.2 ± 4.5 kg, respectively, while lean body mass was 63.7 ± 6.1 and 63.6 ± 6.1 kg, respectively. Baseline measurements of maximal oxygen consumption ($\dot{V}_{O_2\,max}$) were 4.3 ± 0.1 l min^{-1}. These values decreased as a result of the high altitude (3.0 ± 0.6 l min^{-1}) but returned to BL values upon the provision of supplemental oxygen at altitude, simulating normoxic breathing at sea level (4.4 ± 0.1 l min^{-1}), suggesting no difference in training status between times of data acquisition. For more detailed subject characteristics see Lundby *et al.* (2008). All subjects provided informed, written consent after being presented with oral and written explanations regarding experimental procedures and protocol. The study was conducted in accordance with the principles of the Declaration of Helsinki and was approved by the local ethical committee for Frederiksberg and Copenhagen Communities.

Experimental protocol

A more detailed description of the experimental protocol has been given previously (Robach *et al.* 2007; Lundby *et al.* 2008). Subjects reported to and remained at the laboratory (Copenhagen, 42 m above sea level) 3 days prior to acquisition of BL measurements, where activity was controlled and caloric intake monitored. Subjects later flew to Italy and were transported (including partial hike) to a high-altitude hut (Gnifetti hut, 3647 m), where they stayed for 2 days. On the third day at high altitude, subjects hiked to the Capanna Regina Margherita hut (4559 m), where they remained for the subsequent 9 days. This specific hypoxic exposure to high altitude was chosen because it is long enough to induce some degree of physiological adaptation to hypoxia (Horstman *et al.* 1980; Bender *et al.* 1988; Lundby *et al.* 2003, 2006; Zungu *et al.* 2007; Nordsborg *et al.* 2010), with longer hypoxic exposure facilitating no further changes in oxidative capacity of the leg (Lundby *et al.* 2006). The ascent profile was

Table 1. Blood analyses

Conditions	Serum EPO (mIU ml^{-1})	[Hb] (g l^{-1})	P_{aCO_2} (mmHg)	P_{aO_2} (mmHg)	S_{aO_2} (%)
BL	8.7 ± 3.7	144 ± 8	40.4 ± 2.0	103.2 ± 13.8	98.6 ± 0.5
HA	12.2 ± 3.0*	169 ± 13*	29.2 ± 1.9*	50.5 ± 3.2*	83.4 ± 2.7*

Blood gases, haemoglobin (Hb) and serum erythropoietin (EPO) concentrations were obtained for baseline (BL) measurements in normoxic conditions at sea level and following 11 days (2 days at 3647 m and 7–9 days at 4559 m) of high-altitude (HA) exposure. Abbreviations: P_{aCO_2}, arterial partial pressure of carbon dioxide; P_{aO_2}, arterial partial pressure of oxygen; and S_{aO_2}, percentage arterial oxygen saturation as also reported by Robach *et al.* (2007). The calculation of statistical differences from normoxia was performed using the Wilcoxon test. Values are presented as means ± SD. * Significant difference ($P < 0.01$).

uniform across all subjects. Skeletal muscle biopsies were collected at altitude throughout days 7–9 of exposure to 4559 m (9–11 days of high-altitude exposure in total), with three or four subjects being sampled per day. Three days prior to sample acquisition at high altitude, the subject's activity was controlled as it was at baseline and everyone was fed isocaloric diets with negligible differences in macronutrient content *versus* baseline feeding. No food or caffeine was allowed 12 h prior to skeletal muscle biopsy in either BL or HA conditions. In summary, muscle biopsies were obtained on two separate occasions, the first at BL and the second during HA.

Blood samples

Venous blood was sampled during supine rest from a forearm vein. Blood samples were allowed to clot at 4°C, centrifuged, and the serum was then stored at –20°C for later analysis. Arterial blood was obtained from the right femoral artery for immediate determination of blood gases, as previously described (Calbet *et al.* 2006*a*,*b*).

Blood analyses

Arterial blood was sampled anaerobically in heparinized syringes and was immediately analysed for haemoglobin concentration ([Hb]), oxygen saturation (S_{aO_2}) and the partial pressure of oxygen (P_{aO_2}; ABL700; Radiometer, Copenhagen, Denmark). Serum concentration of erythropoietin (EPO) was assessed with an enzyme-linked immunosorbent assay (ELISA) kit (R&D Systems, Minneapolis, MN, USA). All blood analyses are shown in Table 1. Serum EPO and [Hb] increased from BL to HA, with values changing from 8.7 ± 3.7 to 12.2 ± 3.0 mIU ml^{-1} and from 147 ± 8 to 170 ± 13 g l^{-1} (mean ± SD), respectively. The arterial partial pressure of CO_2 (P_{aCO_2}) diminished from 40.6 ± 2.1 to 29.1 ± 2.0 mmHg as both P_{aO_2} and S_{aO_2} also decreased from 105.7 ± 15.7 and 98.5 ± 0.6 to 50.5 ± 3.0 mmHg and 83.6 ± 2.9%, respectively (Robach *et al.* 2007).

Skeletal muscle sampling

Skeletal muscle biopsies were obtained from the vastus lateralis muscle under local anaesthesia (1% lidocaine) of the skin and superficial muscle fascia, using the Bergstrøm technique (Bergstrom, 1962) with a needle modified for suction. The majority of the biopsy was directly dissected free of fat and connective tissue, frozen in liquid nitrogen, and stored at –80°C for later analysis. A small section of the muscle was then used immediately for measurements of mitochondrial respiration.

Skeletal muscle preparation

The small portion of the muscle biopsy (2–6 mg) that was to be used to measure mitochondrial respiration was immediately placed in ice-cold biopsy preservation solution (BIOPS) containing 10 mM CaK_2EGTA buffer, 7.23 mM K_2EGTA buffer, 0.1 μM free calcium, 20 mM imidazole, 20 mM taurine, 50 mM 2-(*N*-morpholino)ethanesulfonic acid hydrate (K-Mes), 0.5 mM dithiothreitol, 6.56 mM $MgCl_2.6H_2O$, 5.77 mM ATP and 15 mM phosphocreatine (pH 7.1). Muscle samples were then gently dissected with two pairs of sharp forceps, achieving a high degree of fibre separation, which was verified microscopically, followed by chemical permeabilization via incubation in 2 ml of BIOPS with saponin (50 μg ml^{-1}) for 30 min at 4°C (Kuznetsov *et al.* 2004). Samples were washed with a mitochondrial respiration medium (MiR05) containing 0.5 mM EGTA, 3 mM $MgCl_2.6H_2O$, 60 mM potassium lactobionate, 20 mM taurine, 10 mM KH_2PO_4, 20 mM Hepes, 110 mM sucrose and 1 g l^{-1} bovine serum albumin (pH 7.1), weighed, and added to a respiratory chamber. This technique of permeabilization allows for the study of mitochondrial function *ex vivo* in intact skeletal muscle samples with only very small biopsy samples using high-resolution respirometry (Boushel *et al.* 2007).

Mitochondrial respiration

Muscle bundles were blotted and measured for wet weight in a balance controlled for constant relative humidity, providing hydration consistency and stability of weight

measurements. Samples were then added to respective chambers where respiration was observed in MiR05 at 30°C using the high-resolution Oroboros Oxygraph-2k (Oroboros, Innsbruck, Austria). The Oxygraph is a two-chamber titration-injection respirometer with an oxygen detection limit of up to 0.5 pmol s^{-1} ml^{-1}. Standardized instrumental calibrations were performed to correct for back diffusion of oxygen into the chamber from the various components, leak from the exterior, and sensor oxygen consumption. Oxygen flux was resolved by software allowing non-linear changes in the negative time derivative of the oxygen concentration signal (Oxygraph 2k; Oroboros, Innsbruck, Austria). Data obtained at the experimental temperature (30°C) were multiplied by a T-factor corresponding to a Q_{10} of 2 (multiplication factor for a 10°C difference) equalling 1.62 for extrapolation to body temperature adjustments (Gnaiger, 2009). All experiments were carried out in a hyperoxygenated environment (chamber oxygen concentration maintained above 300 nmol ml^{-1}) to prevent potential limitations in oxygen diffusion. All measurements were made in duplicate.

Respiratory titration protocol

Titrations of all of substrates, uncouplers and inhibitors (SUIT) were added in series. Leak respiration in the absence of adenylates (L_N) was induced with the addition of malate (1.5 mM) and octanoyl carnitine (0.2 mM). This state represents the oxygen consumption of an unaltered and intact electron transport system in the absence of adenylates. In the L_N state, the chemiosmotic gradient is at maximum and oxygen flux is at a minimum, indicating proton leak, slip and cation cycling. As all electron transport system complexes are coupled in this state, all oxygen consumption represents the spontaneous dyscoupling of the system (Pesta & Gnaiger, 2012). Lipid oxidative phosphorylation capacity (P_{ETF}) and maximal electron flow through electron-transferring flavoprotein (ETF) was determined following the addition of ADP (4.8 mM). Electron-transferring flavoprotein is located on the matrix face of the inner mitochondrial membrane and supplies electrons from β-oxidation to coenzyme Q (Eaton *et al.* 1996). The ETF-linked transfer of electrons requires the metabolism of acetyl-CoA, hence the addition of malate, in order to facilitate convergent electron flow into the Q-junction from both complex I (CI) and ETF, allowing β-oxidation to proceed. The contribution of electron flow through NADH dehydrogenase, CI, is far below capacity; therefore, the rate-limiting metabolic branch here is electron transport through ETF such that malate- + octanoyl carnitine- + ADP-stimulated respiration is representative of, rather than specific to, electron capacity through ETF (Eaton *et al.* 1996; Saks *et al.* 1998; Gnaiger, 2009; Pesta *et al.* 2011; Pesta & Gnaiger, 2012). Maximal CI specific state 3 respiratory capacity (P_{CI}) was induced with glutamate (19 mM). Previous data have demonstrated that octanolyl carnitine + malate respiration constitute approximately 30% of respiration stimulated by octanoyl carnitine + malate + glutamate (Pesta *et al.* 2011), supporting the suggestion that electron transport through CI in the respiratory state P_{ETF} is not at capacity. Furthermore, following the titration of glutamate into the respiration medium, electron transport through ETF is inhibited, isolating the transport of electrons through CI (Saks *et al.* 1998). Maximal state 3 respiration, oxidative phosphorylation capacity (P), was induced with the addition of succinate (9.5 mM). Maximal state 3 represents respiration that is resultant to saturating concentrations of ADP as well as substrates specific for CI and succinate dehydrogenase, complex II (CII), and demonstrates the mitochondrial capacity to catalyse a sequential set of redox reactions that are partly coupled to the production of ATP via ATP synthase. Convergent electron input to CI and CII has been shown to provide higher respiratory values compared with the isolated respiration of either CI (pyruvate + malate or glutamate + malate) or CII (succinate + rotenone; Gnaiger, 2009) and, accordingly, is more representative and physiologically relevant to the study of mitochondrial function. Inhibition of CI by addition of rotenone (1 μM) led to state 3 respiratory capacity specific to CII (P_{CII}). Oligomycin (1 μM) was added to inhibit ATP synthase, demonstrating oligomycin-induced leak respiration (L_{Omy}). Phosphorylative restraint of electron transport through complex II was assessed by uncoupling ATPsynthase (complex V) from the electron transport system with the titration of the proton ionophore, carbonyl cyanide *p*-(trifluoromethoxy) phenylhydrazone (FCCP; 0.7 μM per addition up to optimal concentrations ranging from 2.5 to 4 μM). The integrity of the outer mitochondrial membrane was assessed with the addition of cytochrome *c* (19 μM). Cytochrome *c* had no additive effect on respiration (3.1 and 5.2% at BL and HA, respectively), confirming mitochondrial membrane intactness throughout all skeletal muscle samples. Finally, antimycin A (12 μM) was added to terminate respiration by inhibiting cytochrome bc_1 complex, allowing for the determination of residual oxygen consumption in the chamber. The concentrations of substrates and inhibitors used were based on prior experiments conducted for optimization of the titration protocols.

Data analysis

For all statistical evaluations, a P value of <0.05 was considered significant. Statistical analysis of differences in mitochondrial respiratory capacity between BL and

HA were calculated using a univariate analysis of variance (SPSS Statistics 17.0, SPSS, Chicago, IL, USA). The effect of high-altitude exposure on blood gases, haemoglobin, serum EPO and maximal oxygen uptake from BL to HA (two repeated measures) were evaluated with the Wilcoxon test (Statview Version 5.0., SAS Institute, Cary, NC, USA).

Results

Mass-specific mitochondrial respiratory states

There were no significant changes in substrate-controlled mass-specific respiration states when comparing BL with HA (Fig. 1) for any respiratory states. There were no differences in mass-specific leak respiration without adenylates (L_N, $P = 0.824$); the capacity for fatty acid oxidation (P_{ETF}, $P = 0.917$); CI-specific oxidative capacity (P_{CI}; $P = 0.479$), CII-specific oxidative capacity (P_{CII}; $P = 0.239$); oligomycin-induced leak (L_{Omy}) respiration ($P = 0.895$); or residual oxygen consumption following the addition of antimycin A ($P = 0.871$) when comparing baseline values with those measured following 9–11 days of high-altitude exposure. There was a trend, however, for maximal oxidative phosphorylation (P) to decrease following acclimatization ($P = 0.059$).

Mitochondrial efficiency and coupling control

Coupling control ratios indicative of the efficiency of chemiosmotic coupling along the respiratory system were examined (Table 2). In skeletal muscle mitochondria, the ETF coupling control (the efficiency of electron transfer

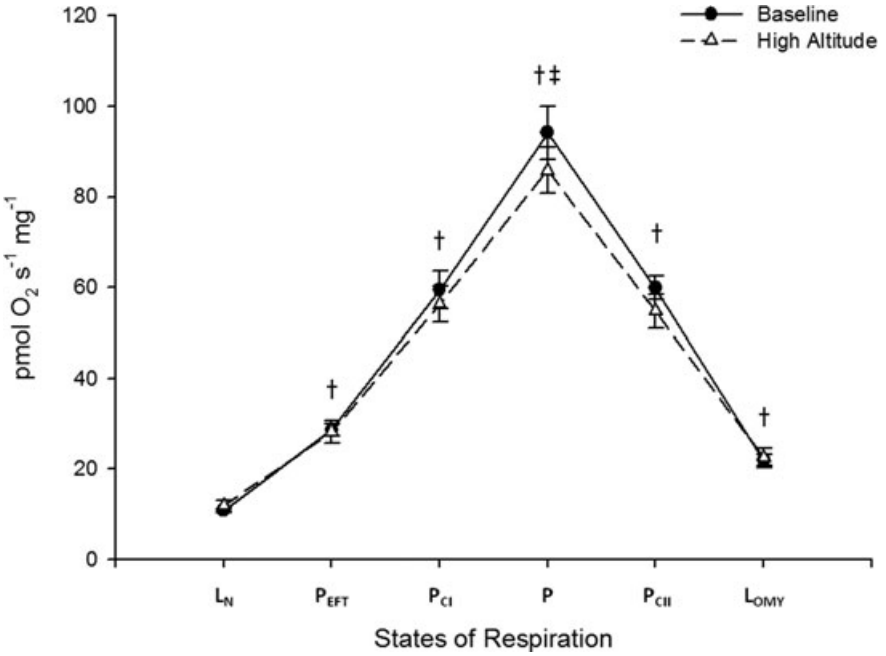

Figure 1. Respiration measurements
Substrate uncoupler inhibitor titration (SUIT) protocol for skeletal muscle samples taken first at sea level, for baseline (BL) measurements, and again following 11 days of high-altitude (HA) exposure (2 days at 3647 m and 7–9 days at 4559 m). All titrations, presented from left to right, were added in series. Leak respiration in the absence of adenylates (L_N) was induced with the addition of malate (1.5 mM) and octanoyl carnitine (0.2 mM). Lipid oxidative phosphorylation capacity (P_{ETF}) and maximal electron flow through electron-transferring flavoprotein (ETF) were determined following the addition of ADP (4.8 mM). Maximal NADH dehydrogenase, complex I (CI), specific state 3 respiratory capacity (P_{CI}) was induced with glutamate (19 mM). Maximal state 3 respiration, oxidative phosphorylation capacity (P), was induced with the addition of succinate (9.5 mM). Inhibition of CI by addition of rotenone (1 μM) led to state 3 respiratory capacity specific to complex II (CII; P_{CII}). Oligomycin (1 μM) was added to inhibit ATP synthase, demonstrating oligomycin-induced leak respiration (L_{Omy}). Differential respiratory capacities across the mitochondrial respiratory system were made evident throughout the SUIT protocol utilized, validating our mitochondrial preparation. In both conditions, BL and HA, respiration increased significantly following the addition of ADP, again with the addition of glutamate, and increased even further in response to succinate. In both conditions, respiration decreased with the inhibition of CI via rotenone, and was further diminished following oligomycin-induced inhibition of ATP synthase. The calculation of statistical differences between respiratory states and groups was performed using a multivariate analysis of variance. Values are presented as means ± SEM in units of picomoles of O_2 consumed per second per milligram tissue wet weight (pmol s^{-1} mg^{-1}). † Difference from the previous state of respiration ($P < 0.001$); and ‡ difference from same BL measurement ($P = 0.059$).

Table 2. Mitochondrial efficiency

Conditions	ETF coupling control	Respiratory control ratio	Leak (L_{Omy}) coupling control
BL	0.39 ± 0.02	4.44 ± 0.42	0.24 ± 0.02
HA	0.42 ± 0.02	4.02 ± 0.30	0.26 ± 0.02

Three separate coupling control ratios were determined from mitochondrial respiration measurements made from skeletal muscle tissue samples obtained at sea level for baseline (BL) measurements and again following 11 days of high-altitude (HA) exposure (2 days at 3647 m and 7–9 days at 4559 m). Electron-transferring flavoprotein (ETF) coupling control is the ratio between leak without adenylates (L_N) and maximal fatty acid oxidative capacity (P_{ETF}); the classic respiratory control ratio (state 3/state 4 respiration) is the ratio of maximal oxidative phosphorylation (P; state 3 respiration) and oligomycin-induced leak respiration (L_{OMY}, state 4 respiration); and leak coupling control is the ratio between L_{Omy} and P. Coupling control ratios are ratios of oxygen flux at a specific and constant mitochondrial substrate state. Values are presented as means ± SEM with $P < 0.05$.

from β-oxidation to coenzyme Q_{10}), the respiratory control ratio and the leak coupling control (the efficiency of electron transfer down the electron transport system) were all unaffected ($P = 0.256$, 0.422 and 0.530, respectively) by exposure to high altitude.

Discussion

The main finding of this study is that mitochondrial function is not greatly affected by 9–11 days of exposure to high altitude. More specifically, the sojourn to high altitude did not affect P_{ETF} or individualized respiration capacity through complex I and II (P_{CI} and P_{CII}, respectively). Chemiosmotic coupling efficiency, as measured by ETF coupling control, leak control coupling and the respiratory control ratio, was not modified following acclimatization. Opposed to declines in TCA- and oxidative phosphorylation-specific enzymatic characteristics (Viganò *et al.* 2008), the functional capacity of mitochondria in skeletal muscle is retained with subacute exposure to high altitude. Of note, however, mass-specific maximal oxidative phosphorylation capacity, P, in human skeletal muscle did express a trend ($P = 0.059$) to decrease after high-altitude exposure.

Hypoxic influence on the mitochondria has become a topic of interest because several mitochondrial proteins have been identified as being regulated by hypoxia-inducible factor (HIF; Semenza *et al.* 2006; Semenza, 2007). Although the data have been inconsistent, it is generally assumed that hypoxic exposure has a diminishing effect on mitochondria. Twenty-four hours of hypoxic exposure reduced oxygen consumption in cell suspensions of primary fibroblasts in a HIF-dependant manner (Papandreou *et al.* 2006). Hypoxic exposure, ranging from 9 to 75 days, has been shown to modify skeletal muscle by affecting biochemical expression and mitochondrial morphology (Mizuno *et al.* 1990, 2008; Hoppeler & Vogt, 2001; Vogt *et al.* 2001; Hoppeler *et al.* 2003; Lundby *et al.* 2003, 2009; Viganò *et al.* 2008; Perrey & Rupp, 2009; Levett *et al.* 2012). The physiological significance of these modifications, however, is far from understood. The present study demonstrates how respirometric analysis of mitochondrial function is largely unaltered despite large (~1.2- to 1.4-fold) changes in mitochondrial proteins specific for the TCA cycle or oxidative phosphorylation (Viganò *et al.* 2008) of similar exposure times. One drastic limitation of many studies investigating biochemical adaptation in skeletal muscle following hypoxic exposure is that they are often limited in analysing only isolated enzymatic modifications. Respirometric measurements allow for more complete analysis of integrated cellular function. As such, the data presented are more comprehensive because they can differentiate between diminished expression of an enzyme *versus* the functional capacity of a subcellular system.

Functional measurements of oxidative capacity of the skeletal muscle were largely unaffected following high-altitude exposure. Supporting these data, we were previously unable to detect differences in various respiratory states using high-resolution respirometry following intermittent hypoxic exposure for 4 weeks at the equivalent of 3000 m for 16 h day^{-1} (Robach *et al.* 2012). The present study did, however, find a trend suggestive of a lessened oxidative capacity in skeletal muscle. The TCA-specific enzymes, such as aconitase and oxoglutarate dehydrogenase, showed a decrease following acclimatization (Viganò *et al.* 2008) and may serve to explain the trend for a decrease in P. Aconitase facilitates the isomerization of citrate to isocitrate; however, this occurs near equilibrium and is not rate limiting. Oxoglutarate dehydrogenase, a rate-limiting enzyme in the TCA cycle, catalyses the decarboxylation of 2-oxoglutarate, the transfer of coenzyme A (CoA) to what becomes succinyl-CoA, and the reduction of NAD^+ to NADH, and functions *in vivo* near maximal enzymatic rate (Read *et al.* 1977; Cooney *et al.* 1981). The enzyme activity of oxoglutarate dehydrogenase has been reported to serve as a reliable marker indicating the capacity of oxygen consumption *in vivo* during maximal exercise involving small and isolated muscle groups (Blomstrand *et al.* 1997, 2011). When using NADH-related substrates, such as malate and glutamate, TCA cycle metabolites citrate and 2-oxoglutarate are exchanged for malate by the tricarboxylate and 2-oxoglutarate carriers, respectively, reducing the contribution of electron transport from NADH produced via the reaction catalysed by oxoglutarate

dehydrogenase (Gnaiger, 2009). As such, the measureable decreases would not be expected for either P_{CI} or P_{CII} but only for total respiratory capacity, P.

Maximal values of oxygen consumption when performed in acute normoxic conditions were no different from BL values (Fig. 2). A slightly depressed P capacity would not be expected to limit $\dot{V}_{O_2\,max}$, because mitochondrial respiratory capacity exceeds maximal oxygen delivery during maximal whole-body exercise (Boushel *et al.* 2011).

In the present study, mitochondria-specific enzymes involved in fatty acid oxidation decreased after high-altitude exposure. Specifically, trans-enoyl-CoA isomerase, enoyl-CoA-hydratase and the carnitine acetyltransferase decreased (Viganò *et al.* 2008). The ETF subunit declined in a similar manner with acclimatization (Viganò *et al.* 2008). These results support previous findings that demonstrate a nutrient-partitioning shift towards a greater dependency on glucose oxidation and a reduction of lipid oxidation following acclimatization (Cartee *et al.* 1991; Azevedo *et al.* 1995; Roberts *et al.* 1996; Braun, 2008). The present study shows that skeletal muscle mitochondria retain respiratory capacity for fat oxidation after high-altitude exposure.

One mechanism thought to affect mitochondrial density in response to hypoxic adaptation is the suppression of mammalian target of rapamycin and subsequent protein synthesis (Murray, 2009). In the present study, mammalian target of rapamycin decreased (Viganò *et al.* 2008), while whole-body protein breakdown increased (Holm *et al.* 2010). This is thought to affect mitochondrial autophagic remodelling and possibly suppress mitochondrial biogenesis. However, maintenance of mitochondria-specific protein synthesis has been reported despite global decreases in cellular proliferation during the energetic stress associated with caloric restriction in mice (Miller *et al.* 2012). Data presented in the present study may suggest, similar to those reported during caloric restriction, that overall mitochondria-specific protein synthesis is maintained along with functional parameters.

The fractional synthetic protein rate in the present study was previously reported to increase in myofibrillar compartments of the skeletal muscle but not in sarcoplasmic compartments, suggesting that protein turnover in the myofibrillar compartments may be maintained while the subsarcolemmal compartment experiences losses (Holm *et al.* 2010). Potential hypoxia-mediated changes in mitochondrial physiology may affect subpopulations of mitochondria in the skeletal muscle differently. Two separate mitochondrial populations exist in the skeletal muscle, the intermyofibrillar (IMF) and the subsarcolemmal (SS) populations. The IMF populations are situated near myofibrils and primarily support the energetic requirements of muscle contraction, while SS populations exist immediately beneath the sarcolemma and support energetic requirements that sustain membrane transport and cytoplasmic processes. The biochemical characterization and regulation of these two populations are different from one another (Krieger *et al.* 1980; Cogswell *et al.* 1993; Iossa *et al.* 2002). Recent evidence supports our previous findings (Holm

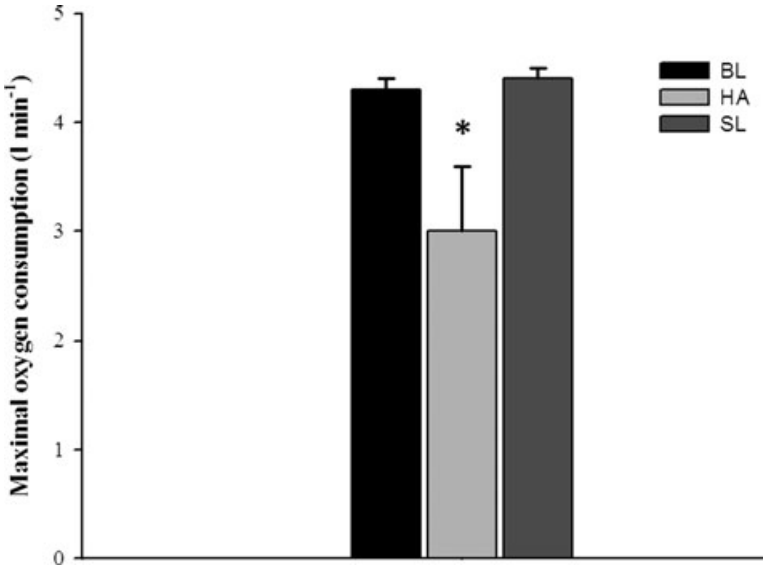

Figure 2. Maximal exercise capacity
Measurements of maximal oxygen consumption (in litres per minute) obtained at baseline sea level (BL), after 9–11 days of high-altitude exposure (HA), and again at high altitude with oxygen supplementation, i.e. acute normoxia representing sea level (SL), using an incremental cycle ergrometer exercise protocol. Values are presented as means ± SEM. * Significant difference from SL ($P < 0.05$).

et al. 2010), because subsarcolemmal mitochondrial populations express a greater reduction in volume density (73.1% loss) compared with intermyofibrillar populations (14.3% loss) following acclimatization by 66 days of high-altitude exposure (Levett *et al.* 2012). The extent to which mitochondrial populations may be affected in response to acclimatization as well as how these different populations affect overall mitochondrial function require further investigation.

Several studies have reported that there is an improvement in mechanical efficiency during exercise at sea level following prolonged or intermittent hypoxic exposure (Green *et al.* 2000*b*; Gore *et al.* 2001; Katayama *et al.* 2004; Saunders *et al.* 2009), while others have not been able to verify any change in mechanical efficiency (Lundby *et al.* 2007; Siebenmann *et al.* 2012). Our data show that 9–11 days of exposure to high altitude has no effect on respiratory chain electron slippage, proton leak or coupling control, suggesting no change in metabolic efficiency in skeletal muscle mitochondria following 9–11 days of exposure to high altitude. In support of these findings, we recently demonstrated, through similar indices of mitochondrial coupling, that there is also no evidence to suggest that respiratory system function or efficiency is altered with 4 weeks of exposure to intermittent hypoxia (Robach *et al.* 2012).

The findings in the present study may have direct application to human performance at sea level and high altitude. We have previously determined that mass-specific oxidative phosphorylation capacity in vastus lateralis is the strongest determinant of endurance capacity at an elevation of approximately 1000 m (Jacobs *et al.* 2011). Oxidative capacity remained largely unaltered following 9–11 days of high-altitude exposure, while haemoglobin concentrations increased (Robach *et al.* 2007; Lundby *et al.* 2008). Perhaps endurance capacity would improve, as opposed to $\dot{V}_{O_2\,max}$ which did not (Fig. 2), along with the ability to transport oxygen upon returning to sea level. Training in hypoxic conditions while living near sea level has been thought possibly to improve exercise performance at sea level. While hypoxic exercise training does result in greater morphometric (Schmutz *et al.* 2010) and biochemical expressions (Vogt *et al.* 2001) suggestive of enhanced oxidative capacity in skeletal muscle, these results do not translate into functional improvements in exercise capacity at sea level (Vogt *et al.* 2001; Schmutz *et al.* 2010; Vogt & Hoppeler, 2010). They do, however, improve exercise capacity in hypoxia (Vogt & Hoppeler, 2010).

Determinants of exercise performance change as elevation increases, shifting from more convective limitations of oxygen transport and peripheral origin of fatigue at lower elevations to diffusive limitations of oxygen and centrally mediated origin of fatigue at higher elevations (Amann *et al.* 2007; Robach *et al.* 2008; Jacobs *et al.* 2012). Approximately 14 days was previously determined appropriate to spend at moderate altitude prior to a competition in order to enhance exercise capacity along with the improvement in oxygen-carrying capacity (Schuler *et al.* 2007). As elevation increases, at somewhere between 3500 and 4500 m and above, the diffusive limitations of oxygen transport negate improvements in oxygen-carrying capacity (Robach *et al.* 2008; Jacobs *et al.* 2012). Thus, maintaining mitochondrial capacity, as is presented in the present study, or even enhancing mitochondrial capacity (Vogt *et al.* 2001; Schmutz *et al.* 2010; Vogt & Hoppeler, 2010) may be necessary in order to maintain, or improve, exercise capacity.

Critical variables that could intervene in the regulation of whole-body exercise and skeletal muscle respiration (i.e. physical activity, the time course of adaptation and the severity of altitude) were taken into consideration in the present study. Subjects were neither overly active nor extensively sedentary prior to and again following high-altitude exposure. Thus, training status did not differ between baseline and high-altitude data collections, which was verified by the similar measurements of exercise capacity at BL and while given supplemental oxygen at high altitude, acute normoxia (SL; Fig. 2). Physical activity was also controlled for 3 days prior to each data collection at both BL and HA. Although physical activity cannot be conclusively ruled out as a means for inducing any modification to mitochondrial function, as a control group was never introduced, there is strong evidence to suggest that our results were not a product of any changes in activity. The adequacy of the time course of acclimatization as well as the severity of altitude are demonstrated by the blood gas analyses, reduction of $\dot{V}_{O_2\,max}$, and increases in both serum EPO and [Hb]. Several changes in different proteins were also detected (Viganò *et al.* 2008). Animals exposed to hypoxia for different lengths of time have shown contrasting results. Rats subjected to 11% O_2 for 2 *versus* 4 weeks were reported to experience a different influence on respiration in mitochondria isolated from the right ventricle and left ventricle. Two weeks of hypoxia significantly increased fatty acid-induced state 3 respiration (malate and palmitoyl-L-carnitine) in mitochondria isolated from the right ventricle but not the left ventricle (Zungu *et al.* 2007), whereas 4 weeks had no effect on right ventricular respiration but reduced left ventricular ETF-specific state 3 respiration (Zungu *et al.* 2008). Whether a longer duration of hypoxic exposure or a different severity of hypoxia would alter the results of the present study is unknown. Owing to reported changes in mitochondrial characteristics in skeletal muscle with longer exposures to high elevations (Green *et al.* 1989; Hoppeler *et al.* 1990, 2003; Howald *et al.* 1990; Levett *et al.* 2012), this question merits further investigation.

In conclusion, mitochondrial function does not appear to be greatly affected by 7–9 days of acclimatization to 4559 m (total of 9–11 days of high-altitude exposure) in healthy lowlanders. We interpret our findings to suggest that during the catabolic physiological state induced by a subacute high-altitude sojourn (Holm *et al.* 2010), muscle mitochondrial function is preserved to maximize oxygen consumption in the face of a pronounced reduction in oxygen transport capacity.

References

Amann M, Romer LM, Subudhi AW, Pegelow DF & Dempsey JA (2007). Severity of arterial hypoxaemia affects the relative contributions of peripheral muscle fatigue to exercise performance in healthy humans. *J Physiol* **581**, 389–403.

Azevedo JL Jr, Carey JO, Pories WJ, Morris PG & Dohm GL (1995). Hypoxia stimulates glucose transport in insulin-resistant human skeletal muscle. *Diabetes* **44**, 695–698.

Bender PR, Groves BM, McCullough RE, McCullough RG, Huang SY, Hamilton AJ, Wagner PD, Cymerman A & Reeves JT (1988). Oxygen transport to exercising leg in chronic hypoxia. *J Appl Physiol* **65**, 2592–2597.

Bergstrom J (1962). Muscle electrolytes in man. *Scand J Clin Lab Invest* **68**, 1–110.

Blomstrand E, Krustrup P, Søndergaard H, Rådegran G, Calbet JA & Saltin B (2011). Exercise training induces similar elevations in the activity of oxoglutarate dehydrogenase and peak oxygen uptake in the human quadriceps muscle. *Pflugers Arch* **462**, 257–265.

Blomstrand E, Rådegran G & Saltin B (1997). Maximum rate of oxygen uptake by human skeletal muscle in relation to maximal activities of enzymes in the Krebs cycle. *J Physiol* **501**, 455–460.

Boushel R, Gnaiger E, Calbet JA, Gonzalez-Alonso J, Wright-Paradis C, Sondergaard H, Ara I, Helge JW & Saltin B (2011). Muscle mitochondrial capacity exceeds maximal oxygen delivery in humans. *Mitochondrion* **11**, 303–307.

Boushel R, Gnaiger E, Schjerling P, Skovbro M, Kraunsøe R & Dela F (2007). Patients with type 2 diabetes have normal mitochondrial function in skeletal muscle. *Diabetologia* **50**, 790–796.

Braun B (2008). Effects of high altitude on substrate use and metabolic economy: cause and effect? *Med Sci Sports Exerc* **40**, 1495–1500.

Calbet JA, Lundby C, Koskolou M & Boushel R (2006*a*). Importance of hemoglobin concentration to exercise: acute manipulations. *Respir Physiol Neurobiol* **151**, 132–140.

Calbet JA, Lundby C, Sander M, Robach P, Saltin B & Boushel R (2006*b*). Effects of ATP-induced leg vasodilation on $\dot{V}_{O_{2peak}}$ and leg O_2 extraction during maximal exercise in humans. *Am J Physiol Regul Integr Comp Physiol* **291**, R447–R453.

Cartee GD, Douen AG, Ramlal T, Klip A & Holloszy JO (1991). Stimulation of glucose transport in skeletal muscle by hypoxia. *J Appl Physiol* **70**, 1593–1600.

Cogswell AM, Stevens RJ & Hood DA (1993). Properties of skeletal muscle mitochondria isolated from subsarcolemmal and intermyofibrillar regions. *Am J Physiol* **264**, C383–C389.

Cooney GJ, Taegtmeyer H & Newsholme EA (1981). Tricarboxylic acid cycle flux and enzyme activities in the isolated working rat heart. *Biochem J* **200**, 701–703.

Eaton S, Bartlett K & Pourfarzam M (1996). Mammalian mitochondrial β-oxidation. *Biochem J* **320**, 345–357.

Gnaiger E (2009). Capacity of oxidative phosphorylation in human skeletal muscle: new perspectives of mitochondrial physiology. *Int J Biochem Cell Biol* **41**, 1837–1845.

Gore CJ, Hahn AG, Aughey RJ, Martin DT, Ashenden MJ, Clark SA, Garnham AP, Roberts AD, Slater GJ & McKenna MJ (2001). Live high:train low increases muscle buffer capacity and submaximal cycling efficiency. *Acta Physiol Scand* **173**, 275–286.

Green H, Roy B, Grant S, Burnett M, Tupling R, Otto C, Pipe A & McKenzie D (2000*a*). Downregulation in muscle Na^+-K^+-ATPase following a 21-day expedition to 6,194 m. *J Appl Physiol* **88**, 634–640.

Green HJ, Roy B, Grant S, Hughson R, Burnett M, Otto C, Pipe A, McKenzie D & Johnson M (2000*b*). Increases in submaximal cycling efficiency mediated by altitude acclimatization. *J Appl Physiol* **89**, 1189–1197.

Green HJ, Sutton JR, Cymerman A, Young PM & Houston CS (1989). Operation Everest II: adaptations in human skeletal muscle. *J Appl Physiol* **66**, 2454–2461.

Green HJ, Sutton JR, Wolfel EE, Reeves JT, Butterfield GE & Brooks GA (1992). Altitude acclimatization and energy metabolic adaptations in skeletal muscle during exercise. *J Appl Physiol* **73**, 2701–2708.

Hochachka PW, Stanley C, Merkt J & Sumar-Kalinowski J (1983). Metabolic meaning of elevated levels of oxidative enzymes in high altitude adapted animals: an interpretive hypothesis. *Respir Physiol* **52**, 303–313.

Holm L, Haslund ML, Robach P, van Hall G, Calbet JA, Saltin B & Lundby C (2010). Skeletal muscle myofibrillar and sarcoplasmic protein synthesis rates are affected differently by altitude-induced hypoxia in native lowlanders. *PLoS One* **5**, e15606.

Hoppeler H, Kleinert E, Schlegel C, Claassen H, Howald H, Kayar SR & Cerretelli P (1990). Morphological adaptations of human skeletal muscle to chronic hypoxia. *Int J Sports Med* **11**(Suppl 1), S3–S9.

Hoppeler H & Vogt M (2001). Muscle tissue adaptations to hypoxia. *J Exp Biol* **204**, 3133–3139.

Hoppeler H, Vogt M, Weibel ER & Fluck M (2003). Response of skeletal muscle mitochondria to hypoxia. *Exp Physiol* **88**, 109–119.

Horstman D, Weiskopf R & Jackson RE (1980). Work capacity during 3-wk sojourn at 4,300 m: effects of relative polycythemia. *J Appl Physiol* **49**, 311–318.

Howald H, Pette D, Simoneau JA, Uber A, Hoppeler H & Cerretelli P (1990). Effect of chronic hypoxia on muscle enzyme activities. *Int J Sports Med* **11**(Suppl 1), S10–S14.

Iossa S, Mollica MP, Lionetti L, Crescenzo R, Botta M & Liverini G (2002). Skeletal muscle oxidative capacity in rats fed high-fat diet. *Int J Obes Relat Metab Disord* **26**, 65–72.

Jacobs RA, Lundby C, Robach P & Gassmann M (2012). Red blood cell volume and the capacity for exercise at moderate to high altitude. *Sports Med* **42** (8), 1–21.

Jacobs RA, Rasmussen P, Siebenmann C, Díaz V, Gassmann M, Pesta D, Gnaiger E, Nordsborg NB, Robach P & Lundby C (2011). Determinants of time trial performance and maximal incremental exercise in highly trained endurance athletes. *J Appl Physiol* **111**, 1422–1430.

Katayama K, Sato K, Matsuo H, Ishida K, Iwasaki K & Miyamura M (2004). Effect of intermittent hypoxia on oxygen uptake during submaximal exercise in endurance athletes. *Eur J Appl Physiol* **92**, 75–83.

Krieger DA, Tate CA, McMillin-Wood J & Booth FW (1980). Populations of rat skeletal muscle mitochondria after exercise and immobilization. *J Appl Physiol* **48**, 23–28.

Kuznetsov AV, Schneeberger S, Seiler R, Brandacher G, Mark W, Steurer W, Saks V, Usson Y, Margreiter R & Gnaiger E (2004). Mitochondrial defects and heterogeneous cytochrome *c* release after cardiac cold ischemia and reperfusion. *Am J Physiol Heart Circ Physiol* **286**, H1633–H1641.

Levett DZ, Radford EJ, Menassa DA, Graber EF, Morash AJ, Hoppeler H, Clarke K, Martin DS, Ferguson-Smith AC, Montgomery HE, Grocott MP & Murray AJ (2012). Acclimatization of skeletal muscle mitochondria to high-altitude hypoxia during an ascent of Everest. *FASEB J* **26**, 1431–1441.

Lundby C, Boushel R, Robach P, Moller K, Saltin B & Calbet JA (2008). During hypoxic exercise some vasoconstriction is needed to match O_2 delivery with O_2 demand at the microcirculatory level. *J Physiol* **586**, 123–130.

Lundby C, Calbet JA & Robach P (2009). The response of human skeletal muscle tissue to hypoxia. *Cell Mol Life Sci* **66**, 3615–3623.

Lundby C, Calbet JA, Sander M, van Hall G, Mazzeo RS, Stray-Gundersen J, Stager JM, Chapman RF, Saltin B & Levine BD (2007). Exercise economy does not change after acclimatization to moderate to very high altitude. *Scand J Med Sci Sports* **17**, 281–291.

Lundby C, Pilegaard H, van Hall G, Sander M, Calbet J, Loft S & Møller P (2003). Oxidative DNA damage and repair in skeletal muscle of humans exposed to high-altitude hypoxia. *Toxicology* **192**, 229–236.

Lundby C, Sander M, van Hall G, Saltin B & Calbet JA (2006). Maximal exercise and muscle oxygen extraction in acclimatizing lowlanders and high altitude natives. *J Physiol* **573**, 535–547.

MacDougall JD, Green HJ, Sutton JR, Coates G, Cymerman A, Young P & Houston CS (1991). Operation Everest II: structural adaptations in skeletal muscle in response to extreme simulated altitude. *Acta Physiol Scand* **142**, 421–427.

Miller BF, Robinson MM, Bruss MD, Hellerstein M & Hamilton KL (2012). A comprehensive assessment of mitochondrial protein synthesis and cellular proliferation with age and caloric restriction. *Aging Cell* **11**, 150–161.

Mizuno M, Juel C, Bro-Rasmussen T, Mygind E, Schibye B, Rasmussen B & Saltin B (1990). Limb skeletal muscle adaptation in athletes after training at altitude. *J Appl Physiol* **68**, 496–502.

Mizuno M, Savard GK, Areskog NH, Lundby C & Saltin B (2008). Skeletal muscle adaptations to prolonged exposure to extreme altitude: a role of physical activity? *High Alt Med Biol* **9**, 311–317.

Murray AJ (2009). Metabolic adaptation of skeletal muscle to high altitude hypoxia: how new technologies could resolve the controversies. *Genome Med* **1**, 117.

Nordsborg NB, Calbet JA, Sander M, van Hall G, Juel C, Saltin B & Lundby C (2010). Human muscle net K^+ release during exercise is unaffected by elevated anaerobic metabolism, but reduced after prolonged acclimatization to 4,100 m. *Am J Physiol Regul Integr Comp Physiol* **299**, R306–R313.

Papandreou I, Cairns RA, Fontana L, Lim AL & Denko NC (2006). HIF-1 mediates adaptation to hypoxia by actively downregulating mitochondrial oxygen consumption. *Cell Metab* **3**, 187–197.

Perrey S & Rupp T (2009). Altitude-induced changes in muscle contractile properties. *High Alt Med Biol* **10**, 175–182.

Pesta D & Gnaiger E (2012). High-resolution respirometry: OXPHOS protocols for human cell cultures and permeabilized fibers from small biopsies of human muscle. *Methods Mol Biol* **810**, 25–58.

Pesta D, Hoppel F, Macek C, Messner H, Faulhaber M, Kobel C, Parson W, Burtscher M, Schocke M & Gnaiger E (2011). Similar qualitative and quantitative changes of mitochondrial respiration following strength and endurance training in normoxia and hypoxia in sedentary humans. *Am J Physiol Regul Integr Comp Physiol* **301**, R1078–R1087.

Read G, Crabtree B & Smith GH (1977). The activities of 2-oxoglutarate dehydrogenase and pyruvate dehydrogenase in hearts and mammary glands from ruminants and non-ruminants. *Biochem J* **164**, 349–355.

Reynafarje B (1962). Myoglobin content and enzymatic activity of muscle and altitude adaptation. *J Appl Physiol* **17**, 301–305.

Robach P, Cairo G, Gelfi C, Bernuzzi F, Pilegaard H, Vigano A, Santambrogio P, Cerretelli P, Calbet JA, Moutereau S & Lundby C (2007). Strong iron demand during hypoxia-induced erythropoiesis is associated with down-regulation of iron-related proteins and myoglobin in human skeletal muscle. *Blood* **109**, 4724–4731.

Robach P, Calbet JA, Thomsen JJ, Boushel R, Mollard P, Rasmussen P & Lundby C (2008). The ergogenic effect of recombinant human erythropoietin on $\dot{V}O_2$max depends on the severity of arterial hypoxemia. *PLoS One* **3**, e2996.

Robach P, Siebenmann C, Jacobs RA, Rasmussen P, Nordsborg NB, Pesta D, Gnaiger E, Diaz V, Christ A, Fiedler J, Crivelli N, Secher NH, Pichon A, Maggiorini M & Lundby C (2012). The role of hemoglobin mass on VO2max following normobaric "live high – train low" in endurance-trained athletes. *Br J Sports Med*, doi: 10.1136/bjsports-2012-091078.

Roberts AC, Butterfield GE, Cymerman A, Reeves JT, Wolfel EE & Brooks GA (1996). Acclimatization to 4,300-m altitude decreases reliance on fat as a substrate. *J Appl Physiol* **81**, 1762–1771.

Saks VA, Veksler VI, Kuznetsov AV, Kay L, Sikk P, Tiivel T, Tranqui L, Olivares J, Winkler K, Wiedemann F & Kunz WS (1998). Permeabilized cell and skinned fiber techniques in studies of mitochondrial function in vivo. *Mol Cell Biochem* **184**, 81–100.

Saunders PU, Telford RD, Pyne DB, Hahn AG & Gore CJ (2009). Improved running economy and increased hemoglobin mass in elite runners after extended moderate altitude exposure. *J Sci Med Sport* **12**, 67–72.

Schmutz S, Dapp C, Wittwer M, Durieux AC, Mueller M, Weinstein F, Vogt M, Hoppeler H & Fluck M (2010). A hypoxia complement differentiates the muscle response to endurance exercise. *Exp Physiol* **95**, 723–735.

Schuler B, Thomsen JJ, Gassmann M & Lundby C (2007). Timing the arrival at 2340 m altitude for aerobic performance. *Scand J Med Sci Sports* **17**, 588–594.

Semenza GL (2007). Oxygen-dependent regulation of mitochondrial respiration by hypoxia-inducible factor 1. *Biochem J* **405**, 1–9.

Semenza GL, Shimoda LA & Prabhakar NR (2006). Regulation of gene expression by HIF-1. *Novartis Found Symp* **272**, 2–8; discussion 8–14, 33–16.

Siebenmann C, Robach P, Jacobs RA, Rasmussen P, Nordsborg N, Diaz V, Christ A, Olsen NV, Maggiorini M & Lundby C (2012). "Live high-train low" using normobaric hypoxia: a double-blinded, placebo-controlled study. *J Appl Physiol* **112**, 106–117.

Tappan DV, Reynafarje B, Potter VR & Hurtado A (1957). Alterations in enzymes and metabolites resulting from adaptation to low oxygen tensions. *Am J Physiol* **190**, 93–98.

Valdivia E (1958). Total capillary bed in striated muscles of guinea pigs native to the Peruvian mountains. *Am J Physiol* **194**, 585–589.

Viganò A, Ripamonti M, De Palma S, Capitanio D, Vasso M, Wait R, Lundby C, Cerretelli P & Gelfi C (2008). Proteins modulation in human skeletal muscle in the early phase of adaptation to hypobaric hypoxia. *Proteomics* **8**, 4668–4679.

Vogt M & Hoppeler H (2010). Is hypoxia training good for muscles and exercise performance? *Prog Cardiovasc Dis* **52**, 525–533.

Vogt M, Puntschart A, Geiser J, Zuleger C, Billeter R & Hoppeler H (2001). Molecular adaptations in human skeletal muscle to endurance training under simulated hypoxic conditions. *J Appl Physiol* **91**, 173–182.

Zungu M, Alcolea MP, García-Palmer FJ, Young ME & Essop MF (2007). Genomic modulation of mitochondrial respiratory genes in the hypertrophied heart reflects adaptive changes in mitochondrial and contractile function. *Am J Physiol Heart Circ Physiol* **293**, H2819–H2825.

Zungu M, Young ME, Stanley WC & Essop MF (2008). Expression of mitochondrial regulatory genes parallels respiratory capacity and contractile function in a rat model of hypoxia-induced right ventricular hypertrophy. *Mol Cell Biochem* **318**, 175–181.

Acknowledgements

This study was financially supported by the Novo Nordisk Fonden to C.L. while working at the Copenhagen Muscle Research Center, Rigshospitalet, Copenhagen, Denmark, and by Fonds de la Recherche en Sante Quebec (R.B.).

The FASEB Journal article fj.12-218206. Published online September 11, 2012.

Twenty-eight days at 3454-m altitude diminishes respiratory capacity but enhances efficiency in human skeletal muscle mitochondria

Robert A. Jacobs,[*,†] Christoph Siebenmann,[*,‡] Mike Hug,[‡] Marco Toigo,[*,‡,§] Anne-Kristine Meinild,[‡] and Carsten Lundby[*,‡,1]

[*]Zurich Center for Integrative Human Physiology (ZIHP), [†]Institute of Veterinary Physiology, Vetsuisse Faculty, and [‡]Institute of Physiology, University of Zurich, Zurich, Switzerland; and [§]Department of Exercise Physiology, Institute of Human Movement Sciences, Eidgenössische Technische Hochschule Zurich, Zurich, Switzerland

ABSTRACT **Modifications of skeletal muscle mitochondria following exposure to high altitude (HA) are generally studied by morphological examinations and biochemical analysis of expression. The aim of this study was to examine tangible measures of mitochondrial function following a prolonged exposure to HA. For this purpose, skeletal muscle biopsies were obtained from 8 lowland natives at sea level (SL) prior to exposure and again after 28 d of exposure to HA at 3454 m. High-resolution respirometry was performed on the muscle samples comparing respiratory capacity and efficiency. Exercise capacity was assessed at SL and HA. Respirometric analysis revealed that mitochondrial respiratory capacity diminished in complex I- and complex II-specific respiration in addition to a loss of maximal state-3 oxidative phosphorylation capacity from SL to HA, all independent from alterations in mitochondrial content. Leak control coupling, respiratory control ratio, and oligomycin-induced leak respiration, all measures of mitochondrial efficiency, improved in response to HA exposure. SL respiratory capacities correlated with measures of exercise capacity near SL, whereas mitochondrial efficiency correlated best with exercise capacity following HA. This data demonstrate that 1 mo of exposure to HA reduces respiratory capacity in human skeletal muscle; however, the efficiency of electron transport improves.—Jacobs, R. A., Siebenmann, C., Hug, M., Toigo, M., Meinild, A.-K., Lundby, C. Twenty-eight days at 3454-m altitude diminishes respiratory capacity but enhances efficiency in human skeletal muscle mitochondria. *FASEB J.* 26, 000–000 (2012). www.fasebj.org**

Key Words: acclimatization · exercise · mitochondrial efficiency · respiratory control

THE MAJORITY OF OUR understanding regarding skeletal muscle mitochondrial changes when exposed to hypoxia comes from morphological examinations and biochemical analysis of expression following some degree of hypoxic exposure. Studies conducted in combination with mountain climbing expeditions to Mt. Everest have reported severe decrements in mitochondrial volume (1, 2) paralleled by losses in mitochondria-specific enzymes (1, 3) attendant to an extended exposure to extreme high altitude (HA; ≥5000 m). Other studies fail to corroborate these findings (4–6), as they report negligible losses in mitochondrial enzymes following extreme HA exposure. Another complication to data interpretation is the allusion that these static measurements can accurately characterize changes in functional parameters of mitochondria.

We previously reported that 9–11 d of exposure to HA did not largely affect oxidative capacity or efficiency of electron transport in human skeletal muscle (7). The preservation of mitochondrial function occurred in the face of pronounced reductions in several mitochon-

Abbreviations: BIOPS, biopsy preservation solution; CI, complex I (NADH dehydrogenase); CII, complex II (succinate dehydrogenase); COX, cytochrome-*c* oxidase; CS, citrate synthase; ETF, electron-transferring flavoprotein; ETS, electron transport system respiratory capacity; F_iO_2, oxygen fraction of inspired air; FCCP, carbonyl cyanide *p*-(trifluoromethoxy) phenylhydrazone; HA, high altitude; HH, hypobaric hypoxia; LCR, leak control ratio; LCR_{ETS}, leak control ratio of oligomycin-induced leak respiration to electron transport system respiratory capacity; L_N, normal leak respiration; L_{OMY}, oligomycin-induced leak respiration; MiR05, mitochondrial respiration medium 05; MiR06, mitochondrial respiration medium 06 (MiR05 + catalase); MOM, mitochondrial outer membrane; NH, normobaric hypoxia; P, maximal state 3 respiration or oxidative phosphorylation capacity; P_{CI}, submaximal state 3 respiration specific to complex I; P_{CII}, submaximal state 3 respiration specific to complex II; P_{ETF}, fatty acid oxidative capacity; RCR, respiratory control ratio; ROX, residual oxygen consumption; SL, sea level; TMPD, *N,N,N′,N′*-tetramethyl-1,4-benzenediamine, dihydrochloride; $\dot{V}O_{2max}$, maximal oxygen consumption; W_{max}, maximal power output; ww, wet weight

[1] Correspondence: Institute of Physiology, ZIHP, University of Zürich, Office 23 H 6, Winterthurerstrasse 190, 8057 Zürich, Switzerland. E-mail: carsten.lundby@access.uzh.ch

doi: 10.1096/fj.12-218206

dria-specific proteins (8). Duration of hypoxic exposure, however, has considerable effect on physiological adaptation. Shorter durations of hypoxic exposure have failed to affect mitochondrial volume density (1) and mitochondrial enzyme expression (9) while longer durations led to a decrease in both parameters (1, 9).

Our previous findings (7) directly demonstrated that relying exclusively on static measurements for the characterization of mitochondrial function and oxidative potential is insufficient. Respirometric analysis in conjunction with biochemical assessments is more appropriate to differentiate between changes in enzymatic expression *vs.* an alteration in the functional capacity of a subcellular system. In the current study, we assessed mitochondrial respiratory chain function and biochemical expression of mitochondria-specific enzymes in permeabilized skeletal muscle fibers near sea level (SL) and again after 28 d of exposure to HA. We hypothesized that the previous trend for a diminished oxidative phosphorylation capacity (7) will become more pronounced following a longer exposure to HA.

MATERIALS AND METHODS

Ethical approval

Experimental protocols involving human subjects were approved by the Ethical Committee for the Eidgenössische Technische Hochschule Zürich (EK 2011-N-51), in accordance with the declaration of Helsinki. Prior to the start of the experiments, informed oral and written consents were obtained from all participants.

Subjects

Eight young and physically active lowland male subjects voluntarily participated in this study. Subject characteristics (means±SD) were age 26 ± 4 yr, height 180 ± 1 cm, and weight 76 ± 6 kg. All subjects were recreationally active; they were neither excessively sedentary nor highly trained. The subjects had a baseline maximal oxygen uptake ($V\dot{O}_{2max}$) of 3.9 ± 0.3 L/min and maximal power output (W_{max}) of 321 ± 28 W, assessed during an incremental test to exhaustion at SL. None of the subjects were taking any medications or had any known family history of type 2 diabetes, severe obesity, or cardiovascular diseases. Subjects were scanned for body composition in a dual-energy X-ray absorptiometer (Lunar iDXA; GE Healthcare, Madison, WI, USA) prior to HA ascent and again 1–3 d after return to sea level.

Experimental design

Subjects reported to the laboratory in Zurich (432 m) several times throughout a 5-wk duration prior to HA ascent for acquisition of baseline (SL) measurements. Subsequently, subjects were transported by train to an HA research station located at the Jungfraujoch Research Station in the Swiss Alps (3454 m). Here, all subjects remained for the next 28 d. The ascent profile was uniform across all subjects.

Exercise tests

Exercise tests to obtain values of $V\dot{O}_{2max}$ were completed on an electronically braked bicycle ergometer (Monark, Varberg, Sweden). The exercise protocol started with a 5-min collection of resting $V\dot{O}_2$ followed by 2 consecutive absolute submaximal workloads, 100 and 150 W, in normoxia and 75 and 125 W in hypoxia, that were maintained for 5 min each. Thereafter, the workload increased 25 W/min until voluntary exhaustion. During the last minutes of the test, subjects were vigorously encouraged to perform to complete exhaustion, and the achievement of $V\dot{O}_{2max}$ was established by standard criteria in all tests (10). Subjects wore a face mask covering their mouth and nose for breath collection (Hans Rudolph, Kansas City, MO, USA), and O_2 and CO_2 concentrations in the expired gas were continuously measured and monitored as breath-by-breath values (Innocor, Innovision, Odense, Denmark). The gas analyzers and the flowmeter of the applied spirometer were calibrated prior to each test.

In total, subjects completed 4 maximal exercise tests. The first was an initial normobaric normoxia test (SL baseline). At 3 d after the SL test, a normobaric hypoxia (NH) test took place where the subjects breathed a hypoxic mixture (oxygen fraction of inspired air F_iO_2=0.134; Alti-Trainer; SMTEC, Nyon, Switzerland), approximately the equivalent of breathing at 3500 m. The third test was a short-term hypobaric hypoxia (HH) test, performed on d 8 following arrival at 3454 m. The last test was a chronic hypobaric hypoxia $V\dot{O}_{2max}$ test completed within the final 2 d of the 28-d exposure to 3454 m (HA test).

Skeletal muscle sampling

Skeletal muscle biopsies were obtained from the m. vastus lateralis at SL and again after 28 d of exposure to HA at 3454 m. Samples were collected under local anesthesia (1% lidocaine) of the skin and superficial muscle fascia, using the Bergström technique (11) with a needle modified for suction. The biopsy was immediately dissected free of fat and connective tissue and divided into sections for measurements of mitochondrial respiration.

Skeletal muscle preparation

The biopsy was sectioned into parts to measure mitochondrial respiration. Each part was immediately placed in ice-cold biopsy preservation solution (BIOPS) containing 2.77 mM CaK_2EGTA buffer, 7.23 mM K_2EGTA buffer, 0.1 μM free calcium, 20 mM imidazole, 20 mM taurine, 50 mM 2-(*N*-morpholino)ethanesulfonic acid hydrate (K-MES), 0.5 mM dithiothreitol (DTT), 6.56 mM $MgCl_2 \cdot 6H_2O$, 5.77 mM ATP, and 15 mM phosphocreatine (pH 7.1). Muscle samples were then gently dissected with the tip of two 18-gauge needles, achieving a high degree of fiber separation verified microscopically, followed by chemical permeabilization *via* incubation in 2 ml of BIOPS with saponin (50 μg/ml) for 30 min in 4°C (12). Lastly, samples were washed with mitochondrial respiration medium 05 (MiR05) containing 0.5 mM EGTA, 3 mM $MgCl_2 \cdot 6H_2O$, 60 mM K-lactobionate, 20 mM taurine, 10 mM KH_2PO_4, 20 mM HEPES, 110 mM sucrose, and 1 mg/ml BSA (pH 7.1) for 10 min in 4°C.

Mitochondrial respiration measurements

Muscle bundles were blotted dry and measured for wet weight (ww) in a balance-controlled scale (XS205 DualRange Analytical Balance; Mettler-Toledo AG, Greifensee, Switzerland) maintaining constant relative humidity, providing hydration consistency, as well as stability of weight measurements. Respiration measurements were performed in mitochondrial respiration medium 06 (MiR06; MiR05 + catalase 280 IU/ml). Measurements of oxygen consumption were performed

at 37°C using the high-resolution Oxygraph-2k (Oroboros, Innsbruck, Austria) with all additions in each substrate, uncoupler, and inhibitor titration protocol added in series. Standardized instrumental calibrations were performed to correct for back diffusion of oxygen into the chamber from the various components, leak from the exterior, oxygen consumption by the chemical medium, and sensor oxygen consumption at SL and at HA. Chemical calibrations were performed to determine, and later control for, the amount of nonmitochondrial autooxidation that occurs in the respiratory chambers during cytochrome-*c* oxidase (COX) analysis at SL and HA. For this calibration, we measured oxygen consumption over time in the respiratory chamber using MiR06, free of any biological sample, with the additions of cytochrome *c* (10 μM), ascorbate (2 mM), and *N,N,N′,N′*-tetramethyl-1,4-benzenediamine, dihydrochloride (TMPD; 500 μM) titrated into the chamber. With this calibration, we are able to establish the linear relationship between the degree of nonbiological oxygen consumption *via* auto-oxidation of chemicals added to the medium across different oxygen concentrations within the chamber. Oxygen flux was resolved by software, allowing nonlinear changes in the negative time derivative of the oxygen concentration signal (DatLab; Oroboros, Innsbruck, Austria). All experiments were carried out in a hyperoxygenated environment to prevent any potential oxygen diffusion limitation, with oxygen concentration within the chamber ranging between 250 and 400 μM.

Respiratory titration protocols

Two different titration protocols were applied in the study (**Table 1**). Each protocol was specific to the examination of individual aspects of respiratory control through a sequence of coupling and substrate states induced *via* separate titrations. Protocol 1 was specific for the analysis of respiratory capacity and coupling control efficiency during both fatty acid oxidation and maximal oxidative phosphorylation, and also coupling control efficiency during submaximal state 3 respiration specific to complex II [CII (succinate dehydrogenase); P_{CII}]. Protocol 2 was specific for the analysis of respiratory capacity and coupling control efficiency during submaximal state 3 respiration specific to complex I [CI (NADH dehydrogenase); P_{CI}], as well as respiratory capacities of maximal state 3 respiration and P_{CII}. All respirometric analyses were made in duplicates, and all titrations were added in series as presented. The concentrations of substrates, uncouplers, and inhibitors used were based on prior experiments conducted for optimization of the titration protocols. Protocols 1 and 2 were modified from refs. 7 and 13, respectively.

TABLE 1. *Titration protocols*

Protocol	Substrate, uncoupler, and inhibitor concentrations
1	M (2 mM), OC (0.2 mM), ADP (5 mM). P (5 mM), G (10 mM,) S (10 mM), Cyt C (10 μM), O (1 μM), FCCP (1.5–3 μM), Rot (0.5 μM), AmA (2.5 μM)
2	M (2 mM), P (5 mM), G (10 mM), ADP (5 mM), S (10 mM), Cyt C (10 μM), Rot (0.5 μM), AmA (2.5 μM), Asc (2 mM), [a] TMPD (500 μM)[a]

Two different titration protocols were used in this study, and are indicated as protocol 1 and protocol 2 in the left column. Right column shows the sequence and concentration of substrates, uncouplers, and inhibitors added during respirometric analysis. M, malate; OC, octanoyl carnitine; ADP, adenosine diphosphate; P, pyruvate; G, glutamate; S, succinate; Cyt C, cytochrome *c*; O, oligomycin; FCCP, carbonyl cyanide *p*-(trifluoromethoxy) phenylhydrazone; Rot, rotenone; AmA, anti-mycin a; Asc, ascorbate; TMPD, *N,N,N′,N′*-tetramethyl-1,4-benzenediamine, dihydrochloride. [a]Immediate sequential, nearly simultaneous, addition to the respiration medium within the chamber.

Protocol 1

Normal leak respiration (L_N) in absence of adenylates was induced with the addition of malate and octanoyl carnitine. The L_N state represents the resting oxygen consumption of an unaltered and intact electron transport system free of adenylates. Maximal electron flow through electron-transferring flavoprotein (ETF) and fatty acid oxidative capacity (P_{ETF}) were determined following the addition of ADP. In the P_{ETF} state, the ETF-linked transfer of electrons requires the metabolism of acetyl-CoA, hence, the addition of malate, in order to facilitate convergent electron flow into the *Q* junction from both CI and ETF, allowing β-oxidation to proceed. The contribution of electron flow through CI is far below capacity, and so, here, the rate-limiting metabolic branch is electron transport through ETF, such that malate + octanoyl carnitine + ADP-stimulated respiration is representative of, rather than specific to, electron capacity through ETF (7, 14–17). P_{CI} was induced following the additions of pyruvate and glutamate. Maximal state 3 respiration or oxidative phosphorylation capacity (P) was then induced with the addition of succinate. This maximal state 3 state represents respiration that is resultant to saturating concentrations of ADP and substrate supply for both CI and CII. Convergent electron input to CI and CII provides higher respiratory values compared to the isolated respiration of either CI (pyruvate/glutamate + malate or glutamate + malate) or CII (succinate + rotenone) (15, 18). Consequently, P presents more physiological relevance to the study of mitochondrial function (19) and is necessary to establish confirmation of a complete and intact electron transport system. P demonstrates a naturally intact electron transport system's capacity to catalyze a sequential set of redox reactions that are partially coupled to the production of ATP *via* ATP synthase. Compared to a correspondent leak state with an equivalent substrate supply, P maintains a lower electrochemical gradient across the inner mitochondrial membrane. That gradient is dictated by the degree of coupling to the phosphorylation system (15, 16). As an internal control for compromised integrity of the mitochondrial preparation, the mitochondrial outer membrane (MOM) was assessed with the addition of cytochrome *c*. Oligomycin was added, inhibiting ATP synthase, demonstrating oligomycin-induced leak respiration (L_{OMY}). The L_{OMY} state is the corresponding leak state to P and is comparable to classic state 4 respiration (20). In L_{OMY}, the chemiosmotic gradient is at maximum, resultant to the combination of maximal substrate supply and inhibition of ATP synthase. Oxygen flux is at a minimum and is representative of proton leak, slip, cation cycling, and overall dyscoupling (15, 16, 19, 21). Phosphorylative restraint of electron transport was assessed by uncoupling ATP synthase (complex V) from the electron transport system with the titration of the proton ionophore, carbonyl cyanide *p*-(trifluoromethoxy) phenylhydrazone (FCCP) reaching the electron transport system respiratory capacity (ETS) state. The inner mitochondrial membrane potential is completely collapsed, with an open transmembrane proton circuit, in the ETS respiratory state. The uninhibited flow of electrons through the respiratory system can, therefore, indirectly serve as an indication of maximal mitochondrial membrane potential. Rotenone and

antimycin A were added, in sequence, to terminate respiration by inhibiting CI and complex III (cytochrome bc_1 complex), respectively. With CI inhibited, P_{CII} can be measured. Inhibition of respiration with antimycin A then allows for the determination and correction of residual oxygen consumption (ROX), indicative of nonmitochondrial oxygen consumption in the chamber.

Protocol 2

L_N was induced with the addition of malate, pyruvate, and glutamate. P_{CI} and maximal electron flow through CI were determined following the addition of ADP. P was then induced with the addition of succinate. Cytochrome *c* was added to validate the integrity of the MOM. Rotenone was added to inhibit electron flow through CI to achieve P_{CII}. Antimycin A was added, inhibiting respiration through complex III, allowing for the determination of ROX. Finally, ascorbate and TMPD were simultaneously titrated into the chambers to assess COX (complex IV) activity. TMPD and ascorbate are redox substrates that donate electrons directly to COX, and activity was measured by pmol $O_2 \cdot min^{-1} \cdot mg\ ww^{-1}$. COX activity has been shown to strongly correlate with mitochondrial volume density and total cristae area (both measured *via* transmission electron microscopy) in addition to respiratory capacity (21).

Validation of titration protocols and mitochondrial membrane integrity

Differences in individual respiratory state capacities across the mitochondrial respiratory system were made evident throughout each of the titration protocols utilized at both SL and HA. Respirometric analysis from protocol 1 is represented in **Fig. 1*A***. Sequential changes in respiratory states at SL and HA confirm that all skeletal muscle preparations and protocols were successful in producing valid responses. Malate- and octanoyl carnitine-induced leak respiration, L_N, increased ($P<0.001$) following the addition of ADP, signifying the capacity for fatty acid oxidation, P_{ETF}. There was another increase from P_{ETF} following the addition of pyruvate and glutamate, stimulating P_{CI} ($P<0.001$). Respiration again increased ($P<0.001$) with succinate addition, representing P. There was no increase ($P=0.894$) from P after cytochrome *c* addition, verifying an intact MOM. Respiration did then decrease ($P<.001$) following the addition of oligomycin into the respiration medium, achieving L_{OMY}. Uncoupling electron transport through complexes I–IV from ATP synthase increased ($P<0.001$) oxygen consumption to a maximum at ETS state. Respiration was reduced ($P<0.001$) after inhibition of CI with rotenone, generating P_{CII}. Finally, respiration diminished ($P<0.001$) to an absolute minimum following the addition of anti-mycin, achieving ROX.

Respirometric analysis from protocol 2 is represented in Fig. 1*B*. Both SL and HA measurements show that malate-, pyruvate-, and glutamate-induced L_N increased ($P<0.001$) with the addition of ADP, signifying P_{CI}. Respiration increased ($P<0.001$) again following succinate addition, reaching P. There was no increase ($P=0.807$) from P once cytochrome *c* was added, verifying an intact MOM. Respiration then decreased ($P<0.001$) following the addition of rotenone after inhibition of CI with rotenone, achieving P_{CII}, and again ($P<0.001$) following the addition of anti-mycin, achieving ROX.

Citrate synthase (CS) activity

CS activity was assayed in homogenates of the skeletal muscle samples used in respiration measurements. The contents of the Oxygraph-2k chambers (2 ml each) were removed after each respiration experiment and washed once with 2 ml of MiR05. Triton X-100 (1%) and 2 μl of a protease inhibitor cocktail (cat. 539134; Sigma-Aldrich, St. Louis, MO, USA) were added to the combined solutions (content and wash) and then homogenized for 30 s with a T10 basic Ultra-Turrax homogenizer (IKA, Staufen, Germany) near maximum speed. The homogenate was then centrifuged for 15 min at 4°C, and the supernatant was removed, frozen in liquid nitrogen, and stored at −80°C. As has been previously described (22), CS activity was measured fluorometrically at 412 nm and 25°C (CS assay kit; Sigma-Aldrich), according to the manufacturer. The

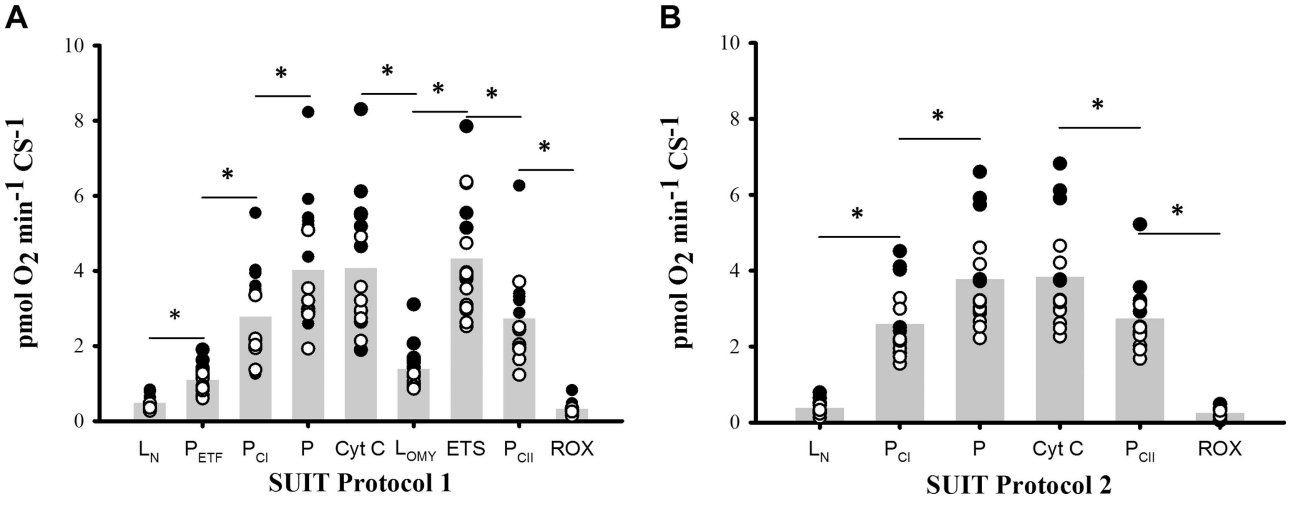

Figure 1. Respirometric analysis protocols. Titration protocols for skeletal muscle samples with all titrations, presented from left to right, added in series. *A*) Protocol 1 induced L_N; maximal electron flow through ETF and P_{ETF}; P_{CI}; P, an internal control for compromised integrity of the mitochondrial preparation, the MOM, assessed with the addition of cytochrome *c* (Cyt C); L_{OMY}; ETS state; P_{CII}; and ROX. *B*) Protocol 2 induced L_N; P_{CI}; P, assessed with Cyt C; $P_{CII;}$ and ROX. Shaded bars indicate the collective average from all baseline (SL) and HA respirometric measurements. Individual data are reported for each respective respiratory state as SL measurements (solid circles) or HA measurements (open circles). $^*P < 0.001$.

strength of association between CS activity and mitochondrial volume density, total cristae area, and respiratory capacity has previously been demonstrated (21).

Data analysis

For all statistical evaluations, a value of $P < 0.05$ was considered significant. Various statistical models were used for analysis (SPSS Statistics 17.0; SPSS, Chicago, IL, USA). Paired-sample *t* tests were used to test the null hypothesis stating no difference between SL and HA values for body composition, body weight, CS and COX activities, mitochondrial respiratory capacities (normalized to corresponding CS activities), and mitochondrial efficiency. The sequential $\dot{V}O_{2max}$ and W_{max} were analyzed by a 1-way ANOVA on repeated measurements. In addition to CS activity, mass-specific respiration was also normalized to COX activity [(respiratory state/COX) × 100], and respiratory capacities as a percentage of COX were analyzed with a 1-way ANOVA. Whenever an ANOVA showed significance, the differences were examined using pairwise comparisons with a Bonferroni adjustment. Linear regression was used to calculate the strength of association between P and COX activity, as well as parameters of mitochondrial respiratory capacity and efficiency, with corresponding measurements of exercise capacity at both SL and HA.

RESULTS

Body composition and weight

Neither percentage body fat from total mass (16.3±4.7 to 16.1±4.6%), as measured by DEXA, nor body weight (76.1±5.8 to 75.8±5.6 kg) were different following altitude exposure.

Maximal exercise capacity and power output

All $\dot{V}O_{2max}$ and W_{max} data are presented in **Fig. 2**. SL $\dot{V}O_{2max}$ values (52.0±4.3 ml·min^{-1}·kg^{-1}) were significantly greater ($P \leq 0.001$) than NH (44.4±3.7 ml·min^{-1}·kg^{-1}), HH (43.8±3.6 ml·min^{-1}·kg^{-1}), and HA (42.8±ml·min^{-1}·kg^{-1}) values. There was no difference in $\dot{V}O_{2max}$ values across all tests done in hypoxia. W_{max} also decreased ($P<0.05$) from the SL (321±28 W) test when compared to HN (254±20 W; $P=0.001$), HH (277±20 W; $P=0.037$), and HA (275±41 W; $P=0.029$). There were no differences in W_{max} values across all tests done in hypoxia.

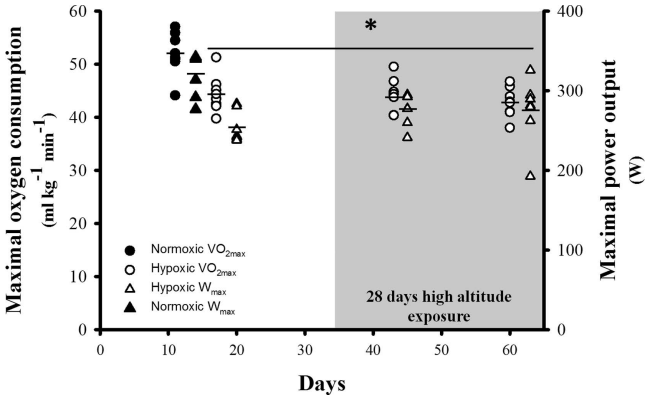

Figure 2. Maximal oxygen consumption and power output. Measurements of $\dot{V}O_{2max}$ (left *y* axis) are represented by circles and W_{max} (right *y* axis) by triangles throughout the duration of the study (*x* axis). *$P < 0.05$ *vs.* normoxic values.

CS and COX activities

There were no measurable changes in skeletal muscle mitochondrial content over time from SL to HA, as indicated by the negligible changes in CS (22.6±6.7 to 24.5±4.9 nmol·min^{-1}·mg ww^{-1}, $P=0.560$) and COX (112±21 to 116±51 pmol O_2·min^{-1}·mg ww^{-1}, $P=0.845$) activities.

Respirometric analysis across time, in response to HA exposure

Respiratory states that were achieved in both titration protocols (L_N, P_{CI}, P, and P_{CII}) did not significantly differ between protocols at SL or HA and were consequently grouped together, with respect to time, for analysis. The respiratory states that significantly changed in response to HA exposure were L_N ($P=0.036$), P_{CI} ($P=0.035$), P ($P=0.042$), P_{CII} ($P=0.031$), and L_{OMY} ($P=0.007$). All respiratory states exhibited a loss of capacity following the altitude exposure (**Fig. 3*A***).

Associations between COX activity and oxidative phosphorylation capacity

When normalizing respiration rates to COX activity, analysis also showed that P_{CI} ($P=0.002$), P ($P=0.002$), and P_{CII} ($P=0.027$) diminished from SL to HA (Fig. 3*B*). L_N respiration had a tendency ($P=0.06$) to decrease. Pearson correlation analysis of mass-specific (pmol O_2·min^{-1}·mg ww^{-1}) P and COX (**Fig. 4**) show a positive correlation at both SL ($P=0.022$) and at HA ($P=0.013$), with Pearson correlation coefficients of 0.782 and 0.819, respectively.

Mitochondrial coupling efficiency

Mitochondrial leak control and coupling control ratios were analyzed (**Table 2**). The leak control ratio (LCR) of L_{OMY} to ETS respiratory state (LCR_{ETS}), indicative of coupling efficiency across the entire respiratory chain, demonstrated an improvement ($P=0.047$) following HA exposure. The respiratory control ratio (RCR), ratio of maximal state 3 respiration, P, to state 4 respiration, L_{OMY}, was the only coupling control ratio that significantly ($P=0.037$) improved with HA exposure.

Association between mitochondrial parameters and maximal whole-body oxygen consumption near SL and at HA

Independent linear regression analyses showed strong positive relationships between SL mitochondrial respiratory capacities and SL $\dot{V}O_{2max}$ values, including P_{CI}

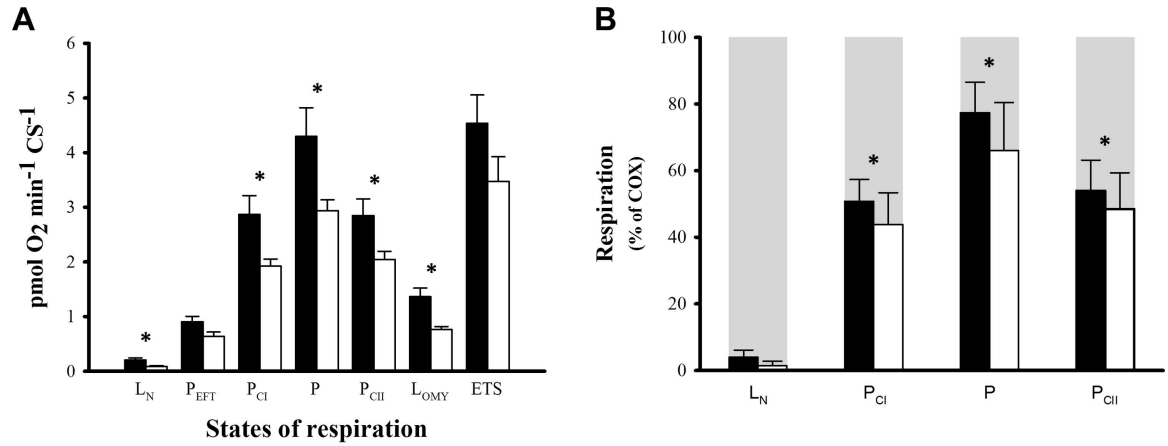

Figure 3. Mitochondrial respiratory capacities. Respirometric analysis was collected from the skeletal muscle in 8 subjects during baseline (SL) collections and then again following 28 d of HA exposure at 3454 m (HA) *A*) L_N, P_{ETF}, P_{CI}, P, P_{CII}, L_{OMY}, and ETS state. Solid bars represent SL measurements; open bars represent HA measurements. Data are presented as means ± SE. *B*) Analysis of L_N, P_{CI}, P, and P_{CII} as a percentage of COX activity. Shaded bars represent COX activity, set to 100%. Solid bars represent SL measurements, open bars represent HA measurements. Data are presented as means ± SD. $^*P < 0.05$ for HA *vs.* SL values.

and P as the best (r^2=0.594 and 0.575, P=0.021 and 0.024, respectively), while there were no significant correlations with SL mitochondrial efficiency. Alternatively, exercise capacity measured at HA following 28 d of HA exposure correlated best with indices of mitochondrial efficiency, specifically RCR and LCR_{ETS} (r^2=0.442 and 0.464, respectively, P=0.05). All significant correlations between exercise capacity and mitochondrial respiratory capacity were lost following HA exposure, with the best correlation being P_{ETF} (r^2=0.204, P=0.154).

DISCUSSION

There are several new findings gained through these experiments. First, respiratory capacity of the skeletal muscle is attenuated with 28 d of exposure to 3454 m altitude. Second, this loss occurred independently from any decrement in mitochondrial content, as indicated by unchanged CS and COX activities. Third, indices of mitochondrial efficiency improved following HA exposure, providing evidence for an enhancement in skeletal muscle mitochondria coupling efficiency. Fourth, whereas mitochondrial respiratory capacity strongly correlates with exercise capacity near sea level, exercise capacity in hypoxia following HA exposure exhibits better concordance with the efficiency of electron transport in skeletal muscle.

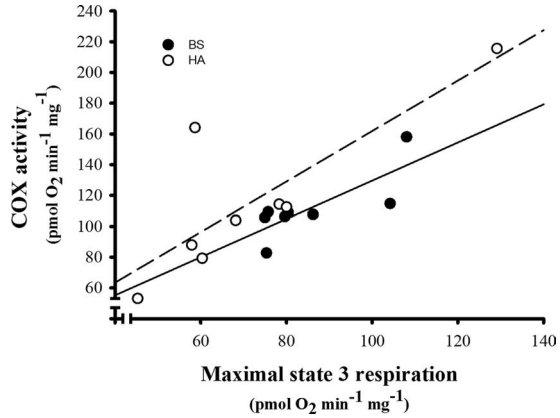

Figure 4. Correlation between COX and P. Pearson correlation coefficients were calculated to investigate the correlation between P and COX activity at baseline (SL; black circles) and again following 28 d exposure to 3454 m (HA; white circles) with Pearson correlation coefficients of 0.782 and 0.819, respectively. Solid line represents the regression line for the correlation at SL; dotted line represents the regression line for the correlation at HA.

Respiratory control with HA exposure

We have previously shown negligible changes in mitochondrial function in 10 human subjects following 2 d of exposure to 3647 m and another 9 at 4559 m (7). There was, however, a tendency (P=0.059) for respiration to decrease with HA exposure. Here, we show that mitochondrial oxidative capacity is diminished with 28 d of HA exposure (Fig. 3). Our past findings combined with these current results suggest that there is a progressive loss of skeletal muscle respiratory capacity with HA exposure, and this attenuation is dependent on the length of exposure. The influence of elevation on these mitochondrial alterations cannot be stated, as only one altitude (3454 m) has been shown to alter respiratory control of the muscle.

Morphological *vs.* functional changes in mitochondria with HA exposure

The current study detected a loss of respiratory capacity independent from changes in mitochondria-specific enzymes, CS and COX. Although we previously reported the loss of certain proteins specific to the mitochondria (8), we did not assess alterations in either CS or COX. Both of these enzymes possess extremely

TABLE 2. *Mitochondrial efficiency*

Condition	LCR_{ETF}	LCR_{CI}	LCR_{CII}	LCR_{ETS}	RCR	PSCR
SL	0.23 ± 0.13	0.08 ± 0.03	0.50 ± 0.10	0.31 ± 0.09	3.23 ± 0.85	1.10 ± 0.34
HA	0.13 ± 0.08	0.04 ± 0.03	0.42 ± 0.12	0.23 ± 0.06*	3.84 ± 0.78*	1.17 ± 0.18

Data are presented as means ± SD. Various determinations of mitochondrial coupling efficiency were collected at baseline (SL) and then again after 28 d of exposure to 3454 m (HA). Indices of efficiency included leak control ratios (LCRs) for the efficiency of electron transfer through ETF during β oxidation (LCR_{ETF}; ratio of L_N to P_{ETF}); during CI respiration (LCR_{CI}; ratio of L_N to P_{CI}); CII respiration (LCR_{CII}; ratio of L_{OMY} to P_{CII}); and efficiency across the entire electron transport system (LCR_{ETS}; ratio of L_{OMY} to ETS state); and coupling control ratios for the degree of coupling across the entire respiratory system with the respiratory control ratio (RCR; ratio of P to L_{OMY}) and for the degree of dyscoupling as a result of the phosphorylative restraint on electron transport through complexes I–IV by ATPsynthase, phosphorylation system control ratio (PSCR; ratio of ETS to P). Difference between SL and HA calculations: $P = 0.109$, 0.063, 0.091, 0.047, 0.037, and 0.662 for indices of mitochondrial coupling efficiency from left to right. *$P < 0.05$ *vs.* SL.

tight associations with mitochondrial volume density, total cristae area, and mass-specific respiratory capacity of human skeletal muscle and thus serve as reliable biomarkers of mitochondrial volume and content in skeletal muscle (21). We confirm these reports, as we found COX activity to strongly correlate with mass-specific P at both SL and HA (Fig. 4). Previous studies have failed to observe a change in CS after a 21-d expedition to 6194 m (4), after 14 and 31–32 d of incremental hypoxic exposure (9), and following 75 d of exposure to 5250 m (6). We also failed to detect a change in CS activity, suggesting that functional modifications of cellular oxygen utilization occur in skeletal muscle mitochondria with hypoxic exposure.

Several studies report that lowland natives participating in high/extreme-altitude expeditions experience losses of mitochondrial volume and content by ~20–25% (1–3). However, the experimental designs of these studies were to accompany mountain climbing expeditions to extreme altitudes and record the physiological adaptations during such a tremendous event. The energy expenditure resulting from the extreme physical rigors of high/extreme-altitude mountaineering alone (23) often results in significant losses in both body and skeletal muscle mass (2, 6, 9, 24). This limits the ability to distinguish hypoxia-facilitated changes in mitochondria from those associated with either participation in extreme endurance events or energy balance (25). Negligible differences in body fat percentages along with preservation of total body mass and W_{max} in the present study imply maintenance of energy balance and suggest that the effects on the mitochondria were the result of HA exposure *per se*.

Mitochondrial efficiency with HA exposure

Indices of coupling efficiency improved (Table 2), while L_{OMY} respiration decreased, with 28 d of HA exposure (Fig. 3*A*), all of which demonstrate an improvement in mitochondrial efficiency. The leak state L_{OMY} is directly reflective of proton leak across the mitochondrial inner membrane using *in situ* mitochondrial preparations (19). We previously failed to observe improvements in several indices of mitochondrial efficiency following 4 wk of exposure to the equivalent of 3000 m normobaric hypoxia for 16 h/d (26) and then again in subjects exposed to 4559 m for 11 d (7). Here, we calculated both leak control and coupling control ratios as an indication of mitochondrial efficiency. LCRs are produced between two respiratory states, a leak state (*i.e.*, low respiration, state 4) to a higher respiratory state (*i.e.*, fatty acid oxidation, submaximal state 3). These corresponding states are paired by an identical substrate supply. The reference state is defined by the leak state, *i.e.*, flux in the P_{ETF} state is greater than in the L_N state, given the same substrate supply (malate + octanoyl carnitine) and serves as the reference state. LCRs help describe mitochondrial coupling efficiency, with a theoretical minimum of 0.0, indicating a fully coupled system, to a value of 1.0, representing a fully noncoupled (dyscoupled) system (15). Alternatively, coupling control ratios are based on the theory that a tightly coupled electron transport system is distinguished from a dyscoupled system by the magnitude of difference between two steady respiratory states, with the reference state being the state defined by the minimum oxygen flux (20). The most common coupling control ratio is the RCR (state 3 respiration/state 4 respiration). In the previous study in which we failed to identify a change in mitochondrial efficiency following 4 wk of intermittent hypoxic exposure, we analyzed the LCR for efficiency of electron transport through CI (LCR_{CI}; leak state being malate- + pyruvate-stimulated L_N and respiratory state being P_{CI}) and the reciprocal coupling control ratio (P_{CI}/L_N) (26). Here, we support these findings, as there were also no improvements to these specific indices of mitochondrial coupling efficiency following HA exposure (Table 2). We did, however, fail to observe the current findings when subjects were exposed to HA for only 11 d (7). Thus, alterations in mitochondrial efficiency also appear to be dependent on duration of hypoxic exposure.

Phosphorylation efficiency has been reported to drop with ADP limitation at high oxygen levels, and then improve at low oxygen tensions (27). Proton leak and uncoupled respiration were found to be repressed in low oxygen, which, in turn, reduces energy expenditure for membrane potential maintenance (27). This hypoxia-induced improvement in bioenergetic efficiency suggests a decrease of mitochondrial oxidant production, as mitochondrial production of superoxide is closely related to mitochondrial coupling effi-

ciency during respiration (28). This adaptation to HA exposure may occur as a response to the initial increase in oxidative stress common with HA exposure (29, 30).

Mitochondria and exercise capacities near SL and at HA

Normoxic $\dot{V}O_{2max}$ values are known to correlate strongly with mitochondrial characteristics, including volume density (31) and oxidative capacity of the muscle (32). We verify this correlation as $\dot{V}O_{2max}$, and both P_{CI} and P exhibited strong correlations. The best predictor of endurance performance in highly trained athletes is skeletal muscle oxidative capacity (13). Less is known on how mitochondrial parameters associate with performance in a hypoxic environment. The degree to which $\dot{V}O_{2max}$ is lost from normoxia to moderate hypoxia in endurance athletes has been partially attributed to differences in mitochondrial function independent of respiration capacity (33). Here, we show that respiration capacity loses its relationship to exercise capacity following HA exposure. Moreover, $\dot{V}O_{2max}$ values following 28 d of exposure to HA correlated with HA indices of mitochondrial efficiency as opposed to respiratory capacities. These data suggest that the importance of mitochondrial parameters on exercise performance shift from a primary significance of respiratory capacity (13) to one of efficiency when going from normoxic to hypoxic exercise. The efficiency of cellular oxygen utilization becomes paramount because of the increasing diffusion limitations of oxygen transport that parallel the increase in elevation (34) *vs.* the convective limitation in oxygen delivery near sea level (35).

Study limitations

The correlational evidence of exercise capacity with respiratory capacity and efficiency at SL and HA, respectively, are based on a small sample size using individual univariate regression analyses. Interpretation of correlational analysis, especially with small sample sizes, should always be tempered. In addition, this study lacks data that provide evidence of potential mechanisms that may explain the loss of mitochondrial respiration capacity or the reciprocal improvement in coupling efficiency. While it is speculation, one potential mechanism that may explain the improvement in mitochondrial efficiency is a decrease in uncoupling protein 3 (UCP3) concentration. Cycling efficiency is inversely proportional to UCP3 concentration in the skeletal muscle (36), and UCP3 has previously been reported to decrease in parallel with improvements in mitochondrial efficiency in cardiac muscle following hypoxic exposure in mice (37). A loss of UCP3 in human skeletal muscle has been reported to occur following hypoxic exposure (1), and this may serve to explain the improvement in skeletal muscle mitochondrial coupling efficiency shown in the present study.

CONCLUSIONS

We find that 28 d of exposure to 3454 m reduces oxidative capacity in human skeletal muscle mitochondria. These alterations in oxidative capacity occur independent from changes in mitochondrial content. In addition to the loss of oxidative capacity in the skeletal muscle is an improvement in mitochondrial coupling efficiency with HA exposure. Lastly, correlation of these mitochondrial parameters to measures of exercise capacity suggest that respiratory capacity is the most important mitochondrial characteristic relative to exercise performance near SL, as mitochondrial efficiency correlates more with performance in hypoxic environments. FJ

The authors sincerely thank Dr. Mikael Sander and Dr. Mattias Hilty for assistance in collection of the skeletal muscle biopsies. The experiments were performed at the Institute of Physiology at University of Zurich. Author contributions: R.A.J., C.S., and C.L. conceived and designed the experiments; R.A.J., M.H., M.T., and A.K.M. collected, analyzed, and interpreted data; R.A.J., C.S., M.H., M.T., and C.L. drafted the article and critically revised it for important intellectual content.

REFERENCES

1. Levett, D. Z., Radford, E. J., Menassa, D. A., Graber, E. F., Morash, A. J., Hoppeler, H., Clarke, K., Martin, D. S., Ferguson-Smith, A. C., Montgomery, H. E., Grocott, M. P., and Murray, A. J. (2012) Acclimatization of skeletal muscle mitochondria to high-altitude hypoxia during an ascent of Everest. *FASEB J.* **26,** 1431–1441
2. Hoppeler, H., Kleinert, E., Schlegel, C., Claassen, H., Howald, H., Kayar, S. R., and Cerretelli, P. (1990) Morphological adaptations of human skeletal muscle to chronic hypoxia. *Int. J. Sports. Med.* **11,** S3–S9
3. Howald, H., Pette, D., Simoneau, J. A., Uber, A., Hoppeler, H., and Cerretelli, P. (1990) Effect of chronic hypoxia on muscle enzyme activities. *Int. J. Sports Med.* **11,** S10–S14
4. Green, H., Roy, B., Grant, S., Burnett, M., Tupling, R., Otto, C., Pipe, A., and McKenzie, D. (2000) Downregulation in muscle Na^+-K^+-ATPase following a 21-day expedition to 6,194 m. *J. Appl. Physiol.* **88,** 634–640
5. Green, H. J., Sutton, J. R., Wolfel, E. E., Reeves, J. T., Butterfield, G. E., and Brooks, G. A. (1992) Altitude acclimatization and energy metabolic adaptations in skeletal muscle during exercise. *J. Appl. Physiol.* **73,** 2701–2708
6. Mizuno, M., Savard, G. K., Areskog, N. H., Lundby, C., and Saltin, B. (2008) Skeletal muscle adaptations to prolonged exposure to extreme altitude: a role of physical activity? *High Alt. Med. Biol.* **9,** 311–317
7. Jacobs, R. A., Boushel, R., Wright-Paradis, C., Calbet, J. A., Robach, P., Gnaiger, E., and Lundby, C. (2012) Mitochondrial function in human skeletal muscle following high-altitude exposure. *Exp Physiol.* In Press
8. Vigano, A., Ripamonti, M., De Palma, S., Capitanio, D., Vasso, M., Wait, R., Lundby, C., Cerretelli, P., and Gelfi, C. (2008) Proteins modulation in human skeletal muscle in the early phase of adaptation to hypobaric hypoxia. *Proteomics* **8,** 4668–4679
9. Green, H. J., Sutton, J. R., Cymerman, A., Young, P. M., and Houston, C. S. (1989) Operation Everest II: adaptations in human skeletal muscle. *J. Appl. Physiol.* **66,** 2454–2461
10. Ross, R. M. (2003) ATS/ACCP Statement on cardiopulmonary exercise testing. *Am. J. Respir. Crit. Care Med.* **167,** 211–277
11. Bergström, J. (1962) Muscle electrolytes in man. *Scand. J. Clin. Lab. Invest.* **68,** 1–110
12. Kuznetsov, A. V., Schneeberger, S., Seiler, R., Brandacher, G., Mark, W., Steurer, W., Saks, V., Usson, Y., Margreiter, R., and

Gnaiger, E. (2004) Mitochondrial defects and heterogeneous cytochrome *c* release after cardiac cold ischemia and reperfusion. *Am. J. Physiol. Heart Circ. Physiol.* **286,** H1633–H1641
13. Jacobs, R. A., Rasmussen, P., Siebenmann, C., Diaz, V., Gassmann, M., Pesta, D., Gnaiger, E., Nordsborg, N. B., Robach, P., and Lundby, C. (2011) Determinants of time trial performance and maximal incremental exercise in highly trained endurance athletes. *J. Appl. Physiol.* **111,** 1422–1430
14. Eaton, S., Bartlett, K., and Pourfarzam, M. (1996) Mammalian mitochondrial beta-oxidation. *Biochem. J.* **320,** 345–357
15. Gnaiger, E. (2009) Capacity of oxidative phosphorylation in human skeletal muscle: new perspectives of mitochondrial physiology. *Int. J. Biochem. Cell Biol.* **41,** 1837–1845
16. Pesta, D., and Gnaiger, E. (2011) High-resolution respirometry. OXPHOS Protocols for Human Cell Cultures and Permeabilized Fibres from Small Biopsies of Human Muscle. *Methods Mol. Biol.* **810,** 25–58
17. Saks, V. A., Veksler, V. I., Kuznetsov, A. V., Kay, L., Sikk, P., Tiivel, T., Tranqui, L., Olivares, J., Winkler, K., Wiedemann, F., and Kunz, W. S. (1998) Permeabilized cell and skinned fiber techniques in studies of mitochondrial function in vivo. *Mol. Cell. Biochem.* **184,** 81–100
18. Rasmussen, U. F., and Rasmussen, H. N. (2000) Human skeletal muscle mitochondrial capacity. *Acta Physiol. Scand.* **168,** 473–480
19. Brand, M. D., and Nicholls, D. G. (2011) Assessing mitochondrial dysfunction in cells. *Biochem. J.* **435,** 297–312
20. Chance, B., and Williams, G. R. (1955) Respiratory enzymes in oxidative phosphorylation. III. The steady state. *J. Biol. Chem.* **217,** 409–427
21. Larsen, S., Nielsen, J., Neigaard Nielsen, C., Nielsen, L. B., Wibrand, F., Stride, N., Schroder, H. D., Boushel, R., Helge, J. W., Dela, F., and Hey-Mogensen, M. (2012) Biomarkers of mitochondrial content in skeletal muscle of healthy young human subjects. *J. Physiol.* **590,** 3349–3360
22. Srere, P. A. (1969) Citrate synthase. *Methods Enzymol.* **13,** 3–11
23. Westerterp, K. R., Kayser, B., Brouns, F., Herry, J. P., and Saris, W. H. (1992) Energy expenditure climbing Mt. Everest. *J. Appl. Physiol.* **73,** 1815–1819
24. MacDougall, J. D., Green, H. J., Sutton, J. R., Coates, G., Cymerman, A., Young, P., and Houston, C. S. (1991) Operation Everest II: structural adaptations in skeletal muscle in response to extreme simulated altitude. *Acta Physiol. Scand.* **142,** 421–427
25. Hochli, D., Schneiter, T., Ferretti, G., Howald, H., Claassen, H., Moia, C., Atchou, G., Belleri, M., Veicsteinas, A., and Hoppeler, H. (1995) Loss of muscle oxidative capacity after an extreme endurance run: the Paris-Dakar foot-race. *Int. J. Sports. Med.* **16,** 343–346
26. Robach, P., Siebenmann, C., Jacobs, R. A., Rasmussen, P., Nordsborg, N. B., Pesta, D., Gnaiger, E., Diaz, V., Christ, A., Fiedler, J., Crivelli, N., Secher, N. H., Pichon, A., Maggiorini, M., and Lundby, C. (2012) The role of hemoglobin mass on VO2max following normobaric "live high – train low" in endurance-trained athletes. *Br. J. Sports Med.* **46,** 822–827
27. Gnaiger, E., Mendez, G., and Hand, S. C. (2000) High phosphorylation efficiency and depression of uncoupled respiration in mitochondria under hypoxia. *Proc. Natl. Acad. Sci. U. S. A.* **97,** 11080–11085
28. Yin, Y., Yang, S., Yu, L., and Yu, C. A. (2010) Reaction mechanism of superoxide generation during ubiquinol oxidation by the cytochrome bc1 complex. *J. Biol. Chem.* **285,** 17038–17045
29. Moller, P., Loft, S., Lundby, C., and Olsen, N. V. (2001) Acute hypoxia and hypoxic exercise induce DNA strand breaks and oxidative DNA damage in humans. *FASEB J.* **15,** 1181–1186
30. Lundby, C., Pilegaard, H., van Hall, G., Sander, M., Calbet, J., Loft, S., and Moller, P. (2003) Oxidative DNA damage and repair in skeletal muscle of humans exposed to high-altitude hypoxia. *Toxicology* **192,** 229–236
31. Mathieu, O., Krauer, R., Hoppeler, H., Gehr, P., Lindstedt, S. L., Alexander, R. M., Taylor, C. R., and Weibel, E. R. (1981) Design of the mammalian respiratory system. VII. Scaling mitochondrial volume in skeletal muscle to body mass. *Respir. Physiol.* **44,** 113–128
32. Pesta, D., Hoppel, F., Macek, C., Messner, H., Faulhaber, M., Kobel, C., Parson, W., Burtscher, M., Schocke, M., and Gnaiger, E. (2011) Similar qualitative and quantitative changes of mitochondrial respiration following strength and endurance training in normoxia and hypoxia in sedentary humans. *Am. J. Physiol. Regul. Integr. Comp. Physiol.* **301,** R1078–R1087
33. Ponsot, E., Dufour, S. P., Doutreleau, S., Lonsdorfer-Wolf, E., Lampert, E., Piquard, F., Geny, B., Mettauer, B., Ventura-Clapier, R., and Richard, R. (2010) Impairment of maximal aerobic power with moderate hypoxia in endurance athletes: do skeletal muscle mitochondria play a role? *Am. J. Physiol. Regul. Integr. Comp. Physiol.* **298,** R558–R566
34. Jacobs, R. A., Lundby, C., Robach, P., and Gassmann, M. (2012) Red blood cell volume and the capacity for exercise at moderate to high-altitude. *Sports Med.* **42,** 1–21
35. Andersen, P., and Saltin, B. (1985) Maximal perfusion of skeletal muscle in man. *J. Physiol.* **366,** 233–249
36. Mogensen, M., Bagger, M., Pedersen, P. K., Fernstrom, M., and Sahlin, K. (2006) Cycling efficiency in humans is related to low UCP3 content and to type I fibres but not to mitochondrial efficiency. *J. Physiol.* **571,** 669–681
37. McCarthy, J., Lochner, A., Opie, L. H., Sack, M. N., and Essop, M. F. (2011) PKCepsilon promotes cardiac mitochondrial and metabolic adaptation to chronic hypobaric hypoxia by GSK3beta inhibition. *J. Cell. Physiol.* **226,** 2457–2468

Received for publication July 30, 2012.
Accepted for publication August 27, 2012.

J Appl Physiol 111: 1422–1430, 2011.
First published September 1, 2011; doi:10.1152/japplphysiol.00625.2011.

Determinants of time trial performance and maximal incremental exercise in highly trained endurance athletes

R. A. Jacobs,[1,2] P. Rasmussen,[2,3,4] C. Siebenmann,[2,3] V. Díaz,[1,2,5] M. Gassmann,[1,2] D. Pesta,[6] E. Gnaiger,[6] N. B. Nordsborg,[7] P. Robach,[8] and C. Lundby[2,3]

[1]*Institute of Veterinary Physiology, University of Zurich;* [2]*Center for Integrative Human Physiology (ZIHP); and* [3]*Institute of Physiology, University of Zurich, Zurich, Switzerland;* [4]*Institute of Pharmacology and Neuroscience, University of Copenhagen, Copenhagen, Denmark;* [5]*Department of Health and Human Performance, Universidad Politécnica de Madrid, Madrid, Spain;* [6]*Department of Transplant Surgery, D. Swarovski Research Laboratory, Innsbruck Medical University, Innsbruck, Austria;* [7]*Department of Exercise and Sport Sciences, University of Copenhagen, Copenhagen, Denmark; and* [8]*Ecole Nationale des Sports de Montagne, Chamonix, France*

Submitted 19 May 2011; accepted in final form 25 August 2011

Jacobs RA, Rasmussen P, Siebenmann C, Díaz V, Gassmann M, Pesta D, Gnaiger E, Nordsborg NB, Robach P, Lundby C. Determinants of time trial performance and maximal incremental exercise in highly trained endurance athletes. *J Appl Physiol* 111: 1422–1430, 2011. First published September 1, 2011; doi:10.1152/japplphysiol.00625.2011.—Human endurance performance can be predicted from maximal oxygen consumption ($\dot{V}O_{2max}$), lactate threshold, and exercise efficiency. These physiological parameters, however, are not wholly exclusive from one another, and their interplay is complex. Accordingly, we sought to identify more specific measurements explaining the range of performance among athletes. Out of 150 separate variables we identified 10 principal factors responsible for hematological, cardiovascular, respiratory, musculoskeletal, and neurological variation in 16 highly trained cyclists. These principal factors were then correlated with a 26-km time trial and test of maximal incremental power output. Average power output during the 26-km time trial was attributed to, in order of importance, oxidative phosphorylation capacity of the vastus lateralis muscle ($P = 0.0005$), steady-state submaximal blood lactate concentrations ($P = 0.0017$), and maximal leg oxygenation (sO_{2LEG}) ($P = 0.0295$), accounting for 78% of the variation in time trial performance. Variability in maximal power output, on the other hand, was attributed to total body hemoglobin mass (Hb_{mass}; $P = 0.0038$), $\dot{V}O_{2max}$ ($P = 0.0213$), and sO_{2LEG} ($P = 0.0463$). In conclusion, *1*) skeletal muscle oxidative capacity is the primary predictor of time trial performance in highly trained cyclists; *2*) the strongest predictor for maximal incremental power output is Hb_{mass}; and *3*) overall exercise performance (time trial performance + maximal incremental power output) correlates most strongly to measures regarding the capability for oxygen transport, high $\dot{V}O_{2max}$ and Hb_{mass}, in addition to measures of oxygen utilization, maximal oxidative phosphorylation, and electron transport system capacities in the skeletal muscle.

mitochondria; oxidative phosphorylation; oxygen transport and utilization; skeletal muscle; hemoglobin

THE PRODUCT of an athlete's maximal oxygen consumption ($\dot{V}O_{2max}$) × lactate threshold × exercise efficiency can predict endurance performance (4, 44–46). This general calculation of performance is likely appropriate because it broadly accounts for most physiological parameters involved in exercise. The purpose of this study is therefore to isolate the most dominant physiological variables of performance and identify the strongest determinant(s) of exercise performance in highly trained endurance athletes.

An individual's $\dot{V}O_{2max}$ is limited primarily by cardiac output, locomotor muscle blood flow, and oxygen-carrying capacity of the blood (1, 47, 52) while also expressing a strong linear correlation with mitochondrial volume density (85). The constraint of oxygen consumption has been recognized to limit exercise performance for nearly a century (20, 33), and a large $\dot{V}O_{2max}$ is a prerequisite for high endurance capability (72, 74, 78). The ability to maintain a given workload with lower blood lactate concentrations, however, correlates more reliably to endurance performance than $\dot{V}O_{2max}$ among groups of trained individuals (17, 22, 70) and is said to be the strongest broad-spectrum predictor of exercise performance in highly trained endurance athletes (17, 55). The lactate threshold is a theoretical workload facilitating an accelerated accumulation of blood lactate attendant to a disproportionate rise in glycolytic flux and lactate appearance over oxidative phosphorylation and lactate disposal, respectively (9, 24). The physiological determinants of maintaining relatively low concentrations of lactate are believed to parallel the mitochondrial capacity of the skeletal muscle (35, 84). Additionally, skeletal muscle oxidative capacity, once thought to be indicated by percentage of type 1 (oxidative) muscle fibers (2), correlates strongly with exercise efficiency (18), which also accounts for a significant variation in exercise performance among highly trained athletes (14, 58). Oxidative phosphorylation capacity of the skeletal muscle appears central to all three physiological components used to predict endurance performance ($\dot{V}O_{2max}$, lactate threshold, and exercise efficiency) although its relation to exercise performance in a homogeneous group of trained athletes has never been directly demonstrated.

Accordingly, during a recent study involving 16 highly trained endurance cyclists (Siebenmann C, Robach P, Jacobs RA, Rasmussen P, Nordsborg N, Díaz V, Christ A, Olsen NV, Maggiorini M, Lundby C, unpublished observations), we acquired a considerable physiological data set and correlated these to time trial performance and maximal incremental exercise capacity. As oxidative capacity of the skeletal muscle appears to have the most common interrelation between $\dot{V}O_{2max}$, lactate threshold, and exercise efficiency we hypothesize that maximal oxidative phosphorylation capacity of the skeletal muscle is the strongest determinant of time trial performance in highly trained athletes.

Address for reprint requests and other correspondence: C. Lundby, Institute of Physiology, ZIHP, Univ. of Zurich, Office 23 H 6, Winterthurerstr. 190, 8057 Zürich, Switzerland (e-mail: carsten.lundby@access.uzh.ch).

METHODS

Volunteers

Sixteen highly trained endurance athletes (15 men, 1 woman, age 29 ± 6 yr, height 179 ± 8 cm, body weight 69 ± 9 kg) from various countries in North America and Europe were volunteers in the current study. All of them regularly participated in endurance competitions on at least the national level in disciplines related to cycling, i.e., road cycling, triathlon, cycle cross, and/or mountain bike. All volunteers gave written informed consent to participate in the study. The study was approved by the Ethics Committee of Zürich (2010–066/0) and Vaud (215/10) (Switzerland), and conformed to the Declaration of Helsinki.

Experimental Protocols

All the experimental procedures of the study were performed at the hospital La Vallée (Le Sentier, Switzerland). At least 24 h was given to all subjects in between separate exercise tests.

Maximal incremental exercise capacity. This measure of performance was tested on an electronically braked bicycle-ergometer in an upright position (Monark 839E, Varberg, Sweden). The exercise protocol started with a warm-up period of 5 min at a workload of 150 W followed by 5 min at 200 W except for the female athlete who warmed up at 100 and 150 W. Thereafter, the workload was increased by 25 W/min until failure. During the last minutes of the test, volunteers were vigorously encouraged to perform to complete exhaustion. Volunteers wore a face mask covering mouth and nose for breath collection, and O_2 and CO_2 concentration in the expired gas were continuously measured and monitored as breath-by-breath values. The gas analyzers and the flowmeter of the applied spirometer (Quark, Cosmed, Rome, Italy) were calibrated prior to each test. After the test breath-by-breath values were visually controlled and averaged over 30 s. The highest average value was determined for $\dot{V}O_{2max}$, and all the other parameters were selected at the same time except for maximal workload (W_{max}), which was calculated as $W_{max} = W_{compl} + 25 \times (t/60)$, with W_{compl} being the last completed workload and t the number of seconds in the not-completed workload.

Time trial performance. To evaluate exercise performance in a scenario similar to competitions, volunteers performed a time trial using their own personal bike mounted on an electrically braked cycle trainer (Fortius Virtual Reality Trainer, Tacx, Rotterdam, Netherlands). The combination with a commercially available software allowed for the simulation of a predefined route on a portable computer. We selected a final section of the Milan-San Remo race with a length of 26.15 km. This route consists of a first flat part (4.8 km, average incline 0.23%), a first climb (5.5 km, 4.19%), a downhill part (3.1 km, −6.79%), a second flat part (8.6 km, 0.25%) and the final climb (4.15 km, 3.13%). Volunteers' body weight was measured before each trial for software-based calculation of the appropriate resistance. After warming up for a minimum of 10 min volunteers could rest again and start the test whenever they felt ready. Throughout the test volunteers were free to manually change gears, drink and eat ad libitum, and were allowed visual feedback on the computer screen that displayed their speed and covered distance. The rear wheel of each bike was fitted with a power meter (Powertap Highly trained+, CycleOps, Madison, WI), which monitored power output over the whole course. Volunteers were vigorously encouraged during all tests.

Exercise efficiency. We assessed $\dot{V}O_2$ and respiratory exchange ratio (RER) at an absolute set submaximal steady-state cycling. Breath-by-breath values during the last minute of 5-min increments (150 W and 200 W for men; 100 W and 150 W for the woman) were averaged. Energy expenditure (EE) per minute was calculated from submaximal $\dot{V}O_2$ values and RERs (57). Delta efficiency (DE) was then calculated as the ratio of the change in work (kcal/min) by the change in energy expended (kcal/min) at the two submaximal workloads multiplied by 100: DE (%) = (ΔWork rate/ΔEE)·100.

Arterial blood measurements. After local anesthesia with 2% lidocaine, a 20-gauge catheter (model 80115.09R, Vygon laboratories, Ecouen, France) was inserted percutaneously using the Seldinger technique into the radial artery. Arterial blood was sampled anaerobically in heparinized syringes and immediately analyzed for hemoglobin concentration ([Hb]), O_2 saturation (Sa_{O_2}), O_2 tension (Pa_{O_2}), and lactate concentration by means of the ABL 800 Flex (Radiometer, Copenhagen, Denmark). Blood O_2 content (Ca_{O_2}) was computed from the following formula: $Ca_{O_2} = (1.34 \times [Hb] \times Sa_{O_2}) + (0.003 \times Pa_{O_2})$. Arterial samples were collected at rest, 150 W, 200 W, and at exhaustion.

Intravascular volumes. Hemoglobin mass (Hb_{mass}) was quantified by a modified (56) carbon monoxide (CO)-rebreathing technique (11). After the subject had stayed for 20 min in a semirecumbent position, 2 ml of blood was sampled from an antecubital vein without stasis through a 20-gauge catheter and immediately analyzed in quadruplicate for *1*) percent carboxyhemoglobin (%HbCO) and hemoglobin concentration ([Hb]) on a hemoximeter (ABL 800 Flex, Radiometer, Copenhagen, Denmark), and *2*) hematocrit (4 min at 13,500 rpm). A bolus (1.5 ml/kg) of 99.997% CO (CO N47, Air Liquide) containing <0.1 ppm of nickel tetracarbonyl or ferrous pentacarbonyl was then rebreathed for 8 min. At the end of the rebreathing period, another similarly obtained and analyzed 2-ml blood sample was obtained. The change in %HbCO between the first and second measurement was used to calculate Hb_{mass}, taking into account the amount of CO remaining in the rebreathing circuit at the end of the procedure (2.2%) (11). The RCV, blood and plasma volumes were derived from Hb_{mass}, [Hb], and hematocrit (11) as assessed by the same operator for the entire study. The Hb_{mass} values expressed the average of duplicate measurement. The coefficient of variation for Hb_{mass}, assessed from duplicate baseline during the lead-in period, and expressed as the percent typical error (i.e., SD of difference scores/$\sqrt{2}$), was 2.6%.

Near-infrared spectroscopy (NIRS). Thigh (sO_{2LEG}) and cerebral (sO_{2BRAIN}) measures of tissue oxygenation were obtained by NIRS (NIRO-200, Hamamatsu, Japan). The method has been previously described (69). Briefly, both measurements assume a homogeneous medium and use spatially resolved spectroscopy coupled to an analytical solution of the diffusion equation (69). NIRS reflects primarily capillary oxygenation although the signal is also affected by the arterial and venous blood and, for the muscle, myoglobin. The NIRO-200 uses an internal calibration derived independently from the pathway length of the infrared light. Changes in cerebral sO_{2BRAIN} oxygenation were relative to the values obtained at rest and reported as cerebral ΔsO_{2BRAIN}. NIRS measurements in skeletal muscle provide the oxygenation status of the hemoglobin in the microvasculature of the tissue (with a small contribution from myoglobin in skeletal muscle) thereby reflecting the balance between oxygen consumption (drive to reduce oxygenation) and delivery (drive to maintain oxygenation). NIRS values have been shown to correlate well with femoral venous oxygen saturation and can serve as a substitute measure of oxygen extraction (21).

Middle cerebral artery velocity. Transcranial doppler (TCD) measurements of cerebral blood velocity were performed (Dopplerbox, DWL, überlingen, Germany). The TCD-transducer was fixed above the temporal bone with a headband to carry out measurements on the proximal part of the middle cerebral artery (MCA). To achieve the best signal-to-noise ratio both probe position and insonation depth (40–60 mm) were carefully adjusted for each individual. The MCA velocity was computed from the integral of the maximum frequency Doppler shifts over one heartbeat and averaged over 30 s.

Blood pressure. Arterial pressure was measured with a transducer (MLT844, AD Instruments, Australia) connected to the arterial line placed at the level of the heart (4th intercostal space). Blood pressure data were collected and stored with Powerlab (AD Instruments, Australia).

Muscle function. Volunteers were seated on a wooden plate with no backrest and the angle of the knee joint was between 85 and 95 degrees. A mark was made on the subject's thigh in relation to the edge of the chair to ensure precise repositioning. A strap was placed around the lower leg, just above the ankle joint. The strap was secured to a rigid pole that was attached to a strain gauge. The strain gauge was calibrated twice a day, once in the morning and again in the afternoon. Force recordings were sampled at 1 kHz. Self adhesive electrodes (5 × 9 cm, Platinium Neurostimulation Electrodes, Axelgaard, Fallbrook, CA) were placed on the rectus femoris muscle at 25% of the distance from spina iliaca anterior superior to the proximal part of patella. The electrodes were fixed by tape (Fixomull stretch, BSN medical GmbH, Hamburg, Germany) and remained in position for the rest of the experiment. This was done to ensure no measurement errors due to repositioning of electrodes and to reduce the time elapsed from the end of exercise to investigation. Five to ten submaximal and close to maximal contractions were performed prior to determination of the optimal stimulation intensity. The stimulation intensity used was 440 ± 70 mA with a range between 220 and 500 mA. The stimulations were delivered using a single 200-μs pulse, and voltage was 400 V (Digitimer DS7AH, Digitimer, Hertfordshire, UK). Optimal stimulation intensity was determined by increasing stimulation current from 50 mA until the current was at least 20% higher than the current eliciting a maximal twitch response. At first, an optimal stimulation intensity was determined by rapid increments of stimulation currents. When an optimal intensity was determined a stimulation current vs. twitch force curve was constructed with increments of 50 mA or less to ensure that a maximal twitch response was obtained. After determination of the optimal stimulation intensity, the subject was asked to perform a 5-s maximal voluntary contraction (MVC) with stimulation occurring 3 s into the 5 s contraction (superimposed twitch, T_{WS}). Five seconds after the MVC another stimulation was performed to determine the twitch force (T_W). This procedure was repeated every minute, three times in total. Maximal values for MVC, T_{WS}, and T_W were recorded. The superimposed twitch force was related to the twitch force recorded 5 s after the MVC and termed percent voluntary activation: $VA\% = [1 - (T_{WS}/T_W)] \times 100$. One minute after the third MVC the subject was asked to generate ~50% of the force recorded during MVC. When the force was constant after 5–20 s a stimulation was performed. After another minute of rest, the procedure was repeated at ~75% of MVC. The measurements were performed to ensure that the applied procedure could be used to assess %VA. The control measurements revealed %VA to be 64.3 ± 12.3 and 84.2 ± 9.1 at 50% and 75% of MVC, respectively. After the time trial, volunteers were rapidly moved to the wooden plate and repositioned as they were previously. After 45 s, a 5-s MVC was performed with a stimulation again being delivered 3 s into and 5 s after the MVC, as described above. The procedure was repeated three times starting every 30 s. Following 5 min of recovery the same series of 3 MVC and stimulations were performed. This protocol was used to assess central (neuromuscular) vs. peripheral (skeletal muscle) fatigue following time trial performance. The aim prior to exercise was to determine maximal twitch force. Accordingly, sufficient time, 60 s, was allowed to elapse between stimulations to avoid stimulation-induced fatigue. Following exercise, however, the aim was to examine whether a loss of twitch force had occurred with concern that maximal twitch force could recover during the elapsed time between measurements. Therefore the compromise was to allow only 30 s between stimulations after exercise. Since we used the maximal obtained twitch force in the calculations there is no error in the interpretation of the data with this approach.

Skeletal muscle biopsy. Under local anesthetics using the Bergström technique (6) with a needle modified for suction, skeletal muscle biopsies were obtained while the subject was at rest and a minimum of 24 h following last exercise training bout. The biopsy was dissected free of fat and connective tissue and divided into sections for mitochondrial respiration and muscle buffer capacity measurements. The section used for muscle buffer capacity was frozen immediately.

Mitochondrial respiration. A subsample of the biopsy (~20 mg) was sectioned into four parts to measure mitochondrial respiration. Each part was immediately placed in ice-cold biopsy preservation solution (BIOPS) containing 2.77 mM CaK_2EGTA buffer, 7.23 mM K_2EGTA buffer, 0.1 μM free calcium, 20 mM imidazole, 20 mM taurine, 50 mM 2-(*N*-morpholino)ethanesulfonic acid hydrate (MES), 0.5 mM dithiothreitol, 6.56 mM $MgCl_2 \cdot 6H_2O$, 5.77 mM ATP, and 15 mM phosphocreatine (pH 7.1). Muscle samples were then gently dissected using forceps and fibers were chemically permeabilized via incubation in 2 ml of BIOPS containing saponin (50 μg/ ml) for 30 min (49). Before each sample was added to its respective respiration chamber, the wet weight was measured (XS205 DualRange Analytical Balance, Mettler-Toledo AG, Switzerland). Respiration measurements were performed in mitochondrial respiration medium 06 (MiR06) containing 0.5 mM EGTA, 3 mM $MgCl_2 \cdot 6H_2O$, 60 mM K-lactobionate, 20 mM taurine, 10 mM KH_2P04, 20 mM HEPES, 110 mM sucrose, 1 g/l bovine serum albumin, and catalase 280 IU/ml (pH 7.1). Measurements of oxygen consumption were performed in duplicate at 37°C using the high-resolution Oxygraph-2k (Oroboros, Innsbruck, Austria) with all additions of substrates, uncouplers, and inhibitors added in series. All experiments were carried out in a hyperoxygenated environment to prevent any potential oxygen diffusion limitation. Two substrates, uncoupler, and inhibitor titration (SUIT) protocols were used in the study. Each protocol was specific to the examination of individual aspects of respiratory control through a sequence of coupling and substrate states induced via separate titrations. A more complete listing of and thorough explanations for the standard nomenclature regarding various respiratory states, SUIT protocols, coupling control, and flux control ratios can be found in detail elsewhere (67, 68). Briefly, oxidative phosphorylation (OXPHOS) capacity (P; usually compared with originally defined state 3 respiration) is the ADP-activated mitochondrial respiratory state of oxidative phosphorylation with saturating concentrations of ADP, inorganic phosphate, oxygen, and defined reduced substrates. Mitochondrial electron transfer system capacity, E, is the experimentally induced noncoupled (fully uncoupled) state, in which ADP, inorganic phosphate, oxygen, and defined substrates are present at saturating levels along with the titration of an established amount of uncoupler to optimum concentrations facilitating maximal noncoupled respiration through the electron transport system (ETS) (67).

The specific SUIT protocol was used to measure OXPHOS capacity (P) in the permeabilized skeletal muscle preparations. Maximal values of P were induced with the additions of malate (2 mM), octanoyl carnitine (0.2 mM), glutamate (10 mM), succinate (10 mM), and saturating adenosine diphosphate concentrations (ADP; 5 mM). Such a protocol provides saturating concentrations of substrates for both NADH dehydrogenase, complex I, and succinate dehydrogenase, complex II. The integrity of the outer mitochondrial membrane was assessed with the addition of cytochrome *c* (10 μM). The addition of cytochrome *c* had no additive effect on respiration with negligible increases of 3.4%, respectively, confirming intact and viable mitochondria in the skeletal muscle samples. Maximal noncoupled ETS respiration (E) was then measured following the titration of carbonyl cyanide *p*-(trifluoromethoxy)phenylhydrazone (FCCP; a total of 1.5 μM in steps of 0.5 μM). Last, residual oxygen consumption, indicative of nonmitochondrial oxygen consumption, was assessed following

the inhibition of complexes I and III with the addition of rotenone (0.5 μM) and antimycin A (2.5 μM), respectively.

Citrate synthase activity. Citrate synthase (CS) activity was assayed in homogenates of all skeletal muscle samples used for respiration measurements. The content of the oxygraph chamber (2 ml) was removed after each respiration experiment and washed twice with 2 ml of MiR06. The solutions were combined, homogenized for 60 s with an Ultra-Turrax homogenizer at maximum speed, frozen in liquid nitrogen, and stored at −80°C. The activity of citrate synthase was measured spectrophotometrically at 412 nm and 37°C. Eight-hundred microliters of homogenate was added to 200 μl medium containing 0.1 mM 5,5-dithio-bis-(2-nitrobenzoic) acid (DTNB), 0.5 mM oxaloacetate, 0.31 mM acetyl coenzyme A, 5 mM triethanolamine hydrochloride, 50 μM EDTA, and 0.1 M Tris-HCl (pH 8.1) (81).

Skeletal muscle buffer capacity. The method was previously described in Ref. 39. After having adjusted pH of the sample to 7.1 with 0.01 M NaOH, the sample was titrated to pH 6.0 by serial additions of 0.01 M HCl followed by titration back to pH 7.1 by serial additions of 0.01 M NaOH. The pH was measured after each addition. The non-HCO_3^- physiochemical buffer capacity was determined from the number of moles of H^+ required to change pH from 7.1 to 6.5 and was expressed as micromoles H^+ per kilogram dry weight per unit of pH (59). The in vivo muscle buffer capacity was calculated as the change in muscle lactate from rest to exhaustion divided by the change in muscle pH (79).

Statistics

From the studies we obtained 6 intravascular volumes, 22 measures of mitochrondrial function, 40 measures of pulmonary gas exchange, 6 measurements of exercise efficiency, 24 arterial blood gas or metabolite measurements, 36 measures of cardiac performance and blood pressure, 4 measurements of cerebral blood flow, and 14 measures of vastus lateralis and cerebral oxygenation. In total 152 different measurements were recorded and all were the average of 2–6 separate exercise tests. We recorded two separate measures of exercise performance, and these are presented along with $\dot{V}O_{2max}$ for our 16 volunteers in Table 1.

The first objective of the analysis was to reduce the number of variables to <16 to have sufficient degrees of freedom to perform a statistical analysis. Of the 152 potential determinants we excluded 59 variables because they were either redundant (i.e., showed high correlation with a related variable) or because no a priori hypothesis could be justified. This left 73 variables for further evaluation for the main analysis. Those variables were grouped into six groups relating them to efficiency, pulmonary performance, cerebral factors, muscular factors, cardiac-vascular factors, or oxygen transport. If appropriate, each variable was allowed to enter two groups as long as the total number of variables in one group did not exceed 15 ($n - 1$). Following calculation of a nonparametric correlation matrix (Kendall's tau-b), we performed a multiple stepwise regression (Pearson) of the principal factors in each group to identify the variables for which the majority of the variance could be attributed. Factor analysis describes variability among observed variables in terms of a potentially lower number of unobserved variables called factors. The underlying unobserved, or latent, variable, however, is not of interest for this study and principal factor analysis was simply used to reduce the number of variables entering the analysis. Only the variables with loadings on the first three principal factors larger than 0.6 were considered for further analysis. The resulting variables selected are presented in Fig. 1.

RESULTS

Maximal Incremental Power Output

Following multiple stepwise regression analysis for determinants of maximal incremental power output, Hb_{mass} was identified as best single parameter ($r^2 = 0.48$, $P = 0.0027$).

Table 1. *Measures of exercise performance along with $\dot{V}O_{2max}$*

			$\dot{V}O_{2max}$, ml·min^{-1}·kg^{-1}		TT_{mean}, W/kg		$Incremental_{max}$, W/kg	
Subject	Height, cm	Weight, kg	Ranking	Value	Ranking	Value	Ranking	Value
				First quartile				
O	177	70	*1*	80.44	*7*	4.35	*2*	6.31
B	180	72	*2*	77.32	*8*	4.34	*7*	5.99
C	176	65	*3*	76.87	*1*	5.06	*1*	6.89
L	193	76	*4*	74.30	*2*	4.62	*3*	6.28
				Second quartile				
I	173	62	*5*	72.24	*4*	4.50	*9*	5.88
F	176	62	*6*	71.95	*6*	4.43	*5*	6.08
P	175	76	*7*	71.79	*10*	3.98	*10*	5.86
S	164	63	*8*	71.51	*12*	3.91	*15*	4.89
				Third quartile				
N	178	65	*9*	71.44	*5*	4.48	*4*	6.20
M	173	60	*10*	69.39	*14*	3.64	*8*	5.94
G	188	74	*11*	69.20	*3*	4.52	*6*	6.05
H	183	69	*12*	68.36	*9*	4.14	*11*	5.82
				Fourth quartile				
Q	183	80	*13*	68.00	*16*	3.60	*14*	5.37
K	170	59	*14*	64.15	*13*	3.74	*12*	5.79
T	182	76	*15*	63.12	*11*	3.93	*13*	5.55
J	194	87	*16*	58.33	*15*	3.61	*16*	4.88
Mean	179	70		70.53		4.18		5.86
SD	8	8		5.57		0.42		0.51

Numbers in italics preceding values identify subjects according to their ranking, e.g., *subject O* ranks 1st in maximal oxygen consumption ($\dot{V}O_{2max}$), 7th in average time trial power (TT_{mean}), and 2nd in maximal power output during an incremental test ($Incremental_{max}$).

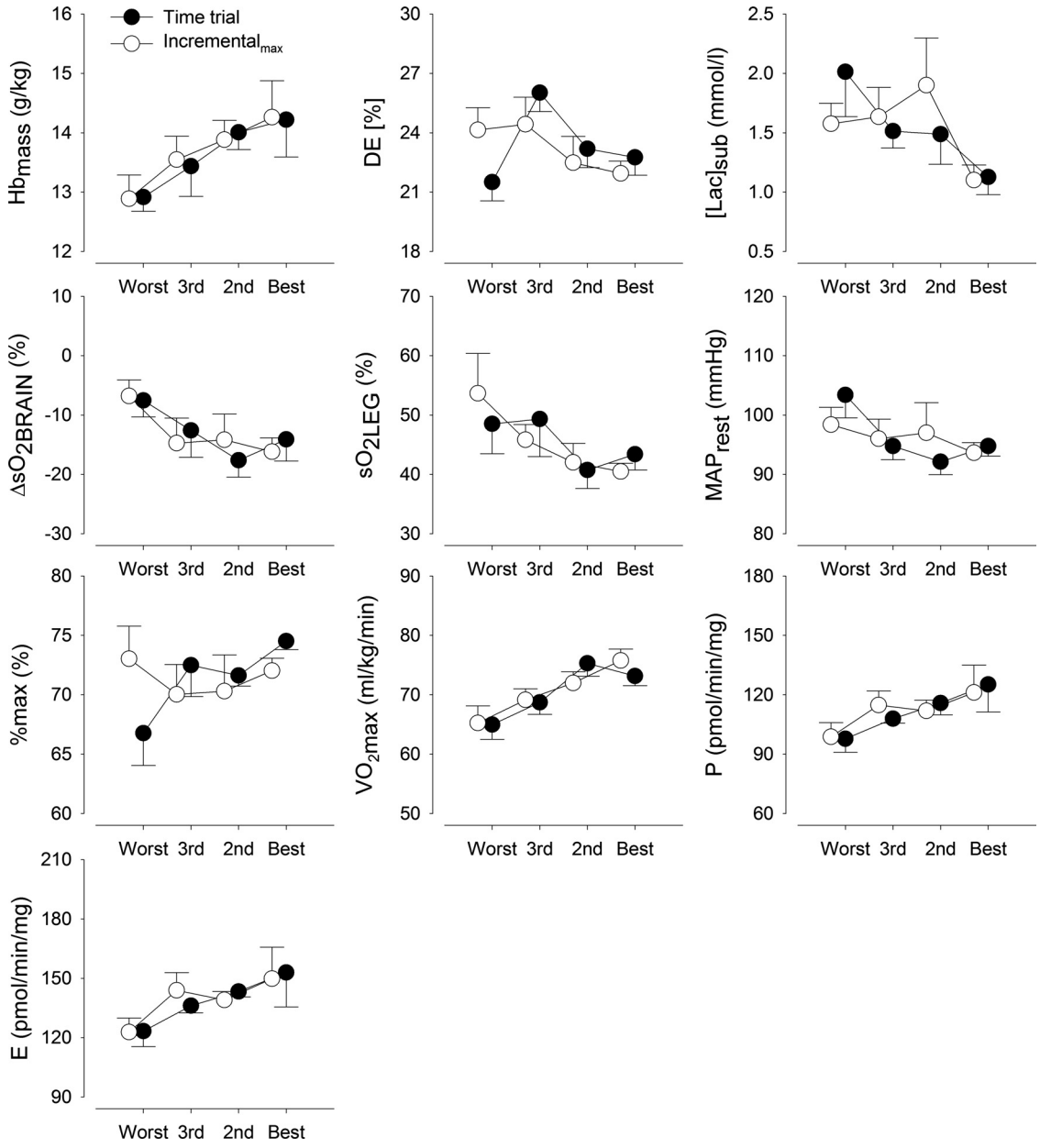

Fig. 1. Predictor variables correlation with exercise performance in highly trained cyclists. Ten principal factors of exercise performance (*y*-axis) plotted according to exercise performance ranked quartiles from worst to best (*x*-axis). Range of exercise performance (W/kg) in each quartile was 3.60–3.74, 3.91–4.14, 4.34–4.48, and 4.50–5.06 for worst to best average time trial power outputs (black circles); and 4.88–5.55, 5.79–5.88, 5.94–6.08, and 6.20–6.89 for worst to best maximal incremental power outputs (open circles). MAP_{rest}, resting mean arterial pressure; P, maximal oxidative phosphorylation capacity in skeletal muscle; E, electron transport system capacity in skeletal muscle; DE, percentage ratio of the change in work performed per minute (5 min at 150 W to 5 min at 200 W) to the change in energy expended per minute; sO_2, tissue oxygenation; ΔsO_2, changes in tissue oxygenation from rest to maximal exercise at the end of the incremental test; %max, workload during time trial as percent of maximal power output during the incremental test; Hb_{mass}, total body hemoglobin; $[Lac]_{sub}$, mean blood lactate concentrations during 5 min at 150 W and 5 min at 200 W; $\dot{V}O_{2max}$, maximal oxygen consumption. Data are presented as means ± SE.

Best two-parameter model included $\dot{V}O_{2max}$ ($r^2 = 0.69$, $P = 0.0005$). The best fit three-parameter model, 78% ($P = 0.0003$) of the variation in maximal incremental power output, could be explained by Hb_{mass} ($P = 0.0038$), $\dot{V}O_{2max}$ ($P = 0.0213$), and sO_{2LEG} ($P = 0.0463$).

Time Trial Performance

We performed multiple stepwise regression analysis on the selected parameters and mean power output during the time trial. This analysis revealed that for a single-parameter model the oxidative phosphorylation capacity of the skeletal muscle, P, provided the best fit ($r^2 = 0.47$, $P = 0.0035$). For a two-parameter model submaximal lactate concentration improved the fit significantly ($r^2 = 0.68$, $P = 0.0006$). Finally, for the best fit three-parameter model, 78% ($P = 0.0002$) of the variation in time trial performance could be explained by P ($P = 0.0005$), submaximal blood lactate concentrations ($P = 0.0017$), and the leg oxygenation (sO_{2LEG}) at exhaustion ($P = 0.0295$).

Overall Exercise Performance

Performance of our two functional tests of exercise capacity strongly correlated with one another. Average power output during the time trial correlated with maximal power output during the incremental exercise test ($r^2 = 0.82$, $P < 0.001$).

Finally, we performed cluster analyses on the correlation matrix between performance parameters and predictor variables. For this we included the 10 main predictors as well as 9 "second tier" variables last excluded by the principal factor analysis. We clustered variables on their correlation strength (Kendall's tau) with measures of aerobic performance, i.e., time trial mean power output and maximal incremental power output. This analysis revealed that overall exercise performance positively correlates best (Fig. 1) with parameters of oxygen transport ($\dot{V}O_{2max}$, Hb_{mass}), extraction (sO_{2LEG}), and skeletal muscle oxidative capacity (both P and electron transport system capacity, E).

DISCUSSION

This study presents several main findings regarding specific determinants of exercise performance: *1*) Hb_{mass} correlates the strongest with maximal incremental power output; *2*) maximal oxidative phosphorylation capacity of the skeletal muscle, P, is the strongest determining factor relating to 26-km time trial performance; and *3*) primary factors determining overall (time trial and maximal incremental power output) include measures regarding the capability for oxygen transport, high $\dot{V}O_{2max}$ and Hb_{mass}, in addition to measures of oxygen utilization, P and electron transport system capacities, E, in the skeletal muscle.

Maximal Incremental Power Output

Overall, 78% of the variance in maximal incremental power output was attributable to, in order of significance, Hb_{mass}, $\dot{V}O_{2max}$, and sO_{2LEG}. An individual's $\dot{V}O_{2max}$ establishes the upper limit of aerobic capacity and is a requirement for highly trained endurance capability (72, 74) with oxygen consumption proportion to exercise workload. This study confirms previous findings in showing that $\dot{V}O_{2max}$ is a significant correlate to maximal incremental power output. Convective limitations in oxygen delivery appear to be the primary physiological bottleneck of maximal oxygen consumption in humans (1, 4, 45). Maximal oxidative phosphorylation capacity, P, in the skeletal muscle has been shown to exceed the upper limit of oxygen delivery during whole body maximal exercise (8) and thus would not be expected as a significant correlate of maximal incremental whole body exercise. The results from the present study agree with and emphasize the importance of convective oxygen capacity for maximal exercise intensities. Hb_{mass} is the physiological factor that correlates the strongest to maximal incremental power output in highly trained endurance athletes accounting for 48% of the variation. This supports previous findings that have shown strong relationships between Hb_{mass} and $\dot{V}O_{2max}$ (28, 47, 61). While total blood volume is also understood to complement Hb_{mass} (47, 61, 77) we did not examine the correlation between total blood volume and maximal incremental power output. Of the variables we excluded from the potential 152 variables of interest, blood volume was among them because of its redundancy (high correlation inherently resulting from method of calculation) with Hb_{mass}. Convective transport of oxygen is also highly reliant on the pumping capacity of the heart as maximal cardiac output is understood to be a limiting factor at maximal workloads engaging a significant percentage of total body muscle mass (1, 52). As we did not directly assess cardiac output in the present study, high $\dot{V}O_{2max}$ values and the capacity for oxygen delivery to the leg are both indirectly indicative of high cardiac capacity and support maximal cardiac output as a dominant determinant in maximal aerobic power output. Cardiac output and leg blood flow both increase in parallel with an increase in work output (12, 76). Accordingly, although not directly measured, the significance of maximal cardiac output capacity is indirectly suggested as vital to maximal incremental power output in the present study.

The third strongest correlate to maximal incremental power output in the best fit three-parameter model was sO_{2LEG}. Muscle oxygen extraction increases with increasing workload during exercise (12). Maximal values of oxygen extraction averaging 91% have been observed in healthy cyclists during maximal exercise with values ranging from 87% to as high as 95% (27). As oxygen extraction is known to improve with training (73) the present study demonstrates its relation to maximal power output in highly trained athletes.

Time Trial Performance

The present study demonstrates that skeletal muscle oxidative capacity is the strongest correlate to exercise endurance among highly trained cyclists (average $\dot{V}O_{2max} = 70.53$ $ml \cdot kg^{-1} \cdot min^{-1}$; Table 1), accounting for 47% of the variation in 26-km time trial performance. This specific mitochondrial state, P, demonstrates the mitochondrial capacity to catalyze a sequential set of redox reactions that are partially coupled to the production of ATP via ATP synthase. Mitochondrial enzymes, content, volume density, and respiratory capacity all increase linearly in response to training (19, 23, 34–36, 83) and are elevated in trained vs. untrained counterparts (5, 23, 26, 37, 50, 51) as well as in moderate vs. highly trained athletes (17). Acute reduction of mitochondrial oxidative capacity limits maximal oxygen consumption in skeletal muscle (31, 62, 71). Exercise training has a direct dose response on endurance performance, skeletal muscle respiratory capacity, and mitochondrial markers in skeletal muscle of rats (23); however, these animals varied significantly in level of training, unlike the athletes in the present study. Homogeneous groups of athletes have displayed differences in exercise efficiency (75), lactate threshold, and endurance performance (16) without differences in static measurements of mitochondrial content. When normalizing mitochondrial respiratory rates to skeletal muscle CS concentration, respiratory differences between trained and untrained groups are ostensibly lost (23, 63). The present study differentiates the importance of dynamic mitochondrial properties (e.g., maximal oxidative phosphorylation and electron transport system capacities) on exercise performance as opposed to previously quantified static mitochondrial characteristics such as CS activity, which is used as a common measure of mitochondrial content. CS activity did not significantly correlate with time trial performance in the present study, highlighting the importance of functional mitochondrial analyses in combination with instantaneous "snap-shot" measurements of individual mitochondrial characteristics.

Submaximal arterial lactate concentrations, along with oxidative phosphorylation capacity, accounted for 68% of the variation in time trial performance. The ability to maintain a given workload with lower blood lactate concentrations correlates with endurance performance in trained individuals (17, 22, 53, 55, 70, 75) and this study confirms these results. World class cyclists have been reported to maintain blood lactate concentrations below 3 mM while cycling for 20 min at 80% of their maximal workload: ~86% of $\dot{V}O_{2max}$ (54). Despite similar aerobic capacities, cyclists with higher lactate thresholds were able to maintain exercise at 88% of their $\dot{V}O_{2max}$, which happened to be at a slightly higher absolute power output, for twice as long as those with comparatively low lactate thresholds (16). The single strongest predictor of performance has been repeatedly attributed to $\dot{V}O_{2max}$ percentage at lactate threshold (16, 55).

Trained individuals oxidize more fat and less carbohydrate than untrained counterparts at a given submaximal workload (10, 32). As the subjects who performed best on the 26-km time trial exercise test in the present study typically presented with, respectively, lower arterial lactate concentrations for a given submaximal workload (Fig. 1), those values did not, however, correlate with quantification of fat oxidation via respiratory exchange ratio values ($R^2 = 0.02$; data not presented). Furthermore, maximal octanoyl-carnitine stimulated respiration capacity, representative of the capacity for fatty acid oxidation and maximal electron flow through electron-transferring-flavoprotein dehydrogenase in the inner mitochondrial membrane, neither differed between subjects nor did values correlate with exercise performance. We included all relevant respiratory states in the factor analysis (1st step) and only used those that could contribute for a large part of the variation in the data set for the stepwise regression analysis (2nd step). Thus we did examine measures of maximal fat oxidative capacity in the analysis and they were not "significant" in relation to exercise performance. Thus the oxidative potential of the skeletal muscle can be thought to directly relate to blood lactate measurements more so than nutrient partitioning. More robust oxidative capacities in skeletal muscle limit the disproportionate increase in glycolytic flux at greater workloads. This, in turn, maintains a lower lactate concentration, as lactate production is more effectively matched by pathways of lactate disposal (84), explaining why skeletal muscle oxidative capacity and low arterial lactate concentrations, together, correlate well with time trial performance.

Human skeletal muscle respiratory capacity, more so than fiber type, corresponds with time to fatigue during short intensive exercise (41). Although fiber type is believed to be important to endurance performance as exercise efficiency has been primarily attributed to both percentage of type I fibers (18, 29, 38, 48, 63) along with concentration of uncoupling protein isotype 3 (63), it is the capillary density of the muscle that is directly proportional to the respiratory capacity of that muscle and not the fiber type (40). The importance of exercise efficiency and its role on exercise performance has oft been a topic of discussion (7, 15, 18, 38, 42, 43, 54, 64, 65). Suggested increases in efficiency of 1% has been proposed and to drop ~63 s off a 40-km time trial performance (43) while an 1.8% greater efficiency has shown to parallel a 9% improvement in work output obtained during a 1-h cycling performance test (38). However, most empirical evidence demonstrates no difference in efficiency between elite, trained, or novice athletes (7, 60, 64, 66, 82), denoting that exercise efficiency is not a predictor of endurance performance in elite level cycling (64). The present study calculated DE via two relatively low-intensity power outputs (150 and 200 W, corresponding to 50% and 63% $\dot{V}O_{2max}$, respectively). This may have introduced more variability in DE values compared with those if more measurements during steady-state exercise ranging from 50 to 90% $\dot{V}O_{2max}$ were collected. Regardless, this study confirms and supports previous findings as DE was not identified as a primary contributing physiological factor of endurance performance among a homogeneous group of highly trained athletes.

The third strongest correlate with time trial performance was sO_{2LEG} as the stronger athletes were able to reduce tissue oxygenation the greatest (Fig. 1). Oxygen extraction significantly correlates with oxygen consumption over various workloads (13) and oxidative capacity in the skeletal muscle has been proposed to assist in facilitating the extraction of oxygen during exercise (13). Measurement of sO_{2LEG} was the only variable strongly predictive of both maximal incremental power output and time trial performance. The relationship between oxygen extraction and oxidative capacity of the muscle is not well understood and requires further investigation.

Overall Exercise Performance

This study demonstrated a high correlation of performance between exercise tests in highly trained athletes. Maximal incremental power output and time trial performance are strongly correlated to one another ($r^2 = 0.82$, $P < 0.001$). Peak power output obtained in these subjects during an all-out 30-s sprint was also significantly correlated to maximal incremental power outputs and time trial performance ($P < 0.01$, data not shown). Peak power output has been reported to correlate highly with time trial performance (30) but seemingly more so with average power output than time to completion of a time trial (3). Although percent of maximal power output averaged during time trial was 1 of the 10 best correlates of exercise performance in the present study (Fig. 1), other variables were observed to have stronger validity as determinants of exercise performance.

The physiological variables most predictive of overall exercise performance included parameters relating to both the transport of oxygen and the capacity for cellular oxygen utilization (Fig. 1). These data support other studies identifying the collective importance of oxygen delivery and oxidative capacity in regulating oxygen flux (31). The cluster analysis supports regression analyses, as both P and E were strongly predictive of overall exercise performance in highly trained athletes along with $\dot{V}O_{2max}$ and Hb_{mass}. In the specific mitochondrial state E, inner mitochondrial membrane potential is collapsed with an open transmembrane proton circuit and thus serves as an indication of mitochondrial membrane potential (25, 67). As the transport of oxygen to the working skeletal muscle during exercise is firmly recognized as an essential factor determining performance, this study develops our understanding of the limitations to exercise performance in highly trained athletes by illustrating the importance coupling a high oxygen transport capacity with an equally sizable ability for cellular oxygen utilization.

Conclusion

In summary, this study identified several individual and specific physiological variables detailing the determinants of exercise capacity in highly trained cyclists. The primary predictors for time trial performance and maximal incremental power output are skeletal muscle oxidative phosphorylation capacity, P, and Hb_{mass}, respectively. Overall exercise performance is strongly attributed to means of oxygen transport (Hb_{mass}), ability to extract oxygen in the skeletal muscle (sO_{2LEG}), and the capacity for oxygen utilization within the muscle (P, E).

ACKNOWLEDGMENTS

We acknowledge Orobos (Innsbruck, Austria) for making valuable equipment at our disposal during the study period.

GRANTS

This study was funded through grants obtained from the Bundes Amt für Sport (BASPO, Switzerland), Team Denmark (Denmark), and Institut National du Sport, de l'Expertise et de la Performance (INSEP, France).

DISCLOSURES

E. Gnaiger is the founder and managing director of Orobos Instruments, high-resolution respirometry, Scharpfstrasse 18, A-6020 Innsbruck, Austria.

REFERENCES

1. **Andersen P, Saltin B.** Maximal perfusion of skeletal muscle in man. *J Physiol* 366: 233–249, 1985.
2. **Baldwin KM, Klinkerfuss GH, Terjung RL, Mole PA, Holloszy JO.** Respiratory capacity of white, red, and intermediate muscle: adaptative response to exercise. *Am J Physiol* 222: 373–378, 1972.
3. **Balmer J, Davison RC, Bird SR.** Peak power predicts performance power during an outdoor 16.1-km cycling time trial. *Med Sci Sports Exerc* 32: 1485–1490, 2000.
4. **Bassett DR Jr, Howley ET.** Limiting factors for maximum oxygen uptake and determinants of endurance performance. *Med Sci Sports Exerc* 32: 70–84, 2000.
5. **Befroy DE, Petersen KF, Dufour S, Mason GF, Rothman DL, Shulman GI.** Increased substrate oxidation and mitochondrial uncoupling in skeletal muscle of endurance-trained individuals. *Proc Natl Acad Sci USA* 105: 16701–16706, 2008.
6. **Bergstrom J.** Muscle electrolytes in man. *Scand J Clin Lab Invest* 68: 1–110, 1962.
7. **Boning D, Gonen Y, Maassen N.** Relationship between work load, pedal frequency, and physical fitness. *Int J Sports Med* 5: 92–97, 1984.
8. **Boushel R, Gnaiger E, Calbet JA, Gonzalez-Alonso J, Wright-Paradis C, Sondergaard H, Ara I, Helge JW, Saltin B.** Muscle mitochondrial capacity exceeds maximal oxygen delivery in humans. *Mitochondrion* 11: 303–307, 2011.
9. **Brooks GA.** Anaerobic threshold: review of the concept and directions for future research. *Med Sci Sports Exerc* 17: 22–34, 1985.
10. **Brooks GA, Mercier J.** Balance of carbohydrate and lipid utilization during exercise: the "crossover" concept. *J Appl Physiol* 76: 2253–2261, 1994.
11. **Burge CM, Skinner SL.** Determination of hemoglobin mass and blood volume with CO: evaluation and application of a method. *J Appl Physiol* 79: 623–631, 1995.
12. **Calbet JA, Gonzalez-Alonso J, Helge JW, Sondergaard H, Munch-Andersen T, Boushel R, Saltin B.** Cardiac output and leg and arm blood flow during incremental exercise to exhaustion on the cycle ergometer. *J Appl Physiol* 103: 969–978, 2007.
13. **Calbet JA, Holmberg HC, Rosdahl H, van Hall G, Jensen-Urstad M, Saltin B.** Why do arms extract less oxygen than legs during exercise? *Am J Physiol Regul Integr Comp Physiol* 289: R1448–R1458, 2005.
14. **Conley DL, Krahenbuhl GS.** Running economy and distance running performance of highly trained athletes. *Med Sci Sports Exerc* 12: 357–360, 1980.
15. **Coyle EF.** Physiological determinants of endurance exercise performance. *J Sci Med Sport* 2: 181–189, 1999.
16. **Coyle EF, Coggan AR, Hopper MK, Walters TJ.** Determinants of endurance in well-trained cyclists. *J Appl Physiol* 64: 2622–2630, 1988.
17. **Coyle EF, Feltner ME, Kautz SA, Hamilton MT, Montain SJ, Baylor AM, Abraham LD, Petrek GW.** Physiological and biomechanical factors associated with elite endurance cycling performance. *Med Sci Sports Exerc* 23: 93–107, 1991.
18. **Coyle EF, Sidossis LS, Horowitz JF, Beltz JD.** Cycling efficiency is related to the percentage of type I muscle fibers. *Med Sci Sports Exerc* 24: 782–788, 1992.
19. **Daussin FN, Zoll J, Ponsot E, Dufour SP, Doutreleau S, Lonsdorfer E, Ventura-Clapier R, Mettauer B, Piquard F, Geny B, Richard R.** Training at high exercise intensity promotes qualitative adaptations of mitochondrial function in human skeletal muscle. *J Appl Physiol* 104: 1436–1441, 2008.
20. **Dill DB, Edwards HT, Talbott JH.** Studies in muscular activity. VII. Factors limiting the capacity for work. *J Physiol* 77: 49–62, 1932.
21. **Esaki K, Hamaoka T, Radegran G, Boushel R, Hansen J, Katsumura T, Haga S, Mizuno M.** Association between regional quadriceps oxygenation and blood oxygen saturation during normoxic one-legged dynamic knee extension. *Eur J Appl Physiol* 95: 361–370, 2005.
22. **Farrell PA, Wilmore JH, Coyle EF, Billing JE, Costill DL.** Plasma lactate accumulation and distance running performance. *Med Sci Sports* 11: 338–344, 1979.
23. **Fitts RH, Booth FW, Winder WW, Holloszy JO.** Skeletal muscle respiratory capacity, endurance, and glycogen utilization. *Am J Physiol* 228: 1029–1033, 1975.
24. **Gladden LB.** Lactate metabolism: a new paradigm for the third millennium. *J Physiol* 558: 5–30, 2004.
25. **Gnaiger E.** Capacity of oxidative phosphorylation in human skeletal muscle: new perspectives of mitochondrial physiology. *Int J Biochem Cell Biol* 41: 1837–1845, 2009.
26. **Gollnick PD, Armstrong RB, Saubert CWt Piehl K, Saltin B.** Enzyme activity and fiber composition in skeletal muscle of untrained and trained men. *J Appl Physiol* 33: 312–319, 1972.
27. **Gonzalez-Alonso J, Calbet JA.** Reductions in systemic and skeletal muscle blood flow and oxygen delivery limit maximal aerobic capacity in humans. *Circulation* 107: 824–830, 2003.
28. **Gore CJ, Hahn AG, Burge CM, Telford RD.** $\dot{V}O_{2max}$ and haemoglobin mass of trained athletes during high intensity training. *Int J Sports Med* 18: 477–482, 1997.
29. **Hansen EA, Andersen JL, Nielsen JS, Sjogaard G.** Muscle fibre type, efficiency, and mechanical optima affect freely chosen pedal rate during cycling. *Acta Physiol Scand* 176: 185–194, 2002.
30. **Hawley JA, Noakes TD.** Peak power output predicts maximal oxygen uptake and performance time in trained cyclists. *Eur J Appl Physiol Occup Physiol* 65: 79–83, 1992.
31. **Hepple RT, Hagen JL, Krause DJ.** Oxidative capacity interacts with oxygen delivery to determine maximal O_2 uptake in rat skeletal muscles in situ. *J Physiol* 541: 1003–1012, 2002.
32. **Hermansen L, Hultman E, Saltin B.** Muscle glycogen during prolonged severe exercise. *Acta Physiol Scand* 71: 129–139, 1967.
33. **Hill AV, Lupton H.** Muscular exercise, lactic acid, and the supply and utilization of oxygen. *Q J Med* 16: 135–171, 1923.
34. **Holloszy JO.** Biochemical adaptations in muscle. Effects of exercise on mitochondrial oxygen uptake and respiratory enzyme activity in skeletal muscle. *J Biol Chem* 242: 2278–2282, 1967.
35. **Holloszy JO, Rennie MJ, Hickson RC, Conlee RK, Hagberg JM.** Physiological consequences of the biochemical adaptations to endurance exercise. *Ann NY Acad Sci* 301: 440–450, 1977.
36. **Hoppeler H, Howald H, Conley K, Lindstedt SL, Claassen H, Vock P, Weibel ER.** Endurance training in humans: aerobic capacity and structure of skeletal muscle. *J Appl Physiol* 59: 320–327, 1985.
37. **Hoppeler H, Luthi P, Claassen H, Weibel ER, Howald H.** The ultrastructure of the normal human skeletal muscle. A morphometric analysis on untrained men, women and well-trained orienteers. *Pflügers Arch* 344: 217–232, 1973.
38. **Horowitz JF, Sidossis LS, Coyle EF.** High efficiency of type I muscle fibers improves performance. *Int J Sports Med* 15: 152–157, 1994.
39. **Iaia FM, Thomassen M, Kolding H, Gunnarsson T, Wendell J, Rostgaard T, Nordsborg N, Krustrup P, Nybo L, Hellsten Y, Bangsbo J.** Reduced volume but increased training intensity elevates muscle Na^+-K^+ pump alpha1-subunit and NHE1 expression as well as short-term work capacity in humans. *Am J Physiol Regul Integr Comp Physiol* 294: R966–R974, 2008.

40. **Ingjer F.** Effects of endurance training on muscle fibre ATP-ase activity, capillary supply and mitochondrial content in man. *J Physiol* 294: 419–432, 1979.
41. **Ivy JL, Sherman WM, Miller JM, Maxwell BD, Costill DL.** Relationship between muscle QO_2 and fatigue during repeated isokinetic contractions. *J Appl Physiol* 53: 470–474, 1982.
42. **Jeukendrup A, Martin DT, Gore CJ.** Are world-class cyclists really more efficient? *Med Sci Sports Exerc* 35: 1238–1239; discussion 1240–1231, 2003.
43. **Jeukendrup AE, Martin J.** Improving cycling performance: how should we spend our time and money. *Sports Med* 31: 559–569, 2001.
44. **Joyner MJ.** Modeling: optimal marathon performance on the basis of physiological factors. *J Appl Physiol* 70: 683–687, 1991.
45. **Joyner MJ, Coyle EF.** Endurance exercise performance: the physiology of champions. *J Physiol* 586: 35–44, 2008.
46. **Joyner MJ, Ruiz JR, Lucia A.** The two-hour marathon: who and when? *J Appl Physiol* 110: 275–277, 2011.
47. **Kanstrup IL, Ekblom B.** Blood volume and hemoglobin concentration as determinants of maximal aerobic power. *Med Sci Sports Exerc* 16: 256–262, 1984.
48. **Krustrup P, Secher NH, Relu MU, Hellsten Y, Soderlund K, Bangsbo J.** Neuromuscular blockade of slow twitch muscle fibres elevates muscle oxygen uptake and energy turnover during submaximal exercise in humans. *J Physiol* 586: 6037–6048, 2008.
49. **Kuznetsov AV, Schneeberger S, Seiler R, Brandacher G, Mark W, Steurer W, Saks V, Usson Y, Margreiter R, Gnaiger E.** Mitochondrial defects and heterogeneous cytochrome c release after cardiac cold ischemia and reperfusion. *Am J Physiol Heart Circ Physiol* 286: H1633–H1641, 2004.
50. **Lanza IR, Short DK, Short KR, Raghavakaimal S, Basu R, Joyner MJ, McConnell JP, Nair KS.** Endurance exercise as a countermeasure for aging. *Diabetes* 57: 2933–2942, 2008.
51. **Larsen RG, Callahan DM, Foulis SA, Kent-Braun JA.** In vivo oxidative capacity varies with muscle and training status in young adults. *J Appl Physiol* 107: 873–879, 2009.
52. **Levine BD.** $\dot{V}O_{2max}$: what do we know, and what do we still need to know? *J Physiol* 586: 25–34, 2008.
53. **Lorenzo S, Minson CT, Babb TG, Halliwill JR.** Lactate threshold predicting time-trial performance: impact of heat and acclimation. *J Appl Physiol* 111: 221–227, 2011.
54. **Lucia A, Hoyos J, Perez M, Santalla A, Chicharro JL.** Inverse relationship between $\dot{V}O_{2max}$ and economy/efficiency in world-class cyclists. *Med Sci Sports Exerc* 34: 2079–2084, 2002.
55. **Lucia A, Hoyos J, Perez M, Santalla A, Earnest CP, Chicharro JL.** Which laboratory variable is related with time trial performance time in the Tour de France? *Br J Sports Med* 38: 636–640, 2004.
56. **Lundby C, Thomsen JJ, Boushel R, Koskolou M, Warberg J, Calbet JA, Robach P.** Erythropoietin treatment elevates haemoglobin concentration by increasing red cell volume and depressing plasma volume. *J Physiol* 578: 309–314, 2007.
57. **Lusk G.** *The Elements of the Science of Nutrition*. New York: Saunders, 1919.
58. **Mahood NV, Kenefick RW, Kertzer R, Quinn TJ.** Physiological determinants of cross-country ski racing performance. *Med Sci Sports Exerc* 33: 1379–1384, 2001.
59. **Mannion AF, Jakeman PM, Willan PL.** Determination of human skeletal muscle buffer value by homogenate technique: methods of measurement. *J Appl Physiol* 75: 1412–1418, 1993.
60. **Marsh AP, Martin PE, Foley KO.** Effect of cadence, cycling experience, and aerobic power on delta efficiency during cycling. *Med Sci Sports Exerc* 32: 1630–1634, 2000.
61. **Martino M, Gledhill N, Jamnik V.** High $\dot{V}O_{2max}$ with no history of training is primarily due to high blood volume. *Med Sci Sports Exerc* 34: 966–971, 2002.
62. **McAllister RM, Terjung RL.** Acute inhibition of respiratory capacity of muscle reduces peak oxygen consumption. *Am J Physiol Cell Physiol* 259: C889–C896, 1990.
63. **Mogensen M, Bagger M, Pedersen PK, Fernstrom M, Sahlin K.** Cycling efficiency in humans is related to low UCP3 content and to type I fibres but not to mitochondrial efficiency. *J Physiol* 571: 669–681, 2006.
64. **Moseley L, Achten J, Martin JC, Jeukendrup AE.** No differences in cycling efficiency between world-class and recreational cyclists. *Int J Sports Med* 25: 374–379, 2004.
65. **Moseley L, Jeukendrup AE.** The reliability of cycling efficiency. *Med Sci Sports Exerc* 33: 621–627, 2001.
66. **Nickleberry BL Jr, Brooks GA.** No effect of cycling experience on leg cycle ergometer efficiency. *Med Sci Sports Exerc* 28: 1396–1401, 1996.
67. **Pesta D, Gnaiger E.** High-resolution respirometry. OXPHOS protocols for human cell cultures and permeabilized fibres from small biopsies of human muscle. In: *Mitochondrial Bioenergetics: Methods and Protocols*, edited by Palmeira C, Moreno A. New York: Humana, 2011, p. 1–24, 2011.
68. **Pesta D, Hoppel F, Macek C, Messner H, Faulhaber M, Kobel C, Parson W, Burtscher M, Schocke M, Gnaiger E.** Similar qualitative and quantitative changes of mitochondrial respiration following strength and endurance training in normoxia and hypoxia in sedentary humans. *Am J Physiol Regul Integr Comp Physiol* in press: 2011.
69. **Rasmussen P, Dawson EA, Nybo L, van Lieshout JJ, Secher NH, Gjedde A.** Capillary-oxygenation-level-dependent near-infrared spectrometry in frontal lobe of humans. *J Cereb Blood Flow Metab* 27: 1082–1093, 2007.
70. **Ribeiro JP, Cadavid E, Baena J, Monsalvete E, Barna A, De Rose EH.** Metabolic predictors of middle-distance swimming performance. *Br J Sports Med* 24: 196–200, 1990.
71. **Robinson DM, Ogilvie RW, Tullson PC, Terjung RL.** Increased peak oxygen consumption of trained muscle requires increased electron flux capacity. *J Appl Physiol* 77: 1941–1952, 1994.
72. **Robinson S, Edwards HT, Dill DB.** New records in human power. *Science* 85: 409–410, 1937.
73. **Roca J, Agusti AG, Alonso A, Poole DC, Viegas C, Barbera JA, Rodriguez-Roisin R, Ferrer A, Wagner PD.** Effects of training on muscle O2 transport at $\dot{V}O_{2max}$. *J Appl Physiol* 73: 1067–1076, 1992.
74. **Saltin B, Astrand PO.** Maximal oxygen uptake in athletes. *J Appl Physiol* 23: 353–358, 1967.
75. **Saltin B, Kim CK, Terrados N, Larsen H, Svedenhag J, Rolf CJ.** Morphology, enzyme activities and buffer capacity in leg muscles of Kenyan and Scandinavian runners. *Scand J Med Sci Sports* 5: 222–230, 1995.
76. **Saltin B, Radegran G, Koskolou MD, Roach RC.** Skeletal muscle blood flow in humans and its regulation during exercise. *Acta Physiol Scand* 162: 421–436, 1998.
77. **Schmidt W, Prommer N.** Impact of alterations in total hemoglobin mass on $\dot{V}O_{2max}$. *Exerc Sport Sci Rev* 38: 68–75, 2010.
78. **Schuler B, Thomsen JJ, Gassmann M, Lundby C.** Timing the arrival at 2340 m altitude for aerobic performance. *Scand J Med Sci Sports* 17: 588–594, 2007.
79. **Sharp RL, Costill DL, Fink WJ, King DS.** Effects of eight weeks of bicycle ergometer sprint training on human muscle buffer capacity. *Int J Sports Med* 7: 13–17, 1986.
81. **Srere PA.** Citrate synthase. *Methods Enzymol* 13: 3–11, 1969.
82. **Stuart MK, Howley ET, Gladden LB, Cox RH.** Efficiency of trained subjects differing in maximal oxygen uptake and type of training. *J Appl Physiol* 50: 444–449, 1981.
83. **Turner DL, Hoppeler H, Claassen H, Vock P, Kayser B, Schena F, Ferretti G.** Effects of endurance training on oxidative capacity and structural composition of human arm and leg muscles. *Acta Physiol Scand* 161: 459–464, 1997.
84. **Van Hall G, Jensen-Urstad M, Rosdahl H, Holmberg HC, Saltin B, Calbet JA.** Leg and arm lactate and substrate kinetics during exercise. *Am J Physiol Endocrinol Metab* 284: E193–E205, 2003.
85. **Weibel ER, Hoppeler H.** Exercise-induced maximal metabolic rate scales with muscle aerobic capacity. *J Exp Biol* 208: 1635–1644, 2005.

J Appl Physiol 114: 344–350, 2013.
First published December 6, 2012; doi:10.1152/japplphysiol.01081.2012.

Mitochondria express enhanced quality as well as quantity in association with aerobic fitness across recreationally active individuals up to elite athletes

Robert A. Jacobs[1,2,3] and Carsten Lundby[1,3]

[1]*Zurich Center for Integrative Human Physiology, Zurich, Switzerland;* [2]*Institute of Veterinary Physiology, Vetsuisse Faculty, University of Zurich, Zurich, Switzerland; and* [3]*Institute of Physiology, University of Zurich, Zurich, Switzerland*

Submitted 5 September 2012; accepted in final form 30 November 2012

Jacobs RA, Lundby C. Mitochondria express enhanced quality as well as quantity in association with aerobic fitness across recreationally active individuals up to elite athletes. *J Appl Physiol* 114: 344–350, 2013. First published December 6, 2012; doi:10.1152/japplphysiol.01081.2012.—Changes in skeletal muscle respiratory capacity parallel that of aerobic fitness. It is unknown whether mitochondrial content, alone, can fully account for these differences in skeletal muscle respiratory capacity. The aim of the present study was to examine quantitative and qualitative mitochondrial characteristics across four different groups ($n = 6$ each), separated by cardiorespiratory fitness. High-resolution respirometry was performed on muscle samples to compare respiratory capacity and efficiency in active, well-trained, highly trained, and elite individuals. Maximal exercise capacity (ml $O_2 \cdot min^{-1} \cdot kg^{-1}$) differed across all groups, with mean ± SD values of 51 ± 4, 64 ± 5, 71 ± 2, and 77 ± 3, respectively. Mitochondrial content assessed by citrate synthase activity was higher in elite trained compared with active and well-trained (29 ± 7 vs. 16 ± 4 and 19 ± 4 $nmol \cdot min^{-1} \cdot mg\ wet\ wt^{-1}$, respectively). When normalizing respiration to mitochondrial content, the respiratory capacities during maximal fatty acid oxidation ($P = 0.003$), maximal state 3 respiration ($P = 0.021$), and total electron transport system capacity ($P = 0.008$) improved with respect to maximal exercise capacity. The coupling efficiency of β-oxidation, however, expressed no difference across groups. These data demonstrate the quantitative and qualitative differences that exist in skeletal muscle mitochondrial respiratory capacity and efficiency across individuals that differ in aerobic capacity. Mitochondrial-specific respiration capacities during β-oxidation, maximal oxidative phosphorylation, and electron transport system capacity all correspondingly improve with aerobic capacity, independent of mitochondrial content in human skeletal muscle.

exercise; skeletal muscle; fat oxidation

MEASURES OF WHOLE BODY CARDIORESPIRATORY fitness ostensibly represent the state of health in humans (1, 12, 24–26, 31, 34). Although maximal aerobic capacity is primarily limited by the oxygen transport system (3, 44), i.e., maximal cardiac output and oxygen-carrying capacity of the blood, mitochondrial content (7, 18) and skeletal muscle respiratory capacity (9) both also share a strong positive correlation with maximal aerobic capacity in humans. Morphometric examination and analysis of biochemical expression show that mitochondrial density and content increase in response to training (15, 16, 18) and differ between untrained and trained individuals (20, 28, 33, 46). Skeletal muscle oxidative capacity also increases with training (36) and varies across groups differing in activity level (28, 33, 46). There is debate whether the increase in skeletal muscle respiration capacity that parallels aerobic fitness can be explained by quantitative differences in mitochondrial content alone (41, 45), or whether qualitative adaptations, such as functional modifications in respiratory control and capacity, also improve along with whole body aerobic capacity (13).

We previously determined that mitochondrial respiratory capacity, particularly oxidative phosphorylation capacity (P) and electron transport system capacity (ETS), are strongly predictive of overall exercise capacity in highly trained athletes (22). Over many other physiological variables, including total hemoglobin mass and cerebral oxygenation, P, exclusively, was identified as the strongest determinant of endurance performance (22). Mitochondrial content does not always differ between individuals who display significantly different exercise capacities (38, 40), and yet skeletal muscle P is the strongest predictor of endurance performance (22). Moreover, prolonged exposure to hypoxia can diminish respiratory capacity and enhance mitochondrial coupling efficiency, independent from any change in mitochondrial content (23). Together, these data suggest that qualitative differences in mitochondria may exist independent from mitochondrial content.

Previous reported differences in skeletal muscle mitochondria respiratory capacity across groups that differed in level of cardiorespiratory fitness did not control for the significant variation in mitochondrial content between the groups (33, 46). No study has compared functional differences in mitochondria between normal, healthy individuals vs. elite athletes. The aim of this study is to analyze mitochondrial differences, both quantitative and qualitative, across four different groups of healthy and physically active subjects who differ in aerobic capacity. As P is the strongest determining factor in endurance performance (22) among a more homogenous group of athletes with negligible differences in mitochondrial content (38), we hypothesize that differences in mitochondria from AT to ET individuals will possess distinct qualitative differences.

METHODS

Ethical Approval

All experimental protocols involving human subjects were approved by the Eidgenössische Technische Hochschule Zürich for Kanton Zurich (2010–066/0 and EK 2011-N-51) and Kanton Vaud (215/10), Switzerland, in accordance with the declaration of Helsinki. Before the start of the experiments, informed oral and written consents were obtained from all participants.

Subjects and Experimental Design

Subject characteristics are shown in Table 1. Twenty-four young and physically active subjects (23 men and 1 woman) voluntarily participated in this study. No subjects were taking any prescription medications nor had any known family history of type 2 diabetes, severe obesity, or cardiovascular diseases. Previous studies

Address for reprint requests and other correspondence: R. A. Jacobs, Institute of Veterinary Physiology, Vetsuisse Faculty and Zurich Center for Integrative Human Physiology (ZIHP), Winterthurerstrasse 190, CH-8057 Zurich, Switzerland (e-mail: jacobs@vetphys.uzh.ch).

Table 1. *Subject characteristics*

Group	Age, yr	Height, cm	Weight, kg	Absolute $\dot{V}O_{2max}$, l/min	Absolute W_{max}, W	Relative W_{max}, W/kg	Years of Exercise	Time Training/Year, h	Time Training/Week, h
AT	26 ± 4	181 ± 5	77 ± 5	3.96 ± 0.39	326 ± 27	4.2 ± 0.4	8.8 ± 5.6	190 ± 88[b,c,d]	3.7 ± 1.7[b,c,d]
WT	32 ± 8	180 ± 7	73 ± 10	4.68 ± 0.60	378 ± 59	5.2 ± 0.5[a]	13.9 ± 5.3	493 ± 141[a,d]	9.5 ± 2.7[a,d,g]
HT	28 ± 2	175 ± 7	68 ± 10	4.82 ± 0.67[e]	389 ± 45	5.8 ± 0.3[a,f]	9 ± 4.8	636 ± 43[a,d]	12.3 ± 0.8[a,d,f]
ET	28 ± 6	179 ± 8	68 ± 6	5.24 ± 0.52[a]	417 ± 41[a]	6.2 ± 0.3[a,b]	16 ± 6.2	847 ± 126[a,b,c]	16.4 ± 2.6[a,b,c]

Physiological characteristics for all subjects ($n = 24$) are means ± SD. AT, active subjects ($n = 6$); WT, well-trained subjects ($n = 6$); HT, highly trained subjects ($n = 6$); ET, elite athletes ($n = 6$); $\dot{V}O_{2max}$, maximal oxygen consumption; W_{max}, maximal power output. Difference ($P < 0.05$) from [a]AT, [b]WT, [c]HT, and [d]ET. Tendency of difference ($0.05 < P < 0.1$) from [e]AT, [f]WT, [g]HT, and [h]ET.

show no main effect of sex on skeletal muscle oxidative capacity and, consequently, grouped all data according to training status (28, 33, 46), as we have done in the present study. We divided the 24 subjects into four different tiers, dependent on their aerobic capacity: active (AT), well-trained (WT), highly trained (HT), and elite (ET). The AT group performed physical activity or sport (climbing, mountain biking, tennis, karate, road cycling, hockey, skating, running, swimming, or tour skiing) sporadically for an average of 1.58 days/wk, with no regular routine; the WT group participated in some variation of a regular exercise or sport program (climbing, running, Thai boxing, or road cycling) for an average of 2.46 days out of the week; and HT and ET athletes engaged in endurance exercise (triathlon training or road/mountain/cyclo-cross cycling and road or mountain cycling for HT and ET, respectively) on average for 2.49 and 2.81 days/wk, respectively. All individuals were separated into their respective groups based on aerobic capacities, which were obtained via tests of maximal oxygen consumption ($\dot{V}O_{2\,max}$).

Exercise Tests

Exercise tests to obtain values of $\dot{V}O_{2\,max}$ were completed on an electronically braked cycle ergometer (Monark, Varberg, Sweden). The exercise protocol started with a 5-min collection of resting oxygen consumption ($\dot{V}O_2$), followed by two consecutive absolute submaximal workloads, 100 W and 150 W, which were maintained for 5 min each. Thereafter, the workload increased 25 W/min until voluntary exhaustion. During the last minutes of the test, subjects were vigorously encouraged to perform to complete exhaustion, and the achievement of $\dot{V}O_{2\,max}$ was established by standard criteria in all tests (2). Subjects wore a face mask covering their mouth and nose for breath collection (Hans Rudolph, Kansas City, MO), and O_2 and CO_2 concentration in the expired gas was continuously measured and monitored as breath-by-breath values (Quark, Cosmed, Rome, Italy and Innocor, Innovision, Odense, Denmark). The gas analyzers and flowmeters of each applied spirometer were calibrated before each test.

Skeletal Muscle Sampling

Skeletal muscle biopsies were obtained from the *m. vastus lateralis* under local anesthesia (1% lidocaine) of the skin and superficial muscle fascia, using the Bergström technique (6), with a needle modified for suction at rest in the morning, and in a fasted state at least 24 h after the last bout of exercise. The biopsy was immediately dissected free of fat and connective tissue and divided into sections for measurements of mitochondrial respiration.

Skeletal Muscle Preparation

The skeletal muscle samples were sectioned into parts to measure mitochondrial respiration. Each part was immediately placed in ice-cold biopsy preservation solution (BIOPS) containing 2.77 mM CaK_2EGTA buffer, 7.23 mM K_2EGTA buffer, 0.1 μM free calcium, 20 mM imidazole, 20 mM taurine, 50 mM 2-(*N*-morpholino)ethanesulfonic acid hydrate, 0.5 mM dithiothreitol, 6.56 mM $MgCl_2{\cdot}6H_2O$, 5.77 mM ATP, and 15 mM phosphocreatine (pH 7.1). Muscle samples were then gently dissected with the tip of two 18-gauge needles, achieving a high degree of fiber separation verified microscopically. Chemical permeabilization followed via incubation in 2 ml of BIOPS with saponin (50 μg/ml) for 30 min in 4°C (27). Lastly, samples were washed with a mitochondrial respiration medium (MiR05) containing 0.5 mM EGTA, 3 mM $MgCl_2{\cdot}6H_2O$, 60 mM potassium-lactobionate, 20 mM taurine, 10 mM KH_2P0_4, 20 mM HEPES, 110 mM sucrose, and 1 g/l bovine serum albumin (pH 7.1) for 10 min in 4°C.

Mitochondrial Respiration Measurements

Muscle bundles were blotted dry and measured for wet weight in a balance-controlled scale (XS205 DualRange Analytical Balance, Mettler-Toledo), maintaining constant relative humidity and providing hydration consistency as well as stability of weight measurements. Respiration measurements were performed in mitochondrial respiration medium 06 (MiR05 + catalase 280 IU/ml). Measurements of $\dot{V}O_2$ were performed at 37°C using the high-resolution Oxygraph-2k (Oroboros, Innsbruck, Austria) with all additions of each substrate, uncoupler, and inhibitor titration (SUIT) protocol added in series. Standardized instrumental were performed to correct for back-diffusion of oxygen into the chamber from the various components, leak from the exterior, $\dot{V}O_2$ by the chemical medium, and sensor $\dot{V}O_2$. Oxygen flux was resolved by software allowing nonlinear changes in the negative time derivative of the oxygen concentration signal (Oxygraph 2k, Oroboros, Innsbruck, Austria). All experiments were carried out in a hyperoxygenated environment to prevent any potential oxygen diffusion limitation.

Respiratory Titration Protocol

The SUIT protocol applied in the study has been previously described (22). The protocol was specific to the examination of individual aspects of respiratory control through a sequence of coupling and substrate states induced via separate titrations. All respirometric analyses were made in duplicates, and all titrations were added in series as presented. The concentrations of substrates, uncouplers, and inhibitors used were based on prior experiments conducted for optimization of the titration protocols. Leak respiration in absence of adenylates (L_N) was induced with the addition of malate (2 mM) and octanoyl carnitine (0.2 mM). The L_N state represents the resting $\dot{V}O_2$ of an unaltered and intact electron transport system free of adenylates. Maximal electron flow through electron transferring-flavoprotein (ETF) and fatty acid oxidative capacity (P_{ETF}) were both determined following the addition of ADP (5 mM). In the P_{ETF} state, the ETF linked transfer of electrons requires the metabolism of acetyl-CoA, hence the addition of malate, to facilitate convergent electron flow into the Q-junction from both complex I (C1) and ETF, allowing β-oxidation to proceed. The contribution of electron flow through C1 is far below capacity, and so here the rate-limiting metabolic branch is electron transport through ETF, such that malate + octanoyl carnitine + ADP-stimulated respiration is representative of, rather than specific to, electron capacity through ETF (11, 13, 35, 36, 39). State 3 respiratory capacity specific to C1, NADH dehydrogenase (P_{C1}), was induced following the additions of pyruvate (5 mM) and

J Appl Physiol • doi:10.1152/japplphysiol.01081.2012 • www.jappl.org

glutamate (10 mM). P was then induced with the addition of succinate (10 mM). P demonstrates a naturally intact electron transport system's capacity to catalyze a sequential set of redox reactions that are partially coupled to the production of ATP via ATP synthase. P maintains an electrochemical gradient across the inner mitochondrial membrane dictated by the degree of coupling to the phosphorylation system (13, 35). As an internal control for compromised integrity of the mitochondrial preparation, the mitochondrial outer membrane was assessed with the addition of cytochrome *c* (10 μM). There was no indication of mitochondrial damage indicated by the average change in respiration of 1.1% across all subjects ($P = 0.361$) following addition of cytochrome *c*. Phosphorylative restraint of electron transport was assessed by uncoupling ATP synthase (complex V) from the electron transport system with the titration of the proton ionophore, carbonyl cyanide *p*-(trifluoromethoxy) phenylhydrazone (0.5 μM per addition up to optimum concentrations ranging from 1.5 to 3 μM), reaching ETS. Finally, rotenone (0.5 μM) and antimycin A (2.5 μM) were added, in sequence, to terminate respiration by inhibiting C1 and complex III (cytochrome bc_1 complex), respectively. With C1 inhibited, electron flow specific to complex II (C2), succinate dehydrogenase, and state 3 respiration through C2 (P_{C2}) can be measured. Inhibition of respiration with antimycin A then allows for the determination and correction of residual $\dot{V}O_2$, indicative of nonmitochondrial $\dot{V}O_2$ in the chamber.

Citrate Synthase Activities

Citrate synthase (CS) activities were assayed in homogenates of the skeletal muscle samples used in respiration measurements. The contents of the Oxygraph-2k chambers (2 ml each) were removed after each respiration experiment and washed once with 2 ml of MiR05. One percent Triton X-100 and 2 μl of a protease inhibitor cocktail (Sigma Aldrich cat. no. 539134) were added to the combined solutions (content and wash) and then homogenized for 30 s with a T10 basic ULTRA-TURRAX homogenizer near maximum speed. The homogenate was then centrifuged for 15 min at 4°C, and the supernatant was removed, frozen in liquid nitrogen, and stored at −80°C. As has been previously described (42), CS activity was measured fluorometrically at 412 nm and 25°C (Citrate Synthase Assay Kit, Sigma-Aldrich), according to the manufacturer.

Data Analysis

Significance was set at $P = 0.05$, but P values of < 0.10 are also noted. Data are presented as means ± SD. Mitochondria-specific respiration was calculated by dividing mass-specific respiration (pmol $O_2 \cdot min^{-1} \cdot mg$ wet wt^{-1}) by the corresponding CS activity (nmol $\cdot min^{-1} \cdot mg$ wt^{-1}). Comparisons of age, weight, height, absolute and relative $\dot{V}O_{2\,max}$, absolute and relative maximal power (W_{max}), years of exercise, respiratory capacities, CS, and indexes of mitochondrial coupling control were compared using a one-way ANOVA (SPSS Statistics 17.0, SPSS, Chicago, IL). Significant main effects or interactions were further analyzed by Tukey's post hoc test. The time of training per year and per week did not, however, display a Gaussian distribution, and, therefore, a Kruskal-Wallis ANOVA and Mann-Whitney *U*-tests were used to reveal differences between groups. An analysis of covariance was also run on mass-specific respirometric values with CS activities included as the covariant being controlled for. Multiple linear regression analysis with backward elimination was used to identify the strongest association between measurements of mass-specific and mitochondrial-specific respiration to cardiorespiratory fitness.

RESULTS

$\dot{V}O_{2\,max}$

All groups differed in $\dot{V}O_{2\,max}$ (Fig. 1). Group $\dot{V}O_{2\,max}$ values presented as means ± SD, maximum and minimum, respectively, in ml $\cdot min^{-1} \cdot kg^{-1}$, were as follows: AT (51.2 ± 4.1, 46.9 and 55.5); WT (63.9 ± 4.7, 58.9 and 68.8); HT (71.3 ± 1.7, 69.5 and 73.1); and ET (77.3 ± 3.0, 74.1 and 80.4). The AT group was lower ($P < 0.001$) than all other groups. The WT group was higher than AT ($P < 0.001$), but lower than HT ($P = 0.009$) and ET ($P < 0.001$). The HT group was higher than both AT ($P < 0.001$) and WT ($P = 0.009$) groups, but lower than the ET group ($P = 0.04$).

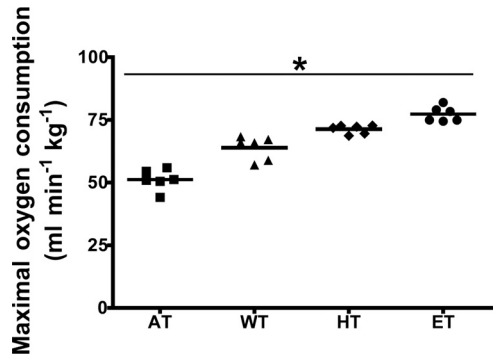

Fig. 1. Aerobic capacities across groups. Individual values of maximal oxygen consumption ($\dot{V}O_{2\,max}$) across groups are shown. AT, active; WT, well trained; HT, highly trained; ET, elite. *Significance of $P < 0.05$.

Subject Characteristics

All subject characteristics are presented in Table 1. There were no differences in age, height, weight, or years of exercise across groups. The absolute W_{max} only differed between the ET and AT groups ($P = 0.01$); however, the relative W_{max} for the AT group was lower than WT, HT, and ET ($P = 0.004$, $P < 0.001$, and $P < 0.001$, respectively). The ET also had a greater relative W_{max} than the WT group ($P = 0.002$), and the HT group showed a tendency for a higher relative W_{max} than the WT group ($P = 0.071$). The time-spent training per week and year demonstrated a progressive increase across groups, as the AT group exhibited the least time-spent participating in some form of physical activity, and the ET group had the most time-spent.

CS Activity

CS values (nmol $\cdot min^{-1} \cdot mg$ wet wt^{-1}) across groups (mean ± SD) were as follows: AT (16.2 ± 4.9), WT (18.6 ± 4.0), HT (25.1 ± 7.1), and ET (28.7 ± 7.0). The only differences detected in CS activity between groups were observed in ET compared with AT ($P = 0.008$) and WT groups ($P = 0.035$). There was a tendency for difference between AT and HT ($P = 0.072$). CS activity is an empirically established and reliable biomarker of mitochondrial content (30). CS activities are presented in Fig. 2.

Respiratory Capacity

Mass-specific respiration. There were no differences in mass-specific respiration (Fig. 3*A*) between AT and WT, WT and HT, or between HT and ET groups at any respiratory states, although P_{ETF} had a tendency to increase from AT to WT ($P = 0.056$). The AT group had lower fat respiration, P_{ETF} ($P = 0.012$ and $P < 0.001$), P ($P = 0.015$ and $P < 0.001$), ETS ($P = 0.003$ and $P < 0.001$), and submaximal P_{C2} ($P = 0.005$ and $P = 0.002$) than the HT and ET groups, respectively. The AT group also expressed lower L_N ($P = 0.019$) and submaxi-

J Appl Physiol • doi:10.1152/japplphysiol.01081.2012 • www.jappl.org

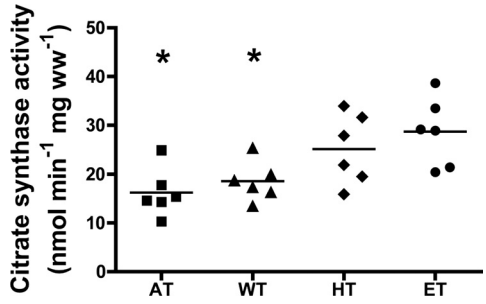

Fig. 2. Citrate synthase (CS) activities. Individual values of CS activities are presented across group as a biomarker of mitochondrial content. *Significance from ET of $P < 0.05$.

mal P_{C1} ($P = 0.033$) vs. the ET group. The WT group expressed lower respiration compared with the ET group during P ($P = 0.009$) and ETS ($P = 0.001$) and had a tendency to have lower P_{ETF} ($P = 0.052$).

Mass-specific respiration when controlling for mitochondrial content. Significant differences in mass-specific respiration were altered when controlling for CS activity as a covariate (data not shown). The lower respiratory capacities of the AT group vs. the HT group were only apparent during ETS and P_{C2} ($P = 0.049$), but showed a tendency for lower P_{ETF}, P, and P_{C2} ($P = 0.069$, 0.079, and 0.052, respectively). The AT group expressed lower respiration compared with the ET group at P_{ETF} ($P = 0.004$), P ($P = 0.005$), and ETS ($P = 0.003$) and had a tendency for lower P_{C2} ($P = 0.067$). The WT group expressed lower ETS than the ET group ($P = 0.033$) and also had a tendency for lower P ($P = 0.067$). There were no differences across groups during L_N or P_{CI}.

Mitochondria-specific respiration. Mass-specific respiration does not take into account differences in mitochondrial content between samples. Accordingly, respirometric analyses were adjusted for CS activity, a biomarker shown to express strong concordance with mitochondrial content and total cristae area, as measured by transmission electron microscopy as well as myocellular respiratory capacity (30). Figure 3*B* illustrates mitochondrial-specific respiration across all groups. There were no differences in mitochondrial-specific respiration between AT, WT, and HT groups across all respiratory states, although there was a tendency for lower respiration in the AT vs. the HT during P_{ETF} ($P = 0.056$). When normalizing respiration to mitochondrial content, P was greater in ET vs. only AT ($P = 0.031$), while P_{ETF} ($P = 0.003$ and 0.048) and ETS ($P = 0.015$ and 0.029) were greater in ET compared with both AT and WT, respectively. There was a tendency for P to be lower in the WT vs. ET group ($P = 0.066$). There were no differences across all groups during L_N, P_{C1}, or P_{C2}.

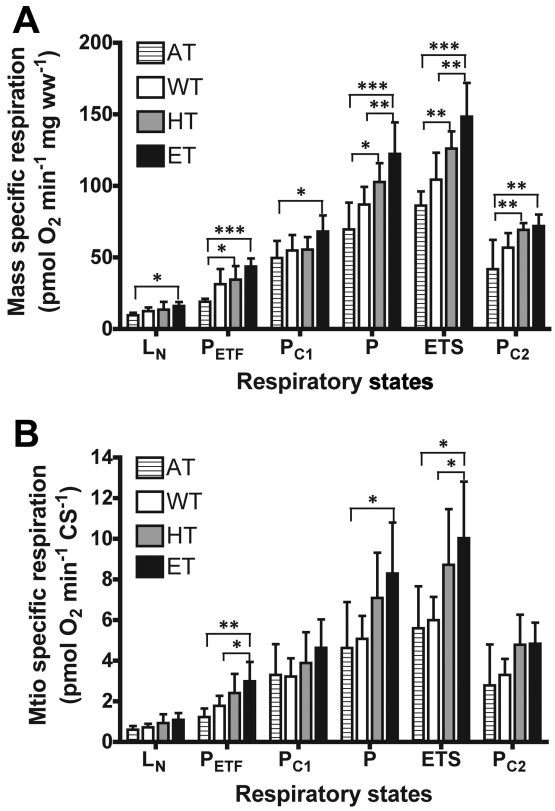

Fig. 3. Mitochondrial respiration control across groups. *A*: mass-specific respiratory capacity. *B*: mitochondria-specific respiratory capacity across groups. L_N, leak respiration in absence of adenylates; P_{ETF}, maximal electron flow through electron-transferring flavoprotein (ETF) and fatty acid oxidative capacity; P_{C1}, submaximal state 3 respiratory capacity specific to complex I; P, maximal state 3 respiration and oxidative phosphorylation capacity; ETS, electron transport system capacity; P_{C2}, submaximal state 3 respiratory capacity specific to complex II. Values are means ± SD. Significant difference of $*P < 0.05$, $**P < 0.01$, and $***P < 0.001$.

Mitochondrial Coupling Efficiency and Respiratory Control

We calculated the leak control ratio (LCR) as indication of electron coupling efficiency during β-oxidation (LCR_{ETF}), as has been fully explained previously (23). The LCR_{ETF} did not express any difference across groups (Fig. 4*A*). The phosphorylation system control ratio (PSCR), ratio of P to ETS expressing the degree of maximal P constraint by the phosphorylation

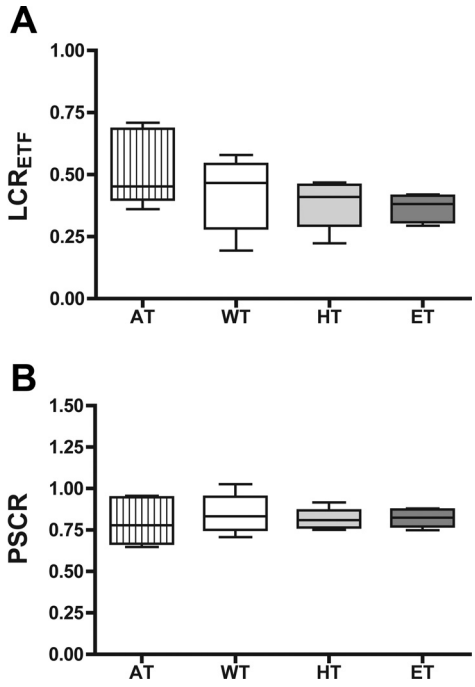

Fig. 4. Mitochondrial coupling efficiency and respiratory control. *A*: leak control ratio (LCR), electron coupling control during β-oxidation (LCR_{ETF}) across groups. *B*: phosphorylation system control ratio (PSCR) across groups.

J Appl Physiol • doi:10.1152/japplphysiol.01081.2012 • www.jappl.org

system or ATP synthase (13), was also determined. While skeletal muscle PSCR differs significantly between mice and humans (21), it did not differ between groups that varied in aerobic capacity (Fig. 4*B*).

Correlation Between Maximal Exercise Respiratory Capacities

All mitochondrial parameters examined in this study expressed a significant correlation to $\dot{V}O_{2\,max}$, except for the PSCR ($R = 0.077$, $P = 0.361$). The second weakest correlation (behind L_N respiration) was between values of mitochondrial content and exercise capacity ($R = 0.635$, $P < 0.001$). The LCR_{ETF} was the only value showing a significant negative correlation ($R = -0.462$, $P = 0.012$). Finally, multiple linear regression analysis using backward elimination for mass-specific (Fig. 5*A*) and mitochondria-specific respiration (Fig. 5*B*), respectively, calculated ETS as the best predictive mitochondrial parameter of $\dot{V}O_{2\,max}$.

DISCUSSION

In this study we divided one large group of healthy subjects ($n = 24$) into four different groups ($n = 6$), dependent on their aerobic capacity and studied mitochondrial function via respirometric analysis. This study presents several novel findings. First, qualitative, independent from quantitative, differences in mitochondrial characteristics are apparent across groups of healthy humans in accordance with $\dot{V}O_{2\,max}$. Fat respiration (P_{ETF}), P, and electron transport across the entire respiratory system (ETS) all improve, in combination with aerobic capacity. Second, efficiency of coupling control during β-oxidation and phophorylative restraint of ATP synthase on electron transport do not appear to differ across individuals with markedly disparate measures of $\dot{V}O_{2\,max}$. Finally, ETS correlates best, among all other respiratory states, to cardiorespiratory fitness in humans.

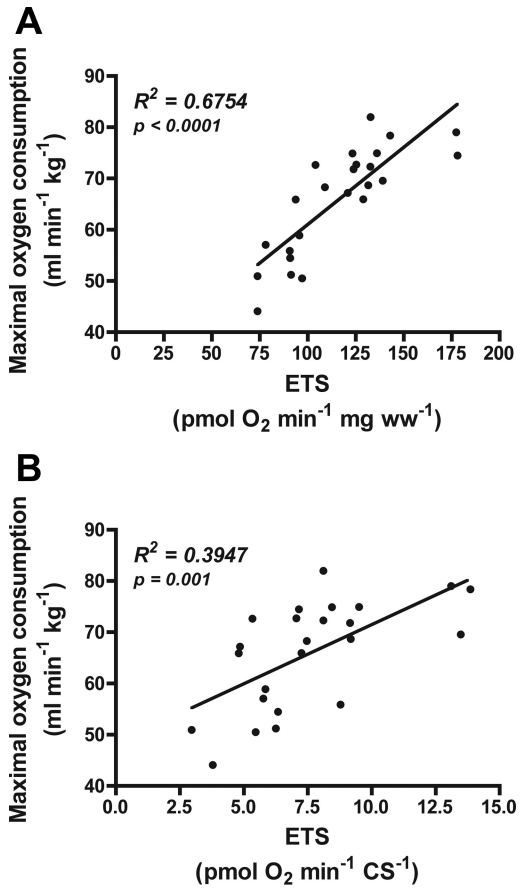

Fig. 5. Correlation of ETS capacity and $\dot{V}O_{2\,max}$ across groups. *A*: mass-specific respiration. *B*: mitochondrial-specific respiration.

There is a strong correlation between mitochondrial content and maximal aerobic capacity in both humans and animals (17, 18, 20, 32). The subjects included in this study displayed this correlation between CS and $\dot{V}O_{2\,max}$ ($P < 0.001$), although differences in mitochondrial content were not apparent between all groups (Fig. 2). It has been suggested that oxidative capacity of skeletal muscle is dependent purely on the quantity of mitochondria in the muscle (19, 41). Here we present strong evidence to suggest that there are qualitative improvements in mitochondria that correspond with whole body aerobic capacity, independent of mitochondrial content. The seemingly inconsistent results between those presented here and past studies (41) may be due to the fact that the former study used substrates for respiration specific to either mitochondrial C1 or C2 individually, but never collectively (41). Our data support these previous findings, as we also failed to identify any respiratory differences between any groups at P_{C1} or P_{C2} respiratory states when normalizing respiration to mitochondrial content (Fig. 3*B*). We stimulated P with saturating concentrations of ADP and substrate supply for both C1 and C2. This convergent electron input of both complexes provides higher respiratory values compared with the isolated respiration of either C1 (pyruvate/glutamate + malate or glutamate + malate) or C2 (succinate + rotenone) (13, 37). Accordingly, P presents with more physiological relevance to the study of mitochondrial function, as substrate provision for both complexes is necessary to confirm a complete and intact electron transport system and measure maximal respiratory capacity in skeletal muscle (8).

Although the capacity for fat respiration differed between AT and ET groups and also showed a tendency for improvement in HT over AT ($P = 0.056$), mitochondrial coupling efficiency during fatty acid oxidation was the same across all groups (Figs. 3*B* and 4*A*). Fat oxidation during exercise has been reported as greater in trained vs. untrained individuals at the same relative workload (43). Moreover, a greater percentage of energy expenditure during exercise comes from fat oxidation in trained vs. untrained subjects at the same absolute workload (43). There is also a greater intramuscular triglyceride content in trained vs. untrained humans (20), which also increases and becomes localized next to the mitochondria in response to exercise training (18) and is increased in active vs. nonactive individuals (14). One training study has reported improvements in mass-specific mitochondrial respiratory capacity, along with improvements in mitochondrial fat metabolism when sedentary individuals trained for 10 wk, while mitochondrial content, as assessed by mitochondrial DNA, did not increase (36). Unfortunately, mitochondrial DNA does not strongly correlate with measures of mitochondrial content and total cristae area, as assessed by transmission electron microscopy or myocellular respiratory capacity (30), and thus does not adequately serve as biomarker of mitochondrial content. Therefore, satisfactory mitochondrial-specific analysis of P_{ETF}

J Appl Physiol • doi:10.1152/japplphysiol.01081.2012 • www.jappl.org

could not be analyzed (36). We extend on previous findings and show that the capacity for fat oxidation improves with cardiorespiratory fitness; however, efficiency appears unaltered.

Another qualitative difference in mitochondria observed across groups differing in aerobic fitness was ETS (Fig. 3*B*). Oxidative capacity of skeletal muscle is known to improve with overall fitness (28), although specific modifications in mitochondrial function in relation to fitness are much less understood. Differences in mass-specific respiration capacity in young and older subjects matched for aerobic capacity are negligible until respiration is normalized to mitochondrial content, where a reduction in respiratory capacity becomes apparent (29). Endurance-trained individuals present with a greater substrate flux through the tricarboxylic acid cycle over sedentary individuals, independent from any difference in ATP synthesis (5). The greater flux through the tricarboxylic acid cycle without an increase in ATP led authors to speculate that resting mitochondrial respiration in endurance-trained individuals is uncoupled from ATP synthesis to a greater degree than their sedentary counterparts (5). Here we show that ET athletes have a greater capacity for electron transport across the entire respiratory chain vs. AT and WT subjects, even though they present with similar phosphorylative restraint of electron transport (Fig. 5*B*). In the ETS state, the inner mitochondrial membrane potential is completely collapsed with an open transmembrane proton circuit. The uninhibited flow of electrons through the respiratory system can, therefore, indirectly serve as an indication of maximal attainable mitochondrial membrane potential. A larger capacity for electron transport with similar phosphorylative restraint allows for a superior uncoupling capacity, which appears to correspond with aerobic capacity. Across all states of respiration measured, ETS fit best with cardiorespiratory fitness (Fig. 5*A*). This correlation remained even when controlling for differences in mitochondrial content across all groups (Fig. 5*B*), further demonstrating the qualitative differences in mitochondrial function that are associated with whole body aerobic fitness in humans.

This study specifically highlights significant qualitative changes in mitochondria by means of respiratory capacity. Less is known in regards to how mitochondrial efficiency fluctuates with aerobic capacity. While an improvement in the coupling efficiency of electron transport during β-oxidation was not apparent across groups, the coupling control across the entire respiratory chain could not be determined with this SUIT protocol. Previous studies utilizing mitochondrial isolation techniques report no change in coupling control (4), while others report an improvement in mitochondrial efficiency between trained vs. sedentary individuals (10, 46). The malleability of mitochondria in response to training merits further attention.

One possible limitation in the present study is the supraphysiological concentrations of oxygen that are required during respirometric analysis to overcome diffusive limitations of the samples (35), and the potential alterations in mitochondrial function that may accompany this hyperoxygenated environment. This, however, is not believed to have influenced our results or conclusions, as all samples were treated similarly and exposed to the same oxygen concentrations.

In summary, both mitochondrial quantity and quality improve with aerobic capacity. Qualitative differences in mitochondria across levels of cardiorespiratory fitness were not fully understood and questioned to even exist. As such, we divided 24 healthy and aerobically fit individuals into four groups that differed in whole body aerobic exercise capacity. Across these healthy individuals, both quantitative and qualitative mitochondrial variations were evident. Those with elite aerobic capacities displayed superior respiratory capacity over those who were active or well-trained. Specifically, these qualitative differences observed across groups were specific to greater capacities for fat oxidation, oxidative phosphorylation, and electron transport across the entire respiratory system. These results make it apparent that mitochondrial modifications with improving cardiorespiratory fitness comprise more than just an increase in mitochondrial content. It is important and necessary to differentiate mitochondrial content from function in future studies.

ACKNOWLEDGMENTS

The authors sincerely thank Drs. Dominik Pesta, Anne-Kristine Meinild, Christoph Siebenmann, and Paul Robach for technical assistance with respirometric analysis, CS measurements, and maximal exercise tests, respectively.

DISCLOSURES

No conflicts of interest, financial or otherwise, are declared by the author(s).

AUTHOR CONTRIBUTIONS

Author contributions: R.A.J. and C.L. conception and design of research; R.A.J. performed experiments; R.A.J. analyzed data; R.A.J. and C.L. interpreted results of experiments; R.A.J. prepared figures; R.A.J. drafted manuscript; R.A.J. and C.L. edited and revised manuscript; R.A.J. and C.L. approved final version of manuscript.

REFERENCES

1. **Aadland E, Robertson L.** Physical activity is associated with weight loss and increased cardiorespiratory fitness in severely obese men and women undergoing lifestyle treatment. *J Obes* 2012: 810594, 2012.
2. **American Thoracic Society; American College of Chest Physicians.** ATS/ACCP statement on cardiopulmonary exercise testing. *Am J Respir Crit Care Med* 167: 211–277, 2003.
3. **Andersen P, Saltin B.** Maximal perfusion of skeletal muscle in man. *J Physiol* 366: 233–249, 1985.
4. **Befroy DE, Petersen KF, Dufour S, Mason GF, de Graaf RA, Rothman DL, Shulman GI.** Impaired mitochondrial substrate oxidation in muscle of insulin-resistant offspring of type 2 diabetic patients. *Diabetes* 56: 1376–1381, 2007.
5. **Befroy DE, Petersen KF, Dufour S, Mason GF, Rothman DL, Shulman GI.** Increased substrate oxidation and mitochondrial uncoupling in skeletal muscle of endurance-trained individuals. *Proc Natl Acad Sci U S A* 105: 16701–16706, 2008.
6. **Bergström J.** Muscle electrolytes in man. *Scand J Clin Lab Invest* 68: 1–110, 1962.
7. **Booth FW, Narahara KA.** Vastus lateralis cytochrome oxidase activity and its relationship to maximal oxygen consumption in man. *Pflügers Arch* 349: 319–324, 1974.
8. **Brand MD, Nicholls DG.** Assessing mitochondrial dysfunction in cells. *Biochem J* 435: 297–312, 2011.
9. **Daussin FN, Zoll J, Dufour SP, Ponsot E, Lonsdorfer-Wolf E, Doutreleau S, Mettauer B, Piquard F, Geny B, Richard R.** Effect of interval vs. continuous training on cardiorespiratory and mitochondrial functions: relationship to aerobic performance improvements in sedentary subjects. *Am J Physiol Regul Integr Comp Physiol* 295: R264–R272, 2008.
10. **Daussin FN, Zoll J, Ponsot E, Dufour SP, Doutreleau S, Lonsdorfer E, Ventura-Clapier R, Mettauer B, Piquard F, Geny B, Richard R.** Training at high exercise intensity promotes qualitative adaptations of mitochondrial function in human skeletal muscle. *J Appl Physiol* 104: 1436–1441, 2008.
11. **Eaton S, Bartlett K, Pourfarzam M.** Mammalian mitochondrial beta-oxidation. *Biochem J* 320: 345–357, 1996.

12. **Gander J, Lee DC, Sui X, Hebert JR, Hooker SP, Blair SN.** Self-rated health status and cardiorespiratory fitness as predictors of mortality in men. *Br J Sports Med* 45: 1095–1100, 2011.
13. **Gnaiger E.** Capacity of oxidative phosphorylation in human skeletal muscle: new perspectives of mitochondrial physiology. *Int J Biochem Cell Biol* 41: 1837–1845, 2009.
14. **Goodpaster BH, He J, Watkins S, Kelley DE.** Skeletal muscle lipid content and insulin resistance: evidence for a paradox in endurance-trained athletes. *J Clin Endocrinol Metab* 86: 5755–5761, 2001.
15. **Holloszy JO.** Biochemical adaptations in muscle. Effects of exercise on mitochondrial oxygen uptake and respiratory enzyme activity in skeletal muscle. *J Biol Chem* 242: 2278–2282, 1967.
16. **Holloszy JO, Booth FW.** Biochemical adaptations to endurance exercise in muscle. *Annu Rev Physiol* 38: 273–291, 1976.
17. **Hoppeler H.** The different relationship of $\dot{V}O_{2\,max}$ to muscle mitochondria in humans and quadrupedal animals. *Respir Physiol* 80: 137–145, 1990.
18. **Hoppeler H, Howald H, Conley K, Lindstedt SL, Claassen H, Vock P, Weibel ER.** Endurance training in humans: aerobic capacity and structure of skeletal muscle. *J Appl Physiol* 59: 320–327, 1985.
19. **Hoppeler H, Hudlicka O, Uhlmann E.** Relationship between mitochondria and oxygen consumption in isolated cat muscles. *J Physiol* 385: 661–675, 1987.
20. **Hoppeler H, Luthi P, Claassen H, Weibel ER, Howald H.** The ultrastructure of the normal human skeletal muscle. A morphometric analysis on untrained men, women and well-trained orienteers. *Pflügers Arch* 344: 217–232, 1973.
21. **Jacobs RA, Diaz V, Meinild AK, Gassmann M, Lundby C.** The C57Bl/6 mouse serves as a suitable model of human skeletal muscle mitochondrial function. *Exp Physiol.* doi:10.1113/expphysiol.2012.07003:2012.
22. **Jacobs RA, Rasmussen P, Siebenmann C, Diaz V, Gassmann M, Pesta D, Gnaiger E, Nordsborg NB, Robach P, Lundby C.** Determinants of time trial performance and maximal incremental exercise in highly trained endurance athletes. *J Appl Physiol* 111: 1422–1430, 2011.
23. **Jacobs RA, Siebenmann C, Hug M, Toigo M, Meinild AK, Lundby C.** Twenty-eight days at 3454-m altitude diminishes respiratory capacity but enhances efficiency in human skeletal muscle mitochondria. *FASEB J* 26: 5192–5200, 2012.
24. **Janssen I, Jolliffe CJ.** Influence of physical activity on mortality in elderly with coronary artery disease. *Med Sci Sports Exerc* 38: 418–417, 2006.
25. **Katzmarzyk PT, Church TS, Blair SN.** Cardiorespiratory fitness attenuates the effects of the metabolic syndrome on all-cause and cardiovascular disease mortality in men. *Arch Intern Med* 164: 1092–1097, 2004.
26. **Kodama S, Saito K, Tanaka S, Maki M, Yachi Y, Asumi M, Sugawara A, Totsuka K, Shimano H, Ohashi Y, Yamada N, Sone H.** Cardiorespiratory fitness as a quantitative predictor of all-cause mortality and cardiovascular events in healthy men and women: a meta-analysis. *JAMA* 301: 2024–2035, 2009.
27. **Kuznetsov AV, Schneeberger S, Seiler R, Brandacher G, Mark W, Steurer W, Saks V, Usson Y, Margreiter R, Gnaiger E.** Mitochondrial defects and heterogeneous cytochrome c release after cardiac cold ischemia and reperfusion. *Am J Physiol Heart Circ Physiol* 286: H1633–H1641, 2004.
28. **Larsen RG, Callahan DM, Foulis SA, Kent-Braun JA.** In vivo oxidative capacity varies with muscle and training status in young adults. *J Appl Physiol* 107: 873–879, 2009.
29. **Larsen S, Hey-Mogensen M, Rabol R, Stride N, Helge JW, Dela F.** The influence of age and aerobic fitness: effects on mitochondrial respiration in skeletal muscle. *Acta Physiol (Oxf)* 205: 423–432, 2012.
30. **Larsen S, Nielsen J, Neigaard Nielsen C, Nielsen LB, Wibrand F, Stride N, Schroder HD, Boushel R, Helge JW, Dela F, Hey-Mogensen M.** Biomarkers of mitochondrial content in skeletal muscle of healthy young human subjects. *J Physiol* 590: 3349–3360, 2012.
31. **Lyerly GW, Sui X, Lavie CJ, Church TS, Hand GA, Blair SN.** The association between cardiorespiratory fitness and risk of all-cause mortality among women with impaired fasting glucose or undiagnosed diabetes mellitus. *Mayo Clin Proc* 84: 780–786, 2009.
32. **Mathieu O, Krauer R, Hoppeler H, Gehr P, Lindstedt SL, Alexander RM, Taylor CR, Weibel ER.** Design of the mammalian respiratory system. VII. Scaling mitochondrial volume in skeletal muscle to body mass. *Respir Physiol* 44: 113–128, 1981.
33. **Mettauer B, Zoll J, Sanchez H, Lampert E, Ribera F, Veksler V, Bigard X, Mateo P, Epailly E, Lonsdorfer J, Ventura-Clapier R.** Oxidative capacity of skeletal muscle in heart failure patients versus sedentary or active control subjects. *J Am Coll Cardiol* 38: 947–954, 2001.
34. **Ortega FB, Lee DC, Sui X, Kubzansky LD, Ruiz JR, Baruth M, Castillo MJ, Blair SN.** Psychological well-being, cardiorespiratory fitness, and long-term survival. *Am J Prev Med* 39: 440–448, 2010.
35. **Pesta D, Gnaiger E.** High-resolution respirometry. OXPHOS protocols for human cell cultures and permeabilized fibers from small biopsies of human muscle. *Methods Mol Biol* 810: 25–58, 2012.
36. **Pesta D, Hoppel F, Macek C, Messner H, Faulhaber M, Kobel C, Parson W, Burtscher M, Schocke M, Gnaiger E.** Similar qualitative and quantitative changes of mitochondrial respiration following strength and endurance training in normoxia and hypoxia in sedentary humans. *Am J Physiol Regul Integr Comp Physiol* 301: R1078–R1087, 2011.
37. **Rasmussen UF, Rasmussen HN.** Human skeletal muscle mitochondrial capacity. *Acta Physiol Scand* 168: 473–480, 2000.
38. **Robach P, Siebenmann C, Jacobs RA, Rasmussen P, Nordsborg NB, Pesta D, Gnaiger E, Diaz V, Christ A, Fiedler J, Crivelli N, Secher NH, Pichon A, Maggiorini M, Lundby C.** The role of hemoglobin mass on $\dot{V}O_{2\,max}$ following normobaric "live high-train low" in endurance-trained athletes. *Br J Sports Med* 46: 822–827, 2012.
39. **Saks VA, Veksler VI, Kuznetsov AV, Kay L, Sikk P, Tiivel T, Tranqui L, Olivares J, Winkler K, Wiedemann F, Kunz WS.** Permeabilized cell and skinned fiber techniques in studies of mitochondrial function in vivo. *Mol Cell Biochem* 184: 81–100, 1998.
40. **Saltin B, Kim CK, Terrados N, Larsen H, Svedenhag J, Rolf CJ.** Morphology, enzyme activities and buffer capacity in leg muscles of Kenyan and Scandinavian runners. *Scand J Med Sci Sports* 5: 222–230, 1995.
41. **Schwerzmann K, Hoppeler H, Kayar SR, Weibel ER.** Oxidative capacity of muscle and mitochondria: correlation of physiological, biochemical, and morphometric characteristics. *Proc Natl Acad Sci U S A* 86: 1583–1587, 1989.
42. **Srere PA.** Citrate synthase. *Methods Enzymol* 13: 3–11, 1969.
43. **van Loon LJ, Jeukendrup AE, Saris WH, Wagenmakers AJ.** Effect of training status on fuel selection during submaximal exercise with glucose ingestion. *J Appl Physiol* 87: 1413–1420, 1999.
44. **Wagner PD.** New ideas on limitations to $\dot{V}O_{2\,max}$. *Exerc Sport Sci Rev* 28: 10–14, 2000.
45. **Weibel ER, Hoppeler H.** Exercise-induced maximal metabolic rate scales with muscle aerobic capacity. *J Exp Biol* 208: 1635–1644, 2005.
46. **Zoll J, Sanchez H, N'Guessan B, Ribera F, Lampert E, Bigard X, Serrurier B, Fortin D, Geny B, Veksler V, Ventura-Clapier R, Mettauer B.** Physical activity changes the regulation of mitochondrial respiration in human skeletal muscle. *J Physiol* 543: 191–200, 2002.

3. Discussion and outlook

The aim of my Ph.D. studies was to put together a compilation of work that contributed to the scientific literature and improved our comprehensive understanding of mitochondrial physiology. Specifically we analyzed: 1.) the mitochondrial potential to utilize lactate; 2.) alterations on respiratory chain function across different skeletal muscle types with age; 3.) similarities and differences in mouse and human skeletal muscle function; 4.) hypoxia-induced alterations on mitochondrial function; and 5.) mitochondrial function and its relation to aerobic capacity and sports performance. Summarized below are the conclusions for each of the six studies for which this dissertationis comprised of.

Study 1: Lactate metabolism in human skeletal muscle mitochondria

Using high-resolution respirometry on mitochondrial preparations of human skeletal muscle *in situ*, a technique that specifically does not alter the native reticular structure of the mitochondria, we observed that mitochondria are capable of utilizing lactate as a substrate for respiration. Lactate stimulated respiration did not occur, however, in the presence of "malate + lactate" alone, as compared to "malate + pyruvate", indicating that lactate is not being shuttled across the MIM intact and oxidized in the mitochondrial matrix. Respiration only occurred when lactate and NAD^+ were titrated into the respiration medium together. This suggests that in order to cross the MIM and be further oxidized, lactate must first be converted to pyruvate by lactate dehydrogenase (LDH). The question is whether LDH exists within the MIS or exclusively in the cytosol? The specific mitochondrial preparation used, saponin-permeabilized or "skinned" skeletal muscle technique, has repeatedly demonstrated the loss of cytosolic components, including LDH (160, 163, 164, 179, 227, 253, 254, 291) providing evidence to suggest that any LDH that was measured in our sample must be entrapped in the mitochondrion itself. The concentration of the LDH measured in our samples was approximately 5% of that previously was measured in whole tissue homogenates. The mitochondrial reticular network accounts for approximately 5% of the volume density of skeletal muscle fibers (117, 119). Finally, exogenous titrations of LDH did not further stimulate respiration. All these observations suggest that LDH is present within the MIS, however we were unable to

empirically verify this postulation. The presence of LDH within mitochondria has repeatedly been demonstrated in different tissues and cell-types across several species (4, 8, 27, 30, 36, 47, 67, 72, 73, 103, 149, 182, 186, 188, 207, 213, 223, 269, 270, 279, 299). Additionally, LDH has even been shown to have a genetic tag for mitochondrial allocation (116). While we cannot definitively exclude the possibility that lactate and NAD^+ stimulated respiration was facilitated by remnants of cytosolic LDH or LDH that may be tethered to the MOM, our data and previous reports of mitochondrial LDH, suggest the existence of LDH is within the MIS but not the matrix, and that the mitochondrion, itself, possesses the ability to oxidize lactate as a substrate.

Study 2: Age-induced alterations in skeletal muscle mitochondria

Here we directly demonstrated impairments of respiratory chain function in aging glycolytic and white skeletal muscle. These impairments were not observed in skeletal muscle that is primarily composed of slow-twitch red oxidative muscle fibers. Therefore our data indicate that skeletal muscle consisting primarily of type 2 fast twitch glycolytic fibers are predisposed to progressive impairments in mitochondrial function with age as type I slow twitch oxidative fibers appear to be protected against functional degradation. Mitochondrial function varies across different skeletal muscle types in general, irrespective of age, however specific alterations with age occur in more glycolytic muscle. These alterations include an increase in submaximal state 3 respiration specific to mitochondrial complex I, P_{CI}, when controlling for complex I protein expression and an increase in maximal state 3 respiration / oxidative phosphorylation capacity, P, when controlling for mitochondrial complex III protein expression. Electron coupling efficiency also declined with age in more glycolytic skeletal muscle whereas it was preserved in oxidative skeletal muscle. The higher respiration through CI and CIII in combination with the deterioration in coupling efficiency all suggests an increase in oxidant production. Though oxidative muscle largely maintained mitochondrial function with age, electron-coupling control during fat oxidation did diminish. Taken together, this is the first study to identify actual and specific alterations in respiratory chain function in skeletal muscle with age (131).

Study 3: Mitochondrial function in mouse vs. man

Robert J. Lefkowitz and Brian K. Kobilka both won the Nobel Prize in Chemistry in 2012 for their work specific to G-protein-coupled receptors (42, 56, 190, 312) while

Sir John B. Gurdon and Shinya Yamanaka won the Nobel Prize in Physiology or Medicine for their work demonstrating that mature cells can be reprogrammed to become pluripotent cells (13, 183, 204, 212). The year prior, the Nobel Prize in Physiology or Medicine was divided between Bruce A. Beutler and Jules A. Hoffmann for their work pertaining to the activation of innate immunity (105, 261, 271, 327) and Ralph M. Steinman for his detection of the dendritic cell and identifying its role in adaptive immunity (45, 125). The work of these Nobel laureates have two things in common: 1) Their work has contributed greatly to their respective fields (obviously!); and 2.) A significant amount of their work was done in a mouse model. The role in which animals play for the development and progression of human medicine is unquestionable and this fact is understated. Murine modeling of human biology across the sciences accounts for a majority of the animal research conducted. Research relating to mitochondrial physiology is no different, as much research uses mouse tissue to mimic that of humans. There have been suggestions, albeit few and far between, that the mouse may not be a proper model for the study of mitochondria (171) or questions concerning which murine muscle best represents that of the human *m. vastus lateralis* (145). The degree of conservation between mouse and human genomes allows for the study of murine biology to largely characterize that of humans (52). There remains, however, a biological divergence between species that is not always so apparent and can lead to scientific misdirection if not properly recognized. Accordingly we empirically determined the resemblance of murine skeletal muscle to that of human. We found that mouse skeletal muscle mitochondrial function does resemble that of human *m. vastus lateralis*, however the semblance across species is highly dependent on the skeletal muscle type (130). It is the mouse quadricep muscle that most closely resembles human quadricep muscle, while murine soleus and gastrocnemius muscle expressed a greater divergence in function. This refutes previous work that suggested that mouse modeling of human skeletal muscle mitochondrial function is inadequate (171) and also that mouse soleus more closely resembles that of human quadricep (145). Overall, we provide evidence that skeletal muscle mitochondrial function, specifically respiratory control and capacity, are similar between mice and humans, however no mouse skeletal muscle provides an exact equivalent to that of human muscle. Thus future research must take into consideration the specific differences and similarities between mouse and human skeletal muscle to help address their specific interests and aims of study.

Studies 4 & 5: Progressive adaptation of skeletal muscle mitochondria to hypoxia

A degree of mitochondrial dysfunction has been identified in individuals suffering from COPD (206), sleep apnea (273), and cystic fibrosis (7, 51), all diseases or disorders that negatively effect oxygen transport throughout the body. It is not known whether the differences in mitochondrial function observed in individuals presenting with these diseases are from the disease *per se* or rather and indirect effect of hypoxia on the tissue. Accordingly, we set out to identify the hypoxia-mediated changes specifically in skeletal muscle mitochondria with high-altitude exposure. Exposure of humans to such altitudes is a challenge to homeostatic maintenance of oxygen flux as a result of the gradual decrease in the partial pressure of oxygen (PO_2) attendant to the diminishing barometric pressure (311).

In the first study (129) we found that acute and short duration exposure to high altitude does not greatly affect mitochondrial function. Exposure to high altitude for 9-11 days (7-9 days at 4,559 m) did not affect the capacity for fat oxidation or individualized respiration capacity through complex I and II, P_{CI} and P_{CII}, respectively, in human skeletal muscle. Chemiosmotic coupling efficiency during fat respiration also did not change following acclimatization. Functional characteristics of mitochondria do not always tightly parallel those of biochemical expression, as declines in TCA-and oxidative phosphorylation-specific enzymatic characteristics (293) did not equate with functional modifications to respiration in our study. Although the functional capacity of mitochondria in skeletal muscle was largely retained with subacute exposure to high altitude, mass specific maximal oxidative phosphorylation capacity, P, in human skeletal muscle did express a trend ($p = 0.059$) to decrease after high altitude exposure. This observation made us question whether our length of high altitude exposure was long enough to allow sufficient adaptation and so we conducted an additional study where subjects remained at high altitude for a longer duration.

In the second study (135) we observed that one month of exposure to 3,454 m led to alteration in respiratory function in skeletal muscle. Respiratory capacity of the

skeletal muscle was attenuated with high altitude exposure and this loss was independent from any indication of a decrease in mitochondrial content. There was also evidence of a reciprocal improvement in mitochondrial electron coupling efficiency. Finally, mitochondrial respiratory capacity correlated best with exercise capacity near sea level, however exercise capacity at 3,454 m following one month of high-altitude exposure was associated with the efficiency of electron transport, and not respiratory capacity, in skeletal muscle. These adaptations indicate that skeletal muscle mitochondria are quite capable and proficient in responding to a reduction in environmental oxygen by limiting respiratory capacities and becoming more efficient in harnessing the oxygen that is delivered to the tissue for bioenergetic purposes. The correlation with mitochondrial parameters and exercise demonstrate that skeletal mitochondria adapts to best exploit the limiting factor in oxygen delivery. At high altitude when the diffusive limitations in oxygen transport become more pronounced and limits the capacity for physical activity (133), mitochondria adapt accordingly to maintain function despite the lower oxygen tensions.

Studies 6 & 7: The role of mitochondria in health, fitness, and sports performance

Athletics and sport around the world serves as a billion dollar industry. For this very reason there is much research aimed at evaluating the most effective training strategies and the most important physiologic variables attributed to sports performance. Human endurance performance can approximated by maximal oxygen consumption (VO_{2max}), lactate threshold, and exercise efficiency (14, 137-139). These physiologic parameters, however, are not wholly exclusive from one another with the common link being association to the mitochondria. Accordingly, we sought to clarify and more precisely identify the physiological variable(s) most tightly correlating to exercise performance. We found that VO_{2max} and total hemoglobin mass were the two physiological variables that could best predict maximal incremental exercise capacity in highly trained athletes. These results suggest that the capacity to transport oxygen to the muscle is limiting, and thus of utmost importance, during maximal incremental exercise to fatigue. This has been demonstrated before (5). The novelty of the study, however, was the variable that we discovered best-predicted endurance performance in these athletes. Maximal state 3 respiration, or mass-specific respiratory capacity of

the *m. vastus lateralis* was the strongest predictor of endurance performance among these athletes (134). Moreover, mitochondrial content as assess by citrate synthase activity, a measurement that has demonstrated a strong correlation with mitochondrial content as assessed by electron transmission microscopy in both humans and horses (118, 169), expressed no relation with performance in this group of athletes. When grouping exercise capacity together, taking into account both incremental exercise and endurance performances, VO_{2max}, total hemoglobin mass, oxidative phosphorylation capacity, and electron transport system capacity were the best predictors of performance. In short, it is the transport and utilization of oxygen that is the most important to exercise performance. Interestingly the predictability of exercise performance by the respiratory capacity of the skeletal muscle has also been demonstrated in elite racehorses, where those horses with the highest respiratory capacity were also the strongest racers (Dominique-Marie Votion, unpublished findings). In summary, if you want to bet on sports performance then put your money on the mitochondria.

With the majority of research investigating the role of mitochondrial "dysfunction" in disease, the role of mitochondria in healthy individuals is much less understood. The research included in this dissertationwas predominately collected from reasonably young and healthy humans and mice, aside from the mature mouse skeletal muscle analyzed.

Health is a universal term that encompasses many states. While health is a broad term and one that is hard to define with a single measurement, maximal exercise capacity (VO_{2max}) may serve as the best individual quantification of overall health in humans (1, 81, 136, 143, 150, 180, 219). After discovering that respiratory capacity of the skeletal muscle best predicts endurance performance in highly trained athletes with no association between performance and mitochondrial content, we were interested in assessing more qualitative differences in mitochondria across an entire "healthy" group separated by aerobic capacity. We found that qualitative measures of mitochondrial function do indeed improve in individuals that possess a higher aerobic capacity. Specifically these improvements include the ability to oxidize fat, total oxidative phosphorylation capacity and also electron transport capacity (132). All these qualitative differences were independent from the differences of mitochondrial content across groups. Again, similar finding exist in horses as they also demonstrate

mitochondrial improvements with training and across different levels of fitness (296, 297).

Closing

There is much that remains unknown regarding mitochondria. The collection of studies presented in this thesis, however, help to illuminate some previous questions regarding mitochondrial physiology. In general, qualitative adjustments in mitochondrial function appear to be more pronounced than previously believed. Specifically, mitochondria possess the ability to oxidize lactate, age-associated modifications in respiratory chain function are apparent in fast-twitch skeletal muscle, mouse and human skeletal muscle mitochondrial function is similar but dependent on skeletal muscle type, exposure to high altitudes facilitates a progressive adaptation in respiratory control and capacity, and finally mitochondrial function is an extremely important variable in sports performance of which differs greatly with aerobic capacity. As there are many more questions to be answered in regards to mitochondria, I look forward to spending my indefinite future further investigating the inner workings of this organelle in its relations with both health and disease.

4. Bibliography

1. **Aadland E, and Robertson L**. Physical activity is associated with weight loss and increased cardiorespiratory fitness in severely obese men and women undergoing lifestyle treatment. *J Obes* 2012: 810594, 2012.

2. **Abrahams JP, Leslie AG, Lutter R, and Walker JE**. Structure at 2.8 A resolution of F1-ATPase from bovine heart mitochondria. *Nature* 370: 621-628, 1994.

3. **Abrahams JP, Lutter R, Todd RJ, van Raaij MJ, Leslie AG, and Walker JE**. Inherent asymmetry of the structure of F1-ATPase from bovine heart mitochondria at 6.5 A resolution. *EMBO J* 12: 1775-1780, 1993.

4. **Agostoni A, Vergani C, and Villa L**. Intracellular distribution of the different forms of lactic dehydrogenase. *Nature* 209: 1024-1025, 1966.

5. **Andersen P, and Saltin B**. Maximal perfusion of skeletal muscle in man. *J Physiol* 366: 233-249, 1985.

6. **Anderson S, Bankier AT, Barrell BG, de Bruijn MH, Coulson AR, Drouin J, Eperon IC, Nierlich DP, Roe BA, Sanger F, Schreier PH, Smith AJ, Staden R, and Young IG**. Sequence and organization of the human mitochondrial genome. *Nature* 290: 457-465, 1981.

7. **Antigny F, Girardin N, Raveau D, Frieden M, Becq F, and Vandebrouck C**. Dysfunction of mitochondria Ca2+ uptake in cystic fibrosis airway epithelial cells. *Mitochondrion* 9: 232-241, 2009.

8. **Baba N, and Sharma HM**. Histochemistry of lactic dehydrogenase in heart and pectoralis muscles of rat. *J Cell Biol* 51: 621-635, 1971.

9. **Babcock GT, and Wikstrom M**. Oxygen activation and the conservation of energy in cell respiration. *Nature* 356: 301-309, 1992.

10. **Baker LA, Watt IN, Runswick MJ, Walker JE, and Rubinstein JL**. Arrangement of subunits in intact mammalian mitochondrial ATP synthase determined by cryo-EM. *Proc Natl Acad Sci U S A* 109: 11675-11680, 2012.

11. **Balaban RS, Nemoto S, and Finkel T**. Mitochondria, oxidants, and aging. *Cell* 120: 483-495, 2005.

12. **Bangsbo J, Gollnick PD, Graham TE, and Saltin B**. Substrates for muscle glycogen synthesis in recovery from intense exercise in man. *J Physiol* 434: 423-440, 1991.

13. **Bao S, Tang F, Li X, Hayashi K, Gillich A, Lao K, and Surani MA**. Epigenetic reversion of post-implantation epiblast to pluripotent embryonic stem cells. *Nature* 461: 1292-1295, 2009.

14. **Bassett DR, Jr., and Howley ET**. Limiting factors for maximum oxygen uptake and determinants of endurance performance. *Med Sci Sports Exerc* 32: 70-84, 2000.

15. **Beckman KB, and Ames BN**. The free radical theory of aging matures. *Physiol Rev* 78: 547-581, 1998.

16. **Bekker A, Holland HD, Wang PL, Rumble D, 3rd, Stein HJ, Hannah JL, Coetzee LL, and Beukes NJ**. Dating the rise of atmospheric oxygen. *Nature* 427: 117-120, 2004.

17. **Belogrudov G, and Hatefi Y**. Catalytic sector of complex I (NADH:ubiquinone oxidoreductase): subunit stoichiometry and substrate-induced conformation changes. *Biochemistry* 33: 4571-4576, 1994.

18. **Bentinger M, Tekle M, and Dallner G**. Coenzyme Q--biosynthesis and functions. *Biochem Biophys Res Commun* 396: 74-79, 2010.

19. **Benz R**. Permeation of hydrophilic solutes through mitochondrial outer membranes: review on mitochondrial porins. *Biochim Biophys Acta* 1197: 167-196, 1994.

20. **Benz R**. Porin from bacterial and mitochondrial outer membranes. *CRC Crit Rev Biochem* 19: 145-190, 1985.

21. **Bergman BC, Wolfel EE, Butterfield GE, Lopaschuk GD, Casazza GA, Horning MA, and Brooks GA**. Active muscle and whole body lactate kinetics after endurance training in men. *J Appl Physiol* 87: 1684-1696, 1999.

22. **Bernstein D**. Exercise assessment of transgenic models of human cardiovascular disease. *Physiol Genomics* 13: 217-226, 2003.

23. **Bloch D, Belevich I, Jasaitis A, Ribacka C, Puustinen A, Verkhovsky MI, and Wikstrom M**. The catalytic cycle of cytochrome c oxidase is not the sum of its two halves. *Proc Natl Acad Sci U S A* 101: 529-533, 2004.

24. **Bowler MW, Montgomery MG, Leslie AG, and Walker JE**. Ground state structure of F1-ATPase from bovine heart mitochondria at 1.9 A resolution. *J Biol Chem* 282: 14238-14242, 2007.

25. **Boyer PD**. The ATP synthase--a splendid molecular machine. *Annu Rev Biochem* 66: 717-749, 1997.

26. **Brand MD**. The sites and topology of mitochondrial superoxide production. *Exp Gerontol* 45: 466-472, 2010.

27. **Brandt RB, Laux JE, Spainhour SE, and Kline ES**. Lactate dehydrogenase in rat mitochondria. *Arch Biochem Biophys* 259: 412-422, 1987.

28. **Brandt U**. Energy converting NADH:quinone oxidoreductase (complex I). *Annu Rev Biochem* 75: 69-92, 2006.

29. **Brandt U, Kerscher S, Drose S, Zwicker K, and Zickermann V**. Proton pumping by NADH:ubiquinone oxidoreductase. A redox driven conformational change mechanism? *FEBS Lett* 545: 9-17, 2003.

30. **Brody IA, and Engel WK**. Isozyme Histochemistry: The Display of Selective Lactate Dehydrogenase Isozymes in Sections of Skeletal Muscle. *J Histochem Cytochem* 12: 689-695, 1964.

31. **Brookes PS, Levonen AL, Shiva S, Sarti P, and Darley-Usmar VM**. Mitochondria: regulators of signal transduction by reactive oxygen and nitrogen species. *Free Radic Biol Med* 33: 755-764, 2002.

32. **Brooks GA**. Cell-cell and intracellular lactate shuttles. *J Physiol* 587: 5591–5600, 2009.

33. **Brooks GA**. Lactate shuttle -- between but not within cells? *J Physiol* 541: 333-334, 2002.

34. **Brooks GA**. Lactate: Glycolytic end product and oxidative substrate during sustained exercise in mammals - the 'lactate shuttle'. In: *Circulation, Respiration, and Metabolism: Current Comparative Approaches*, edited by Gilles R. Berlin: Springer-Verlag, 1985, p. 208-218.

35. **Brooks GA**. Mammalian fuel utilization during sustained exercise. *Comp Biochem Physiol B Biochem Mol Biol* 120: 89-107, 1998.

36. **Brooks GA, Dubouchaud H, Brown M, Sicurello JP, and Butz CE**. Role of mitochondrial lactate dehydrogenase and lactate oxidation in the intracellular lactate shuttle. *Proc Natl Acad Sci U S A* 96: 1129-1134, 1999.

37. **Brooks GA, and Hashimoto T**. Investigation of the lactate shuttle in skeletal muscle mitochondria. *J Physiol* 584: 705-706;author reply 707-708, 2007.

38. **Cahill GF, Jr.** Fuel metabolism in starvation. *Annu Rev Nutr* 26: 1-22, 2006.

39. **Cahill GF, Jr.** Starvation in man. *Clin Endocrinol Metab* 5: 397-415, 1976.

40. **Cardullo RA, and Baltz JM**. Metabolic regulation in mammalian sperm: mitochondrial volume determines sperm length and flagellar beat frequency. *Cell Motil Cytoskeleton* 19: 180-188, 1991.

41. **Carroll J, Fearnley IM, Shannon RJ, Hirst J, and Walker JE**. Analysis of the subunit composition of complex I from bovine heart mitochondria. *Mol Cell Proteomics* 2: 117-126, 2003.

42. **Chen M, Philipp M, Wang J, Premont RT, Garrison TR, Caron MG, Lefkowitz RJ, and Chen W**. G Protein-coupled receptor kinases phosphorylate LRP6 in the Wnt pathway. *J Biol Chem* 284: 35040-35048, 2009.

43. **Chen Q, Vazquez EJ, Moghaddas S, Hoppel CL, and Lesnefsky EJ**. Production of reactive oxygen species by mitochondria: central role of complex III. *J Biol Chem* 278: 36027-36031, 2003.

44. **Chen S, and Guillory RJ**. Studies on the interaction of arylazido-beta-alanyl NAD+ with the mitochondrial NADH dehydrogenase. *J Biol Chem* 256: 8318-8323, 1981.

45. **Cheong C, Matos I, Choi JH, Dandamudi DB, Shrestha E, Longhi MP, Jeffrey KL, Anthony RM, Kluger C, Nchinda G, Koh H, Rodriguez A, Idoyaga J, Pack M, Velinzon K, Park CG, and Steinman RM**. Microbial stimulation fully differentiates monocytes to DC-SIGN/CD209(+) dendritic cells for immune T cell areas. *Cell* 143: 416-429, 2010.

46. **Chretien D, Pourrier M, Bourgeron T, Sene M, Rotig A, Munnich A, and Rustin P**. An improved spectrophotometric assay of pyruvate dehydrogenase in lactate dehydrogenase contaminated mitochondrial preparations from human skeletal muscle. *Clin Chim Acta* 240: 129-136, 1995.

47. **Coleman RA, Ramp WK, Toverud SU, and Hanker JS**. Electron microscopic localization of lactate dehydrogenase in osteoclasts of chick embryo tibia. *Histochem J* 8: 543-558, 1976.

48. **Collinson IR, Skehel JM, Fearnley IM, Runswick MJ, and Walker JE**. The F1F0-ATPase complex from bovine heart mitochondria: the molar ratio of the subunits in the stalk region linking the F1 and F0 domains. *Biochemistry* 35: 12640-12646, 1996.

49. **Collinson IR, van Raaij MJ, Runswick MJ, Fearnley IM, Skehel JM, Orriss GL, Miroux B, and Walker JE**. ATP synthase from bovine heart mitochondria. In vitro assembly of a stalk complex in the presence of F1-ATPase and in its absence. *J Mol Biol* 242: 408-421, 1994.

50. **Colombini M**. VDAC structure, selectivity, and dynamics. *Biochim Biophys Acta* 1818: 1457-1465, 2012.

51. **Conrad DJ, Stenbit AE, Zettner EM, Wick I, Eckhardt C, and Hardiman G**. Frequency of mitochondrial 12S ribosomal RNA variants in an adult cystic fibrosis population. *Pharmacogenet Genomics* 18: 1095-1102, 2008.

52. **Consortium MGS, Waterston RH, Lindblad-Toh K, Birney E, Rogers J, Abril JF, and al. e**. Initial sequencing and comparative analysis of the mouse genome. *Nature* 420: 520-562, 2002.

53. **Covian R, and Trumpower BL**. Regulatory interactions in the dimeric cytochrome bc(1) complex: the advantages of being a twin. *Biochim Biophys Acta* 1777: 1079-1091, 2008.

54. **Davies KM, Anselmi C, Wittig I, Faraldo-Gomez JD, and Kuhlbrandt W**. Structure of the yeast F1Fo-ATP synthase dimer and its role in shaping the mitochondrial cristae. *Proc Natl Acad Sci U S A* 109: 13602-13607, 2012.

55. **Davies KM, Strauss M, Daum B, Kief JH, Osiewacz HD, Rycovska A, Zickermann V, and Kuhlbrandt W**. Macromolecular organization of ATP synthase and complex I in whole mitochondria. *Proc Natl Acad Sci U S A* 108: 14121-14126, 2011.

56. **Day PW, Rasmussen SG, Parnot C, Fung JJ, Masood A, Kobilka TS, Yao XJ, Choi HJ, Weis WI, Rohrer DK, and Kobilka BK**. A monoclonal antibody for G protein-coupled receptor crystallography. *Nat Methods* 4: 927-929, 2007.

57. **De Jong AM, and Albracht SP**. Ubisemiquinones as obligatory intermediates in the electron transfer from NADH to ubiquinone. *Eur J Biochem* 222: 975-982, 1994.

58. **de Vries S, Berden JA, and Slater EC**. Properties of a semiquinone anion located in the QH2:cytochrome c oxidoreductase segment of the mitochondrial respiratory chain. *FEBS Lett* 122: 143-148, 1980.

59. **Demetrius L**. Aging in mouse and human systems: a comparative study. *Ann N Y Acad Sci* 1067: 66-82, 2006.

60. **Desai KH, Sato R, Schauble E, Barsh GS, Kobilka BK, and Bernstein D**. Cardiovascular indexes in the mouse at rest and with exercise: new tools to study models of cardiac disease. *Am J Physiol* 272: H1053-1061, 1997.

61. **Divakaruni AS, and Brand MD**. The regulation and physiology of mitochondrial proton leak. *Physiology (Bethesda)* 26: 192-205, 2011.

62. **Donovan CM, and Pagliassotti MJ**. Quantitative assessment of pathways for lactate disposal in skeletal muscle fiber types. *Med Sci Sports Exerc* 32: 772-777, 2000.

63. **Droge W**. Free radicals in the physiological control of cell function. *Physiol Rev* 82: 47-95, 2002.

64. **Drose S, and Brandt U**. Molecular mechanisms of superoxide production by the mitochondrial respiratory chain. *Adv Exp Med Biol* 748: 145-169, 2012.

65. **Drose S, Hanley PJ, and Brandt U**. Ambivalent effects of diazoxide on mitochondrial ROS production at respiratory chain complexes I and III. *Biochim Biophys Acta* 1790: 558-565, 2009.

66. **Drose S, Krack S, Sokolova L, Zwicker K, Barth HD, Morgner N, Heide H, Steger M, Nubel E, Zickermann V, Kerscher S, Brutschy B, Radermacher M, and Brandt U**. Functional dissection of the proton pumping modules of mitochondrial complex I. *PLoS Biol* 9: e1001128, 2011.

67. **Dubouchaud H, Butterfield GE, Wolfel EE, Bergman BC, and Brooks GA**. Endurance training, expression, and physiology of LDH, MCT1, and MCT4 in human skeletal muscle. *Am J Physiol Endocrinol Metab* 278: E571-579, 2000.

68. **Efremov RG, Baradaran R, and Sazanov LA**. The architecture of respiratory complex I. *Nature* 465: 441-445, 2010.

69. **Eldridge N**. *Life on Earth: An Encyclopedia of Biodiversity, Ecology, and Evolution*. Santa Barbara, CA: ABC-CLIO Inc., 2002.

70. **Elston T, Wang H, and Oster G**. Energy transduction in ATP synthase. *Nature* 391: 510-513, 1998.

71. **Esposito LA, Melov S, Panov A, Cottrell BA, and Wallace DC**. Mitochondrial disease in mouse results in increased oxidative stress. *Proc Natl Acad Sci U S A* 96: 4820-4825, 1999.

72. **Fahimi HD, and Amarasingham CR**. Cytochemical Localization of Lactic Dehydrogenase in White Skeletal Muscle. *J Cell Biol* 22: 29-48, 1964.

73. **Fahimi HD, and Karnovsky MJ**. Cytochemical localization of two glycolytic dehydrogenases in white skeletal muscle. *J Cell Biol* 29: 113-128, 1966.

74. **Fearnley IM, Carroll J, and Walker JE**. Proteomic analysis of the subunit composition of complex I (NADH:ubiquinone oxidoreductase) from bovine heart mitochondria. *Methods Mol Biol* 357: 103-125, 2007.

75. **Ferguson SJ**. ATP synthase: from sequence to ring size to the P/O ratio. *Proc Natl Acad Sci U S A* 107: 16755-16756, 2010.

76. **Ferretti G, Antonutto G, Denis C, Hoppeler H, Minetti AE, Narici MV, and Desplanches D**. The interplay of central and peripheral factors in limiting maximal O2 consumption in man after prolonged bed rest. *J Physiol* 501 (Pt 3): 677-686, 1997.

77. **Fleming JE, Miquel J, Cottrell SF, Yengoyan LS, and Economos AC**. Is cell aging caused by respiration-dependent injury to the mitochondrial genome? *Gerontology* 28: 44-53, 1982.

78. **Galkin A, and Brandt U**. Superoxide radical formation by pure complex I (NADH:ubiquinone oxidoreductase) from Yarrowia lipolytica. *J Biol Chem* 280: 30129-30135, 2005.

79. **Galkin AS, Grivennikova VG, and Vinogradov AD**. -->H+/2e- stoichiometry in NADH-quinone reductase reactions catalyzed by bovine heart submitochondrial particles. *FEBS Lett* 451: 157-161, 1999.

80. **Galkin AS, Grivennikova VG, and Vinogradov AD**. H+/2e- stoichiometry of the nadh:ubiquinone reductase reaction catalyzed by submitochondrial particles. *Biochemistry (Mosc)* 66: 435-443, 2001.

81. **Gander J, Lee DC, Sui X, Hebert JR, Hooker SP, and Blair SN**. Self-rated health status and cardiorespiratory fitness as predictors of mortality in men. *Br J Sports Med* 45: 1095-1100, 2011.

82. **Gao X, Wen X, Esser L, Quinn B, Yu L, Yu CA, and Xia D**. Structural basis for the quinone reduction in the bc1 complex: a comparative analysis of crystal structures of mitochondrial cytochrome bc1 with bound substrate and inhibitors at the Qi site. *Biochemistry* 42: 9067-9080, 2003.

83. **Garland T, Jr., Schutz H, Chappell MA, Keeney BK, Meek TH, Copes LE, Acosta W, Drenowatz C, Maciel RC, van Dijk G, Kotz CM, and Eisenmann**

JC. The biological control of voluntary exercise, spontaneous physical activity and daily energy expenditure in relation to obesity: human and rodent perspectives. *J Exp Biol* 214: 206-229, 2011.

84. **Gibbons C, Montgomery MG, Leslie AG, and Walker JE**. The structure of the central stalk in bovine F(1)-ATPase at 2.4 A resolution. *Nat Struct Biol* 7: 1055-1061, 2000.

85. **Gladden LB**. 200th anniversary of lactate research in muscle. *Exerc Sport Sci Rev* 36: 109-115, 2008.

86. **Gladden LB**. Is there an intracellular lactate shuttle in skeletal muscle? *J Physiol* 582: 899, 2007.

87. **Gladden LB**. Lactate metabolism: a new paradigm for the third millennium. *J Physiol* 558: 5-30, 2004.

88. **Gnaiger E**. Capacity of oxidative phosphorylation in human skeletal muscle: new perspectives of mitochondrial physiology. *Int J Biochem Cell Biol* 41: 1837-1845, 2009.

89. **Gnaiger E, Lassnig B, Kuznetsov A, Rieger G, and Margreiter R**. Mitochondrial oxygen affinity, respiratory flux control and excess capacity of cytochrome c oxidase. *J Exp Biol* 201: 1129-1139, 1998.

90. **Goldblatt C, Lenton TM, and Watson AJ**. Bistability of atmospheric oxygen and the Great Oxidation. *Nature* 443: 683-686, 2006.

91. **Gray MW, Burger G, and Lang BF**. Mitochondrial evolution. *Science* 283: 1476-1481, 1999.

92. **Green H, Roy B, Grant S, Burnett M, Tupling R, Otto C, Pipe A, and McKenzie D**. Downregulation in muscle Na(+)-K(+)-ATPase following a 21-day expedition to 6,194 m. *J Appl Physiol* 88: 634-640, 2000.

93. **Green HJ, Sutton JR, Cymerman A, Young PM, and Houston CS**. Operation Everest II: adaptations in human skeletal muscle. *J Appl Physiol* 66: 2454-2461, 1989.

94. **Green HJ, Sutton JR, Wolfel EE, Reeves JT, Butterfield GE, and Brooks GA**. Altitude acclimatization and energy metabolic adaptations in skeletal muscle during exercise. *J Appl Physiol* 73: 2701-2708, 1992.

95. **Grivennikova VG, and Vinogradov AD**. Generation of superoxide by the mitochondrial Complex I. *Biochim Biophys Acta* 1757: 553-561, 2006.

96. **Guzy RD, Hoyos B, Robin E, Chen H, Liu L, Mansfield KD, Simon MC, Hammerling U, and Schumacker PT**. Mitochondrial complex III is required for hypoxia-induced ROS production and cellular oxygen sensing. *Cell Metab* 1: 401-408, 2005.

97. **Hagerhall C**. Succinate: quinone oxidoreductases. Variations on a conserved theme. *Biochim Biophys Acta* 1320: 107-141, 1997.

98. **Hamilton ML, Van Remmen H, Drake JA, Yang H, Guo ZM, Kewitt K, Walter CA, and Richardson A**. Does oxidative damage to DNA increase with age? *Proc Natl Acad Sci U S A* 98: 10469-10474, 2001.

99. **Han D, Williams E, and Cadenas E**. Mitochondrial respiratory chain-dependent generation of superoxide anion and its release into the intermembrane space. *Biochem J* 353: 411-416, 2001.

100. **Hare JF, and Crane FL**. A durohydroquinone oxidation site in the mitochondrial transport chain. *J Bioenerg* 2: 317-326, 1971.

101. **Harman D**. Aging: a theory based on free radical and radiation chemistry. *J Gerontol* 11: 298-300, 1956.

102. **Hashimoto T, and Brooks GA**. Mitochondrial lactate oxidation complex and an adaptive role for lactate production. *Med Sci Sports Exerc* 40: 486-494, 2008.

103. **Hashimoto T, Hussien R, and Brooks GA**. Colocalization of MCT1, CD147, and LDH in mitochondrial inner membrane of L6 muscle cells: evidence of a mitochondrial lactate oxidation complex. *Am J Physiol Endocrinol Metab* 290: E1237-1244, 2006.

104. **Hayashi T, and Stuchebrukhov AA**. Electron tunneling in respiratory complex I. *Proc Natl Acad Sci U S A* 107: 19157-19162, 2010.

105. **Heilmann K, Hoffmann U, Witte E, Loddenkemper C, Sina C, Schreiber S, Hayford C, Holzlohner P, Wolk K, Tchatchou E, Moos V, Zeitz M, Sabat R, Gunthert U, and Wittig BM**. Osteopontin as two-sided mediator of intestinal inflammation. *J Cell Mol Med* 13: 1162-1174, 2009.

106. **Henderson GC, Horning MA, Lehman SL, Wolfel EE, Bergman BC, and Brooks GA**. Pyruvate shuttling during rest and exercise before and after endurance training in men. *J Appl Physiol* 97: 317-325, 2004.

107. **Hendler RW, Pardhasaradhi K, Reynafarje B, and Ludwig B**. Comparison of energy-transducing capabilities of the two- and three-subunit cytochromes aa3 from Paracoccus denitrificans and the 13-subunit beef heart enzyme. *Biophys J* 60: 415-423, 1991.

108. **Hinkle PC**. P/O ratios of mitochondrial oxidative phosphorylation. *Biochim Biophys Acta* 1706: 1-11, 2005.

109. **Hinkle PC, Kumar MA, Resetar A, and Harris DL**. Mechanistic stoichiometry of mitochondrial oxidative phosphorylation. *Biochemistry* 30: 3576-3582, 1991.

110. **Hirst J**. Towards the molecular mechanism of respiratory complex I. *Biochem J* 425: 327-339, 2010.

111. **Hirst J, Carroll J, Fearnley IM, Shannon RJ, and Walker JE**. The nuclear encoded subunits of complex I from bovine heart mitochondria. *Biochim Biophys Acta* 1604: 135-150, 2003.

112. **Hochachka PW, Stanley C, Merkt J, and Sumar-Kalinowski J**. Metabolic meaning of elevated levels of oxidative enzymes in high altitude adapted animals: an interpretive hypothesis. *Respir Physiol* 52: 303-313, 1983.

113. **Holland HD**. The oxygenation of the atmosphere and oceans. *Philos Trans R Soc Lond B Biol Sci* 361: 903-915, 2006.

114. **Holloszy JO**. Biochemical adaptations in muscle. Effects of exercise on mitochondrial oxygen uptake and respiratory enzyme activity in skeletal muscle. *J Biol Chem* 242: 2278-2282, 1967.

115. **Holloszy JO, and Booth FW**. Biochemical adaptations to endurance exercise in muscle. *Annu Rev Physiol* 38: 273-291, 1976.

116. **Holmes RS, and Goldberg E**. Computational analyses of mammalian lactate dehydrogenases: human, mouse, opossum and platypus LDHs. *Comput Biol Chem* 33: 379-385, 2009.

117. **Hoppeler H**. The different relationship of VO2max to muscle mitochondria in humans and quadrupedal animals. *Respir Physiol* 80: 137-145, 1990.

118. **Hoppeler H**. *The Dynamic State of Muscle Fibers*. Berlin: Walter de Gruyter, 1990.

119. **Hoppeler H, Howald H, Conley K, Lindstedt SL, Claassen H, Vock P, and Weibel ER**. Endurance training in humans: aerobic capacity and structure of skeletal muscle. *J Appl Physiol* 59: 320-327, 1985.

120. **Hoppeler H, Kleinert E, Schlegel C, Claassen H, Howald H, Kayar SR, and Cerretelli P**. Morphological adaptations of human skeletal muscle to chronic hypoxia. *Int J Sports Med* 11 Suppl 1: S3-9, 1990.

121. **Hoppeler H, Luthi P, Claassen H, Weibel ER, and Howald H**. The ultrastructure of the normal human skeletal muscle. A morphometric analysis on untrained men, women and well-trained orienteers. *Pflugers Arch* 344: 217-232, 1973.

122. **Horan MP, Pichaud N, and Ballard JW**. Review: quantifying mitochondrial dysfunction in complex diseases of aging. *J Gerontol A Biol Sci Med Sci* 67: 1022-1035, 2012.

123. **Horton RH**. *Principles of biochemistry*. Upper Saddle River, NJ: Pearson Prentice Hall, 2006.

124. **Howald H, Pette D, Simoneau JA, Uber A, Hoppeler H, and Cerretelli P**. Effect of chronic hypoxia on muscle enzyme activities. *Int J Sports Med* 11 Suppl 1: S10-14, 1990.

125. **Idoyaga J, Lubkin A, Fiorese C, Lahoud MH, Caminschi I, Huang Y, Rodriguez A, Clausen BE, Park CG, Trumpfheller C, and Steinman RM**. Comparable T helper 1 (Th1) and CD8 T-cell immunity by targeting HIV gag p24 to CD8 dendritic cells within antibodies to Langerin, DEC205, and Clec9A. *Proc Natl Acad Sci U S A* 108: 2384-2389, 2011.

126. **Itoh H, Takahashi A, Adachi K, Noji H, Yasuda R, Yoshida M, and Kinosita K**. Mechanically driven ATP synthesis by F1-ATPase. *Nature* 427: 465-468, 2004.

127. **Iwata S, Ostermeier C, Ludwig B, and Michel H**. Structure at 2.8 A resolution of cytochrome c oxidase from Paracoccus denitrificans. *Nature* 376: 660-669, 1995.

128. **Jacobs HT**. The mitochondrial theory of aging: dead or alive? *Aging Cell* 2: 11-17, 2003.

129. **Jacobs RA, Boushel R, Wright-Paradis C, Calbet JA, Robach P, Gnaiger E, and Lundby C**. Mitochondrial function in human skeletal muscle following high altitude exposure. *Exp Physiol* 98: 245-255, 2013.

130. **Jacobs RA, Diaz V, Meinild AK, Gassmann M, and Lundby C**. The C57Bl/6 mouse serves as a suitable model of human skeletal muscle mitochondrial function *Exp Physiol* doi:10.1113/expphysiol.2012.070037: 2012.

131. **Jacobs RA, Diaz V, Soldini L, Haider T, Thomassen M, Nordsborg NB, Gassmann M, and Lundby C**. Fast-twitch glycolytic skeletal muscle is predisposed to age-induced impairments in mitochondrial function. *J Gerontol A Biol Sci Med Sci* doi:10.1093/gerona/gls335: 2013.

132. **Jacobs RA, and Lundby C**. Mitochondria express enhanced quality as well as quantity in association with aerobic fitness across recreationally active individuals up to elite athletes. *J Appl Physiol* doi:10.1152/japplphysiol.01081.2012 2012.

133. **Jacobs RA, Lundby C, Robach P, and Gassmann M**. Red blood cell volume and the capacity for exercise at moderate to high altitude. *Sports Med* 42 (8): 1-21, 2012.

134. **Jacobs RA, Rasmussen P, Siebenmann C, Diaz V, Gassmann M, Pesta D, Gnaiger E, Nordsborg NB, Robach P, and Lundby C**. Determinants of time trial performance and maximal incremental exercise in highly trained endurance athletes. *J Appl Physiol* 111: 1422-1430, 2011.

135. **Jacobs RA, Siebenmann C, Hug M, Toigo M, Meinild AK, and Lundby C**. Twenty-eight days at 3454-m altitude diminishes respiratory capacity but enhances efficiency in human skeletal muscle mitochondria. *FASEB J* 26: 5192-5200, 2012.

136. **Janssen I, and Jolliffe CJ**. Influence of physical activity on mortality in elderly with coronary artery disease. *Med Sci Sports Exerc* 38: 418-417, 2006.

137. **Joyner MJ**. Modeling: optimal marathon performance on the basis of physiological factors. *J Appl Physiol* 70: 683-687, 1991.

138. **Joyner MJ, and Coyle EF**. Endurance exercise performance: the physiology of champions. *J Physiol* 586: 35-44, 2008.

139. **Joyner MJ, Ruiz JR, and Lucia A**. The two-hour marathon: who and when? *J Appl Physiol* 110: 275-277, 2011.

140. **Junge W**. Protons, proteins and ATP. *Photosynth Res* 80: 197-221, 2004.

141. **Kaneda H, Hayashi J, Takahama S, Taya C, Lindahl KF, and Yonekawa H**. Elimination of paternal mitochondrial DNA in intraspecific crosses during early mouse embryogenesis. *Proc Natl Acad Sci U S A* 92: 4542-4546, 1995.

142. **Kato-Yamada Y, Noji H, Yasuda R, Kinosita K, Jr., and Yoshida M**. Direct observation of the rotation of epsilon subunit in F1-ATPase. *J Biol Chem* 273: 19375-19377, 1998.

143. **Katzmarzyk PT, Church TS, and Blair SN**. Cardiorespiratory fitness attenuates the effects of the metabolic syndrome on all-cause and cardiovascular disease mortality in men. *Arch Intern Med* 164: 1092-1097, 2004.

144. **Kay L, Nicolay K, Wieringa B, Saks V, and Wallimann T**. Direct evidence for the control of mitochondrial respiration by mitochondrial creatine kinase in oxidative muscle cells in situ. *J Biol Chem* 275: 6937-6944, 2000.

145. **Kho AT, Kang PB, Kohane IS, and Kunkel LM**. Transcriptome-scale similarities between mouse and human skeletal muscles with normal and myopathic phenotypes. *BMC Musculoskelet Disord* 7: 23, 2006.

146. **Kim I, and Lemasters JJ**. Mitochondrial degradation by autophagy (mitophagy) in GFP-LC3 transgenic hepatocytes during nutrient deprivation. *Am J Physiol Cell Physiol* 300: C308-317, 2010.

147. **Kinosita K, Jr., Yasuda R, Noji H, Ishiwata S, and Yoshida M**. F1-ATPase: a rotary motor made of a single molecule. *Cell* 93: 21-24, 1998.

148. **Kirkwood SP, Munn EA, and Brooks GA**. Mitochondrial reticulum in limb skeletal muscle. *Am J Physiol* 251: C395-402, 1986.

149. **Kline ES, Brandt RB, Laux JE, Spainhour SE, Higgins ES, Rogers KS, Tinsley SB, and Waters MG**. Localization of L-lactate dehydrogenase in mitochondria. *Arch Biochem Biophys* 246: 673-680, 1986.

150. **Kodama S, Saito K, Tanaka S, Maki M, Yachi Y, Asumi M, Sugawara A, Totsuka K, Shimano H, Ohashi Y, Yamada N, and Sone H**. Cardiorespiratory fitness as a quantitative predictor of all-cause mortality and cardiovascular events in healthy men and women: a meta-analysis. *Jama* 301: 2024-2035, 2009.

151. **Koenitzer JR, and Freeman BA**. Redox signaling in inflammation: interactions of endogenous electrophiles and mitochondria in cardiovascular disease. *Ann N Y Acad Sci* 1203: 45-52, 2010.

152. **Koga N, and Takada S**. Folding-based molecular simulations reveal mechanisms of the rotary motor F1-ATPase. *Proc Natl Acad Sci U S A* 103: 5367-5372, 2006.

153. **Kokoszka JE, Coskun P, Esposito LA, and Wallace DC**. Increased mitochondrial oxidative stress in the Sod2 (+/-) mouse results in the age-related decline of mitochondrial function culminating in increased apoptosis. *Proc Natl Acad Sci U S A* 98: 2278-2283, 2001.

154. **Konhauser KO, Lalonde SV, Planavsky NJ, Pecoits E, Lyons TW, Mojzsis SJ, Rouxel OJ, Barley ME, Rosiere C, Fralick PW, Kump LR, and Bekker A**. Aerobic bacterial pyrite oxidation and acid rock drainage during the Great Oxidation Event. *Nature* 478: 369-373, 2011.

155. **Koopman WJ, Nijtmans LG, Dieteren CE, Roestenberg P, Valsecchi F, Smeitink JA, and Willems PH**. Mammalian mitochondrial complex I: biogenesis, regulation, and reactive oxygen species generation. *Antioxid Redox Signal* 12: 1431-1470, 2010.

156. **Kopp RE, Kirschvink JL, Hilburn IA, and Nash CZ**. The Paleoproterozoic snowball Earth: a climate disaster triggered by the evolution of oxygenic photosynthesis. *Proceedings of the National Academy of Sciences of the United States of America* 102: 11131-11136, 2005.

157. **Kraunsoe R, Boushel R, Hansen CN, Schjerling P, Qvortrup K, Stockel M, Mikines KJ, and Dela F**. Mitochondrial respiration in subcutaneous and visceral adipose tissue from patients with morbid obesity. *J Physiol* 588: 2023-2032, 2010.

158. **Kump LR, and Barley ME**. Increased subaerial volcanism and the rise of atmospheric oxygen 2.5 billion years ago. *Nature* 448: 1033-1036, 2007.

159. **Kunz WS, Kudin A, Vielhaber S, Elger CE, Attardi G, and Villani G**. Flux control of cytochrome c oxidase in human skeletal muscle. *J Biol Chem* 275: 27741-27745, 2000.

160. **Kunz WS, Kuznetsov AV, Schulze W, Eichhorn K, Schild L, Striggow F, Bohnensack R, Neuhof S, Grasshoff H, Neumann HW, and Gellerich FN**. Functional characterization of mitochondrial oxidative phosphorylation in saponin-skinned human muscle fibers. *Biochim Biophys Acta* 1144: 46-53, 1993.

161. **Kushnareva Y, Murphy AN, and Andreyev A**. Complex I-mediated reactive oxygen species generation: modulation by cytochrome c and NAD(P)+ oxidation-reduction state. *Biochem J* 368: 545-553, 2002.

162. **Kussmaul L, and Hirst J**. The mechanism of superoxide production by NADH:ubiquinone oxidoreductase (complex I) from bovine heart mitochondria. *Proc Natl Acad Sci U S A* 103: 7607-7612, 2006.

163. **Kuznetsov AV, Kunz WS, Saks V, Usson Y, Mazat JP, Letellier T, Gellerich FN, and Margreiter R**. Cryopreservation of mitochondria and mitochondrial function in cardiac and skeletal muscle fibers. *Anal Biochem* 319: 296-303, 2003.

164. **Kuznetsov AV, Veksler V, Gellerich FN, Saks V, Margreiter R, and Kunz WS**. Analysis of mitochondrial function in situ in permeabilized muscle fibers, tissues and cells. *Nat Protoc* 3: 965-976, 2008.

165. **Lancaster CR**. Succinate:quinone oxidoreductases: an overview. *Biochim Biophys Acta* 1553: 1-6, 2002.

166. **Larsen RG, Callahan DM, Foulis SA, and Kent-Braun JA**. In vivo oxidative capacity varies with muscle and training status in young adults. *J Appl Physiol* 107: 873-879, 2009.

167. **Larsen S, Ara I, Rabol R, Andersen JL, Boushel R, Dela F, and Helge JW**. Are substrate use during exercise and mitochondrial respiratory capacity decreased in arm and leg muscle in type 2 diabetes? *Diabetologia* 52: 1400-1408, 2009.

168. **Larsen S, Kristensen JM, Stride N, Wojtaszewski JF, Helge JW, and Dela F**. Skeletal muscle mitochondrial respiration in AMPKalpha2 kinase-dead mice. *Acta Physiol (Oxf)* 205: 314-320, 2012.

169. **Larsen S, Nielsen J, Neigaard Nielsen C, Nielsen LB, Wibrand F, Stride N, Schroder HD, Boushel R, Helge JW, Dela F, and Hey-Mogensen M**. Biomarkers of mitochondrial content in skeletal muscle of healthy young human subjects. *J Physiol* 590: 3349–3360, 2012.

170. **Larsen S, Stride N, Hey-Mogensen M, Hansen CN, Andersen JL, Madsbad S, Worm D, Helge JW, and Dela F**. Increased mitochondrial substrate sensitivity in skeletal muscle of patients with type 2 diabetes. *Diabetologia* 54: 1427-1436, 2011.

171. **Lemieux H, and Warren BE**. An animal model to study human muscular diseases involving mitochondrial oxidative phosphorylation. *J Bioenerg Biomembr* DOI: 10.1007/s10863-012-9451-2: 2012.

172. **Lenaz G**. A critical appraisal of the mitochondrial coenzyme Q pool. *FEBS Lett* 509: 151-155, 2001.

173. **Lenaz G, Fato R, Formiggini G, and Genova ML**. The role of Coenzyme Q in mitochondrial electron transport. *Mitochondrion* 7 Suppl: S8-33, 2007.

174. **Lesnefsky EJ, Gudz TI, Moghaddas S, Migita CT, Ikeda-Saito M, Turkaly PJ, and Hoppel CL**. Aging decreases electron transport complex III activity in heart interfibrillar mitochondria by alteration of the cytochrome c binding site. *J Mol Cell Cardiol* 33: 37-47, 2001.

175. **Levett DZ, Radford EJ, Menassa DA, Graber EF, Morash AJ, Hoppeler H, Clarke K, Martin DS, Ferguson-Smith AC, Montgomery HE, Grocott MP, and Murray AJ**. Acclimatization of skeletal muscle mitochondria to high-altitude hypoxia during an ascent of Everest. *FASEB J* 26: 1431-1441, 2012.

176. **Liesa M, Palacin M, and Zorzano A**. Mitochondrial dynamics in mammalian health and disease. *Physiol Rev* 89: 799-845, 2009.

177. **Lieser MJ, Park J, Natori S, Jones BA, Bronk SF, and Gores GJ**. Cholestasis confers resistance to the rat liver mitochondrial permeability transition. *Gastroenterology* 115: 693-701, 1998.

178. **Lill R, Hoffmann B, Molik S, Pierik AJ, Rietzschel N, Stehling O, Uzarska MA, Webert H, Wilbrecht C, and Muhlenhoff U**. The role of mitochondria in cellular iron-sulfur protein biogenesis and iron metabolism. *Biochim Biophys Acta* 1823: 1491-1508, 2012.

179. **Lin A, Krockmalnic G, and Penman S**. Imaging cytoskeleton--mitochondrial membrane attachments by embedment-free electron microscopy of saponin-extracted cells. *Proc Natl Acad Sci U S A* 87: 8565-8569, 1990.

180. **Lyerly GW, Sui X, Lavie CJ, Church TS, Hand GA, and Blair SN**. The association between cardiorespiratory fitness and risk of all-cause mortality among women with impaired fasting glucose or undiagnosed diabetes mellitus. *Mayo Clin Proc* 84: 780-786, 2009.

181. **MacDougall JD, Green HJ, Sutton JR, Coates G, Cymerman A, Young P, and Houston CS**. Operation Everest II: structural adaptations in skeletal muscle in response to extreme simulated altitude. *Acta Physiol Scand* 142: 421-427, 1991.

182. **Machado de Domenech E, Domenech CE, Aoki A, and Blanco A**. Association of the testicular lactate dehydrogenase isozyme with a special type of mitochondria. *Biol Reprod* 6: 136-147, 1972.

183. **Maekawa M, Yamaguchi K, Nakamura T, Shibukawa R, Kodanaka I, Ichisaka T, Kawamura Y, Mochizuki H, Goshima N, and Yamanaka S**. Direct reprogramming of somatic cells is promoted by maternal transcription factor Glis1. *Nature* 474: 225-229, 2011.

184. **Maklashina E, and Cecchini G**. The quinone-binding and catalytic site of complex II. *Biochim Biophys Acta* 1797: 1877-1882, 2010.

185. **Malka F, Guillery O, Cifuentes-Diaz C, Guillou E, Belenguer P, Lombes A, and Rojo M**. Separate fusion of outer and inner mitochondrial membranes. *EMBO Rep* 6: 853-859, 2005.

186. **Mattisson AG, Johansson RG, and Bostrom SL**. The cellular localization of lactate dehydrogenase in skeletal muscle of eel (Anguilla anguilla). *Comp Biochem Physiol B* 41: 475-482, 1972.

187. **Mazzeo RS, Brooks GA, Schoeller DA, and Budinger TF**. Disposal of blood [1-13C]lactate in humans during rest and exercise. *J Appl Physiol* 60: 232-241, 1986.

188. **McClelland GB, and Brooks GA**. Changes in MCT 1, MCT 4, and LDH expression are tissue specific in rats after long-term hypobaric hypoxia. *J Appl Physiol* 92: 1573-1584, 2002.

189. **McCord JM**. The evolution of free radicals and oxidative stress. *Am J Med* 108: 652-659, 2000.

190. **McGraw DW, Almoosa KF, Paul RJ, Kobilka BK, and Liggett SB**. Antithetic regulation by beta-adrenergic receptors of Gq receptor signaling via phospholipase C underlies the airway beta-agonist paradox. *J Clin Invest* 112: 619-626, 2003.

191. **Melov S, Schneider JA, Day BJ, Hinerfeld D, Coskun P, Mirra SS, Crapo JD, and Wallace DC**. A novel neurological phenotype in mice lacking mitochondrial manganese superoxide dismutase. *Nat Genet* 18: 159-163, 1998.

192. **Mettauer B, Zoll J, Sanchez H, Lampert E, Ribera F, Veksler V, Bigard X, Mateo P, Epailly E, Lonsdorfer J, and Ventura-Clapier R**. Oxidative capacity of skeletal muscle in heart failure patients versus sedentary or active control subjects. *J Am Coll Cardiol* 38: 947-954, 2001.

193. **Michel H**. Cytochrome c oxidase: catalytic cycle and mechanisms of proton pumping--a discussion. *Biochemistry* 38: 15129-15140, 1999.

194. **Michikawa Y, Mazzucchelli F, Bresolin N, Scarlato G, and Attardi G**. Aging-dependent large accumulation of point mutations in the human mtDNA control region for replication. *Science* 286: 774-779, 1999.

195. **Miller BF, Fattor JA, Jacobs KA, Horning MA, Navazio F, Lindinger MI, and Brooks GA**. Lactate and glucose interactions during rest and exercise in men: effect of exogenous lactate infusion. *J Physiol* 544: 963-975, 2002.

196. **Miller BF, Fattor JA, Jacobs KA, Horning MA, Suh SH, Navazio F, and Brooks GA**. Metabolic and cardiorespiratory responses to "the lactate clamp". *Am J Physiol Endocrinol Metab* 283: E889-898, 2002.

197. **Miller BF, Robinson MM, Bruss MD, Hellerstein M, and Hamilton KL**. A comprehensive assessment of mitochondrial protein synthesis and cellular proliferation with age and caloric restriction. *Aging Cell* 11: 150-161, 2012.

198. **Milner DJ, Mavroidis M, Weisleder N, and Capetanaki Y**. Desmin cytoskeleton linked to muscle mitochondrial distribution and respiratory function. *J Cell Biol* 150: 1283-1298, 2000.

199. **Mitchell P**. Coupling of phosphorylation to electron and hydrogen transfer by a chemi-osmotic type of mechanism. *Nature* 191: 144-148, 1961.

200. **Mitchell P**. Possible molecular mechanisms of the protonmotive function of cytochrome systems. *J Theor Biol* 62: 327-367, 1976.

201. **Mitchell P**. The protonmotive Q cycle: a general formulation. *FEBS Lett* 59: 137-139, 1975.

202. **Mizuno M, Savard GK, Areskog NH, Lundby C, and Saltin B**. Skeletal muscle adaptations to prolonged exposure to extreme altitude: a role of physical activity? *High Alt Med Biol* 9: 311-317, 2008.

203. **Moore LG, Niermeyer S, and Zamudio S**. Human adaptation to high altitude: regional and life-cycle perspectives. *Am J Phys Anthropol* Suppl 27: 25-64, 1998.

204. **Morris SA, Guo Y, and Zernicka-Goetz M**. Developmental plasticity is bound by pluripotency and the Fgf and Wnt signaling pathways. *Cell Rep* 2: 756-765, 2012.

205. **Muller FL, Liu Y, and Van Remmen H**. Complex III releases superoxide to both sides of the inner mitochondrial membrane. *J Biol Chem* 279: 49064-49073, 2004.

206. **Naimi AI, Bourbeau J, Perrault H, Baril J, Wright-Paradis C, Rossi A, Taivassalo T, Sheel AW, Rabol R, Dela F, and Boushel R**. Altered mitochondrial regulation in quadriceps muscles of patients with COPD. *Clin Physiol Funct Imaging* 2010.

207. **Nakae Y, Stoward PJ, Shono M, and Matsuzaki T**. Localisation and quantification of dehydrogenase activities in single muscle fibers of mdx gastrocnemius. *Histochem Cell Biol* 112: 427-436, 1999.

208. **Newmeyer DD, and Ferguson-Miller S**. Mitochondria: releasing power for life and unleashing the machineries of death. *Cell* 112: 481-490, 2003.

209. **Nicholls P, van Buuren KJ, and van Gelder BF**. Biochemical and biophysical studies on cytochrome aa 3 . 8. Effect of cyanide on the catalytic activity. *Biochim Biophys Acta* 275: 279-287, 1972.

210. **Nishizaka T, Oiwa K, Noji H, Kimura S, Muneyuki E, Yoshida M, and Kinosita K, Jr.** Chemomechanical coupling in F1-ATPase revealed by simultaneous observation of nucleotide kinetics and rotation. *Nat Struct Mol Biol* 11: 142-148, 2004.

211. **Noji H, Yasuda R, Yoshida M, and Kinosita K, Jr.** Direct observation of the rotation of F1-ATPase. *Nature* 386: 299-302, 1997.

212. **Nori S, Okada Y, Yasuda A, Tsuji O, Takahashi Y, Kobayashi Y, Fujiyoshi K, Koike M, Uchiyama Y, Ikeda E, Toyama Y, Yamanaka S, Nakamura M, and Okano H**. Grafted human-induced pluripotent stem-cell-derived neurospheres promote motor functional recovery after spinal cord injury in mice. *Proc Natl Acad Sci U S A* 108: 16825-16830, 2011.

213. **Novikoff AB, and Masek B**. Survival of lactic dehydrogenase and DPNH-diaphorase activities after formol-calcium fixation. *J Histochem Cytochem* 6: 217, 1958.

214. **Nuskova H, Vrbacky M, Drahota Z, and Houstek J**. Cyanide inhibition and pyruvate-induced recovery of cytochrome c oxidase. *J Bioenerg Biomembr* 42: 395-403, 2010.

215. **Ogata T, and Yamasaki Y**. Ultra-high-resolution scanning electron microscopy of mitochondria and sarcoplasmic reticulum arrangement in human red, white, and intermediate muscle fibers. *Anat Rec* 248: 214-223, 1997.

216. **Ohnishi T**. Iron-sulfur clusters/semiquinones in complex I. *Biochim Biophys Acta* 1364: 186-206, 1998.

217. **Ohnishi T, Moser CC, Page CC, Dutton PL, and Yano T**. Simple redox-linked proton-transfer design: new insights from structures of quinol-fumarate reductase. *Structure* 8: R23-32, 2000.

218. **Ohnishi T, and Trumpower BL**. Differential effects of antimycin on ubisemiquinone bound in different environments in isolated succinate . cytochrome c reductase complex. *J Biol Chem* 255: 3278-3284, 1980.

219. **Ortega FB, Lee DC, Sui X, Kubzansky LD, Ruiz JR, Baruth M, Castillo MJ, and Blair SN**. Psychological well-being, cardiorespiratory fitness, and long-term survival. *Am J Prev Med* 39: 440-448, 2010.

220. **Paglialunga S, van Bree B, Bosma M, Valdecantos MP, Amengual-Cladera E, Jorgensen JA, van Beurden D, den Hartog GJ, Ouwens DM, Briede JJ, Schrauwen P, and Hoeks J**. Targeting of mitochondrial reactive oxygen species production does not avert lipid-induced insulin resistance in muscle tissue from mice. *Diabetologia* DOI: 10.1007/s00125-012-2626-x: 2012.

221. **Pande SV, and Blanchaer MC**. Preferential loss of ATP-dependent long-chain fatty acid activating enzyme in mitochondria prepared using Nagarse. *Biochim Biophys Acta* 202: 43-48, 1970.

222. **Panke O, Gumbiowski K, Junge W, and Engelbrecht S**. F-ATPase: specific observation of the rotating c subunit oligomer of EF(o)EF(1). *FEBS Lett* 472: 34-38, 2000.

223. **Passarella S, de Bari L, Valenti D, Pizzuto R, Paventi G, and Atlante A**. Mitochondria and L-lactate metabolism. *FEBS Lett* 582: 3569-3576, 2008.

224. **Payne BA, Wilson IJ, Hateley CA, Horvath R, Santibanez-Koref M, Samuels DC, Price DA, and Chinnery PF**. Mitochondrial aging is accelerated by anti-retroviral therapy through the clonal expansion of mtDNA mutations. *Nat Genet* 43: 806-810, 2011.

225. **Penefsky HS**. Mechanism of inhibition of mitochondrial adenosine triphosphatase by dicyclohexylcarbodiimide and oligomycin: relationship to ATP synthesis. *Proc Natl Acad Sci U S A* 82: 1589-1593, 1985.

226. **Pesta D, and Gnaiger E**. High-Resolution Respirometry. OXPHOS Protocols for Human Cell Cultures and Permeabilized Fibres from Small Biopsies of Human Muscle. *Mitochondrial Bioenergetics: Methods and Protocols* 810: 25-58, 2011.

227. **Pesta D, and Gnaiger E**. High-Resolution Respirometry. OXPHOS Protocols for Human Cell Cultures and Permeabilized Fibres from Small Biopsies of Human Muscle. *Methods Mol Biol* 810: 25-58, 2012.

228. **Pesta D, Hoppel F, Macek C, Messner H, Faulhaber M, Kobel C, Parson W, Burtscher M, Schocke M, and Gnaiger E**. Similar qualitative and quantitative changes of mitochondrial respiration following strength and endurance training in normoxia and hypoxia in sedentary humans. *Am J Physiol Regul Integr Comp Physiol* 301: R1078-1087, 2011.

229. **Petersen LC**. The effect of inhibitors on the oxygen kinetics of cytochrome c oxidase. *Biochim Biophys Acta* 460: 299-307, 1977.

230. **Picard M, Ritchie D, Wright KJ, Romestaing C, Thomas MM, Rowan SL, Taivassalo T, and Hepple RT**. Mitochondrial functional impairment with aging is exaggerated in isolated mitochondria compared to permeabilized myofibers. *Aging Cell* 9: 1032-1046, 2010.

231. **Picard M, Taivassalo T, Gouspillou G, and Hepple RT**. Mitochondria: Isolation, Structure and Function. *J Physiol* 589: 4413–4421, 2011.

232. **Picard M, Taivassalo T, Ritchie D, Wright KJ, Thomas MM, Romestaing C, and Hepple RT**. Mitochondrial structure and function are disrupted by standard isolation methods. *PLoS One* 6: e18317, 2011.

233. **Picard M, White K, and Turnbull DM**. Mitochondrial morphology, topology, and membrane interactions in skeletal muscle: a quantitative three-dimensional electron microscopy study. *J Appl Physiol* 114: 161-171, 2013.

234. **Popinigis J, Antosiewicz J, Crimi M, Lenaz G, and Wakabayashi T**. Human skeletal muscle: participation of different metabolic activities in oxidation of L-lactate. *Acta Biochim Pol* 38: 169-175, 1991.

235. **Potter VR, and Dubois KP**. Studies on the Mechanism of Hydrogen Transport in Animal Tissues : Vi. Inhibitor Studies with Succinic Dehydrogenase. *J Gen Physiol* 26: 391-404, 1943.

236. **Pozefsky T, Tancredi RG, Moxley RT, Dupre J, and Tobin JD**. Effects of brief starvation on muscle amino acid metabolism in nonobese man. *J Clin Invest* 57: 444-449, 1976.

237. **Radi R**. Nitric oxide, oxidants, and protein tyrosine nitration. *Proc Natl Acad Sci U S A* 101: 4003-4008, 2004.

238. **Ralph SJ, Moreno-Sanchez R, Neuzil J, and Rodriguez-Enriquez S**. Inhibitors of succinate: quinone reductase/Complex II regulate production of mitochondrial reactive oxygen species and protect normal cells from ischemic damage but induce specific cancer cell death. *Pharm Res* 28: 2695-2730, 2011.

239. **Rand DM, Haney RA, and Fry AJ**. Cytonuclear coevolution: the genomics of cooperation. *Trends Ecol Evol* 19: 645-653, 2004.

240. **Rangarajan A, and Weinberg RA**. Opinion: Comparative biology of mouse versus human cells: modelling human cancer in mice. *Nat Rev Cancer* 3: 952-959, 2003.

241. **Rasmussen HN, van Hall G, and Rasmussen UF**. Lactate dehydrogenase is not a mitochondrial enzyme in human and mouse vastus lateralis muscle. *J Physiol* 541: 575-580, 2002.

242. **Rennie MJ, Selby A, Atherton P, Smith K, Kumar V, Glover EL, and Philips SM**. Facts, noise and wishful thinking: muscle protein turnover in aging and human disuse atrophy. *Scand J Med Sci Sports* 20: 5-9, 2010.

243. **Reynafarje B**. Myoglobin content and enzymatic activity of muscle and altitude adaptation. *J Appl Physiol* 17: 301-305, 1962.

244. **Robertson DE, Prince RC, Bowyer JR, Matsuura K, Dutton PL, and Ohnishi T**. Thermodynamic properties of the semiquinone and its binding site in the ubiquinol-cytochrome c (c2) oxidoreductase of respiratory and photosynthetic systems. *J Biol Chem* 259: 1758-1763, 1984.

245. **Roessler MM, King MS, Robinson AJ, Armstrong FA, Harmer J, and Hirst J**. Direct assignment of EPR spectra to structurally defined iron-sulfur clusters in complex I by double electron-electron resonance. *Proc Natl Acad Sci U S A* 107: 1930-1935, 2010.

246. **Rosca MG, Vazquez EJ, Chen Q, Kerner J, Kern TS, and Hoppel CL**. Oxidation of fatty acids is the source of increased mitochondrial reactive oxygen species production in kidney cortical tubules in early diabetes. *Diabetes* 61: 2074-2083, 2012.

247. **Rubinstein JL, Walker JE, and Henderson R**. Structure of the mitochondrial ATP synthase by electron cryomicroscopy. *EMBO J* 22: 6182-6192, 2003.

248. **Rutter J, Winge DR, and Schiffman JD**. Succinate dehydrogenase - Assembly, regulation and role in human disease. *Mitochondrion* 10: 393-401, 2010.

249. **Sahlin K, Fernstrom M, Svensson M, and Tonkonogi M**. No evidence of an intracellular lactate shuttle in rat skeletal muscle. *J Physiol* 541: 569-574, 2002.

250. **Sahlin K, and Harris RC**. Control of lipid oxidation during exercise: role of energy state and mitochondrial factors. *Acta Physiol (Oxf)* 194: 283-291, 2008.

251. **Saks V, Guzun R, Timohhina N, Tepp K, Varikmaa M, Monge C, Beraud N, Kaambre T, Kuznetsov A, Kadaja L, Eimre M, and Seppet E**. Structure-function relationships in feedback regulation of energy fluxes in vivo in health and disease: mitochondrial interactosome. *Biochim Biophys Acta* 1797: 678-697, 2010.

252. **Saks VA, Belikova YO, and Kuznetsov AV**. In vivo regulation of mitochondrial respiration in cardiomyocytes: specific restrictions for intracellular diffusion of ADP. *Biochim Biophys Acta* 1074: 302-311, 1991.

253. **Saks VA, Kaambre T, Sikk P, Eimre M, Orlova E, Paju K, Piirsoo A, Appaix F, Kay L, Regitz-Zagrosek V, Fleck E, and Seppet E**. Intracellular energetic units in red muscle cells. *Biochem J* 356: 643-657, 2001.

254. **Saks VA, Veksler VI, Kuznetsov AV, Kay L, Sikk P, Tiivel T, Tranqui L, Olivares J, Winkler K, Wiedemann F, and Kunz WS**. Permeabilized cell and skinned fiber techniques in studies of mitochondrial function in vivo. *Mol Cell Biochem* 184: 81-100, 1998.

255. **Sambongi Y, Iko Y, Tanabe M, Omote H, Iwamoto-Kihara A, Ueda I, Yanagida T, Wada Y, and Futai M**. Mechanical rotation of the c subunit oligomer in ATP synthase (F0F1): direct observation. *Science* 286: 1722-1724, 1999.

256. **Sazanov LA**. Respiratory complex I: mechanistic and structural insights provided by the crystal structure of the hydrophilic domain. *Biochemistry* 46: 2275-2288, 2007.

257. **Sazanov LA, and Hinchliffe P**. Structure of the hydrophilic domain of respiratory complex I from Thermus thermophilus. *Science* 311: 1430-1436, 2006.

258. **Scarpulla RC**. Transcriptional paradigms in mammalian mitochondrial biogenesis and function. *Physiol Rev* 88: 611-638, 2008.

259. **Schagger H, Link TA, Engel WD, and von Jagow G**. Isolation of the eleven protein subunits of the bc1 complex from beef heart. *Methods Enzymol* 126: 224-237, 1986.

260. **Schiaffino S, Sandri M, and Murgia M**. Activity-dependent signaling pathways controlling muscle diversity and plasticity. *Physiology (Bethesda)* 22: 269-278, 2007.

261. **Schmeck B, Zahlten J, Moog K, van Laak V, Huber S, Hocke AC, Opitz B, Hoffmann E, Kracht M, Zerrahn J, Hammerschmidt S, Rosseau S, Suttorp N, and Hippenstiel S**. Streptococcus pneumoniae-induced p38 MAPK-dependent phosphorylation of RelA at the interleukin-8 promotor. *J Biol Chem* 279: 53241-53247, 2004.

262. **Schriner SE, Linford NJ, Martin GM, Treuting P, Ogburn CE, Emond M, Coskun PE, Ladiges W, Wolf N, Van Remmen H, Wallace DC, and Rabinovitch PS**. Extension of murine life span by overexpression of catalase targeted to mitochondria. *Science* 308: 1909-1911, 2005.

263. **Schwerzmann K, Hoppeler H, Kayar SR, and Weibel ER**. Oxidative capacity of muscle and mitochondria: correlation of physiological, biochemical, and morphometric characteristics. *Proc Natl Acad Sci U S A* 86: 1583-1587, 1989.

264. **Sebastian D, Hernandez-Alvarez MI, Segales J, Sorianello E, Munoz JP, Sala D, Waget A, Liesa M, Paz JC, Gopalacharyulu P, Oresic M, Pich S, Burcelin R, Palacin M, and Zorzano A**. Mitofusin 2 (Mfn2) links mitochondrial and endoplasmic reticulum function with insulin signaling and is essential for normal glucose homeostasis. *Proc Natl Acad Sci U S A* 109: 5523-5528, 2012.

265. **Senior AE, and Weber J**. Happy motoring with ATP synthase. *Nat Struct Mol Biol* 11: 110-112, 2004.

266. **Shigenaga MK, Hagen TM, and Ames BN**. Oxidative damage and mitochondrial decay in aging. *Proc Natl Acad Sci U S A* 91: 10771-10778, 1994.

267. **Short KR, Bigelow ML, Kahl J, Singh R, Coenen-Schimke J, Raghavakaimal S, and Nair KS**. Decline in skeletal muscle mitochondrial function with aging in humans. *Proc Natl Acad Sci U S A* 102: 5618-5623, 2005.

268. **Shoubridge EA**. Mitochondrial DNA segregation in the developing embryo. *Hum Reprod* 15 Suppl 2: 229-234, 2000.

269. **Sjodin B**. Lactate dehydrogenase in human skeletal muscle. *Acta Physiol Scand Suppl* 436: 1-32, 1976.

270. **Skilleter DN, and Kun E**. The oxidation of L-lactate by liver mitochondria. *Arch Biochem Biophys* 152: 92-104, 1972.

271. **Slack E, Hapfelmeier S, Stecher B, Velykoredko Y, Stoel M, Lawson MA, Geuking MB, Beutler B, Tedder TF, Hardt WD, Bercik P, Verdu EF, McCoy KD, and Macpherson AJ**. Innate and adaptive immunity cooperate flexibly to maintain host-microbiota mutualism. *Science* 325: 617-620, 2009.

272. **Stadtman ER, and Levine RL**. Protein oxidation. *Ann N Y Acad Sci* 899: 191-208, 2000.

273. **Stal PS, and Johansson B**. Abnormal mitochondria organization and oxidative activity in the palate muscles of long-term snorers with obstructive sleep apnea. *Respiration* 83: 407-417, 2012.

274. **Stock D, Leslie AG, and Walker JE**. Molecular architecture of the rotary motor in ATP synthase. *Science* 286: 1700-1705, 1999.

275. **Strauss M, Hofhaus G, Schroder RR, and Kuhlbrandt W**. Dimer ribbons of ATP synthase shape the inner mitochondrial membrane. *EMBO J* 27: 1154-1160, 2008.

276. **Sun F, Huo X, Zhai Y, Wang A, Xu J, Su D, Bartlam M, and Rao Z**. Crystal structure of mitochondrial respiratory membrane protein complex II. *Cell* 121: 1043-1057, 2005.

277. **Sun J, and Trumpower BL**. Superoxide anion generation by the cytochrome bc1 complex. *Arch Biochem Biophys* 419: 198-206, 2003.

278. **Svenson KL, Von Smith R, Magnani PA, Suetin HR, Paigen B, Naggert JK, Li R, Churchill GA, and Peters LL**. Multiple trait measurements in 43 inbred mouse strains capture the phenotypic diversity characteristic of human populations. *J Appl Physiol* 102: 2369-2378, 2007.

279. **Szczesna-Kaczmarek A**. Regulating effect of mitochondrial lactate dehydrogenase on oxidation of cytoplasmic NADH via an "external" pathway in skeletal muscle mitochondria. *Int J Biochem* 24: 657-661, 1992.

280. **Tappan DV, Reynafarje B, Potter VR, and Hurtado A**. Alterations in enzymes and metabolites resulting from adaptation to low oxygen tensions. *Am J Physiol* 190: 93-98, 1957.

281. **Tomitsuka E, Hirawake H, Goto Y, Taniwaki M, Harada S, and Kita K**. Direct evidence for two distinct forms of the flavoprotein subunit of human mitochondrial complex II (succinate-ubiquinone reductase). *J Biochem* 134: 191-195, 2003.

282. **Trumpower BL**. The protonmotive Q cycle. Energy transduction by coupling of proton translocation to electron transfer by the cytochrome bc1 complex. *J Biol Chem* 265: 11409-11412, 1990.

283. **Tsukihara T, Aoyama H, Yamashita E, Tomizaki T, Yamaguchi H, Shinzawa-Itoh K, Nakashima R, Yaono R, and Yoshikawa S**. Structures of metal sites of oxidized bovine heart cytochrome c oxidase at 2.8 A. *Science* 269: 1069-1074, 1995.

284. **Tsukihara T, Aoyama H, Yamashita E, Tomizaki T, Yamaguchi H, Shinzawa-Itoh K, Nakashima R, Yaono R, and Yoshikawa S**. The whole structure of the 13-subunit oxidized cytochrome c oxidase at 2.8 A. *Science* 272: 1136-1144, 1996.

285. **Turrens JF**. Mitochondrial formation of reactive oxygen species. *J Physiol* 552: 335-344, 2003.

286. **Turrens JF, Alexandre A, and Lehninger AL**. Ubisemiquinone is the electron donor for superoxide formation by complex III of heart mitochondria. *Arch Biochem Biophys* 237: 408-414, 1985.

287. **Turrens JF, and Boveris A**. Generation of superoxide anion by the NADH dehydrogenase of bovine heart mitochondria. *Biochem J* 191: 421-427, 1980.

288. **Valdivia E**. Total capillary bed in striated muscles of guinea pigs native to the Peruvian mountains. *Am J Physiol* 194: 585-589, 1958.

289. **van Hall G**. Lactate kinetics in human tissues at rest and during exercise. *Acta Physiol (Oxf)* 199: 499-508, 2010.

290. **Van Hall G, Jensen-Urstad M, Rosdahl H, Holmberg HC, Saltin B, and Calbet JA**. Leg and arm lactate and substrate kinetics during exercise. *Am J Physiol Endocrinol Metab* 284: E193-205, 2003.

291. **Veksler VI, Kuznetsov AV, Sharov VG, Kapelko VI, and Saks VA**. Mitochondrial respiratory parameters in cardiac tissue: a novel method of assessment by using saponin-skinned fibers. *Biochim Biophys Acta* 892: 191-196, 1987.

292. **Verkhovsky MI, Jasaitis A, Verkhovskaya ML, Morgan JE, and Wikstrom M**. Proton translocation by cytochrome c oxidase. *Nature* 400: 480-483, 1999.

293. **Vigano A, Ripamonti M, De Palma S, Capitanio D, Vasso M, Wait R, Lundby C, Cerretelli P, and Gelfi C**. Proteins modulation in human skeletal muscle in the early phase of adaptation to hypobaric hypoxia. *Proteomics* 8: 4668-4679, 2008.

294. **Villani G, Greco M, Papa S, and Attardi G**. Low reserve of cytochrome c oxidase capacity in vivo in the respiratory chain of a variety of human cell types. *J Biol Chem* 273: 31829-31836, 1998.

295. **Vogt M, Puntschart A, Geiser J, Zuleger C, Billeter R, and Hoppeler H**. Molecular adaptations in human skeletal muscle to endurance training under simulated hypoxic conditions. *J Appl Physiol* 91: 173-182, 2001.

296. **Votion DM, Fraipont A, Goachet AG, Robert C, van Erck E, Amory H, Ceusters J, de la Rebiere de Pouyade G, Franck T, Mouithys-Mickalad A, Niesten A, and Serteyn D**. Alterations in mitochondrial respiratory function in response to endurance training and endurance racing. *Equine Vet J Suppl* 268-274, 2010.

297. **Votion DM, Gnaiger E, Lemieux H, Mouithys-Mickalad A, and Serteyn D**. Physical fitness and mitochondrial respiratory capacity in horse skeletal muscle. *PLoS One* 7: e34890, 2012.

298. **Votyakova TV, and Reynolds IJ**. DeltaPsi(m)-Dependent and -independent production of reactive oxygen species by rat brain mitochondria. *J Neurochem* 79: 266-277, 2001.

299. **Walker DG, and Seligman AM**. The use of formalin fixation in the cytochemical demonstration of succinic and DPN- and TPN-dependent dehydrogenases in mitochondria. *J Cell Biol* 16: 455-469, 1963.

300. **Walker JE, and Dickson VK**. The peripheral stalk of the mitochondrial ATP synthase. *Biochim Biophys Acta* 1757: 286-296, 2006.

301. **Walker JE, Lutter R, Dupuis A, and Runswick MJ**. Identification of the subunits of F1F0-ATPase from bovine heart mitochondria. *Biochemistry* 30: 5369-5378, 1991.

302. **Wallace DC**. A mitochondrial paradigm of metabolic and degenerative diseases, aging, and cancer: a dawn for evolutionary medicine. *Annu Rev Genet* 39: 359-407, 2005.

303. **Wallace DC**. Mitochondria and cancer. *Nat Rev Cancer* 12: 685-698, 2012.

304. **Wallace DC**. Mitochondrial diseases in man and mouse. *Science* 283: 1482-1488, 1999.

305. **Wang H, and Oster G**. Energy transduction in the F1 motor of ATP synthase. *Nature* 396: 279-282, 1998.

306. **Watson JD, and Crick FH**. The structure of DNA. *Cold Spring Harb Symp Quant Biol* 18: 123-131, 1953.

307. **Watt IN, Montgomery MG, Runswick MJ, Leslie AG, and Walker JE**. Bioenergetic cost of making an adenosine triphosphate molecule in animal mitochondria. *Proc Natl Acad Sci U S A* 107: 16823-16827, 2010.

308. **Wegrzyn J, Potla R, Chwae YJ, Sepuri NB, Zhang Q, Koeck T, Derecka M, Szczepanek K, Szelag M, Gornicka A, Moh A, Moghaddas S, Chen Q, Bobbili S, Cichy J, Dulak J, Baker DP, Wolfman A, Stuehr D, Hassan MO, Fu XY, Avadhani N, Drake JI, Fawcett P, Lesnefsky EJ, and Larner AC**. Function of mitochondrial Stat3 in cellular respiration. *Science* 323: 793-797, 2009.

309. **Weibel ER, and Hoppeler H**. Exercise-induced maximal metabolic rate scales with muscle aerobic capacity. *J Exp Biol* 208: 1635-1644, 2005.

310. **Weidner U, Geier S, Ptock A, Friedrich T, Leif H, and Weiss H**. The gene locus of the proton-translocating NADH: ubiquinone oxidoreductase in Escherichia coli. Organization of the 14 genes and relationship between the derived proteins and subunits of mitochondrial complex I. *J Mol Biol* 233: 109-122, 1993.

311. **West JB**. The physiologic basis of high-altitude diseases. *Ann Intern Med* 141: 789-800, 2004.

312. **Whalen EJ, Foster MW, Matsumoto A, Ozawa K, Violin JD, Que LG, Nelson CD, Benhar M, Keys JR, Rockman HA, Koch WJ, Daaka Y, Lefkowitz RJ, and Stamler JS**. Regulation of beta-adrenergic receptor signaling by S-nitrosylation of G-protein-coupled receptor kinase 2. *Cell* 129: 511-522, 2007.

313. **WHO**. *World Health Statistics Annual*. Geneva: World Health Organization, 1996.

314. **Wicker U, Bucheler K, Gellerich FN, Wagner M, Kapischke M, and Brdiczka D**. Effect of macromolecules on the structure of the mitochondrial inter-membrane space and the regulation of hexokinase. *Biochim Biophys Acta* 1142: 228-239, 1993.

315. **Wikstrom MK**. Proton pump coupled to cytochrome c oxidase in mitochondria. *Nature* 266: 271-273, 1977.

316. **Wilson MT, Antonini G, Malatesta F, Sarti P, and Brunori M**. Probing the oxygen binding site of cytochrome c oxidase by cyanide. *J Biol Chem* 269: 24114-24119, 1994.

317. **Wu Z, Puigserver P, Andersson U, Zhang C, Adelmant G, Mootha V, Troy A, Cinti S, Lowell B, Scarpulla RC, and Spiegelman BM**. Mechanisms controlling mitochondrial biogenesis and respiration through the thermogenic coactivator PGC-1. *Cell* 98: 115-124, 1999.

318. **Xia D, Yu CA, Kim H, Xia JZ, Kachurin AM, Zhang L, Yu L, and Deisenhofer J**. Crystal structure of the cytochrome bc1 complex from bovine heart mitochondria. *Science* 277: 60-66, 1997.

319. **Yang D, Oyaizu Y, Oyaizu H, Olsen GJ, and Woese CR**. Mitochondrial origins. *Proceedings of the National Academy of Sciences of the United States of America* 82: 4443-4447, 1985.

320. **Yaniv Y, Juhaszova M, Wang S, Fishbein KW, Zorov DB, and Sollott SJ**. Analysis of mitochondrial 3D-deformation in cardiomyocytes during active contraction reveals passive structural anisotropy of orthogonal short axes. *PLoS One* 6: e21985, 2011.

321. **Yankovskaya V, Horsefield R, Tornroth S, Luna-Chavez C, Miyoshi H, Leger C, Byrne B, Cecchini G, and Iwata S**. Architecture of succinate dehydrogenase and reactive oxygen species generation. *Science* 299: 700-704, 2003.

322. **Yasuda R, Noji H, Kinosita K, Jr., and Yoshida M**. F1-ATPase is a highly efficient molecular motor that rotates with discrete 120 degree steps. *Cell* 93: 1117-1124, 1998.

323. **Yin Y, Yang S, Yu L, and Yu CA**. Reaction mechanism of superoxide generation during ubiquinol oxidation by the cytochrome bc1 complex. *J Biol Chem* 285: 17038-17045, 2010.

324. **Yoshida Y, Holloway GP, Ljubicic V, Hatta H, Spriet LL, Hood DA, and Bonen A**. Negligible direct lactate oxidation in subsarcolemmal and intermyofibrillar mitochondria obtained from red and white rat skeletal muscle. *J Physiol* 582: 1317-1335, 2007.

325. **Youle RJ, and van der Bliek AM**. Mitochondrial fission, fusion, and stress. *Science* 337: 1062-1065, 2012.

326. **Yu-Wai-Man P, Griffiths PG, and Chinnery PF**. Mitochondrial optic neuropathies - disease mechanisms and therapeutic strategies. *Prog Retin Eye Res* 30: 81-114, 2011.

327. **Zak DE, Schmitz F, Gold ES, Diercks AH, Peschon JJ, Valvo JS, Niemisto A, Podolsky I, Fallen SG, Suen R, Stolyar T, Johnson CD, Kennedy KA, Hamilton MK, Siggs OM, Beutler B, and Aderem A**. Systems analysis identifies an essential role for SHANK-associated RH domain-interacting protein (SHARPIN) in macrophage Toll-like receptor 2 (TLR2) responses. *Proc Natl Acad Sci U S A* 108: 11536-11541, 2011.

328. **Zhang Z, Huang L, Shulmeister VM, Chi YI, Kim KK, Hung LW, Crofts AR, Berry EA, and Kim SH**. Electron transfer by domain movement in cytochrome bc1. *Nature* 392: 677-684, 1998.

329. **Zhu J, Egawa T, Yeh SR, Yu L, and Yu CA**. Simultaneous reduction of iron-sulfur protein and cytochrome b(L) during ubiquinol oxidation in cytochrome bc(1) complex. *Proc Natl Acad Sci U S A* 104: 4864-4869, 2007.

330. **Zickermann V, Kerscher S, Zwicker K, Tocilescu MA, Radermacher M, and Brandt U**. Architecture of complex I and its implications for electron transfer and proton pumping. *Biochim Biophys Acta* 1787: 574-583, 2009.

331. **Zoll J, Sanchez H, N'Guessan B, Ribera F, Lampert E, Bigard X, Serrurier B, Fortin D, Geny B, Veksler V, Ventura-Clapier R, and Mettauer B**. Physical activity changes the regulation of mitochondrial respiration in human skeletal muscle. *J Physiol* 543: 191-200, 2002.

LIST OF REFEREED JOURNAL PUBLICATIONS DURING DOCTORAL STUDIES

1. **Jacobs RA**, Meinild AK, Nordsborg NB, and Lundby C. Lactate metabolism in human skeletal muscle. *Am J Physiol Endocrinol Metab* Accepted for publication: 2013.
2. **Jacobs RA**, Diaz V, Soldini L, Haider T, Thomassen M, Nordsborg NB, Gassmann M & Lundby C. (2013). Fast-twitch glycolytic skeletal muscle is predisposed to age-induced impairments in mitochondrial function. *J Gerontol A Biol Sci Med Sci* doi:10.1093/gerona/gls335.
3. Siebenmann C, Sorensen H, **Jacobs RA**, Haider T, Rasmussen P & Lundby C. (2013). Hypocapnia during hypoxic exercise and its impact on cerebral oxygenation, ventilation and maximal whole body O(2) uptake. *Respir Physiol Neurobiol* 185, 461-467.
4. **Jacobs RA**, Boushel R, Wright-Paradis C, Calbet JA, Robach P, Gnaiger E & Lundby C. (2013). Mitochondrial function in human skeletal muscle following high altitude exposure. *Exp Physiol* 98, 245-255.
5. **Jacobs RA** & Lundby C. (2012). Mitochondria express enhanced quality as well as quantity in association with aerobic fitness across recreationally active individuals up to elite athletes. *J Appl Physiol* doi:10.1152/japplphysiol.01081.2012

6. **Jacobs RA**, Diaz V, Meinild AK, Gassmann M & Lundby C. (2012). The C57Bl/6 mouse serves as a suitable model of human skeletal muscle mitochondrial function *Exp Physiol* doi:10.1113/expphysiol.2012.070037.
7. **Jacobs RA**, Siebenmann C, Hug M, Toigo M, Meinild AK & Lundby C. (2012). Twenty-eight days at 3454-m altitude diminishes respiratory capacity but enhances efficiency in human skeletal muscle mitochondria. *FASEB J* 26, 5192-5200.
8. Robach P, Siebenmann C, **Jacobs RA**, Rasmussen P, Nordsborg NB, Pesta D, Gnaiger E, Diaz V, Christ A, Fiedler J, Crivelli N, Secher NH, Pichon A, Maggiorini M & Lundby C. (2012). The role of hemoglobin mass on VO2max following normobaric "live high – train low" in endurance-trained athletes. *Br J Sports Med* 46, 822-827. DOI:10.1136/bjsports-2012-091078.
9. **Jacobs RA**, Lundby C, Robach P & Gassmann M. (2012). Red blood cell volume and the capacity for exercise at moderate to high altitude. *Sports Med* 42 (8), 1-21.
10. Schuler B, Vogel J, Grenacher B, **Jacobs RA**, Arras M & Gassmann M. (2012). Acute and chronic elevation of erythropoietin in the brain improves exercise performance in mice without inducing erythropoiesis. FASEB J 26, fj.11-191197.
11. Rasmussen P, Nordsborg N, Taudorf S, Sorensen H, Berg RM, **Jacobs RA**, Bailey DM, Olsen NV, Secher NH, Moller K & Lundby C. (2012). Brain and skin do not contribute to the systemic rise in erythropoietin during acute hypoxia in humans. *FASEB J* 26, 1831-1834.
12. Nordsborg NB, Siebenmann C, **Jacobs RA**, Rasmussen P, Diaz V, Robach P & Lundby C. (2012). Four weeks of normobaric "live high-train low" do not alter muscular or systemic capacity for maintaining pH and K+ homeostasis during intense exercise. *J Appl Physiol* 112, 2027-2036.
13. Zobi F, Blacque O, **Jacobs RA**, Schaub MC & Bogdanova AY. (2012). 17 e-rhenium dicarbonyl CO-releasing molecules on a cobalamin scaffold for biological application. *Dalton Trans* 41, 370-378.
14. Siebenmann C, Robach P, **Jacobs RA**, Rasmussen P, Nordsborg N, Diaz V, Christ A, Olsen NV, Maggiorini M & Lundby C. (2012). "Live high-train low" using normobaric hypoxia: a double-blinded, placebo-controlled study. *J Appl Physiol* 112, 106-117.
15. Diaz V, Lombardi G, Ricci C, **Jacobs RA**, Montalvo Z, Lundby C & Banfi G. (2011). Reticulocyte and haemoglobin profiles in elite triathletes over four consecutive seasons. *Int J Lab Hematol* 33, 638-644.
16. **Jacobs RA**, Rasmussen P, Siebenmann C, Diaz V, Gassmann M, Pesta D, Gnaiger E, Nordsborg NB, Robach P & Lundby C. (2011). Determinants of time trial performance and maximal incremental exercise in highly trained endurance athletes. *J Appl Physiol* 111, 1422-1430.